Spring 2010

The Influence of Mechanical Circulation on Water Column Stability and Dissolved Oxygen in Stratified Lakes

Paal Engebrigtsen
Old Dominion University

THE INFLUENCE OF MECHANICAL CIRCULATION ON WATER COLUMN STABILITY AND DISSOLVED OXYGEN IN STRATIFIED LAKES

by

Paal Engebrigtsen
B.S. in Mechanical Engineering 1996, University of Colorado at Boulder
M.S. in Environmental Engineering 2004, Old Dominion University

A Dissertation Submitted to the Faculty of
Old Dominion University in Partial Fulfillment of the
Requirement for the Degree of

DOCTOR OF PHILOSOPHY

ENVIRONMENTAL ENGINEERING

OLD DOMINION UNIVERSITY
May 2010

Approved by:

Gary C. Schafran (Director)

Müjde Erten-Unal (Member)

Jaewan Yoon (Member)

John C. Little (Member)

ABSTRACT

THE INFLUENCE OF MECHANICAL CIRCULATION ON WATER COLUMN STABILITY AND DISSOLVED OXYGEN IN STRATIFIED LAKES

Paal Engebrigtsen
Old Dominion University, 2010
Director: Dr. Gary C. Schafran

Surface circulators have been used in wastewater and industrial lagoons for many years, but only recently have they been designed for lakes and reservoirs as a water quality management tool. Their relatively low capital investment and operational costs make them an attractive chemical free option for ameliorating the symptoms of eutrophication. Little research has been conducted on their effectiveness in impacting water quality. Today many lake managers are waiting for independent research on surface circulators' performance before installing such systems.

The Occoquan Reservoir was the primary site for a study conducted to examine the influence of surface circulation on water quality. Eight surface circulators were installed in the reservoir in 2006 in an effort to lower iron and manganese by increasing dissolved oxygen in the lower waters. Oxygen and temperature profiles were recorded at three main sampling sites from April through October 2007. These data were compared with historical data collected by the Occoquan Watershed Monitoring Laboratory (OWML) to determine the influence of circulator operation. Near field flow studies were conducted around one circulator using an acoustic doppler velocimeter (ADV).

It was found that the circulators had significantly less influence on the temperature and dissolved oxygen of Occoquan Reservoir. This appeared to be contributed by the low circulation flow rates that were measured.

A modeling effort was also conducted to simulate measured temperature and dissolved oxygen profiles through 2007. Since CE-QUAL-W2 does not explicitly contain a module to directly simulate surface circulation, the pump module was modified to transfer water from a discrete depth in the hypolimnion to the surface. After a satisfactory agreement between measured and simulated temperature and dissolved oxygen profiles was obtained, the unknown zero flow condition of the reservoir was studied. Next, a series of hypothetical lakes were simulated to explore the influence of various lake sizes, circulation flow rates, and intake depths on the temperature and dissolved oxygen distribution. It was found that the vertical temperature distribution was relatively easy to affect, and it responded to the physical mixing from the surface circulators in a conservative manner. The vertical dissolved oxygen distribution was harder to influence since it was controlled by many processes involving oxygen supply and demand in the water column and the sediments.

A new approach for evaluating the circulator performance was developed based on the reduction in sediment area subjected to anoxic overlaying water. This reduction in anoxic sediment area is considered proportional to the reduction in iron and manganese to the lake, and would therefore represent a benefit to the water quality.

Key Words: Surface circulators, temperature and dissolved oxygen profiles, ADV, and CE-QUAL-W2.

AKNOWLEDGMENTS

First and foremost, I want to express my gratitude to Dr. Gary C. Schafran for directing my research and doctoral work. Dr. Schafran has been an inspiration through his vast knowledge within the field of limnology and environmental science. He offered me laboratory training and financial support through many research projects. Through this period, I observed how Dr. Schafran always took a genuine interest in transferring his knowledge to students.

I want to express my appreciation to Dr. Mujde Erten-Unal and Dr. Jaewan Yoon for their contribution within and outside class projects. I feel that each professor has offered me valuable personal support.

I am thankful that Dr. John C. Little accepted the obligation of serving on my doctoral committee. I have found his technical papers valuable in my research.

I would also like to thank Greg Prelewicz with Fairfax Water. He has been a great support and offered priceless information regarding Fairfax Water's reservoir data. He also provided water quality monitoring data generated by OWML under Dr. Tom Gizzard.

Finally, I want to thank my family, Kimberly and Dennis Engebrigtsen, who supported me through my studies. I look forward to spending more weekend and evening time together.

TABLE OF CONTENTS

Page

Page

Page

Page

LIST OF FIGURES

Page

Page

Page

Page

Page

Page

Page

LIST OF TABLES

CHAPTER I

SURFACE CIRCULATION

1.1 Introduction

Cultural Eutrophication of lakes and reservoirs is a world-wide problem that cannot be solved by chemical addition, mechanical equipment, or other treatment techniques alone. These treatment options will only alleviate some of the undesirable symptoms of the eutrophication process. The real cause is rooted in anthropogenic activities within watersheds that generate or release nutrients which eventually find their way into lakes and reservoirs (Cooke et al., 2001). Control of nutrients in watersheds is a continuing challenge and often requires long periods of time before improvements are realized in adjacent aqueous systems. An option to more quickly improve the conditions in a lake undergoing accelerated eutrophication is some type of within-lake remediation effort. One potential option is enhanced mixing provided by surface circulators. The focus of this research is the investigation of how surface circulators affect the temperature and dissolved oxygen distribution in a water supply reservoir and the development/use of a model to simulate circulation created by surface circulators.

Little research has been conducted on the effectiveness of solar-powered surface circulators on improving dissolved oxygen conditions in lakes. To date, both positive and negative qualitative reports exist on this technology's abilities to improve water quality. Caution must be practiced when different situations are compared because lakes have different conditions (e.g. volume, hydrology, depth, biogeochemical processes), and the objectives for adding surface circulation are often also different. The two most

---

The APA Style will be followed.

common objectives for installing a circulation system are to control algae, particularly concentrations of cyanobacteria, and to increase dissolved oxygen concentrations in oxygen depleted regions. Increasing the hypolimnetic dissolved oxygen concentration will have positive implications on iron, manganese, sulfide, ammonia, and phosphorus loading from the sediments and improve the habitat for fish and other aquatic life (McQueen and Lean, 1986; Ashley, 1988). Anoxic conditions are common in the hypolimnion of stratified mesotrophic and eutrophic lakes and lake, and typically reservoir managers are looking for ways to improve dissolved oxygen levels. Solar-powered surface circulators have recently been offered as a solution to low hypolimnetic oxygen concentrations with improved conditions realized through water exchange.

In August 2006, Fairfax Water, a water utility serving northern Virginia, installed eight surface circulators in Occoquan Reservoir's lower region in an effort to reduce the high manganese concentrations developing in the hypolimnion during the summer. The reservoir response to the operation of the eight surface circulators was studied from May 4, 2007 to October 18, 2007 focusing on water column dissolved oxygen concentrations and the thermal structure. Monitoring activities involved collecting weekly temperature and dissolved oxygen profiles at three sampling sites in the reservoir, as well as additional monitoring efforts to explore the near-field and far-field influence of the surface circulators. Temperature data loggers were also employed for a short duration to monitor circulator operation. An acoustic doppler velocimeter (ADV) instrument was also used to investigate the near-field flow around the circulators to discern physical mixing and flow patterns. A water quality model, CE-QUAL-W2, was set up, calibrated, and validated with the field data and then used to simulate the impact of circulator flow

rate and different intake depths on the temperature and dissolved oxygen distribution in several hypothetical lakes.

1.2 Literature Review

Water movement within a lake is complex and affected by atmospheric conditions, wind and wave forces, bathymetry, and most importantly by temperature fluctuations of the water on a diurnal basis and through the year. The importance of heat content has led to the quantification and characterization of heat fluxes (heat budgets) in lakes. Methods for determining the heat budget for lakes has been based on the pioneering limnological work of Birge (1915). A lake's annual heat budget is based on the temperature difference between winter and summer through the water column multiplied by the specific heat value of water (Hutchinson, 1957; Wetzel, 2001). The temperature and density stratification of lakes regulate nearly all the physicochemical processes and consequently metabolism and productivity (Wetzel, 2001). Artificial circulation has been observed to raise the hypolimnetic temperature more significantly than the decrease observed in the epilimnetic temperature (Cooke at al., 1993) – a condition likely related to the volume differences of these two lake regions. Any mixing that is affecting the vertical temperature profile will likely affect the total heat content of the lake.

Thermal stability is by definition the energy necessary to completely mix the water column to a uniform temperature (Birge, 1915). The higher the thermal stability, the less likely it is that weather events or other perturbations will turn over and mix a lake. A lake's stability is influenced by its bathymetry (shape and depth). Lakes deeper

than 5-7 meters generally develop thermal stratification with high enough thermal stability to resist the mixing forces of typical summer weather in temperate regions (Wetzel, 2001). Solar radiation is the greatest source of heat energy to a lake. Heat exchange with the sediments and the atmosphere does occur, but for moderately deep lakes, these heat exchanges are minimal compared to direct light absorption (Wetzel, 2001). Most heat absorption takes place in the shallower depths of a lake since light penetration decreases exponentially with depth. Consequently, within this layer the water temperature will rise. The specific gravity of water decreases as the temperature is increasing making it more buoyant and resistant to vertical mixing (Hutchinson, 1957). The thermal stratification that occurs in lakes has led to the identification of three distinct zones identified by vertical temperature profiles (Figure 1).

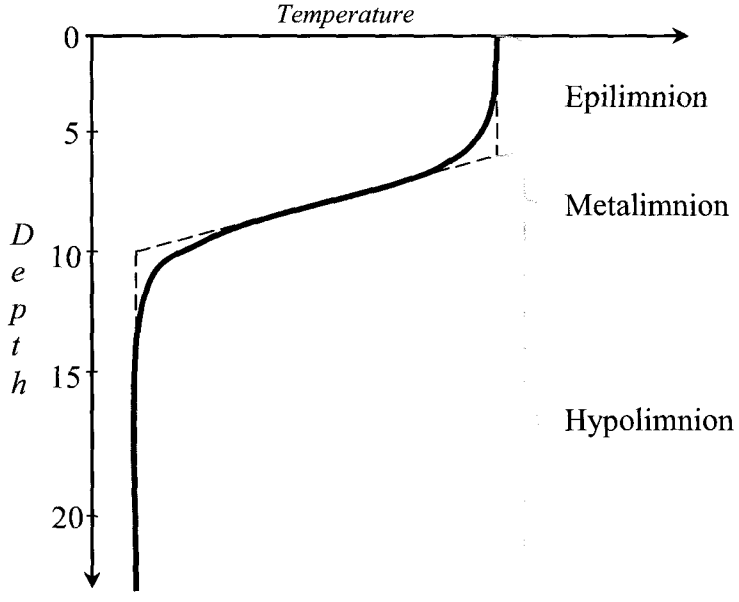

Figure 1. Water column temperature profile during summer stratification and delineation of the epilimnion, metalimnion, and the hypolimnion.

During summer stratification the epilimnion is well mixed, the warmest of the three layers, and typically has a uniform temperature distribution. The hypolimnion is not well mixed, has a uniform or decreasing temperature distribution and is isolated from the atmosphere. The metalimnion is the transition zone between the epilimnion and the hypolimnion where rapid temperature change with depth occurs and where the thermocline resides, defined as the horizontal plane of maximum temperature change (Hutchinson, 1957). All mixing and transport phenomena in a lake are driven by external forces, except molecular diffusion (Imboden and Wuest, 1995). Molecular diffusion is slow, only 10^{-9} m^2/s (20 cm/yr), and an important transport mechanism primarily at the sediment-water interface. External forces on a lake induce waves, seiches, and other oscillating motions that mix the water locally dispersing constituents with it. Horizontal transport is driven by small temperature disturbances which result from mixing and is far more efficient than the vertical transport. These temperature disturbances influence the specific weight of the water and the potential energy balance of the lake. Horizontal transport will take place reestablishing a state of the lowest possible energy (Imboden and Wuest, 1995; Wetzel, 2001). This condition can have a profound effect on the water quality of stratified lakes, particularly highly productive (i.e. eutrophic) lakes. The impact of stratification is generally first observed by way of temperature changes and in the vertical distribution of dissolved oxygen.

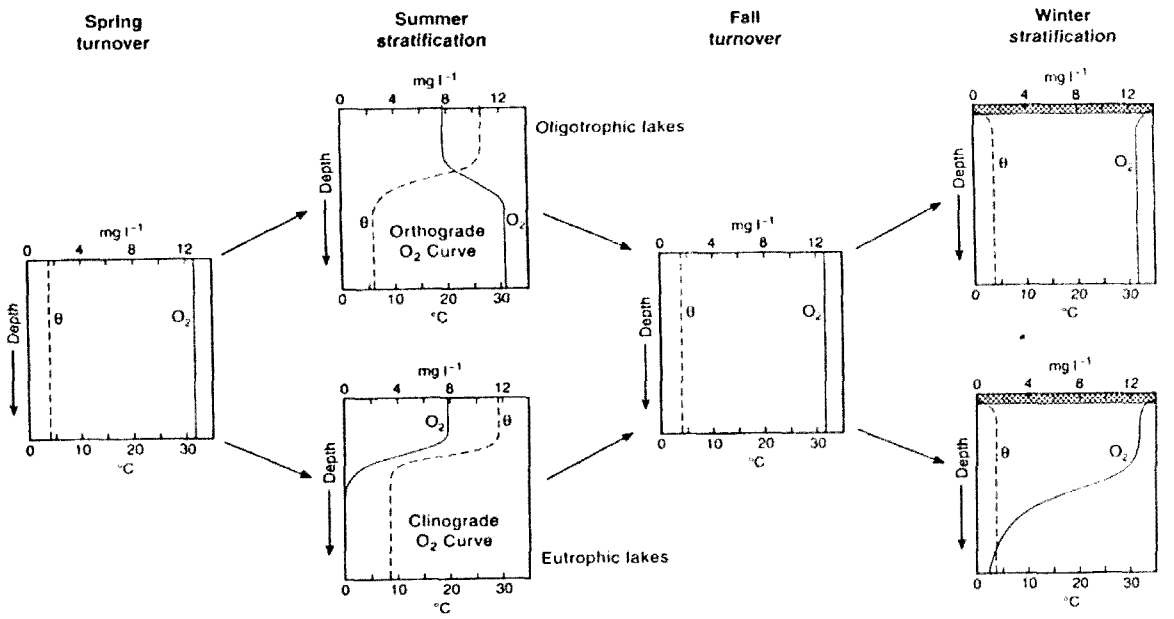

Figure 2. Illustrations of the vertical temperature and dissolved oxygen profiles for eutrophic and oligotrophic of a dimictic lakes (Wetzel, 2001)

During spring turnover the entire water column is often homogenized by vertical mixing. The advective transport is high during this period and the dissolved oxygen concentration can be near saturation. During summer stratification the hypolimnion becomes isolated from the atmospheric oxygen supply by limited vertical transport through the metalimnion. Under these conditions oxygen demand within the water column and in the sediments will consume the hypolimnetic dissolved oxygen until it is depleted (Cole and Hannan, 1990). Occoquan Reservoir has been classified by Occoquan Watershed Monitoring Laboratory as nutrient enriched and eutrophic (Eunpu, 1973) and measured temperature and dissolved oxygen concentrations correspond with the "eutrophic lake" in Figure 2.

The oxygen demand exerted in lakes is almost completely due to microorganisms oxidizing organic matter to satisfy energy needs (Gordon and Higgins, 2001). A lake receives organic matter from the watershed (allochtonous) through contributing streams, rivers, and ground water, and also from in-lake primary production (autochthonous). Microorganisms present in a lake obtain biologically useful energy (BUE) through respiration of organic material using available electron acceptors in order from the highest energy yield to the lowest (Table1). (Bouwen, 1992; Fenchel, 1998).

Table 1. An overview of microbial respiration reactions by their electron acceptors, end products, and BUE yield (Gordon and Higgins, 2007).

Terminal e- Acceptor	End Products	BUE Yield
O_2	H_2O	29.9 kcal/eq
NO_3	N_2	28.4
MnO_2	Mn^{2+}	23.3
FeO(OH)	Fe^{2+}	10.1
SO_4	H_2S	5.9
Organics	Reduced Organics	NA
CO_2	CH_4	5.6

Oxygen is the preferred electron acceptor and represents the greatest amount of biological useful energy. Therefore, it is preferable for microorganisms and will be consumed first in a lake (Gordon and Higgins, 2007). When the available oxygen is depleted nitrification (the process of oxidizing ammonia to nitrate) becomes inhibited by the same lack of oxygen and ammonia accumulates in the water column. Ammonia is toxic to aquatic life, particularly at elevated pH, so it has the potential to negatively

impact aquatic organisms. Denitrification is the next energetically favorable reaction and reduces to N_2 or other gaseous end products removing N from the biologically labile pool. Nitrogen is a key limiting nutrient in many lakes and reservoirs (Wetzel, 2001), which along with phosphorus that is typically released with ammonia, can stimulate phytoplankton growth causing additional organic loading to the sediments, which contributes to anaerobic conditions.

As lake conditions become more reductive, manganese oxide in the sediments will serve as an electron acceptor in a process releasing Mn^{2+} to the porewater and to the water column. Elevated Mn^{2+} in a source water can be problematic and costly for a water treatment plant to remove in the treatment process. High manganese concentration in the drinking water can stain laundry and fixtures at concentrations above 50 µg/L. Iron behaves similarly to manganese with solid phase hydrous oxides of iron reduced to Fe^{2+} followed by diffusion to the water column. Iron is easier to remove than manganese in a treatment plant due to faster oxidation kinetics. As conditions become more reductive, sulfate-reducing bacteria convert sulfate to sulfide where it can accumulate in the bottom waters. Hydrogen sulfide is highly toxic to aquatic biota and can render a lake undesirable as a water source (Beutel, 2008). Under highly reduced conditions methylmercury (methyl-Hg) can also be produced and accumulate in the lower water column. Methylmercury is extremely toxic and accumulates in aquatic biota as well as in humans (Watras et al., 1998). During prolonged periods of anoxic conditions organic materials will be reduced to organic acids and alcohols which are precursors to methane formation. These end products produce an immediate oxygen demand when released to an aerobic environment (Gordon and Higgins, 2007). The least energy favorable

biochemical process is methane formation (methanogenesis) where CO_2 and organic acids are used to form CH_4 gas, which can accumulate in the water column and then escape through the lake surface (Gordon and Higgins, 2007).

In order to quantify the severity of the reducing conditions in a lake, redox potential is widely used. Under well oxygenated aerobic conditions, the redox potential is between 400 and 600 mV. Nitrate reduction typically takes place between 200 to 500 mV. Mn reduction usually occurs between 200 to 400 mV, while Fe reduction typically takes place between 100 to 300 mV. At the lower end of the redox scale, sulfate reduction occurs between 0 to 150 mV. Bohm et al. (2001) provide a list of reduction reactions with the corresponding redox potentials shown in Table 2.

Table 2. List of reduction half reactions with the corresponding redox potential (Bohm et al., 2001).

Reaction	*Eh* at pH 7 (V)	Measured Redox Potential in Soils (V)
O_2 disappearance		
$\frac{1}{2}\,O_2 + 2e^- + 2H^+ = H_2O$	0.82	0.6 to 0.4
NO_3^- disappearance		
$NO_3^- + 2e^- + 2H^+ = NO_2^- + H_2O$	0.54	0.5 to 0.2
Mn^{2+} formation		
$MnO_2 + 2e^- + 4H^+ = Mn^{2+} + 2H_2O$	0.4	0.4 to 0.2
Fe^{2+} formation		
$FeOOH + e^- + 3H^+ = Fe^{2+} + 2H_2O$	0.17	0.3 to 0.1
HS^- formation		
$SO_4^- + 9H^+ + 6e^- = HS^- + 4H_2O$	−0.16	0 to −0.15
H_2 formation		
$H^+ + e^- = \frac{1}{2}H_2$	−0.41	−0.15 to −0.22
CH_4 formation (example of fermentation)		
$(CH_2O)_n = n/2\ CO_2 + n/2\ CH_4$	—	−0.15 to −0.22

Oxygenation of a lake's hypolimnion without disturbing the lake's stratification started in Europe in the 1950s and became an accepted technology in North America in the 1970s (Lorenzen and Fast, 1977). Hypolimnetic aeration was first practiced by Mercier and Perret in 1949 at Lake Bret in Switzerland. Mercier and Perret pumped hypolimnetic water into a shore side splash basin where oxygen was introduced by the atmosphere. The aerated water flowed back to the hypolimnion by gravity (Lorenzen and Fast, 1977). The design worked but suffered from short contact time and poor oxygen transfer to the water. Many different designs have emerged since then. The full lift air injection unit has become a popular design and its performance is well understood (Little, 1995). Ashley (1985) outlines an empirical design approach for this design. A typical unit is illustrated in Figure 3.

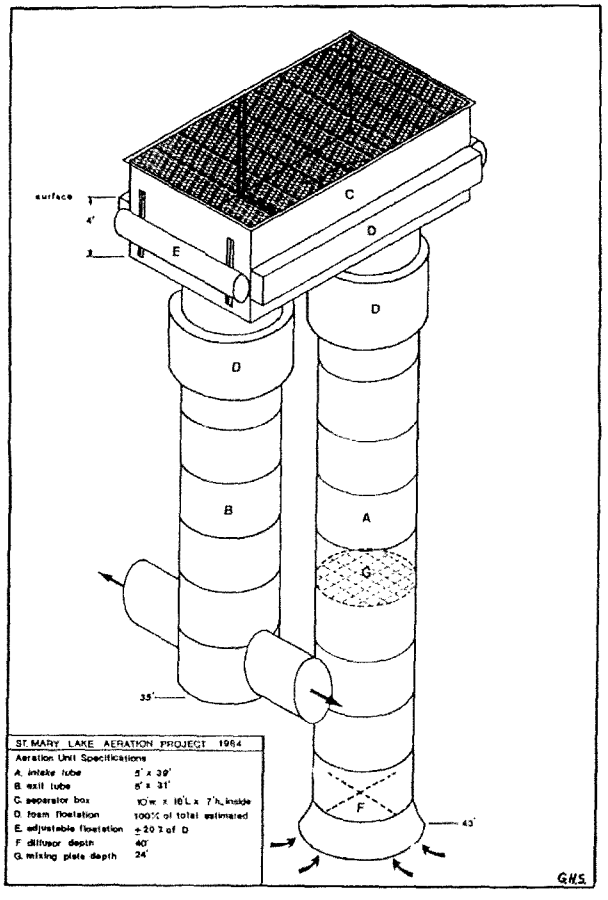

Figure 3. Schematic of a full lift hypolimnetic aerator designed by K. I. Ashley.

Ashley's hypolimnetic aerator design consists of an airlift tube, a gas liquid separation chamber, and a down-comer tube returning the oxygenated water back to the hypolimnion.

This hypolimnetic aerator design was first developed by Bernhardt in 1967 but has been modified many times since then. Full airlift and partial airlift hypolimnetic aerators were later developed to achieve oxygenation in the hypolimnion with higher gas transfer efficiency (Soltero et al., 1994). These designs were variations over the same

aeration principle and have proved to work well in many lakes if designed adequately to satisfy the oxygen demand (Ashley, 1983). It is not recommended to install hypolimnetic aerators in lakes shallower than 12 to 15 meters because erosion of the thermocline can occur (Lorenzen and Fast, 1977). Erosion of the thermocline can lead to adverse water quality such as elevated temperatures in the lower waters and proliferation of blue-green algae at the surface due to nutrient transport to the surface (Cooke et al., 1993). If hypolimnetic aeration is done correctly, it will reduce the iron and manganese levels by increasing oxygen at the sediment-water interface (SWI). By maintaining low concentrations of Fe and Mn in water, municipalities can save money by reducing chemical water treatment. The thermal structure will also be intact so that cold water fish habitats will be preserved.

Phosphorus plays a major role in biological metabolism. It enters a lake from atmospheric precipitation, surface runoff, and ground water (Cooke et al., 1993). Phosphorus is primarily found as inorganic P (orthophosphate) or bound in organic phosphates and cellular compounds in living or dead microorganisms and vegetation (Wetzel, 2001). Bound phosphorus can reach lake sediments with settling detritus and be later released back to the water column by metabolic activities of bacteria and fungi. Phosphorus release has been frequently observed to be inversely correlated with dissolved oxygen concentration at the sediment water interface (SWI) and is inhibited when the dissolved oxygen is above 1 mg/L (Gachter and Wehrli, 1998; Wetzel, 2001). Successfulness in phosphorus reduction varies between aeration projects depending on the system's ability to deliver oxygen concentration to the sediments. Phosphorus

retention is thought to occur if a hypolimnetic aeration system is sufficiently designed and operated (Cooke and Kennedy, 2001).

Empirical design guidelines have been developed for this technology based on hypolimnetic oxygen demand and aerator oxygen supply (Ashley 1985; Cooke et al., 1993). It has been found that the total oxygen demand increased as a result of lake aeration (Lorenzen and Fast, 1977). Soltero et al. 1994, explain this phenomenon as an increased bacteria community at the sediments and the additional inorganic oxygen demand such as iron and manganese oxidation. It was also suggested that hypolimnetic aeration may be re-suspending sediments, which could contribute to an increased oxygen demand. This increase in oxygen demand caused many early hypolimnetic aeration systems to be under designed (McQueen et al., 1984). Long term hypolimnetic aeration was expected to reduce the total oxygen demand of a lake by oxidation of accumulated organic and inorganic sediments (McQueen et al., 1984); however, this effect has not been documented in the literature. The oxygen transfer from hypolimnetic aerators and bubble plume aerators are now well understood (Singleton and Little, 2006; Bernard et al., 2000).

Another approach to improving the oxygen conditions in a stratified lake is artificial circulation. This method is based on the free bubble plume principle. Air bubbles are released directly into the water column by a diffuser network located near the sediments. The bubbles rise freely through the water column entraining water on their way. A buoyant plume develops and ascends towards the surface creating circulation and destratification within the lake. The gas transfer from the air bubbles only accounts for a small part of the overall oxygenation. Most of the oxygen that is transferred to the lake

comes from the atmosphere by transporting anoxic hypolimnetic water to the epilimnion (Lorenzen and Fast, 1977), (Cooke et al., 1993). Pure oxygen is also injected into the lake in a free bubble plume manner to improve the dissolved oxygen concentration. The oxygen transfer from the pure oxygen bubbles will be significant; however, these systems are not designed to weaken the thermal stratification of the water body. Typically, the O_2 gas flow is set so that the bubbles are not lost at the surface. In deep lakes, the bubbles will be completely dissolved within the hypolimnion, and therefore the thermal structure of the lake is maintained (Ganzer, 2007). Consequently, compressed air is used for artificial circulation. The recommended airflow is 9.2 $m^3/min{\cdot}km^2$ (Lorenzen and Fast, 1977) to maintain a destratified lake and to obtain an adequate dissolved oxygen concentration. Figure 4 shows percent destratification versus Flow rate in $m^3/min{\cdot}km^2$ with the critical airflow highlighted.

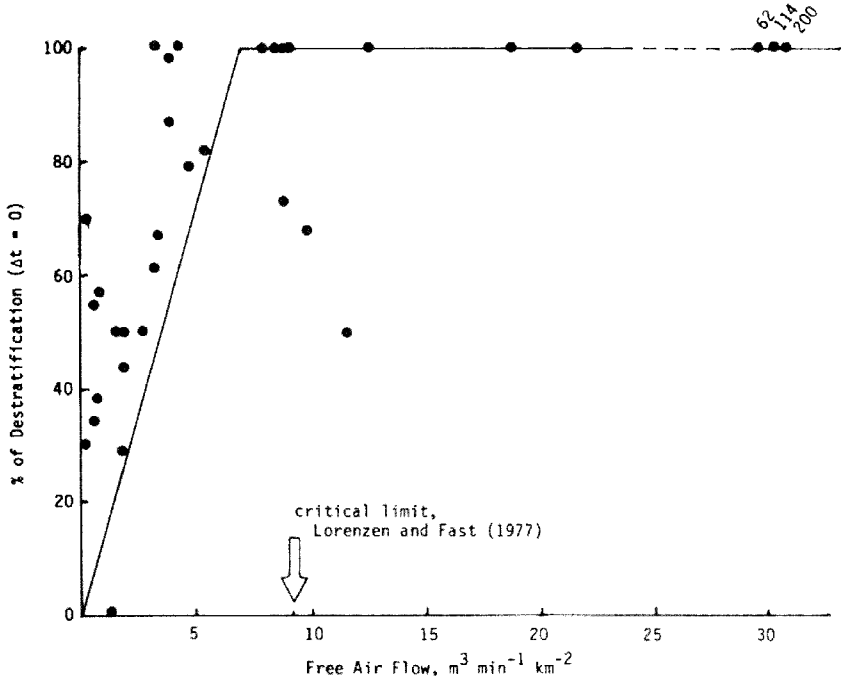

Figure 4. Various artificial circulation projects plotted based on % destratification versus air flow. Lorenzen and Fast's critical airflow limit is shown (Lorenzen and Fast, 1977).

The hypolimnetic temperature will rise dramatically during artificial circulation, and the epilimnetic temperature will normally drop slightly. The overall heat energy in the lake will increase during artificial stratification (Schladow and Fisher, 1995). The dramatic increase in bottom temperatures makes artificial circulation undesirable if maintaining a cold water fish habitat is a concern. The algae concentration will in most cases be reduced by forcing the algae out of their productive zone causing light starvation (Jungo et al., 2001; Cooke et al., 1993). Nutrient limited lakes have reported algae blooms as a consequence of artificial destratification. Algae blooms can occur when nutrients from the hypolimnion are introduced to the nutrient-limited epilimnion (Cooke

et al., 1993). Artificial circulation has a good record of increasing dissolved oxygen, reducing Fe and Mn, reducing ammonium, and improving the habitat for warm water fish species (Cooke et al., 1993).

Surface circulators, surface jet plume installations, and mechanical aeration devices have been explored as possible technologies to add oxygen to lakes but have proven to be limited in efficiency (Lorenzen and Fast, 1977). Their limitation becomes particularly apparent as the lake and its hypolimnetic volume becomes large. Literature is scarce, but Lorenzen and Fast (1977) described various mechanical mixers. A recent report from Myphonga, Reservoir, Australia described how two large-scale surface circulators were assisting an artificial destratification system (Lewis et al., 2001). The circulators' goal was to completely destratify the reservoir. Each surface circulator was operated with a downward flow through a 13 meter depth, 5 meter diameter tube. The flow rate was 3.5 m^3/s through each circulator. Myphonga was successfully destratified leading to improved dissolved oxygen concentrations, reduced metal concentration, and reduced algae and cyanobacteria. The two circulators were efficient, but most of the vertical mixing was done by the artificial destratification system (Lewis et al., 2001). Kirke and Gezawy (1997) showed that surface circulators can be an energy efficient method of circulating water from the surface to the hypolimnion as long as the circulation started before the stratification developed.

A new design of surface circulators has recently emerged on the market as a solution to alleviate eutrophication symptoms in ponds, lakes, and reservoirs. They were first designed to operate in shallow lakes or within the epilimnion but have lately been configured for hypolimnetic circulation. A general schematic is displayed in Figure 5.

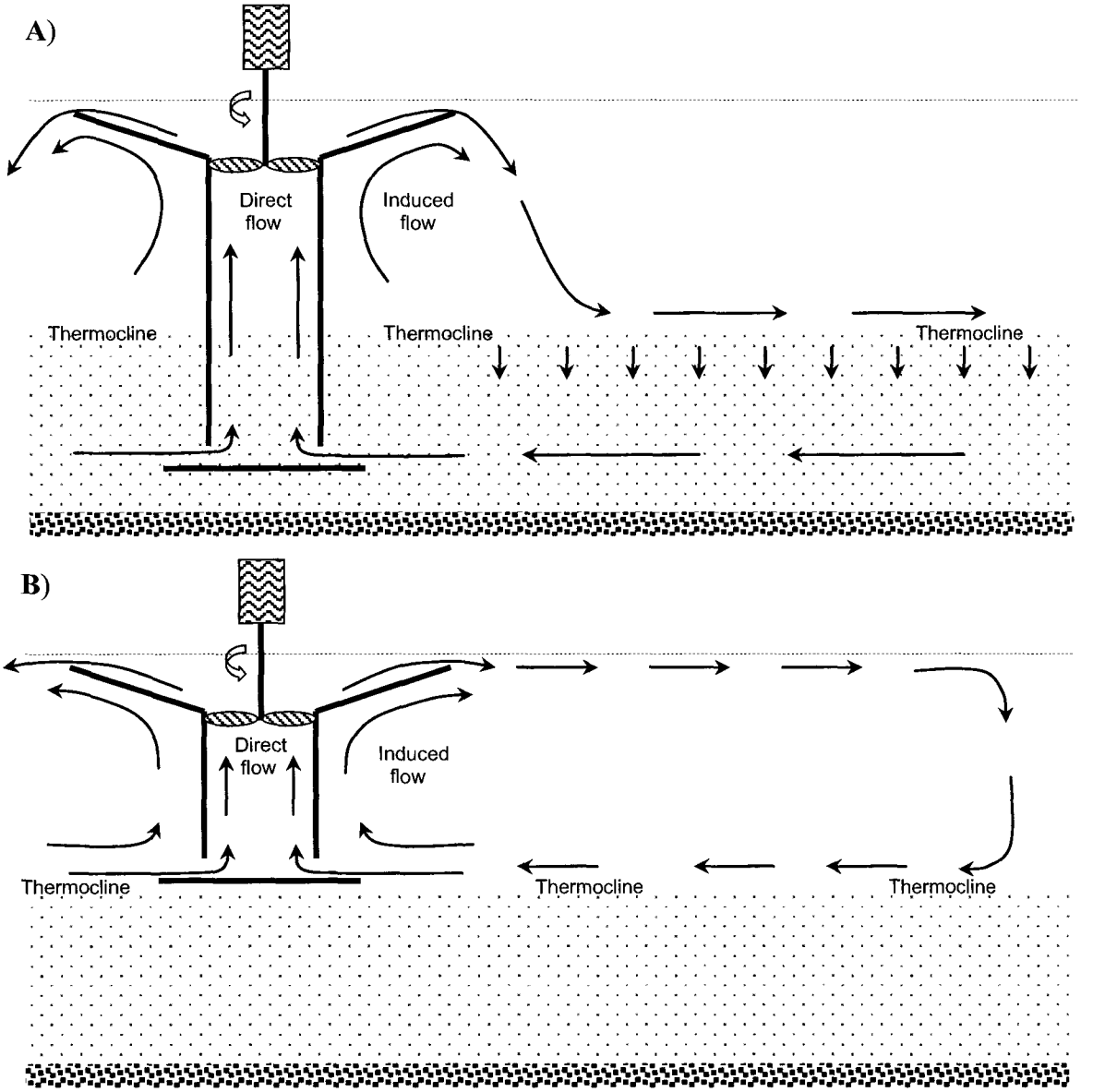

Figure 5. A) Schematic of possible flow pattern for hypolimnetic circulation. B) Schematic of possible flow pattern for epilimnetic circulation.

When the intake is set for epilimnetic circulation (Figure 5 b), hypolimnetic waters would be expected to show no direct influence of operation since water movement/mixing would be confined to the epilimnion. Cyanobacteria (blue-green algae)

that prefer a habitat at the surface many be negatively impacted by movement away from their optimal habitat. This potentially could shift the phytoplankton community to one creating fewer water quality problems. Literature reports that aeration systems have the effect of reducing blue-green algae concentration in lakes/reservoirs (Jungo et al., 2001); however, this has not yet been confirmed objectively for surface circulators. The City Of Houston installed and operated surface circulators with this intake configuration and reported a reduction in their powder activated carbon dosage based on a reduction of blue-green algae (Belhateche et. al., 2007). Recently, surface circulators configured as in Figure 5 a have been deployed in deep stratified lakes to increase the dissolved oxygen in the hypolimnion. There are currently no reliable reports of successful hypolimnetic oxygenation from these circulators. Cooke et al., (1993) describe how an insufficient aerator design could make water quality conditions worse. It is important to avoid an insufficient vertical mixing in an aeration system. This could lead to transport of hypolimnetic nutrients to the light rich and nutrient-limited epilimnion, without providing sufficient mixing at the surface to push the algae out of their preferred distance from the surface. An under-designed aeration system will likely set the stage for an algae bloom. Low flow rates appear to be the normal situation for the new solar powered surface circulators. They introduce hypolimnetic water to the epilimnion without completely destratifying the water column. Cooke et al., (1993) suggest that a complete destratification will dilute the nutrients to a level too low for algae blooms to occur. Also, the vertical mixing will inhibit the algae blooms.

1.3 Study Site

The study site for field monitoring and associated efforts to understand the operations and influence of operating surface circulators on lake/reservoir conditions was the Occoquan reservoir. The Occoquan Reservoir (38°41'40" N, 77°16'37" W) is located in northern Virginia about 50 km southwest of Washington D.C. Its watershed covers 1515 square kilometers including 616 ha of reservoir surface area. The Occoquan watershed is hydrologically divided into two sub-watersheds. The Occoquan River sub-watershed occupies the southern part of the watershed with Broad Run and Cedar Run as the major streams. The Bull Run sub-watershed covers the northern area of the Occoquan watershed with the principle stream being Bull Run. Occoquan watershed is illustrated in Figure 6.

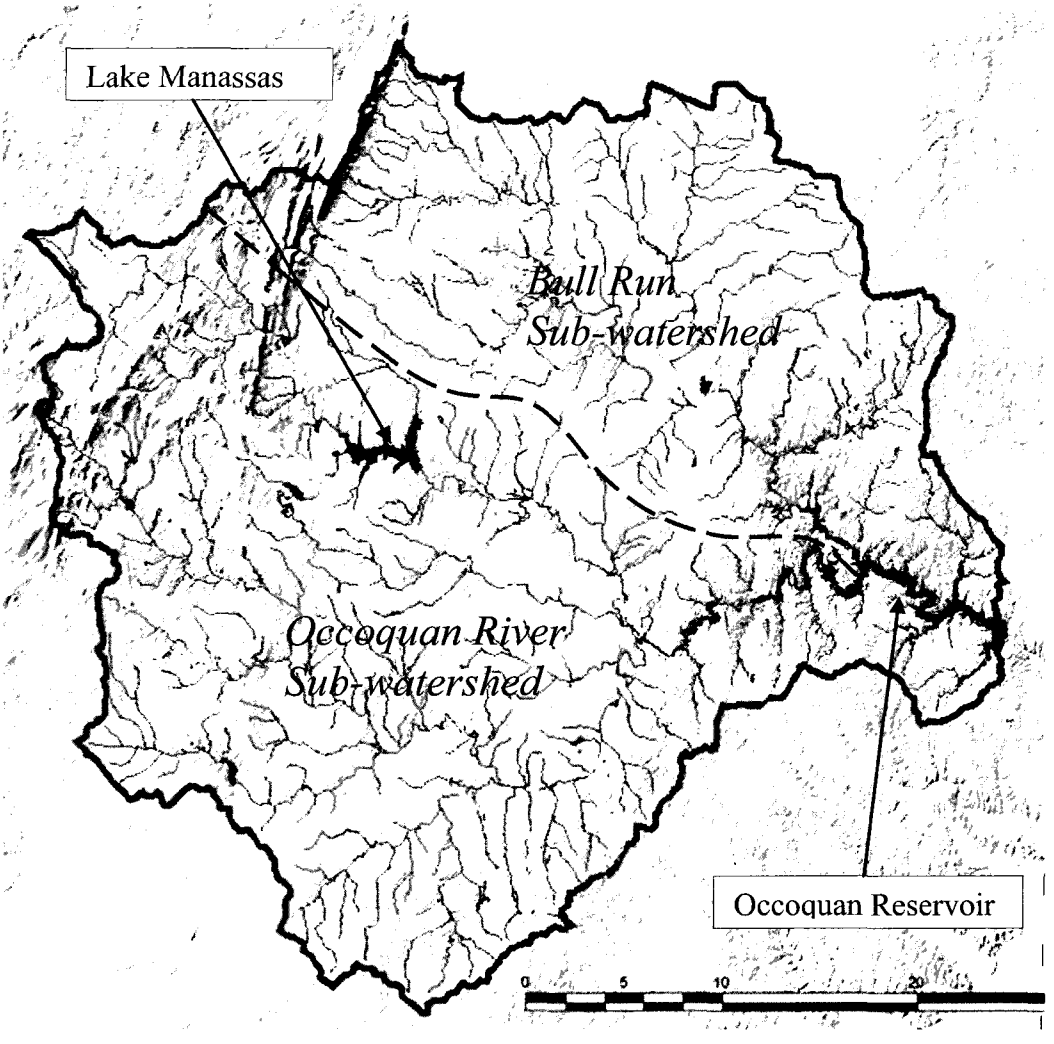

Figure 6. Occoquan watershed including sub-watersheds and large water bodies.

Occoquan Reservoir lies on the boundary between Fairfax county and Prince William county and serves as a major drinking water source for Fairfax Water, a water utility providing drinking water to 1.3 million residents in northern Virginia. It also serves as a major recreational site and is the location of active organizations such as Prince William Rowing Club. Fish species native to Occoquan Reservoir include

largemouth bass, bluegill, black and white crappie, channel catfish, flathead catfish, northern pike, and white perch.

Occoquan Reservoir was impounded by Fairfax County Water Authority in 1950 at its current location above the City of Occoquan. The current "tall dam" was built seven years later to increase the water supply and meet the demand of the fast growing region. In the 1960s the declining water quality in Occoquan Reservoir was attributed to development spreading through the watershed. In 1971, the Virginia Water Control Board and the Virginia Department of Health decided to create the Upper Occoquan Service Authority (UOSA). UOSA was tasked with providing state-of-the-art wastewater treatment for the Occoquan Watershed. Because the UOSA wastewater treatment plant discharges into Bull Run upstream of Occoquan Reservoir, Fairfax County Water Authority along with the Virginia Health Department established a particularly high treatment standard for UOSA. Today, UOSA's 42 MGD discharge is considered a valuable contribution to Occoquan Reservoir's safe yield. In 1973, Occoquan Watershed Monitoring Laboratory (OWML) was established as an independent entity that would continuously monitor the watershed's streams and Occoquan Reservoir. OWML was also tasked with providing guidance on protective measures of Occoquan Reservoir to Fairfax Water.

Occoquan Reservoir is the largest drinking water reservoir in northern Virginia with a surface area of 616 ha. The spillway crest is at 37.2 meter above msl, resulting in a 31.4 billion liter storage volume. Bull Run and Occoquan Creek are the two major contributors entering the reservoir 15 kilometers upstream of the dam. Occoquan Reservoir is moderately deep with an average depth of 5 meters and a maximum depth of

20 meters. The reservoir stratifies during early May and lasts to October. The reservoir is relatively narrow with a maximum width of 330 meters, which is not unusual for a run-of-the-river impoundment such as Occoquan Reservoir. The ratio of watershed drainage area to reservoir area is 194:1. This ratio is relatively high and is the reason for its short flushing rate (The average hydraulic residence time is 20 days) and combined with the narrow width makes the reservoir's condition riverine. The water quality is particularly influenced by severe storm events that bring elevated levels of TSS from the watershed. OWML has described the reservoir as having a plug flow behavior. During the stratified period the inflow is typically warm and overflows the hypolimnion so that the hydraulic residence time is shorter for the epilimnion than the hypolimnion. OWML has labeled the reservoir as nutrient enriched, and eutrophic symptoms are common such as algae and cyanobacteria blooms, elevated iron and manganese levels are common, particularly during the temperate season when there is no flow over the spillway. The fish habitat is also limited by the anoxic hypolimnion during the summer. Figure 8 illustrates the bathymetry with the lower basin enlarged to show the locations of the eight surface circulators deployed from summer 2006 through December 2007. Occoquan Reservoir's characteristics are listed in Table 2.

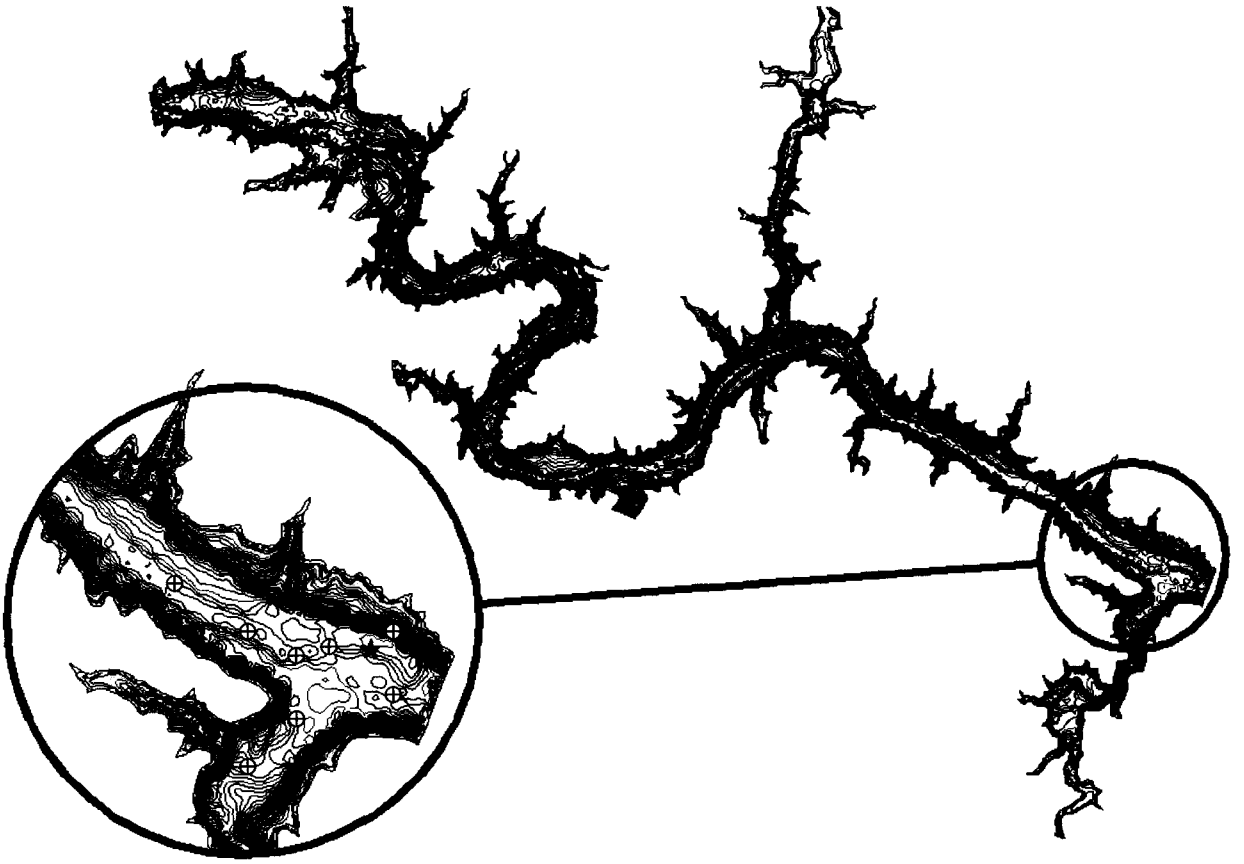

Figure 7. Bathymetry description of Occoquan Reservoir from Ryan's dam to the inlet. The lower basin is enlarged to show the layout of the circulators including the WB sampling site.

Table 3. Occoquan Reservoir characteristics.

Characteristics:	Value:
Reservoir volume	31.4 billion liters (8.3 billion gallons)
Surface area	6.16 km2 (616 ha)
Length	22.5 km (14 mi)
Mean depth	5.1 m (16.7 ft)
Maximum depth	20 m (65 ft)
Maximum width	275 m (900 ft)
Natural safe yield	250,000 m3/d (65 mgd)
Reclaimed water inflow	91,000 m3/d (24 mgd)
Average inflow	1,600 m3/d (422 mgd)
Dam height	37.2 m above sea level (122 ft)
Average residence time	19.6 days

During the late 1960s poor water quality during the summer and early fall was a yearly occurrence. Searching for a solution to this problem, Fairfax County Water Authority examined the benefits of an artificial destratification system. A bubble plume aeration system was installed in 1970 and operated annually from April through October until 2006. Water quality improved dramatically after the bubble plume aeration system was installed with higher dissolved oxygen concentrations recorded much deeper into the water column, elimination of hydrogen sulfide, reduced iron and manganese concentration, and elimination of algae blooms (Eunpu, 1973).

Occoquan Reservoir's spillway is located at an elevation of 37.2 meters above sea level. Fairfax Water has a withdrawal from 35 to 38 MGD through their intake structure at the dam and normally an excess hydraulic inflow to the reservoir during the winter period causing water to spill over the spillway. The surface elevation normally stays within one meter of the crest throughout the summer; however, 2007 was a particularly dry year, and the surface elevation was as low as 3.5 meters below the crest during the late summer of 2007. This can be seen when OWML's surface elevations are plotted from 2000 to 2008 (Figure 8).

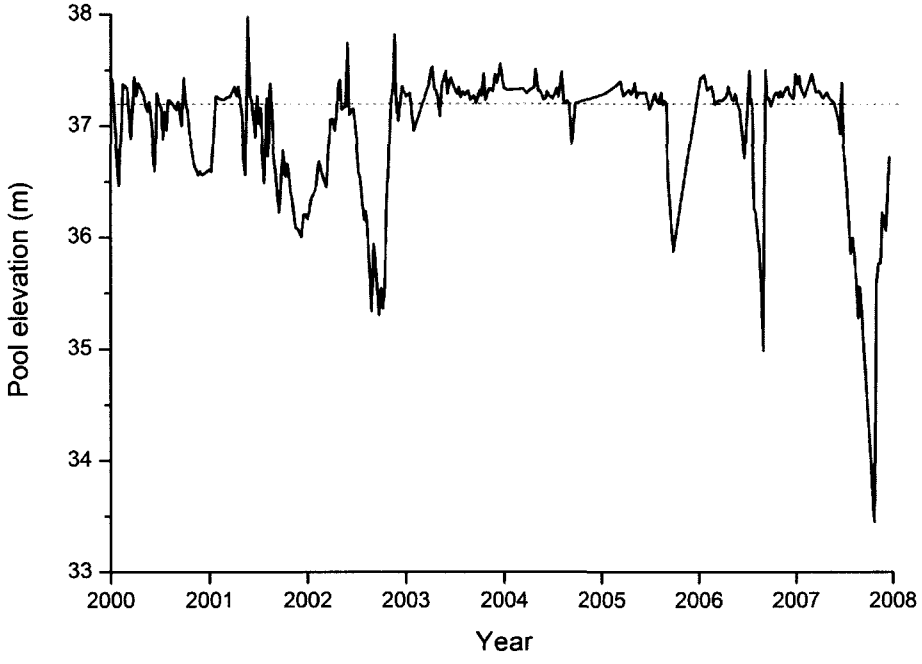

Figure 8. Surface elevation of Occoquan Reservoir from 2000 through 2007.

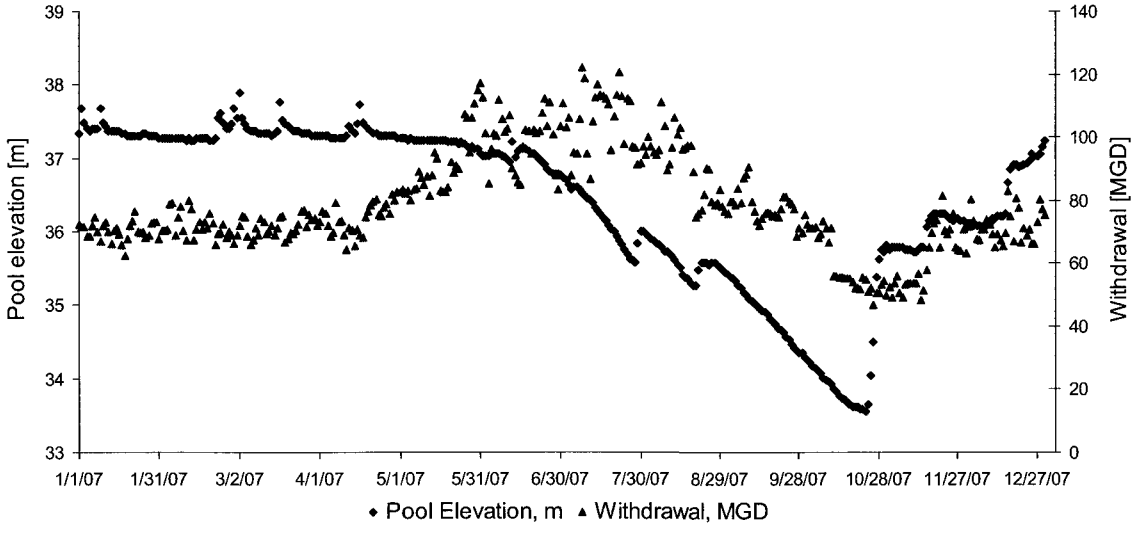

Figure 9. Surface elevation of Occoquan Reservoir for 2007 including Fairfax Water's daily withdrawal.

Daily pool elevations for 2007 and the daily withdrawal to the treatment plant are displayed in Figure 9 and will be used in Chapter 4 for the modeling effort.

1.4 Research Goals

The study reported here focused on investigating the influence of surface circulator operation on the thermal structure and dissolved oxygen concentration of a moderately- deep, stratified lake. It has been reported that surface circulators are controlling algae and cyanobacteria successfully when they are set up for epilimnetic circulation (Belhateche et. al., 2007). Less information is available for systems operating to improve dissolved oxygen conditions. The focus for this work was to determine to what extent surface circulators operating in "deep-draft" circulation mode could improve dissolved oxygen concentrations and affect water column stability and stratification.

1.5 Objectives and Scope of Research

The overall objective for this research was to investigate the influence that operation of surface circulators has on water column stability and dissolved oxygen concentration. Four objectives were set:

Objective 1: Investigate through a field monitoring program the effect that operation of eight surface circulators in the Occoquan Reservoir had on dissolved oxygen and temperature.

Objective 2: Utilize a water quality model to simulate conditions in Occoquan Reservoir focusing on dissolved oxygen and temperature.

Objective 3: Investigate through the simulation of hypothetical lakes of different sizes how circulators operating at different total flow rates and for draft tubes set at different depths influence the temperature and dissolved oxygen distribution of stratified lakes.

Objective 4: Summarize findings from the hypothetical simulations and make recommendations for surface circulator deployment.

CHAPTER II

INFLUENCE OF SURFACE CIRCULATOR OPERATION ON THERMAL STRATIFICATION IN OCCOQUAN RESERVOIR

2.1 Introduction

Temperature's influence on water's specific gravity is fundamental to a lake's movement and behavior (Imboden, 2007). Occoquan Reservoir is a warm monomictic lake that does not usually develop ice during winter. During this period, there is no thermal stratification, so external forces (such as wind) keep the water column well mixed. Thermal stratification typically develops in early May, as can be seen later in this Chapter. The thermal stratification greatly affects the vertical transport (Wetzel, 2001), which is reflected in the smaller vertical turbulent diffusion coefficient. Comparatively, a general horizontal turbulent diffusion coefficient in a stratified lake is from 0.1 m^2/s, and a general vertical turbulent diffusion coefficient is only from $5*10^{-4}$ m^2/s (Csanady, 1973).

A hypolimnetic surface circulator will theoretically affect the transport and mixing dynamics in a lake/reservoir, as initial mixing will occur with the ambient surface water, as cold hypolimnetic water is discharged at the surface. The water mixture will then descend to a depth of equal density (McGinnis et al., 2004), and move away from the circulator as new hypolimnetic water is discharged by the circulator. The circulator operation will cause some water strata to move while other strata are not. Shear forces between these strata will create mixing by eddy diffusion (Mortimer, 1974). According to hydrodynamic theory, there should be little impact on the water column much below

the depth of equal density, other than the effect of drawing down the thermocline by removing hypolimnetic water volume through the circulator intake.

2.2 Aeration History - Temperature

Because Occoquan watershed experienced a growth from rural to suburban development, nutrient loading increased and caused water quality conditions in Occoquan Reservoir to deteriorate. A free bubble plume aeration system was installed in 1970 to improve water quality conditions and was operated through 2006. The aeration system initially consisted of seven 500-foot sections of perforated air supply tubing and 25,000 feet of weighted feeder tubing. Compressed air was provided by three rotary oil-free compressors located at the base of the dam delivering a total of 225 cfm at 50 psi. Diffuser hoses were laid so that the bubbles were evenly distributed out at the bottom of Occoquan Reservoir's lower basin from the dam extending 2,000 feet upstream (Eunpu, 1973). Both the compressors and the diffuser system were modified and improved after the initial installation. A layout of the current diffuser grid is shown in Figure 10.

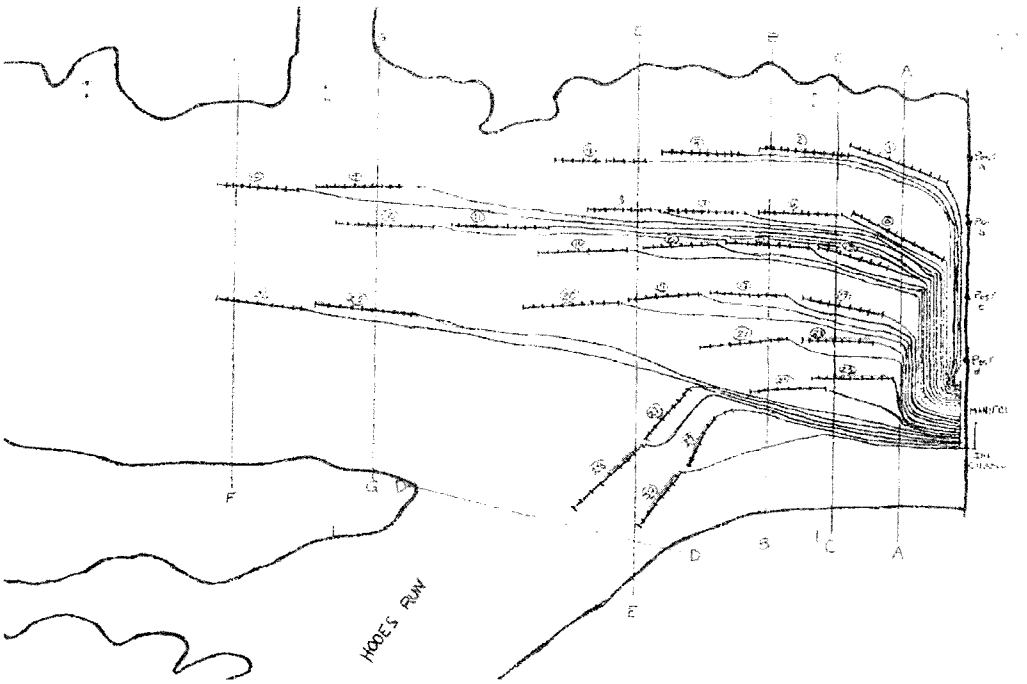

Figure 10. Plan view of diffuser hose and air feeder tubing layout in Occoquan Reservoir. The diffuser hoses are colored red.

Little data are currently available from before the installation of the aeration system in 1970. The only source discovered in this effort was from the 1973 paper by Eunpu, where a table of monthly vertical temperature profiles from 1969 was displayed. These "pre –aeration" temperature data were compared with OWML's "post-aeration" temperature profiles from 1973; both data sets were recorded close to the dam. July and August profiles from both years were plotted together for comparison (Figure 11).

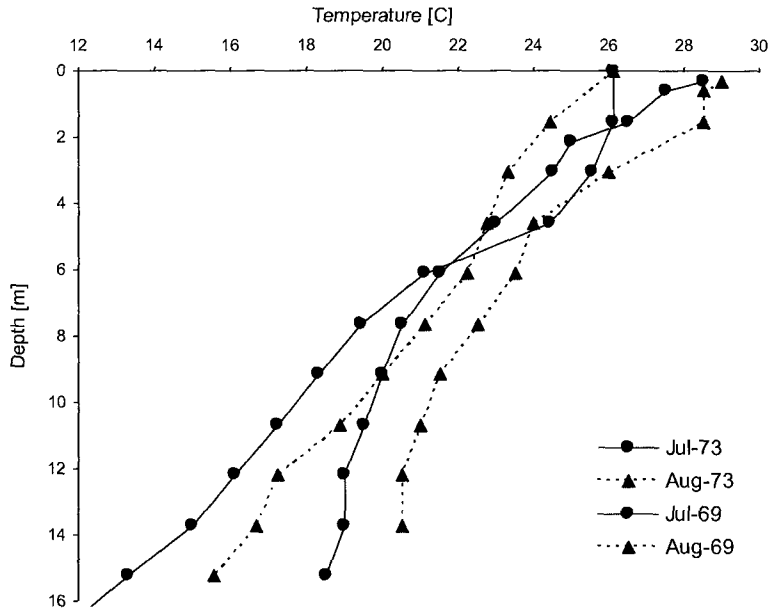

Figure 11. Temperature profiles from pre-aeration conditions (1969) and post-aeration conditions (1973).

As the fine bubbles are released at the bottom of the reservoir, they begin to rise towards the surface due to their buoyancy. Water and bubbles create an upward moving plume referred to as a bubble plume or a bubble curtain if the diffuser is configured as a line. A bubble plume will entrain and detrain water as bubbles rise through the water column creating increased vertical mixing and weakening or preventing a reservoir's thermal stratification (McGinnis et al., 2004). Because of this enhanced mixing the hypolimnion can exhibit an increase in temperature, and the epilimnion can become colder through the mixing process (Schladow, 1995). Hypolimnetic temperatures in the Occoquan Reservoir were higher in July and August in 1973 consistent with the operation of the aeration system; however, the epilimnion appears to be warmer during the aeration period as well. Another observation is that the hypolimnetic temperature

increased 2 to 3 °C between the July and August recordings. The hypolimnetic temperature increased as a response to the artificial aeration in response to the vertical mixing.

Fairfax Water experienced extensive failure of their diffuser grid during June 2006. This failure forced them to shut down the operation of the aeration system. A new solution for maintaining sufficient water quality in the reservoir was introduced in August 2006. Eight surface circulators manufactured by Solar Bee (Model SB 10000v12) were deployed within the lower part of the reservoir. Their layout is illustrated in Figure 7. These surface circulators were powered by solar panels and fitted with batteries storing enough energy to run the circulators through the night. Their intake depths were all set to 10 meters below the water surface, which was one meter below Fairfax Water's main raw water intake to the water treatment plant. Surface circulators are building on a different working principle to achieve increased dissolved oxygen in the reservoir than the aeration approach. According to information from meetings between Fairfax Water and Solar Bee, the goal for the eight circulators was to increase the oxygen levels to 10 meters. This would create an oxygen boundary at this depth that would oxygenate dissolved manganese in the water column, reducing the manganese concentration in the water withdrawn to the treatment plant at a depth of 8.3 meters.

2.3 Methods and Analysis

2.3.1 Water Quality Data

The main objective for this research was to investigate the influence of circulator operation on the temperature and dissolved oxygen concentrations in a water supply

reservoir. There was a substantial amount of historic water quality information available for Occoquan Reservoir due to the establishment of OWML in 1973, and these data represented multiple depths and sites beginning in 1973 and continuing through 2007. Some parameters were only analyzed at the surface and near the bottom of the reservoir while more complete vertical profiles were recorded for other parameters including temperature and dissolved oxygen.

2.3.2 Monitoring buoys

Access was also provided to data collected by Fairfax Water's two monitoring buoys. The buoys were model Environmental Monitoring Module 550s with YSI 6820 multiparameter sondes mounted with fixed sensors at one meter below the surface with an internal data logger. Both monitoring buoys recorded water temperature, conductivity, dissolved oxygen, pH, turbidity, and chlorophyll-a every 30 minutes. The main monitoring buoy located by the dam at site WB also had weather monitoring instrumentation attached providing air temperature, relative humidity, wind speed, wind direction, solar radiation, and PAR (Figure 12). This buoy was launched in March 2005 and data were through August 2007 for this effort.

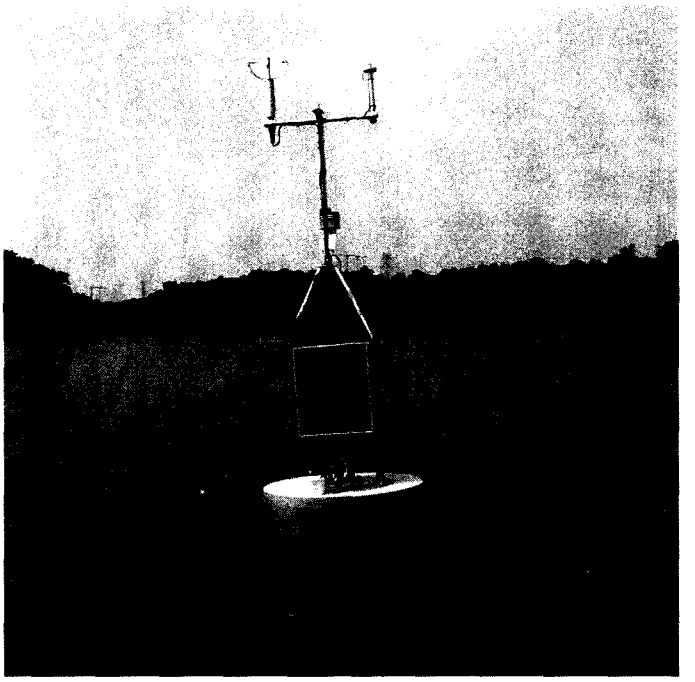

Figure 12. Fairfax Water's monitoring buoy with weather monitoring instruments.

The data from the buoys generally appeared to be of good quality; however, the wind data from the anemometer had periodic irregularities as the wind speed occasionally froze at unrealistically high values. The turbidity sensor periodically showed signs of fouling despite Fairfax Water's regular cleaning. Dissolved oxygen and chlorophyll-a values spiked on occasion and exhibited occasional drifts that are believed to be related to fouling of the sensors. Data sonde-collected data for July 2007 are displayed in Figure 13 and illustrate diurnal fluctuations in temperature, dissolved oxygen, and chlorophyll-a (as a measure of algae). Fluctuations in algal concentrations were not reflected in turbidity measurements suggesting that other forms of particulate material in the water column contribute significantly to turbidity.

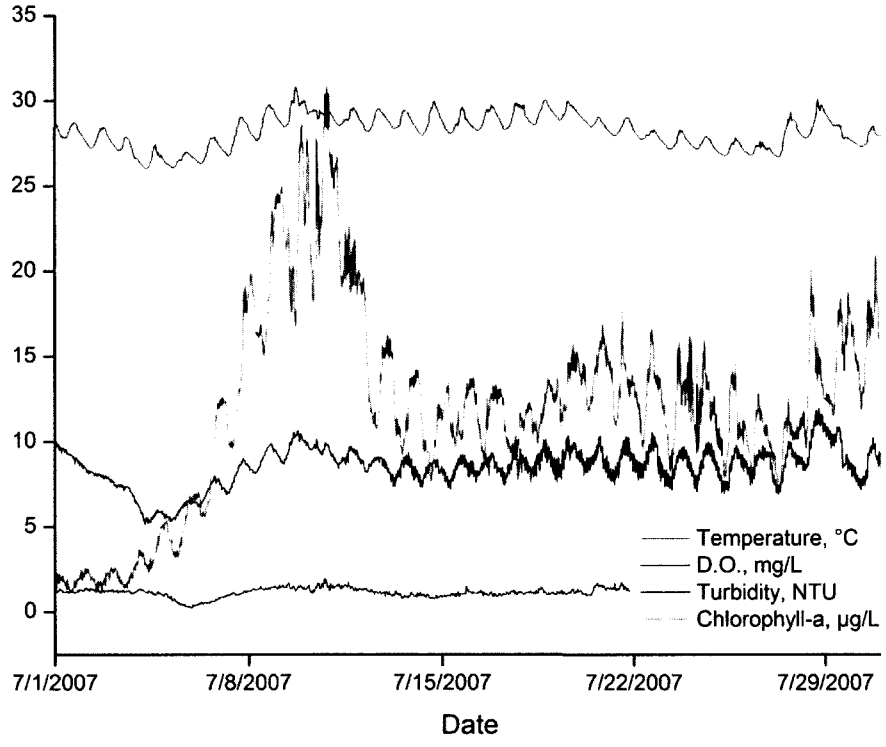

Figure 13. Example of water quality data from July 2007 at the WB buoy (depth of 1 meter).

2.3.3 Occoquan Reservoir and Sample Site

A bathymetry survey was conducted on Occoquan Reservoir in 2005 by OWML, and an AutoCAD file with this information was used to characterize bathymetric details of the reservoir. Because the wind sensor on the monitoring buoy experienced sporadic periods of spurious values, weather data for Dulles International Airport were downloaded from NOAA's web site provided by the U.S. National Weather Service for the 2007 season.

Water quality monitoring of Occoquan Reservoir started April 8, 2007, and three sample sites were monitored regularly until October 18, 2007 (Figure 14). The primary sampling site is designated "weather buoy" (WB) due to the proximity of the sampling

location to Fairfax Water's weather (and water quality monitoring) buoy. It was located centrally among the circulators and above the deepest part of the reservoir. The second sample site was approximately two kilometers upstream on the other side of a straight stretch of the reservoir that was marked with buoys for a rowing course. This site was designated northwest (NW) due to its location relative to the primary sampling site. On the third sampling trip an additional sampling site was added about four kilometers upstream of the NW site. Fairfax Water has a second buoy at this location; hence, the site was named WB2. OWML also monitors Occoquan Reservoir and has long-term water quality monitoring sites (RE02 and RE10) observed to be in close proximity to WB and WB2, respectfully.

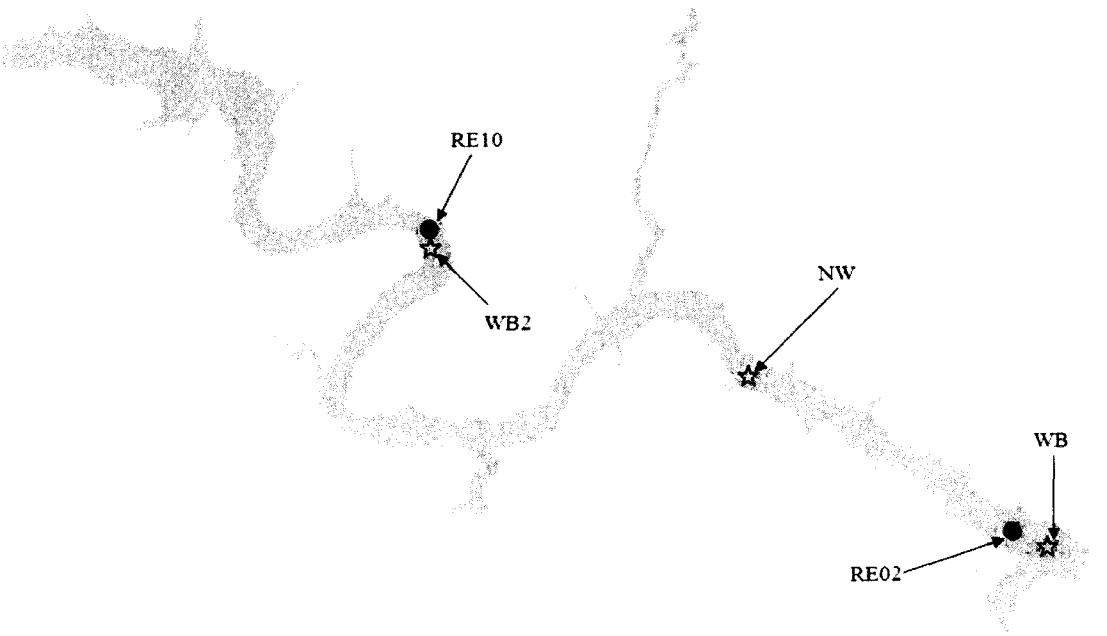

Figure 14. Sampling locations from this study (WB,NW,WB2) and monitored by OWML (RE02,RE10).

2.3.4 Water Quality Data Collection and Vertical Profiling

An 18-foot open boat with a 30 Hp outboard engine was used for the sampling effort. The sampling procedure started by recording the secchi depth at each sample site by lowering a secchi disk into the water on the shady side of the boat until it disappeared from sight. It was then raised slowly until it became visible again and lowered and raised a second time to confirm the reading. The depth for each raising/lowering was recorded to the nearest 0.1 meter.

Vertical profiles of temperature, dissolved oxygen, pH, conductivity, chlorophyll-a, and cyanobacteria were measured with a Hydrolab DS5 multifunctional probe from April through October. Calibration procedures for the individual sensors are described in the instrument calibration chapter. Data were transferred to a laptop via a 30 meter cable using the Hydras 3 LT v.2.02 software from OTT. During the first sample trip the Hydrolab was held at 0.5 meter increments through the water column until the readings stabilized, then the recording was triggered manually. This method was subsequently changed to improve depth resolution by setting data recordings to every second while the instrument was lowered slowly through the water column. It took approximately 10 to 15 minutes to lower the Hydrolab through the water column to allow sensor stabilization at each depth. A typical profile is illustrated in Figure 15.

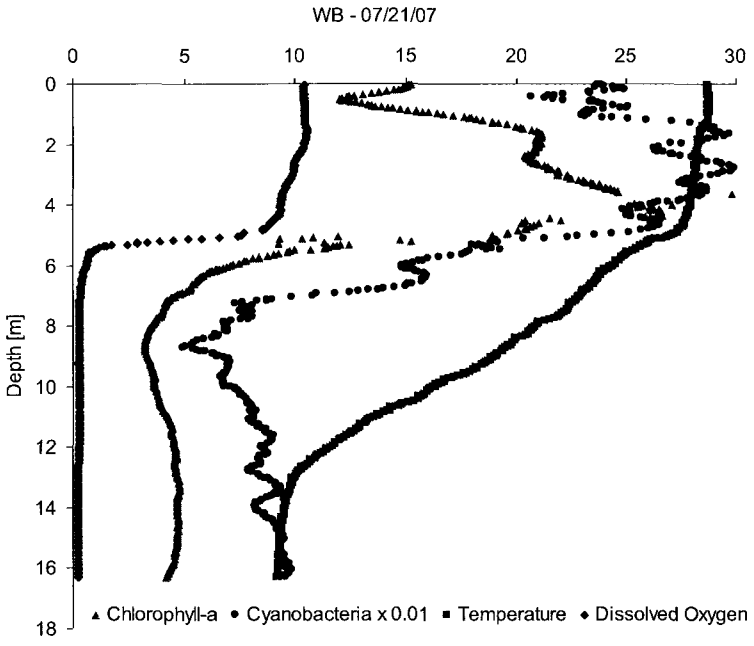

Figure 15. A multi-parameter profile recorded at WB on 7/21/2007.

2.3.5 Collection of Water Samples and Analytical Procedure

Water samples were collected during nine sample trips in period from 31 May 2007 to 13 August 2007. Samples were collected at all three sample sites (WB, NW, and WB2) in two-meter increments from the surface using a peristaltic pump and HDPE sample tubing. Sample containers were 500-mL polycarbonate bottles that were acid washed and DI rinsed. Samples were kept in an ice cooler until analytical work was completed the following day. The samples were analyzed for various water quality parameters in ODU's water quality laboratory and included turbidity, total nitrogen, fluoride, chloride, nitrate, and sulfate readings. A prime reason for collecting water samples was to analyze manganese concentrations that developed through the stratified season. Manganese was analyzed using an atomic absorption spectrophotometer (Perkin

Elmer) by flame atomic absorption using a five point calibration curve. Water samples were also analyzed for total nitrogen using a Shimadzu carbon analyzer (TOC-Vcsn) with a total nitrogen module (TNM-1) attached. Turbidity was recorded using a HACH 2100AN turbidimeter and anions were measured with a Dionex DX-500 ion chromatograph with an IonPac AS11 analytical column. In addition to monitoring the three sample sites, several special monitoring efforts took place during the summer of 2007.

2.3.6 Transects at the Lower Reservoir

Three transects were conducted from NW to WB in June using the Hydrolab DS5. These transects consisted of a series of vertical profiles recorded 200 meters apart. The location for each profiling site was located by a Garmin GPS. Each vertical profile was collected by setting the Hydrolab to record values every second and lowering it slowly through the water column. Post-processing was conducted in MS Excel, and isopleths of temperature and dissolved oxygen were assembled using the software OriginPro v.8.

2.3.7 Circulation Discharge Water Monitoring

The composition of water discharged at the surface by the circulators was measured on a regular basis using a Hydrolab DS5. The purpose of these measurements was to examine the composition of the circulation water released at the surface relative to the composition of water at the intake elevation. These measurements were always conducted on circulator 3 (designated the main circulator) which was closest to the dam and 100 meters from the WB sampling site. The Hydrolab probe was submerged in the

water overflowing the distribution pan taking care to avoid the probe contacting the circulator's impeller. The Hydrolab was set to record data every second and was kept motionless for three minutes. Data from the first minute was deleted and data collected over the next two minutes was used to calculate the average value for each parameter and then recorded.

2.3.8 Circulator Near-field Temperature Measurements

The near-field flow pattern around the circulators was of great interest and was studied by using several instruments. The main instrument used to measure the near-field water quality parameters was the Hydrolab DS5. Because the circulators were moored by a single chain and had the freedom to move within the length of their chain, the position was fixed for circulator 3 by deploying two anchors with tight anchor lines in a triangular pattern with tight anchor lines. A 2x4 wood post was then bridged from the top of the circulator to a flotation device five meters from the circulator. Attachments for a pulley were distributed along the 2x4 to support the Hydrolab while the boat was kept at 5 to 6 meter distance from the circulator during measurements. The position of the boat away from the circulator was important to avoid the boat influencing the flow in the vicinity of the circulator. Vertical profiles were collected every 0.25 meters (laterally) during the first meter and 0.5 meter intervals (laterally) for the next four meters. The data were post processed in Excel and plotted using OriginPro v.8.

Two efforts were conducted expanding the near field measurements at circulator 3. During the first effort, Hydrolab profiles were recorded at 20-meter increments from the circulator to a distance of 100 meters. The second effort was conducted by spacing

the Hydrolab profiles at10 meter increments out to a distance of 50 meters. The post-processing and plotting were similar to the previously described transects.

2.3.9 Circulator Near-field Flow Measurements

Understanding the flow and fate of the hypolimnetic water after it leaves the circulator is a crucial part of understanding the mechanism(s) that affect the temperature and dissolve oxygen in the lake. To better understand the movement of water exiting the circulators, the velocity field around circulator 3 was measured using an acoustic doppler velocimeter (ADV). The instrument was a Vectrino (Nortek) outfitted with a field probe (Figure 18). The Vectrino is a high resolution acoustic velocimeter that measures water velocity in three dimensions (x, y, and z velocities). The Vectrino's coordinate system is oriented after a marked "finger" on the probe that indicates the positive x-axis. The y-axis is 90 degrees to the left when the x-axis is pointing upward and the probe is facing toward the user. The z-axis is then pointing in the same direction as the probe. The Vectrino provides x, y, and z velocities according to its own orientation, so the instrument must be held in an exact position and orientation.

To maintain the Vectrino's position and orientation in the circulator's near-field, a PVC apparatus was constructed to hold the instrument in place. This apparatus had a T-shape that the Vectrino was attached to by tie raps and pole sections that could be attached to lengthen the reach. The pole attachments were marked with an orientation line which had to be pointing towards the center of the circulator and depth markings so that the Vectrino could be held in 0.5 meter increments. The apparatus and the attachment system can be seen in Figures 16 and 17. The Vectrino instrument was

operated from a laptop with Vectrino Plus software. The sampling rate was adjusted down from 200Hz to 50Hz, and each recording was set to terminate after 2000 samplings. The z-velocities were always close to zero, indicating that the flow was moving parallel to the instrument's x-y plane. The post-processing was intensive before a vector-field plot could be made in OriginPro. Each recording (a series of 2000 x, y, and z velocities) was marked with its depth and distance from the circulator, then exported from ASCII format to Excel. The x- and y-velocities were then averaged to a final velocity. The raw data ranged from zero to 0.14 m s^{-1} with a variability of $\pm$0.01m s^{-1}. In order to generate a vector plot in OriginPro, the x-and y-velocities had to be transferred to a velocity and angle format. The velocity vector field was finally overlaid on plots of the temperature and dissolved oxygen concentrations to help evaluate the influence of circulation on water column conditions in the near field.

2.3.10 Circulator Flow Rate Measurements

The Vectrino was also used to measure the flow rate of water passing through each circulator. This was accomplished by measuring the velocity of the water flowing over the outer edge of the circulator distribution pan and multiplying the water velocity by the area at the outer pan edge through which the water flowed. To hold the Vectrino motionless at the edge of the distribution pan, a PVC rig was made to support the Vectrino while it was recording the water velocities (Figure 18 b). The Vectrino's x-axis was oriented so that it was pointing directly away from the center of the circulator and 2000 measurements were collected at 50 Hz; only the x-velocity values were used from these recordings. The velocities were measured 3 to 4 cm below the surface. It was

important to measure all three sectors of the distribution pan, as the surface currents on the reservoir induced by wind forces could influence the discharged flow to be distributed unevenly around the pan. The pan could also be out of alignment so that one side was at a lower elevation than the other side, causing an uneven flow distribution. Due to these factors, the velocities were measured at the midpoint between the floats and then averaged to compensate uneven flow. Based on the average flow over the pan and the area it flowed through, the total flow through the circulator was calculated.

The flow profile over the distribution pan was also measured by the ADV. The elevation of the Vectrino was adjusted so that its sampling volume was located just under the surface, as the velocity was recorded. The Vectrino was then incrementally moved by 1 cm as recordings were made. One assumption of this method is that the velocity measured at 2 inches outside the distribution pan is the same as at the distribution pan.

Data Logging thermistors by Onset were used to investigate the temperature near-field around circulator 3. Twelve thermistors attached at 0.5 meter increments to a line (i.e. a thermistor chain) with a weight tied to the end were attached to the 2x4 used for the previously discussed near-field studies. The line was left undisturbed for 30 minutes, recording temperature measurements at 10-second intervals, before it was quickly switched to the next position 0.5 meter further out on the 2x4 arm. This procedure was done until temperature profiles were out to five meters from the circulator. The thermistors were then stopped and downloaded to a laptop and subsequently post processed using Excel. Data points recorded within five minutes of the start and the ending of each 30 minute recording interval were deleted, and the temperature was

averaged over the remaining 20 minutes of data. The temperature data ranged from 15.01 °C to 27.42 °C with a standard deviation of 0.09 °C.

The data logging thermistors were also used to record the temperature of water flowing over the circulator distribution pans of all circulators during the period. This study was conducted to discern any variations in temperature that could indicate variations in circulator operation. Since water being drawn up and discharged over the distribution pan from 10-meters depth during the period studied would be substantially colder than the surface waters, variations in temperature could be used to assess variations in circulator operation and mixing with lake water at the point of discharge.

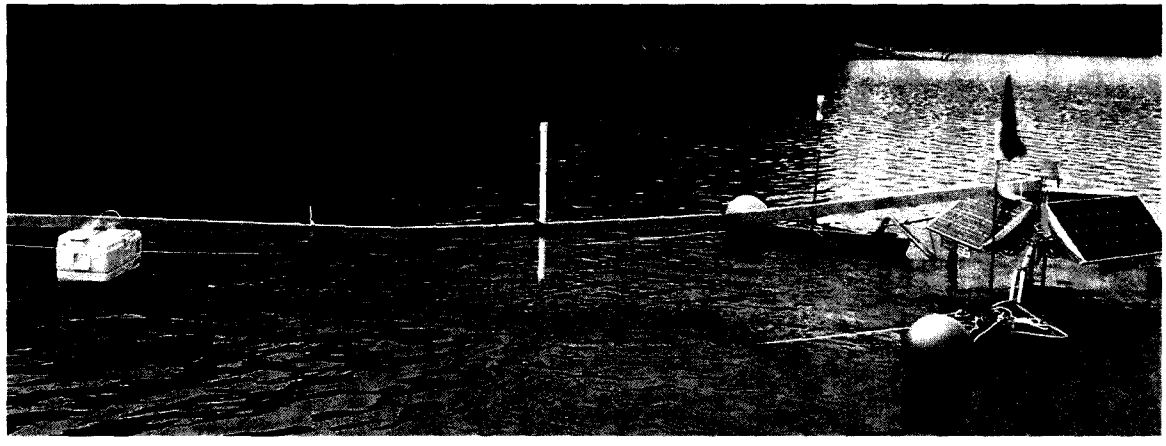

Figure 16. Support arrangement for near-field data study.

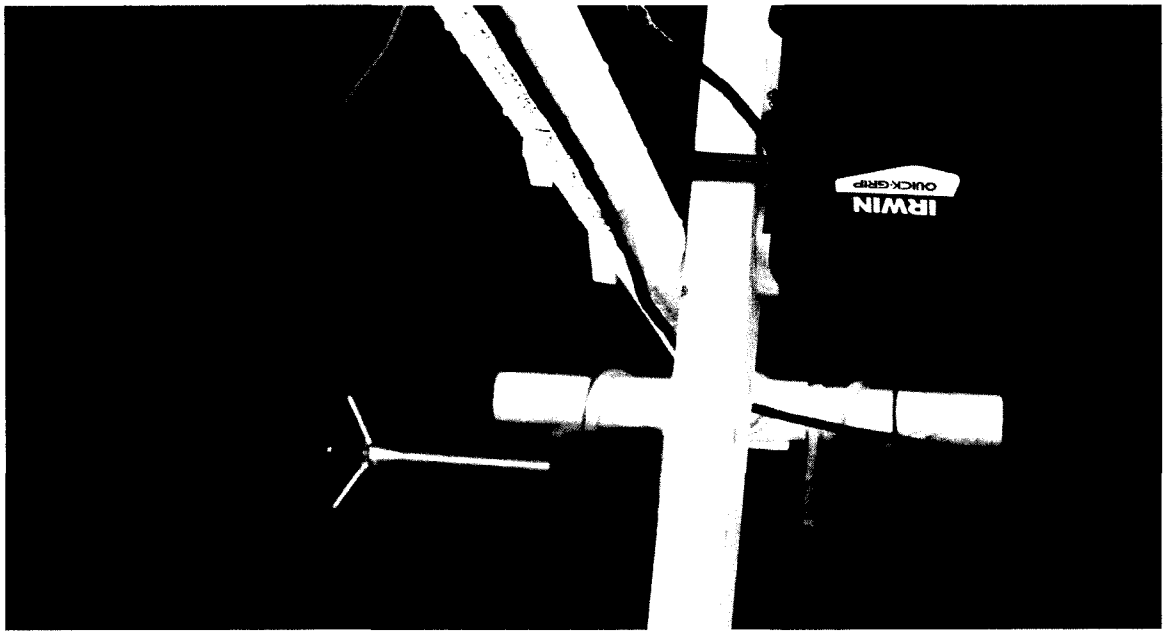

Figure 17. Attachment system for the Vectrino during the near-field velocity measurement.

Figure 18 A) Vectrino field probe with x-axis marking. B) Vectrino and attachment rig for flow velocities.

2.3.11 Change in Heat Content Calculation

The volume to depth relationship was developed for the lower section of Occoquan Reservoir. This relationship was based on a survey conducted by OWML in 2005. A bathymetry file was imported into AutoCAD, and accurate surface areas were calculated at intervals of two feet. The derived volume to depth relationship was then used to calculate the change in heat content in this part of the reservoir through the warm season during an aeration year (2005) and during the circulation year (2007).

The seasonal change in heat content was calculated for the epilimnion (down to 5 meters) and for the hypolimnion (below 5 meters) based on monthly temperature profiles recorded at WB or RE02. Each temperature profile was divided into depth intervals. These temperatures were multiplied by the volume associated with each depth interval and then multiplied by the specific heat constant for water (4.186 Joule/Δ °C* mL).

2.3.12 Activity Schedule

Some sampling activities were conducted on every trip on the reservoir, and other activities were only conducted on specific dates. Table 4 shows an overview of activities that were conducted on specific dates.

Table 4. Sampling activity overview.

Sampling activity:	4/8/2007	5/4/2007	5/18/2007	5/31/2007	6/14/2007	6/21/2007	6/28/2007	6/29/2007	6/30/2007	7/7/2007	7/14/2007	7/18/2007	7/21/2007	7/22/2007	7/23/2007	7/24/2007	7/25/2007	7/29/2007	7/30/2007	7/31/2007	8/13/2007	8/27/2007	9/5/2007	9/20/2007	9/30/2007	########
Secchi depth - all sites	X*	X	X	X	X	X	X*	X	X	X	X	X*	X				X		X		X	X*	X	X	X	X
HydroLab profile - all sites	X*	X	X	X	X	X	X*	X	X	X	X	X*	X				X		X		X	X*	X	X	X	X
Water sampling - all sites				X	X	X	X			X		X					X				X					
HydroLab - inside C-3		X		X	X			X	X		X		X				X		X							
HydroLab near-field					X		X																			
HydroLab trnst. NW-WB					X	X			X																	
HOBO - circ. plate						X				X	X		X										X	X		X
HOBO near-field study														X	X	X	X									
ADV circ. flow											X		X													
ADV near-field												X						X		X						
HydroLab medium-field																						X	X			

2.4 Field instrument calibration and verification

The Hydrolab DS5 (Hach) was used for temperature and dissolved oxygen measurements during monitoring in 2007. It was fitted with a Hach LDO™ Sensor that uses luminescent dissolved oxygen technology to measure dissolved oxygen. It was calibrated every two weeks using the 100% oxygen-saturated water method described by the instrument manufacturer. The dissolved oxygen concentrations that were collected using the Hydrolab were in good agreement with OWML's dissolved oxygen data.

The Hydrolab's temperature sensor (thermister) is factory calibrated and cannot be adjusted by the user. The thermister calibration was checked in the laboratory using a mercury thermometer and across a temperature range of 0 to 35 °C (Figure 19). The correlation between the reference thermometer and the Hydrolab thermister indicated a 4.3 °C negative bias. Consequently, all data collected by the Hydrolab thermister was adjusted by adding 4.3 to the instrument reading.

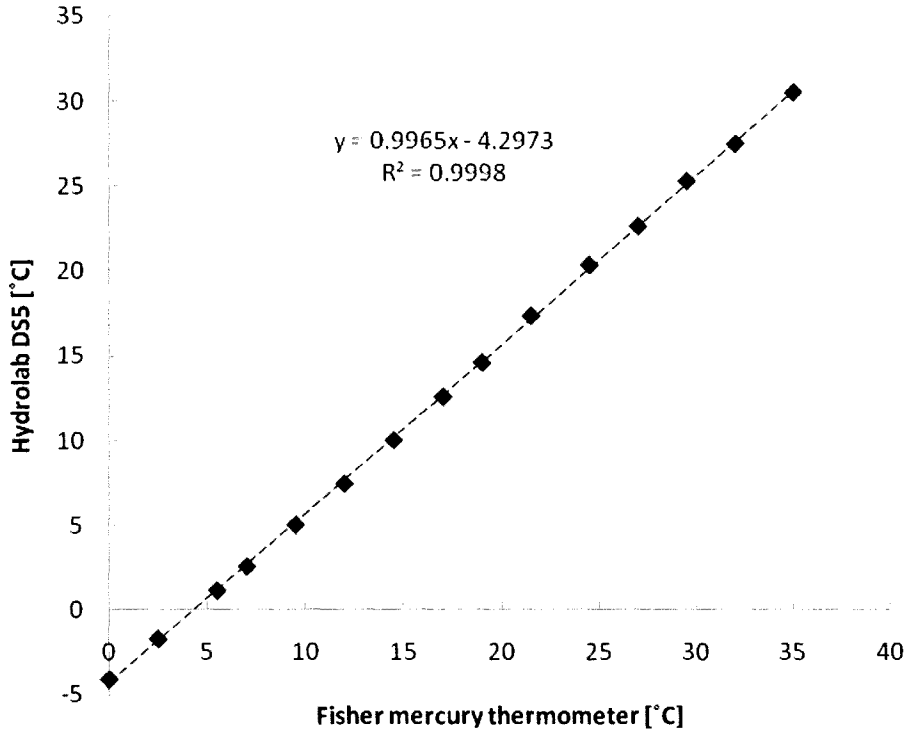

Figure 19. Calibration curve for the Hydrolab thermister against a Fisher mercury thermometer.

The Vectrino from Nortek was also factory calibrated. However, the instrument's calibration was verified in ODU's long wave tank by pulling the instrument at a controlled speed with Vectrino's probe in the water. The x-axis and the y-axis were calibrated separately. The Vectrino was calibrated at four speeds, 0.0, 0.1, 0.2, and 0.3 m/s, using a cart that was pushed by hand on top of the tank. The speed was controlled by marking the tank with a tape strip that had to be passed by the cart every second. The speeds were recorded in triplicates for the x-direction and the y-direction. The post processing involved deleting the first few seconds and the last few seconds of each run. The average speed was calculated using the remaining data points for each run. Then the

average of the three recordings at each speed was taken for the final velocity value. The photograph in Figure 20 shows the Vectrino attached to the cart during the calibration verification. Figure 21 shows the result of the wave tank verification. The high correlation and slope near 1.00 is proof that the Vectrino's calibration was accurate and needed no correction.

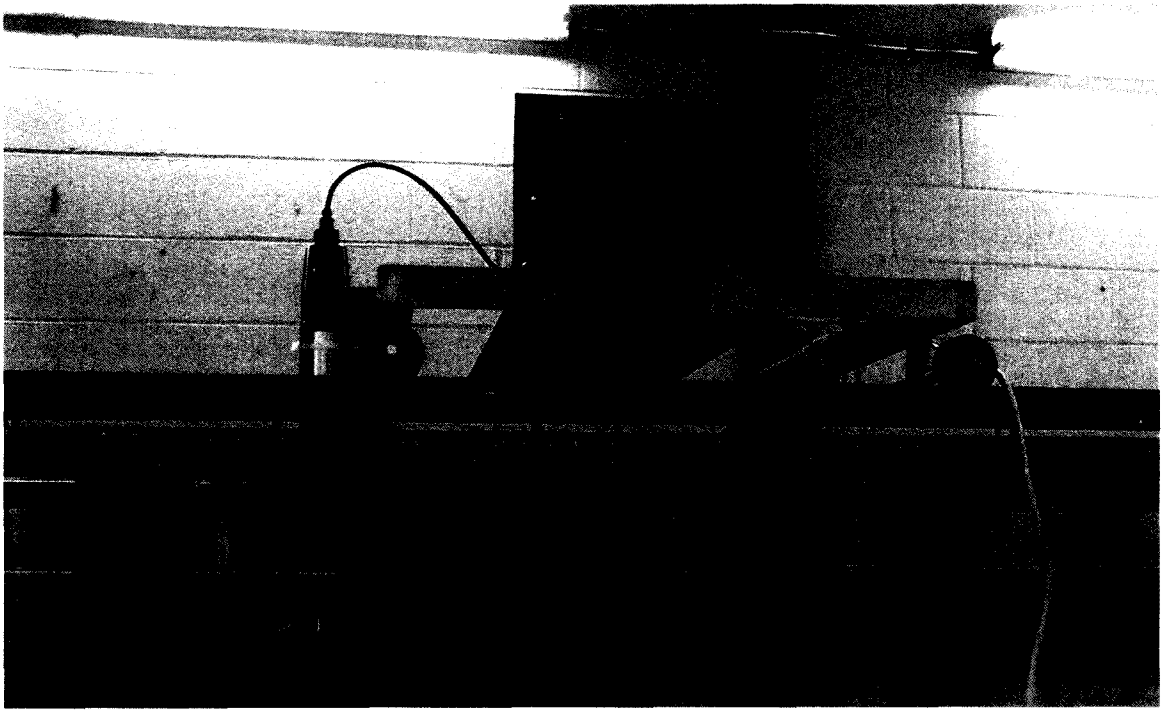

Figure 20. The arrangement of the Vectrino ADV in ODU's hydraulic laboratory's wave tank.

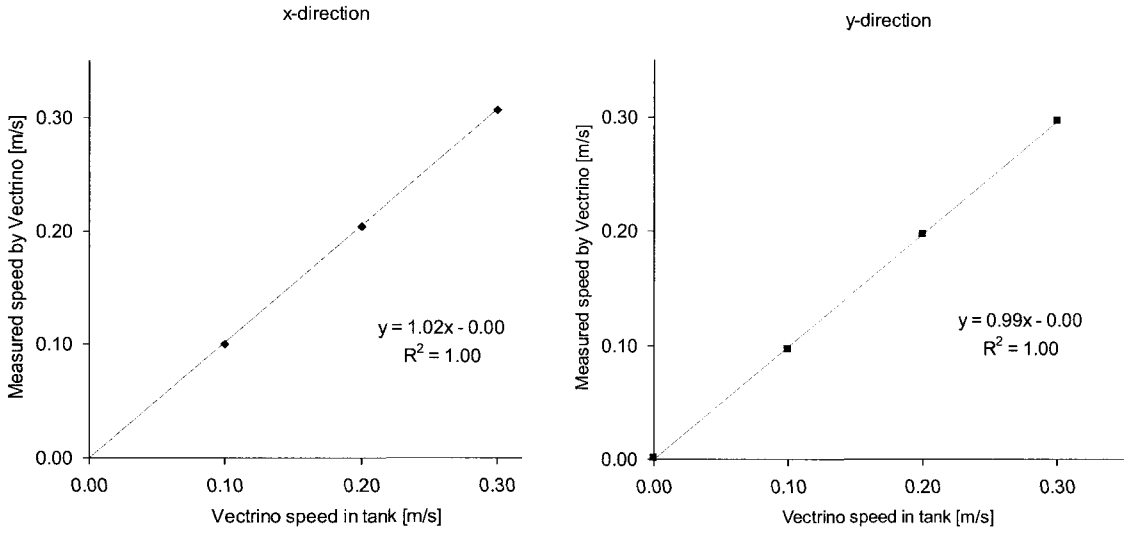

Figure 21. Correlation between wave tank cart speed and Vectrino ADV measured values.

2.5 Results

2.5.1 Thermal Stratification during Aeration and Circulation Periods

To compare temperature conditions from years when the aeration system was in operation with conditions in 2007 when the surface circulators were operational, REO2 temperature profiles from 2000 to 2007 were plotted together. The 2006 profile was excluded from this analysis because the aeration system was not operating properly and was shut down during periods in 2006. The temperature profiles examined here were recorded in late July and are shown in Figure 22.

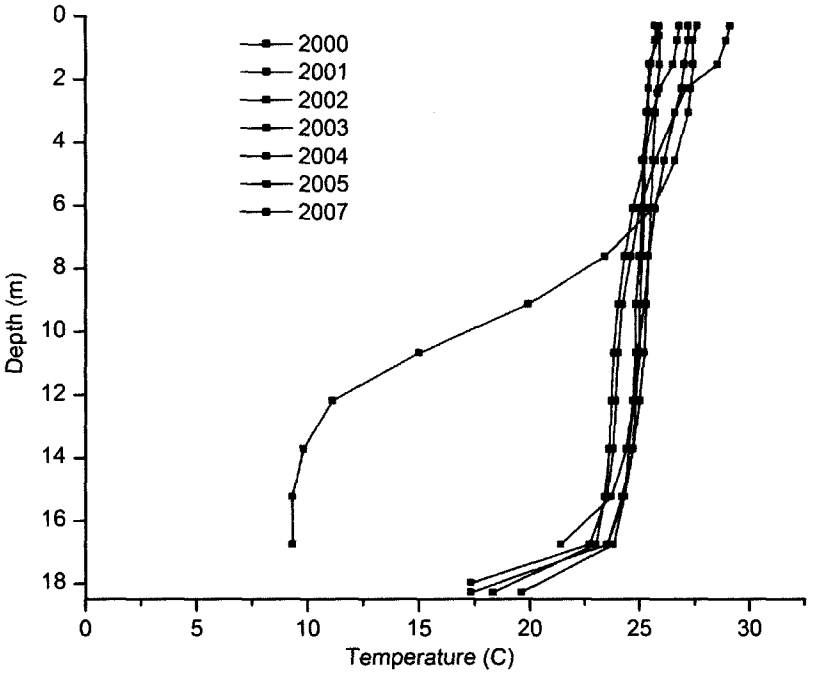

Figure 22. Late July temperature profiles for the Occoquan Reservoir lower basin from 2000 to 2007

It is clear that the 2007 temperature distribution is substantially different than the comparison years with a much colder hypolimnion than the years when the aeration system was operated. This finding is in good agreement with the observations summarized by Cooke et al., (1993) on the influence of a bubble plume's ability to destratify water columns and thus increase hypolimnetic temperature. The dramatic difference in the temperature profile of the circulator year (2007) and the years during aeration (2000-2005) illustrate the substantially different amount of vertical mixing imparted by these two systems. It is clear that the aeration system maintained destratified conditions in late July while the water column profile during the same period in 2007 exhibited strongly stratified conditions. While the water column in July 2007 appeared

strongly stratified the depth of the epilimnion (approximately 7 meters) is likely to have been deeper than under natural conditions (no circulation and no aeration). This supposition is based on observations in other Virginia reservoirs where late July epilimnetic depths have been observed at depths typically shallower than 5 meters.

To better examine the differences between the 2007 circulation year and the previous years when aeration was practiced, temperature plots for the entire seasons between 2000 and 2007 were developed. Six depths (0.3, 3.0, 6.1, 10.7, 13.7, and 15.2 meters) approximately evenly distributed between the surface and the sediments were examined (Figure 23).

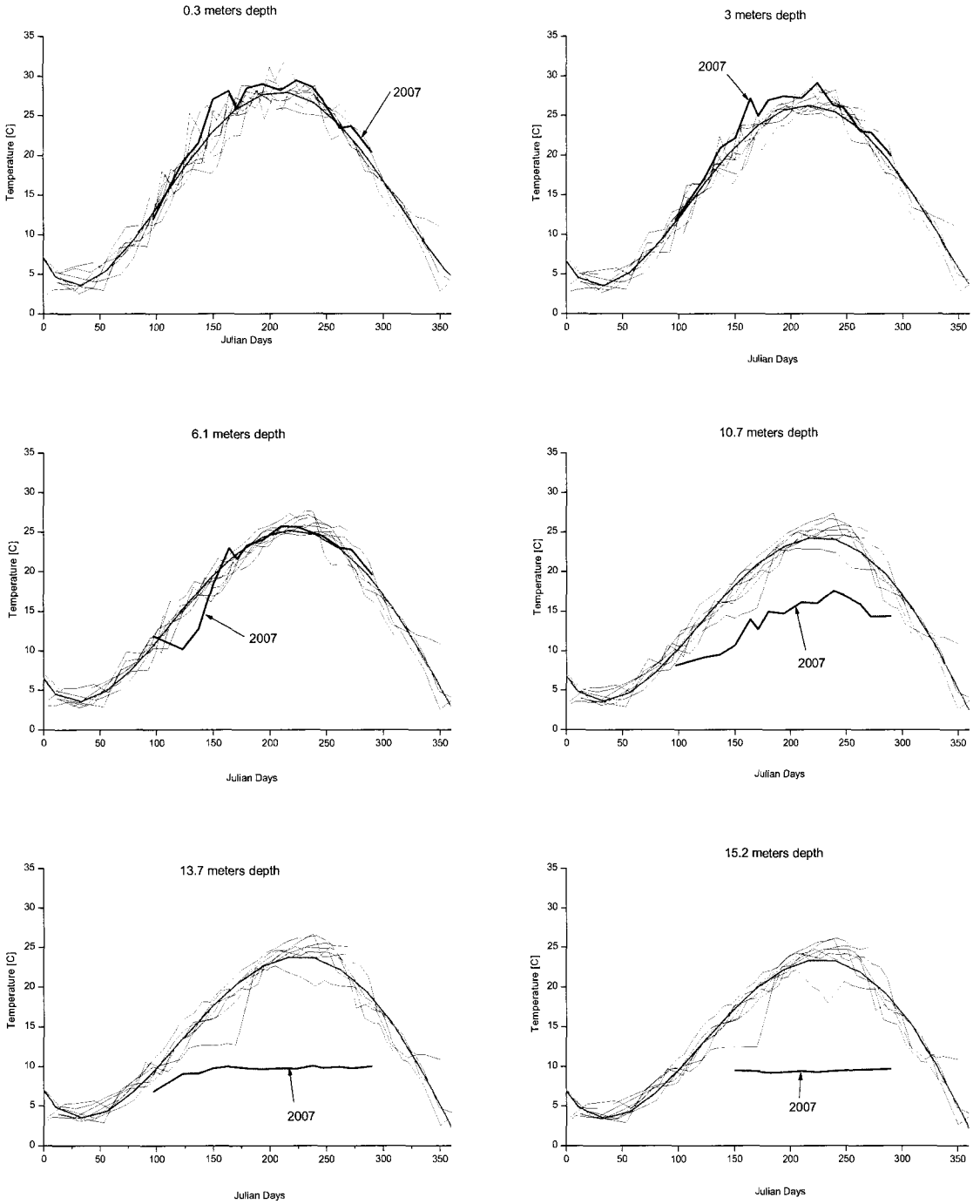

Figure 23. Temperature plots at six depths for Occoquan Reservoir's lower basin. A curve is displayed for every year from 2000 to 2007. Solid green curve represents the average temperature for years 2000-05 at each depth.

At the two shallowest depths examined (0.3 and 3.0 m) the circulator season (red curve) was slightly warmer than the mean temperature at 0.3 m but within the range of previous seasons. At 6.1 meters (approximate base of the epilimnion) there was no significant difference between the seasons. For the 10.7 (metalimnion), 13.7, and the 15.2 meter plots (hypolimnion) the circulator season was clearly colder than the aeration seasons. Again, one can see that the aeration system's ability to homogenize the water column is greater than the surface circulator's ability.

Physical mixing due to aeration has been taking place in Occoquan Reservoir since 1970. No reliable data are available describing the natural behavior of the reservoir without any enhanced mixing. Therefore, comparison of circulation conditions to no circulator or no aeration conditions is not possible. While it is not possible to use historical data from the circulated region of the reservoir for comparison purposes, regions farther up the reservoir that would not be affected by aeration or circulation have the potential to be used to compare the circulation year to non circulation years. The comparison would allow determination of whether 2007 was a typical /atypical year for the period being examined. OWML has not monitored the NW area consistently during the aeration period, so no comparison could be used from this area. OWML has routinely monitored RE10 which is comparable to the WB2 location (Figure 14). Consequently, the temperature conditions from 2000 to 2007 at RE10/WE2 were examined (Figure 24).

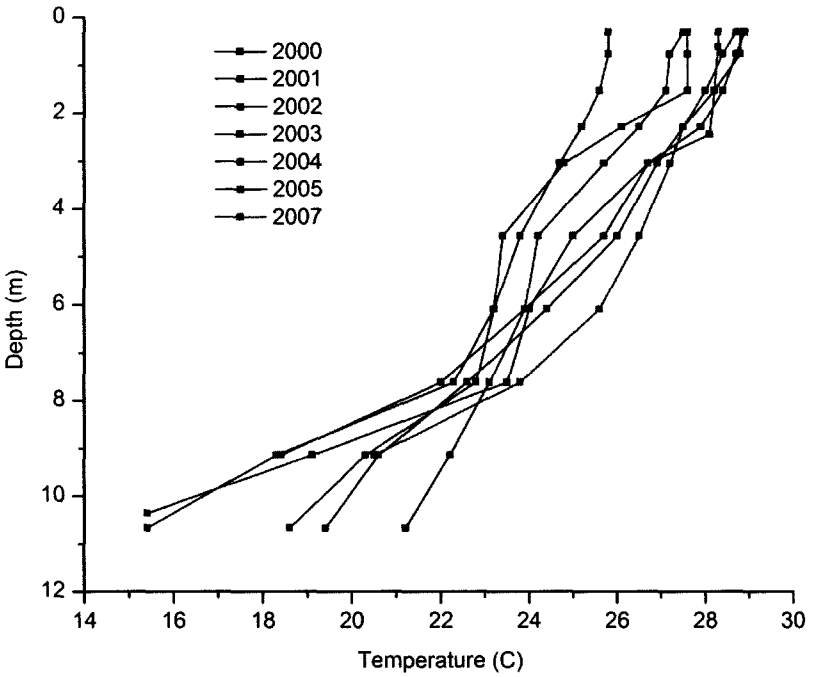

Figure 24. Late July temperature profiles for RE10 from 2000 to 2007

The 2007 profile exhibited generally warmer temperatures than the other seasons, suggesting that water temperatures in Occoquan Reservoir were naturally higher in July 2007 than other years in the comparison. This situation suggests that the slightly higher temperatures exhibited in the surface waters in Figures 12 and 13 may reflect natural variation. While the RE15/WB2 location is shallower than the reservoir it is believed to be an accurate reflection of lake conditions without mixing induced by surface circulators or the aeration system.

To better illustrate both the temporal and spatial variations in temperature between aeration and circulation conditions, isopleths were developed for 2007 representing surface circulation and 2002 representing aeration (Figure 25). The year

2002 was selected because it was the most robust (i.e. well populated) of the data sets for the 2000 to 2005 period. The isopleths clearly show that the aeration system provides more vertical mixing than the surface circulators. An interesting observation for the circulation conditions is that the thermocline developed at a depth of ten meters, which corresponds to the intake depth of the circulators. If the natural temperature distribution of the reservoir was known, then one could determine if the circulators lowered the thermocline to the intake depth or if the thermocline naturally developed at this depth. This question cannot be answered with certainty but is discussed further in chapter four.

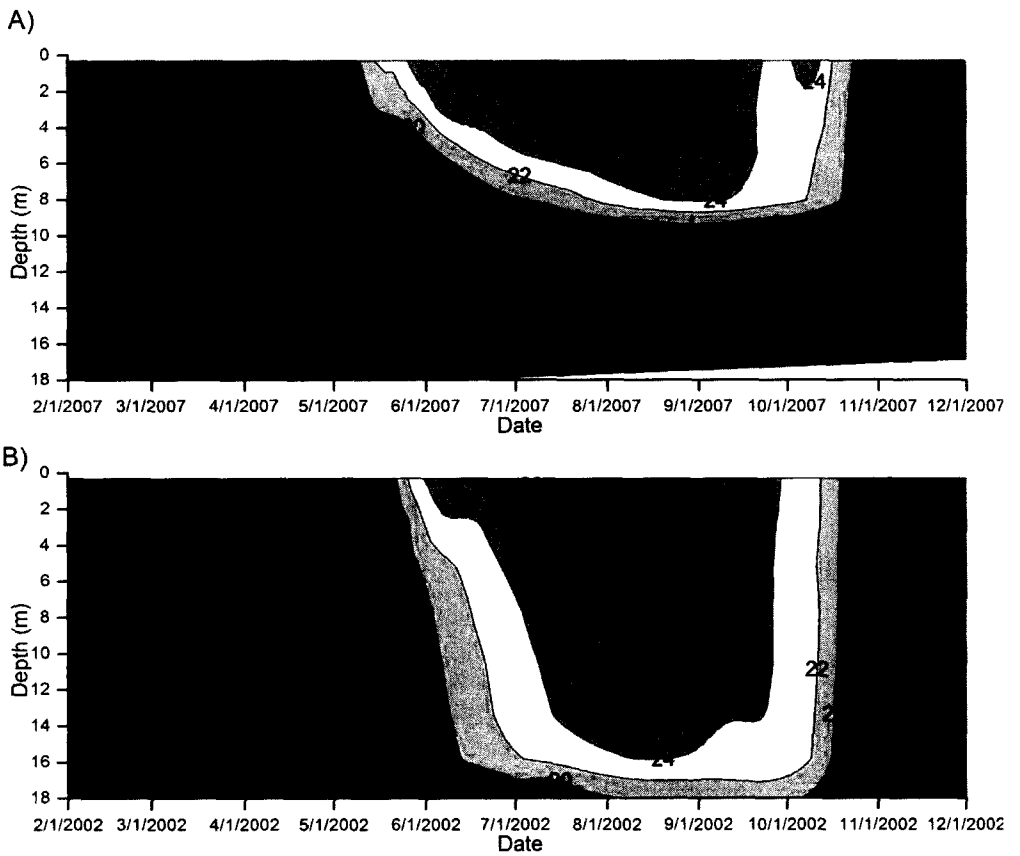

Figure 25. A) Temperature [C] at WB for the 2007 season during the surface circulation period. B) Temperature [C] at WB for the 2002 season during the aeration period.

In order to study the spatial influence from the circulators' temperature, profiles from WB, NW, and WB2 were examined for a common date (13 August 2007). Each profile is based on the direct output from the Hydrolab DS5. These profiles were based on a one second recording interval as the Hydrolab was slowly lowered through the water column. The depth scale is set to ten meters to better observe variations. The profiles are nearly identical except for the 3-4.5 meter interval. The temperature is about 1 °C warmer at WB between 3 and 4.5 meters depth and is consistent with the circulators increasing the water volume at this depth, so the colder water strata below are pushed down. However, the circulators are located in the region of the reservoir where the highest wind speeds may occur and this variation may reflect this situation.

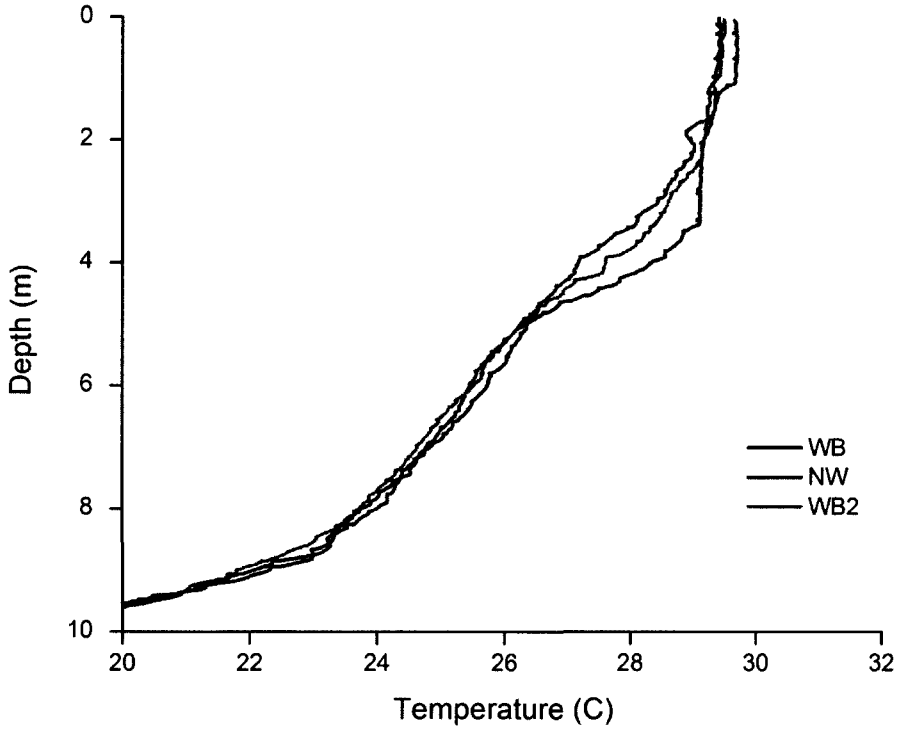

Figure 26. Temperature [C] comparison of August 13th 2007 profiles from WB, NW, and WB2.

2.5.2 Measurement of Circulation Flow Rates

The flow through the circulators was estimated by using acoustic Doppler velocimeter and converting point measurements of velocity and depth to volumetric flow. An example of the velocity variation of water flowing over the distribution plan illustrates the velocity field exiting the circulator (Figure 29). The final flow is based on the average depth and flow velocity for each circulator. The total flow of all eight circulators was 0.5 m^3/s.

Table 5. Depth measurements of the distribution pan at three locations with the corresponding velocities recorded on the 7/14/07. Flow rates for each circulator are shown.

	Cir-1	Cir-2	Cir-3	Cir-4	Cir-5	Cir-6	Cir-7	Cir-8
RPM	59	60	60	60	60	60	60	60
Depth A [m]	0.065	0.075	0.056	0.079	0.067	0.065	0.069	0.071
Depth B [m]	0.060	0.069	0.064	0.070	0.080	0.072	0.065	0.075
Depth C [m]	0.065	0.060	0.068	0.070	0.060	0.067	0.070	0.074
Velocity A [m/s]	0.168	0.172	0.197	0.123	0.200	0.187	0.205	0.172
Velocity B [m/s]	0.192	0.205	0.127	0.143	0.152	0.196	0.135	0.210
Velocity C [m/s]	0.149	0.188	0.152	0.173	0.161	0.139	0.174	0.156
Avg. depth [m]	0.063	0.068	0.063	0.073	0.069	0.068	0.068	0.073
Avg. velocity [m/s]	0.170	0.188	0.159	0.146	0.171	0.174	0.171	0.179
Flow [L/s]	67.2	80.1	62.2	66.8	73.8	74.0	72.8	82.2

According to information from the circulator manufacturer, the flow rate that passes through the lift tube is 3,000 gpm or 190 L/s. It is clear that these flow rates are considerably lower than what the manufacturer claims. On average, the measured flow

rates are only 37% of what is listed in the data sheet for this circulator model. The sum of all the circulators resulted in a total flow rate of 0.58 m^3/s.

The velocity measurements shown in Table 5 were recorded 3 cm below the surface. A velocity profile was also recorded at circulator 2, and is displayed in Figure 27. One can see how the flow field is slowed down near the distribution pan due to friction. The lowest bar that was recorded at 8 cm below the surface was likely in the flow field that is induced from below the pan.

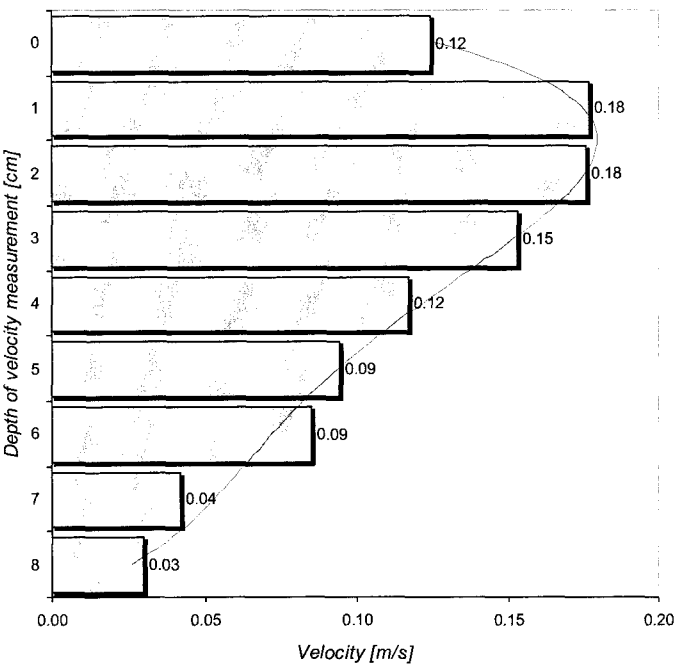

Figure 27. Velocities over the distribution pan at one centimeter increments recorded on the 7/14/2007.

2.5.3 Circulator Slot

During a discussion with the manufacturer, it became clear that there was a slot below the distribution pan that was designed to release flow to widen the radius of influence of the circulator. It was not possible to measure the flow rate through this slot after this discussion; however, observations of particles in the surface water failed to confirm this flow. Because of this slot, there are some uncertainties about the performance of the circulators. It is possible that the flow is negligible or even directed into the distribution pan (reverse flow). This slot is discussed further in Chapter 3.

2.5.4 Circulator Flow Variation

Data Logging thermistors were used to investigate the temporal temperature changes of the water flow that was passing through the circulators. This was done to see if diurnal temperature patterns would occur based on solar heating during daytime. It was expected to be insignificant because the temperature at an intake depth of 10 meters is not affected by the sun's radiation. A single thermistor programmed to record temperature every 30 seconds was attached to the top of each circulator's distribution pan and completely submerged in water flowing over the distribution pan. The thermistors were attached to the circulators for 9 days then retrieved and data downloaded to a laptop.

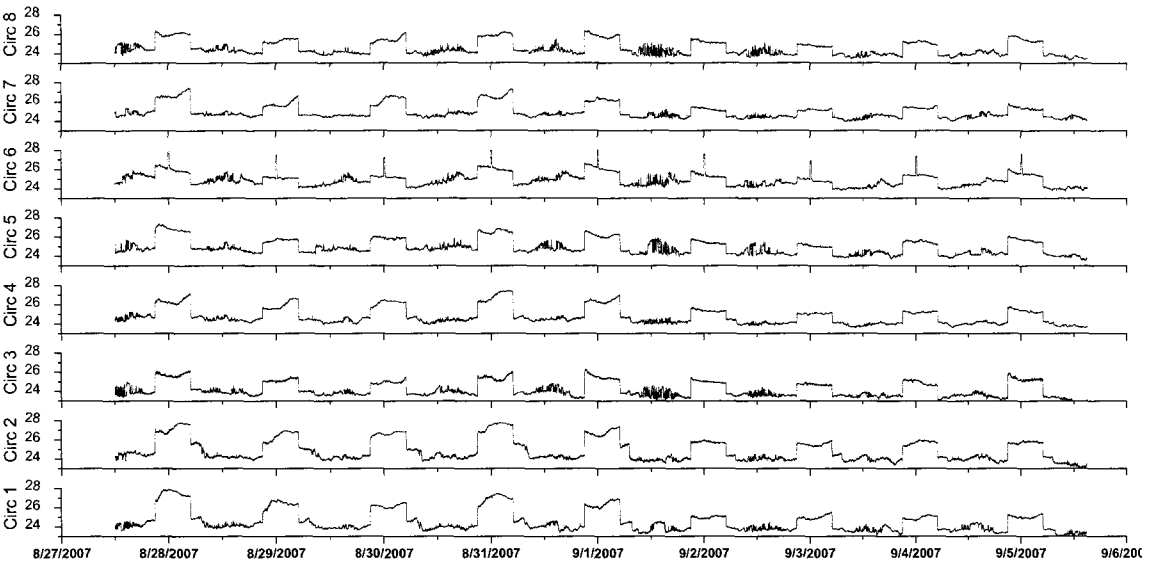

Figure 28. Temperature [C] time series collected of the circulation water on the circulator's distribution pan.

The temperature of water exiting from the circulators exhibited a consistent trend across the nine days and with all circulators (Figure 28). Consistently in early morning the temperature decreased and similarly in evening in a step-function type manner, the temperature increased. This temperature observation for July 19, 2007 at circulator 3 highlights the consistent variation (Figure 29). At 5:00 the temperature dramatically decreased 3 ˚C and increased as dramatically at 21:00. In response to inquiries about this observation the manufacturer noted that the circulator was programmed to operate at 40% capacity to save battery power during the 21:00 to 5:00 period each night.

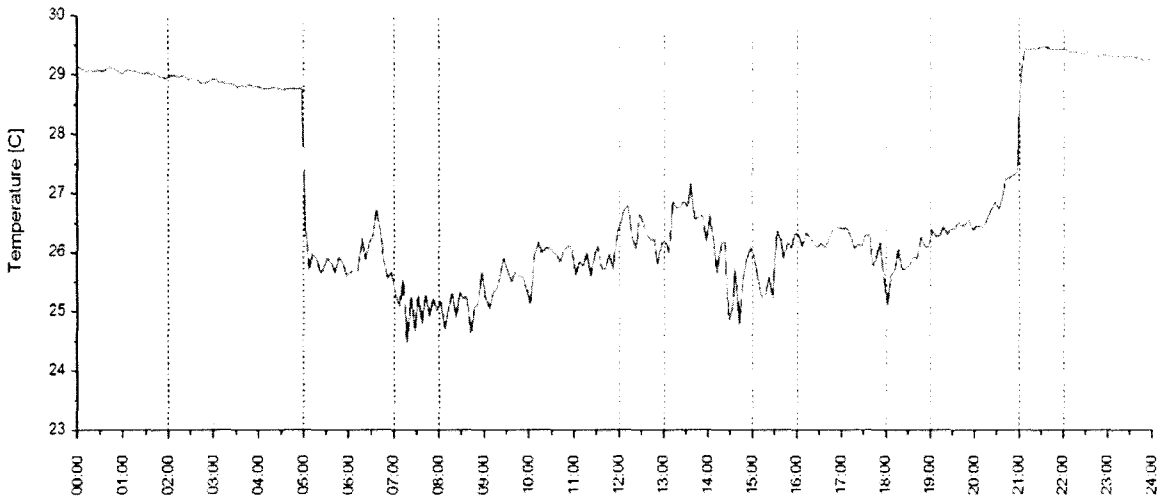

Figure 29. Temperature [°C] time series for water overlying the distribution pan of circulator 3.

Daytime fluctuations in the temperature recordings also occurred and are likely related to the circulator being free to move within the length of its chain to the mooring. The thermistor was attached to a support strut close to the edge of the distribution pan so that wind-induced surface currents could enter onto the distribution pan given the right wind and orientation of the circulator. The temperatures were much smoother during night operation raising the question of whether the circulators were operating between 9:00 PM and 5:00 AM. The WB surface temperature recorded at 2:00 PM on July 18, 2007 by routine monitoring was 29.6 °C, which is in good agreement with the nighttime temperatures on this date. This observation added to the suspicion that the circulators turned off completely during the night, although it is possible that a reduced circulator speed could cause the flow through the slot below the distribution pan to be reversed. If this was the case, the night temperature would be slightly warmer as surface water (about 40 cm depth) mixed into the circulation flow.

2.5.5 The Circulators Total Flow Rate

The eight surface circulators (Solar Bee Model SB 10000v12) operating in Occoquan Reservoir during the 2007 season were rated at 3,000 GPM each through the lift tube for a total of 24,000 GPM (1.5 m^3/s). This flow is three times larger than the estimated flow based on the Vectrino measurements. A discussion with the circulator manufacturer revealed a slot that was located under the distribution pan which the manufacturer stated was the source of the large discrepancy between the rated flow and the measured flow. This flow through the slot was never measured or verified. Taking into account that the circulators were slowing down or shutting off from 9:00 PM to 5:00 AM as revealed by the thermistors, the operation was shortened by 8 hours a day which yields a 20% overall reduction in operation.

To find the flow rate through the circulators was important for this research in order to understand the impact from the circulators. Finding the correct flow rate is also a key parameter in setting up a water quality model for this reservoir, as described in chapter 4. The maximum possible flow is based on the theoretical rating from the manufacturer (1.5 m^3/s) without reducing the flow during the night. The flow rate that represents the minimum likely flow experienced is based on the measured flow over the distribution pan with the assumption that the circulators shut down during the night (0.35 m^3/s.). The range between these two flow rates is considerable. As discussed later, the flow assumption will play an important part in the modeling of the reservoir in a later chapter.

2.5.6 Change in Reservoir Heat Content

The density stratification that is caused by heat energy entering and leaving the reservoir through the progression of the seasons regulates nearly all the physicochemical processes that take place in a water body. Laws of thermodynamics dictate that heat cannot disappear but has to be conserved within the system (reservoir). Heat energy primarily comes from the sun and has to enter and leave the reservoir through the surface (Hutchinson, 1957). To study the circulator's impact on heat energy dynamics versus the aeration system's impact, a series of plots were constructed. The change in heat energy was calculated for the epilimnion and hypolimnion based on temperature profiles from RE02 between 2004 and 2007on a monthly basis. Only the 2005 season is displayed with monthly values in Figure 30. 2007 is also shown with monthly values in Figure 31.

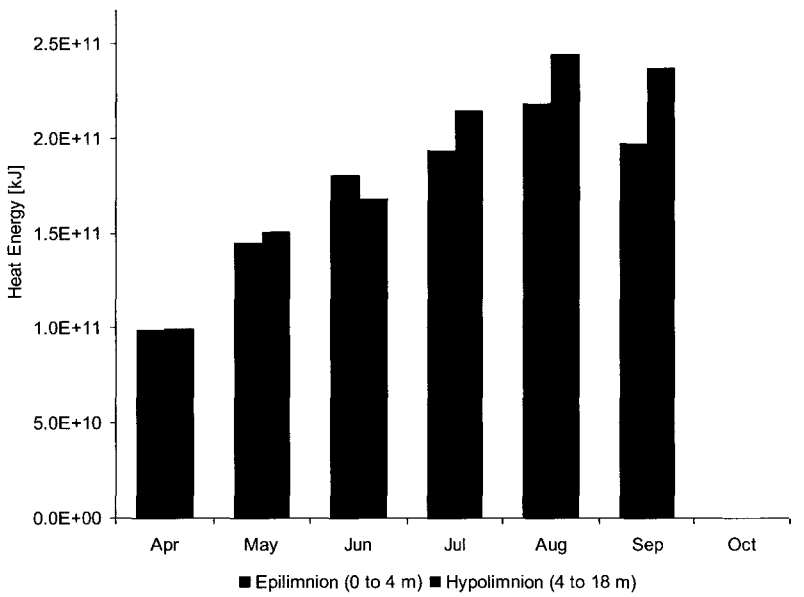

Figure 30. Heat energy for Occoquan Reservoir lower basin during summer 2005 (No circulators, aeration system operated).

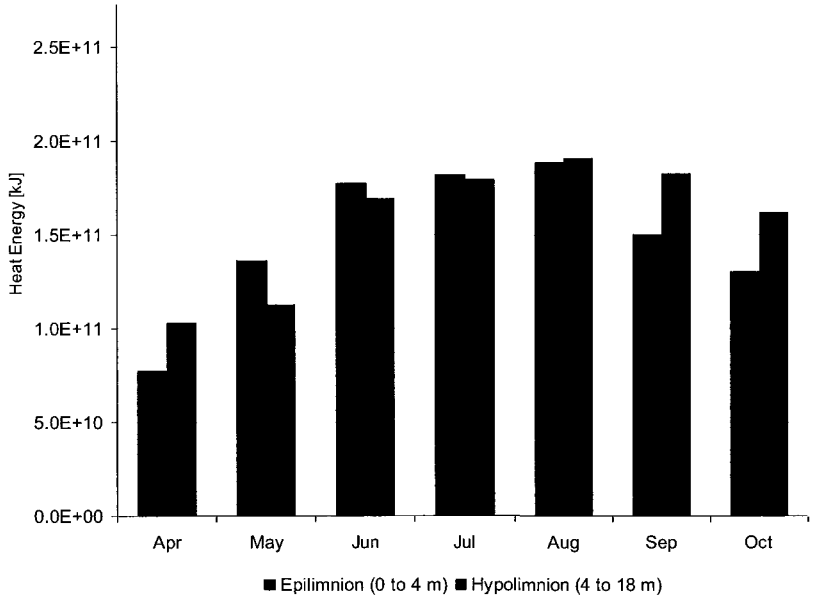

Figure 31. Heat energy for Occoquan Reservoir lower basin during summer 2007 (with circulators).

The difference in the change in heat content between the two years suggests that vertical mixing from the aeration system caused the reservoir to absorb more heat energy than the surface circulators. This effect has been described by Cooke (1993) and can be verified by the previous temperature distributions (Figure 22). The epilimnetic and hypolimnetic change in heat energy through the temperate season from 2004 through 2007 is displayed in Figure 32. It illustrates the reduced change in heat content during the circulation (2007) compared to the normal aeration years (2004 and 2005). It can be seen that 2006 (partial aeration) had a moderate change in heat energy somewhere between the aeration and the circulation results.

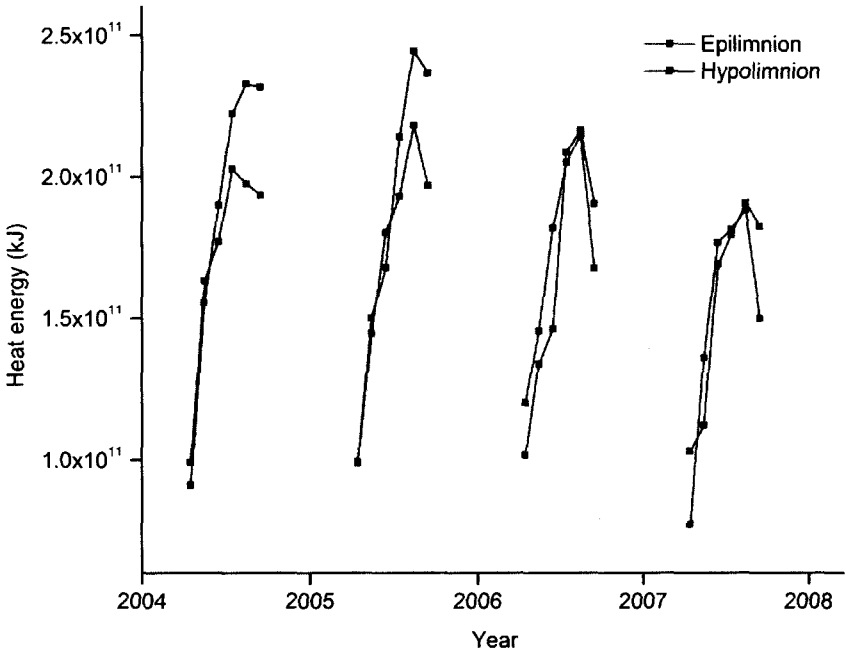

Figure 32. Monthly heat energy values for Occoquan Reservoir's lower basin for 2004, through 2007.

Because it is not possible to distinguish the impact of these periods separately, 2006 will not be used in further comparison. The most important observation is that the heat energy was much higher in the hypolimnion during the aeration period in 2004 and 2005 than during the circulation period in 2007. This is strong evidence of increased vertical convective transport during the aeration years causing warmer waters from the epilimnion to mix with the deeper waters of the hypolimnion. The epilimnion is more similar during aeration and circulation periods.

2.5.7 Circulator Impact on Temperature in the Near-Field

The near-field is thought to represent the area around each circulator where the highest degree of physical mixing is likely to take place. The near-field of circulator 3 was studied in 2007 using several techniques during no-wind or low-wind conditions since even a small breeze will create a surface current (Wetzel, 2001). This influence was confirmed by visual observation of water exiting the circulator being pushed to the leeward side of the distribution pan, causing an assumed uneven mixing pattern in the near-field. It was particularly important to have quiescent conditions during the measurements of the near-field flow pattern because the velocimeter was sensitive to movement, and the smallest amount of waves would lead to false readings. The circulators in Occoquan Reservoir are attached to their mooring by a single chain, leaving them moving freely as wind changes direction. Before studying the near-field of circulator 3, two separate anchors were set in a 120-degree angle to the mooring chain and the lines drawn taut.

Initially, the near-field was measured by taking a series of profiles in close proximity to each other. Each profile was obtained at 0, 0.25, 0.5, 0.75, 1.0, 1.5, 2.0, 2.5, 3.0, 3.5, 4.0, 4.5, and 5.0 meters from the circulator's distribution pan. Figure 33 illustrates the temperature distribution five meters from the edge of the circulator and to a depth of 5 meters. The overlaid arrows represent velocity vectors with the length of each arrow reflecting the magnitude of the water velocity at the point of the arrow. The cold hypolimnetic water can be observed at the upper left corner of the plot as it leaves the distribution pan. It appears to mix rapidly with the ambient epilimnetic water being pulled up from underneath the distribution pan. As it flows away from the circulator it

mixes with the epilimnetic water and quickly loses its velocity. After the initial mixing the circulation water is still colder than the ambient epilimnetic water in the reservoir, and it appears that the plume continues to mix as it sinks lower in the water column to a depth of about four meters. Evidence of this movement can be seen in Figure 33 at three meters distance and two to three meters depth. It appears that the circulation plume remains at the lower part of the epilimnion (4 to 5 meter) where its density would reflect that of the surrounding water.

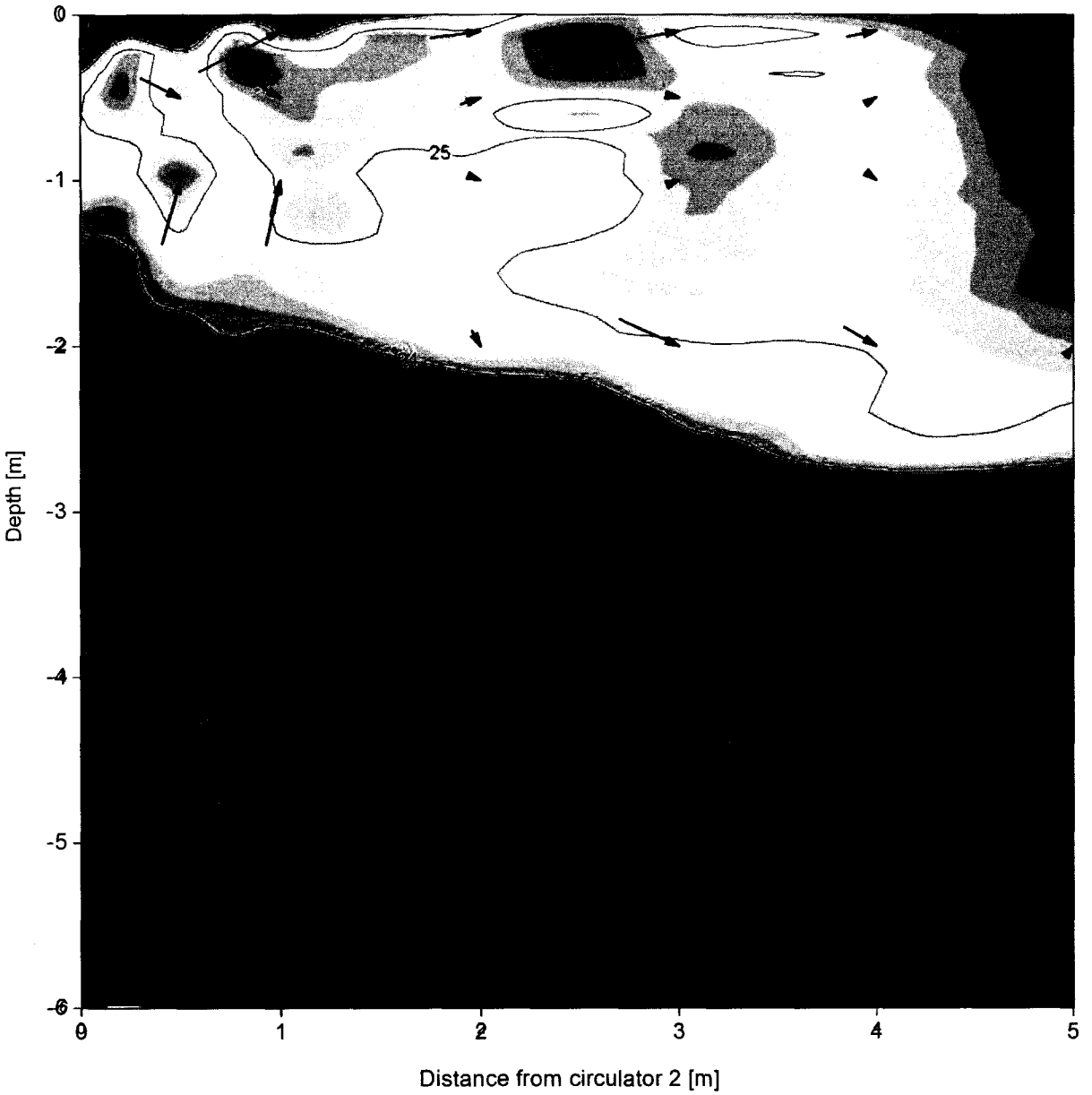

Figure 33. Near field temperature [C] including the flow field described by vectors around circulator 2 on July 2007. Water discharging from the circulator occurs at 0,0 meters on the graph.

The water velocities become too small to measure outside a five meter radius from the circulator due to radical spreading and momentum decline. The water being pulled up

from under the distribution pan is likely water originating from 3 to 4 meters depth. Water currents could also be the result of the slot below the pan, but neither velocity vectors nor the temperature measurements suggest this is a large portion of the total flow. It is not observed, but it is likely that some mixing is occurring where water is rotating around the circulator in a doughnut shape flow.

Another procedure that was used to measure the near-field temperatures around the circulators was to deploy a thermistor chain. Twelve thermistors were distributed at approximately 0.5 meter distances along a five-meter long line and then installed at various distances from the circulator for 20-minute periods so that the vertical temperature profile was recorded. The results of this analysis show a similar temperature distribution as observed with the shorter-term vertical profiles.

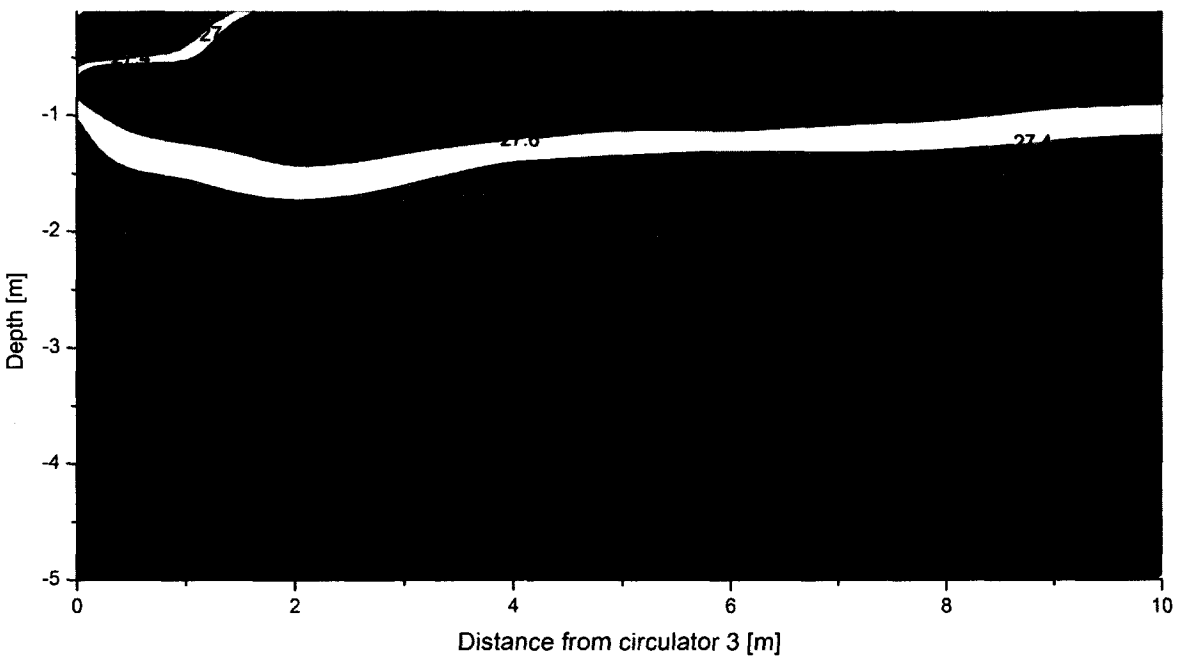

Figure 34. Near field temperature [C] distribution around circulator 3 measured by thermistor chain.

2.5.8 Circulator's Temperature Impact on the Far-Field

Three transects along the longitudinal axis of Occoquan Reservoir were made on three separate dates in June 2007 between the NW site and the dam (Figure 35). The last vertical profile of each transect was collected close to circulator 3, but it is referred to as WB in this chapter (100 meters apart). Each transect consisted of a series of vertical temperature profiles collected every 200 meters using the Hydrolab DS5.

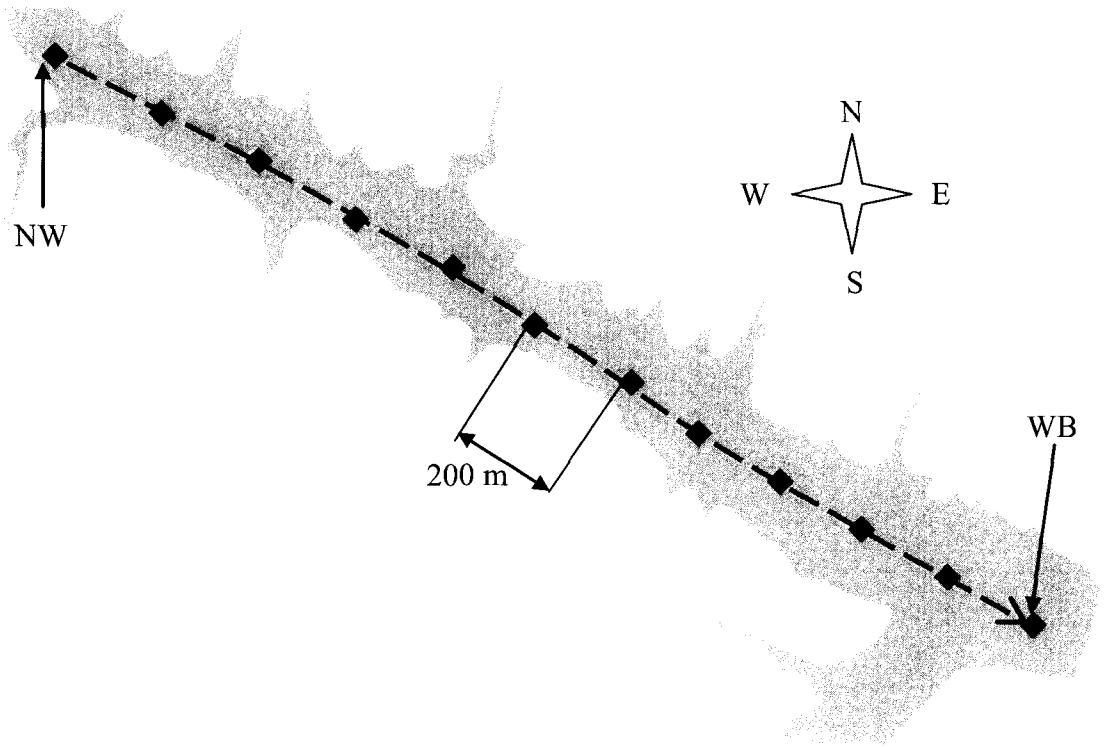

Figure 35. Occoquan Reservoir from NW to WB with the transect sampling sites displayed.

The purpose for these transects was to examine the spatial distribution temperature to determine any influence of circulator operation in the far-field. A temperature isoplot from each transect date (06/15/2007, 06/21/2007, and 06/30/2007) is displayed below.

All three transects showed similar temperature distribution between NW and WB. These temperature distributions are "snap shots" of the temperature profile at the time they were taken but are potentially an opportunity to characterize long range transport mechanisms driven by potential energy differences in the water caused by the circulators mixing. As the epilimnion becomes colder and its volume increases around the circulators, this water will move upstream at the depth of equal density. This transport is driven by the increased potential energy that the circulators induce to the epilimnion as cold hypolimnetic water is mixed into the epilimnion.

The following isopleths (Figure 36-39) show the temperature distribution from NW to WB. The small arrows at the upper edge illustrate the approximate location of the circulators as a reference to where the added hypolimnetic water is entering the epilimnion. While there would appear to be little influence of circulator operation along a transect when examined over the entire water column (Figure 36), if the temperature profile is examined over a narrower depth range, a spatial variation in temperature is apparent. The iso-lines below five meters are horizontal, which indicates a homogeneous temperature distribution and no apparent circulator-induced effect.

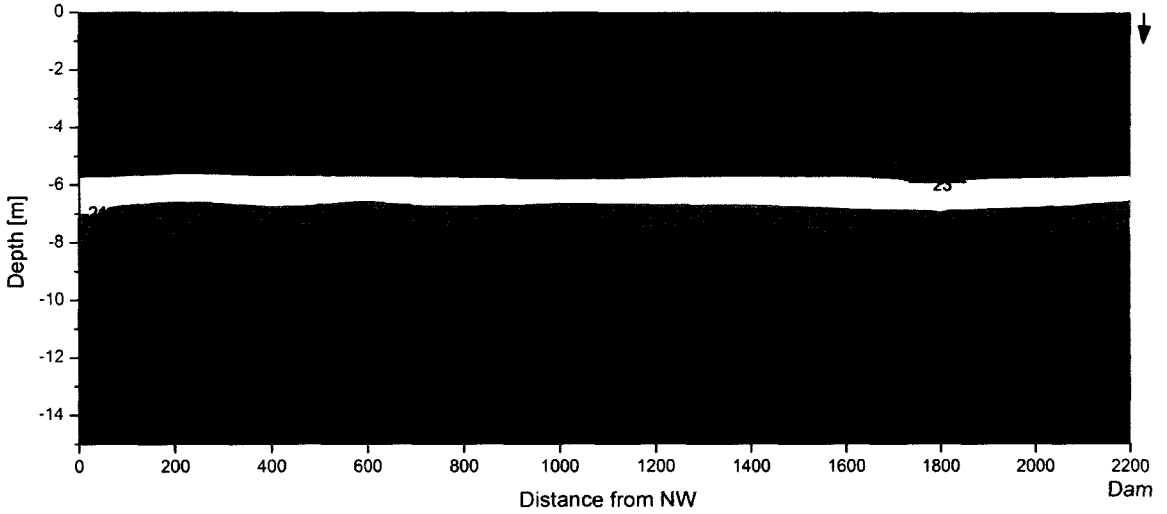

Figure 36. Temperature [C] variation from NW to WB recorded on 06/15/2007.

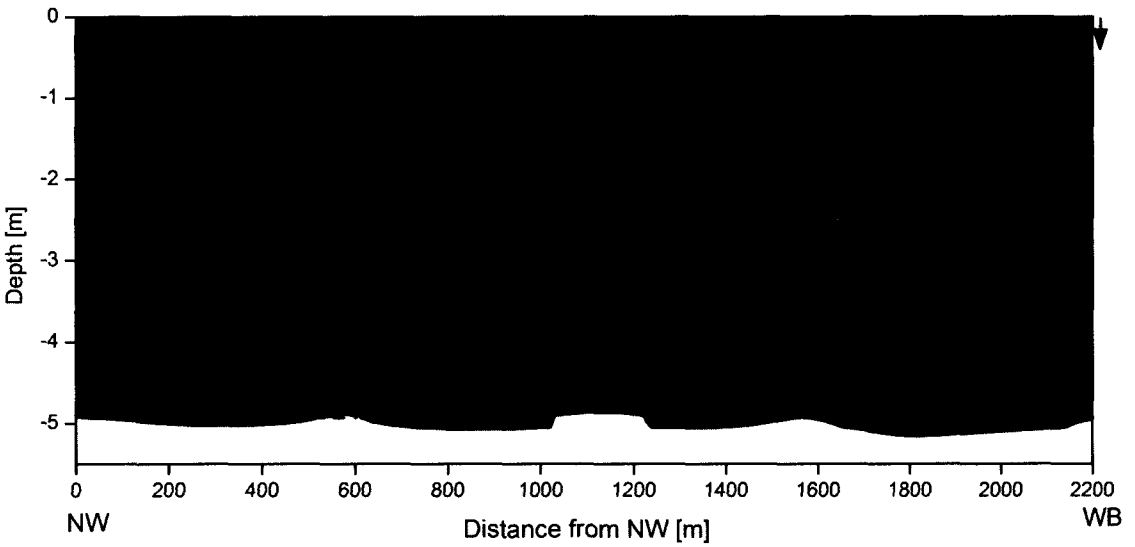

Figure 37. Temperature [C] variation from NW to WB recorded on 06/15/2007.

Figure 37 shows the same transect as in Figure 36 but with a depth scale set from 0 to 5.5 meters. The temperature variation displays an unstable water column consistent

with a colder circulator plume mixing with surface waters and causing a cooling of the water column in the lower epilimnion. This colder and denser water could displace warmer surface water further up the reservoir and ultimately reduce the temperature near the dam. The first transect that was conducted (Figure 37) shows a different trend than the two following transects (Figures 38 and 39). The colder temperature range of the epilimnion (24 °C to 25 °C) is more pronounced near the dam, which is consistent with the introduction of colder circulator water at the surface. It is not clear why colder water strata at greater depths are not pushed deeper close to the dam by the increased hypolimnetic volume in this area from the circulation. The added specific weight of the water would also contribute to a thicker epilimnion near the dam. It is thought that this particular temperature distribution is related to the relatively recently established thermal stratification. The weather data was studied within a week before this event, and no major wind event occurred that could cause a seiche.

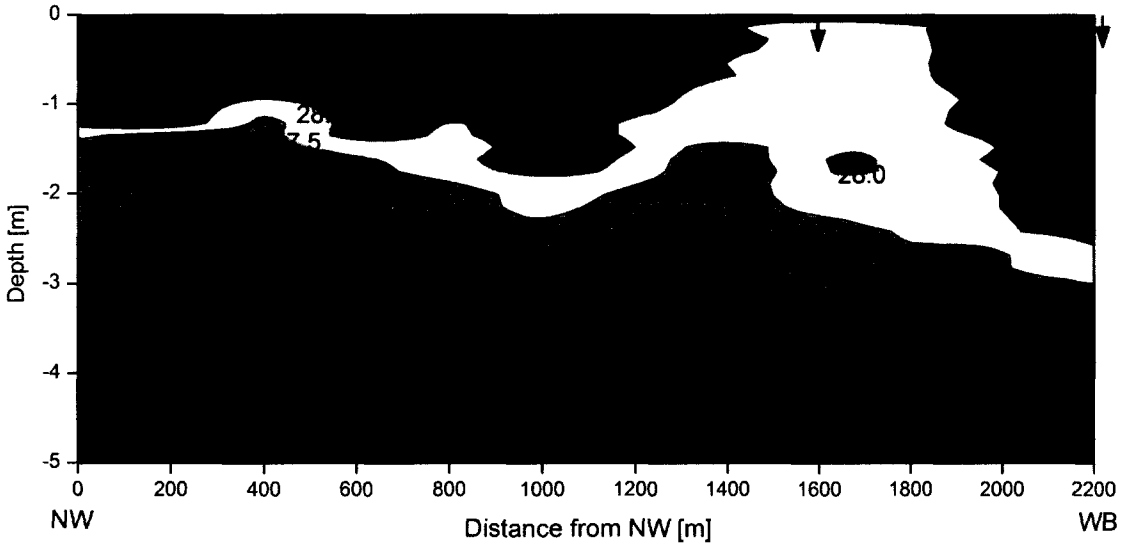

Figure 38. Temperature [C] variation from NW to WB recorded on 06/21/2007.

The second transect was conducted on June 21, 2007, and the spatial distribution temperature suggests the operation of the circulators caused colder water layers beneath to be lowered due to withdrawal through the circulators. The second transect shows a cooling of the surface water that did not appear during the first transect.

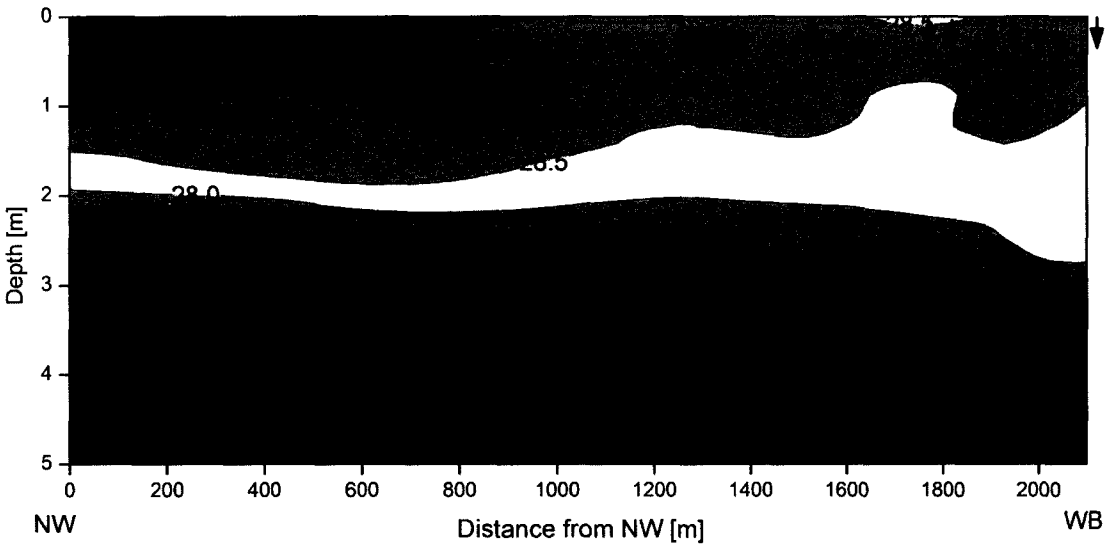

Figure 39. Temperature [C] variation from NW to WB recorded on 06/30/2007.

The spatial variation in temperature for the third transect conducted on June 30, 2007 displays a similar tendency to the June 21 transect. The epilimnion was colder in the upper two meters near the circulators in response to the addition of the cold hypolimnetic water. The increase in volume in the epilimnion combined with withdrawal from 10-meters depth appears to have caused the colder water strata to migrate downward.

Another method of displaying the spatial impact from the surface circulators is to compare the temperature difference between NW and WB. Comparison was conducted by examining the temperature difference (ΔT) for comparable depths at these two sites.

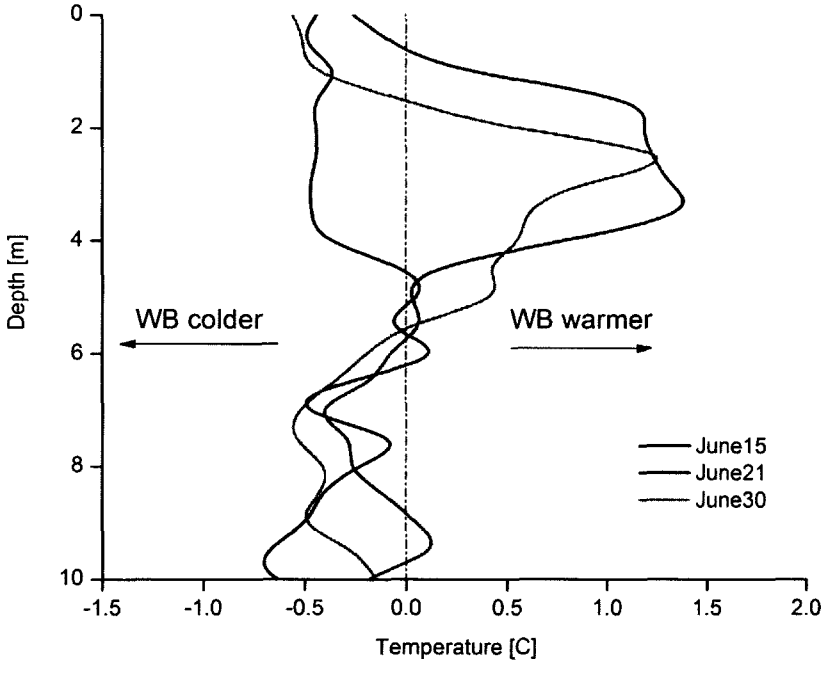

Figure 40. Variation in temperature [C] between the first transect profile (NW) minus the last transect profile (WB) for all three transects.

Figure 40 shows that the surface water temperature was higher at WB than at NW. This is consistent with mixing cold hypolimnetic water at the surface. Then the June 21st and the June 30th transects show a warmer temperature at WB from two meters to five meters. This can easily be misinterpreted. This temperature difference arrives from displacement

of deeper water strata being pushed down in the vicinity of the WB by the increased epilimnetic volume from the circulators.

2.6 Conclusion

An aeration system was installed in Occoquan Reservoir in 1970. It was operated seasonally until the summer of 2006, when the diffuser grid failed. By studying the water quality data from this period it becomes clear that this system represented a significant vertical mixing of the reservoir.

When a late July temperature profile from the surface circulation period (WB - 2007) was compared to the temperature profiles from the aeration period (WB - 2000 to 2005), a significant difference became apparent. The temperature profiles from the aeration period showed no significant thermal stratification, but the 2007 season was significantly stratified. The difference in vertical temperature distribution under circulation conditions caused the change in heat content of the reservoir to be reduced. This is also strong evidence of the reduced vertical mixing during the circulation period.

The circulator flow rate was measured using an ADV. It was found that the direct flow (inside the lift tube) was much less than the manufacturer's specifications. It is calculated that the circulator performance was only about 40% of the specified flow rate. Thermistors mounted to the top of the circulator distribution pans (within the discharge stream) revealed that the circulator performance was reduced during night (from 9:00 pm to 5:00 am).

The near-field of circulator 2 was studied in July 2007 by collection of temperature data within a 5 meter distance from the circulator. Velocity measurements

were also conducted within this field by an ADV. The data showed that significant mixing occurred between the cold discharge water and the warm ambient surface water near the distribution pan. Small evidence of a weak gravity flow could be seen in the velocity field, as the slightly colder mixed water was drifting away from the circulator. The data suggested that no influence occurred below 4 meters depth at the time of the study (July, 2007).

The far-field of the circulators were studied by a 2 km transect from the NW site to the WB site. The main observation from three transects conducted in June 2007 was that the temperature of the epilimnion was not significantly reduced by the operation of the circulators; however, an accumulation of epilimnetic water occurred near the circulators, pushing down the thermocline (by displacement) in this area and the depth of the colder water strata. At the near-field, there was no influence on the temperature distribution below 4 meters depth at the time of the study (June 2007). This suggested that the circulator discharge water was ending up at the lower epilimnion.

CHAPTER III

INFLUENCE OF SURFACE CIRCULATOR OPERATION ON DISSOLVED OXYGEN DISTRIBUTION IN OCCOQUAN RESERVOIR

3.1 Introduction

Dissolved oxygen is perhaps the most important parameter in a reservoir because it has substantial influence on almost every biogeochemical process, and also establishes the habitat necessary for aquatic life. A reservoir considered "high quality" is typically well oxygenated and maintains dissolved oxygen down to the sediments through stratification periods. One significant benefit of well oxygenated reservoirs is the lower release of iron, manganese, and phosphorus from the sediments. Lakes of this type are generally oligotrophic. Mesotrophic and eutrophic lakes have higher oxygen demands in the water column and at the sediments and can experience periods of complete oxygen depletion in the hypolimnion. Hutchinson (1957) reported that a dissolved oxygen concentration above 1.5 mg/L is necessary to keep iron, manganese, and phosphorus from leaching from the sediments to the water column, though manganese may be released at even higher dissolved oxygen concentrations (Carlson and Knocke, 1999). The release of phosphorus is called internal loading and can trigger new cycles of primary production in the reservoir. Prolonged anoxic conditions at the sediment water interface with high internal loading may cause a reservoir to advance into a higher eutrophic state.

There are two main sources of dissolved oxygen in a reservoir. Oxygen can diffuse into the lake from the atmosphere, or it can be added to the photic zone by algal photosynthesis. Algae typically affect epilimnetic dissolved oxygen concentrations in a

diurnal pattern, elevating the oxygen levels during daytime and reducing dissolved oxygen concentrations at night. The phytoplankton community is lake specific and is affected by light and nutrient availability as well as other factors. High concentrations of algae are problematic because on death they become organic detritus and sink through the water column where they can become an organic loading to lower waters where they will represent an oxygen demand (Wetzel, 2001).

The amount of dissolved oxygen that water can hold is strongly dependent on temperature; thus, seasonal variations in water temperature have significant influence on oxygen. The temperature range observed in Occoquan Reservoir is from zero to 30 °C and saturation dissolved oxygen concentrations for this temperature range are 14.6 mg/L to 7.6 mg/L. Atmospheric pressure variations can also influence the saturation concentration, but within a given region these variations have little effect.

Temperature has a secondary impact on the dissolved oxygen distribution of a lake. As discussed in Chapter 2, temperature controls the specific gravity of water, which causes thermal stratification to develop during summer. Thermal stratification controls vertical transport in reservoirs, inhibiting atmospheric oxygen's downward transport across the thermocline. The dissolved oxygen in the hypolimnion will therefore be depleted whenever oxygen demand in this region exceeds vertical (downward) transport from the oxygenated epilimnion/ metalimnion.

There are many sinks of dissolved oxygen in a reservoir. Organic matter originating from the watershed allochtonous and transported to the reservoir by contributing streams is an allochtonous source, and its importance to overall oxygen consumption is a function of its labile nature and the loading relative to internal sources

(autochthonous) of organic matter (e.g., macrophytes). When this biomass dies, it slowly settles through the water column as detritus. Detritus serves as a food source and is metabolized by microorganisms consuming dissolved oxygen in the process. Most of the detritus in moderately deep and productive lakes is not consumed in the water column but accumulates as sediment where the metabolic activities continue along with the dissolved oxygen consumption (Matthews, 2006).

In limnology, the total hypolimnetic oxygen demand (THOD) consists of two categories: the sediment oxygen demand (SOD) and the oxygen demand that takes place in the water column. The amount of oxygen demand that takes place in the water column and at the sediments will vary depending on the reservoir depth and the loading of labile organic matter from the watershed. A reservoir with a deeper hypolimnion will provide a longer time for the organic matter and detritus to be oxidized as it slowly sinks down to the sediments. A more complete oxidation of the organic matter in the water column will lead to a smaller SOD. Beutel (2003) suggested that for reservoirs of high productivity the SOD is typically 75% of the THOD in moderately deep lakes (10 to 15 meters).

The epilimnion in a reservoir is generally well oxygenated because the oxygen exchange with the atmosphere is unhindered. The convective transport within the epilimnion is normally adequate for a complete homogenization. Complete oxygen depletion typically develops at the sediment boundary first. This is due to the high SOD and lack of transport through the thermal boundary. The main mechanism for oxygen depletion is biological respiration of accumulated detritus or other organic matter originating from the watershed and from the lake's primary production. Once the dissolved oxygen in the hypolimnion is depleted, oxygen can no longer serve as an

electron acceptor, so microorganisms must utilize alternative electron acceptors for respiration. Nitrate is the next favorable electron acceptor, and its dissimilatory reduction is referred to as denitrification. Once nitrate is depleted, bacteria successively utilize manganese and iron oxides and then sulfate to satisfy their need for an electron acceptor. These reactions release reduced end products such as ferrous iron (Fe^{2+}), manganous manganese (Mn^{2+}), and sulfide into the water column. The result can be elevated concentrations of metals, sulfides, and nutrients that accumulate in the hypolimnion throughout the period of thermal stratification. A water utility that draws water from above the thermocline will experience a sudden increase in iron and manganese during the fall turn-over as the hypolimnion becomes mixed with the entire water column. This event can be problematic from a treatment point of view.

3.2 Aeration History

Occoquan Reservoir was classified as a "highly eutrophic reservoir" in 1969 based on an intensive study of limnological conditions (Eunpu,1973), and severe taste and odor problems in the late 1960s were attributed to prolific blue-green algae blooms frequently occurring at the upper part of the reservoir. During this period the reservoir also suffered from low dissolved oxygen levels, particularly below a depth of three meters. This severe anoxic condition triggered common water quality problems such as hydrogen sulfide development and elevated iron and manganese concentrations. In 1969, Fairfax County Water Authority (FCWA) embarked upon a program to improve the water quality in Occoquan Reservoir. An artificial destratification system was put into service on April 15, 1970 with the expectation that the thermal stratification of the lower

basin would be reduced to only a few degrees Celsius and the dissolved oxygen concentrations in the hypolimnion would be maintained by the increase in the vertical mixing. The aeration system that was placed into service consisted of three 225-cfm air compressors at 50 psi pressure feeding 3,500 linear feet of air supply tubing and 25,000 feet of weighted piping (Eunpu,1973). The aeration system was tuned by adjusting air valves so that an even bubble distribution was achieved.

Only a small amount of data is available describing the water quality before the aeration system was installed in 1970. Eunpu (1973) published a table containing dissolved oxygen data recorded in 1969 in the vicinity of the dam. These data have been converted into an isoplot illustrating the 1969 dissolved oxygen distribution (Figure 41). It is clear that dissolved oxygen in Occoquan Reservoir was seriously depleted prior to operating the aeration system in 1970. No dissolved oxygen existed at the sediment water interface (SWI) from early May to November, and the redoxcline developed at a depth of three meters in August 1969.

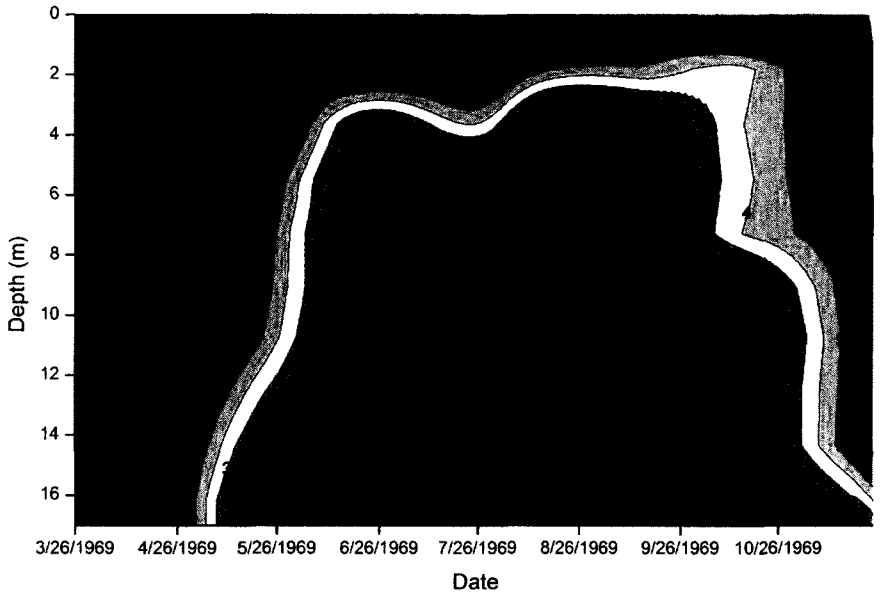

Figure 41. Variation in dissolved oxygen [mg/L] for Occoquan Reservoir lower basin recorded in 1969 (Eunpu, 1973).

A similar plot was constructed based on OWML's data recorded by the dam during 1974 (Figure 42). It is clear that the dissolved oxygen condition was improved by the operation of the aeration system; however, the aeration system did not eliminate hypolimnetic anoxia based on the anoxic event that occurred throughout the summer in 1974. The anoxic boundary was lowered from three to six meters during summer, and the anoxic event was shortened by several months compared to pre-aeration conditions (Figure 42). The shortening of the anoxic period is particularly evident in the fall where the turnover time was accelerated from November to September as a result of operating the aeration system.

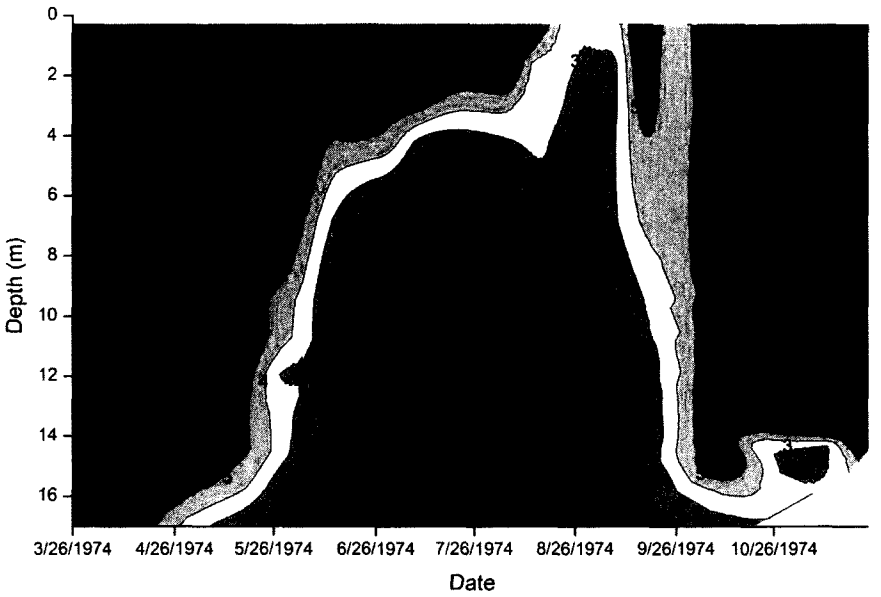

Figure 42. Variation in dissolved oxygen [mg/L] for Occoquan Reservoir lower basin recorded in 1974 (OWML).

Eunpu (1973) concluded that the hydrogen sulfide, iron, and manganese concentration were reduced as a consequence of the increased oxygen concentrations from the aeration system. No prolific algae occurrences were reported after 1970, but copper sulfate was still applied regularly to the upper region of the reservoir where the influence of the aeration system was small. By reducing the algae levels, FCWA was able to use less chlorine and activated carbon at the treatment plant after the aeration system was placed into service (Eunpu, 1973). It was estimated that the aeration system had a pay-back period of four years based on the savings in treatment costs.

3.3 Surface Circulator Operation

When the diffuser lines of the aeration system ruptured in early summer of 2006, Fairfax Water decided to deploy solar powered circulators at the lower basin of Occoquan Reservoir. The circulator manufacturer initially suggested that 20 units should be deployed to ensure an oxygenation significant enough to reduce the manganese levels that were normal during the operation of the aeration system. Due to financial constraints, only eight surface circulators were installed near the dam and in Hooves Cove. The circulator intakes were all set to 10 meters below the surface to build up an oxygen barrier at this depth that would inhibit the Mn from entering the intake at 8 meters.

A schematic of a single surface circulator with its potential influence on dissolved oxygen is illustrated in Figure 43. In this operational condition, colder, oxygen depleted water is withdrawn from the hypolimnion and discharged at the surface where it mixes with the surface water and descends to a depth of equal density. The circulator intake is configured with a bottom plate that is expected to allow water to enter from depths at or above the intake plate.

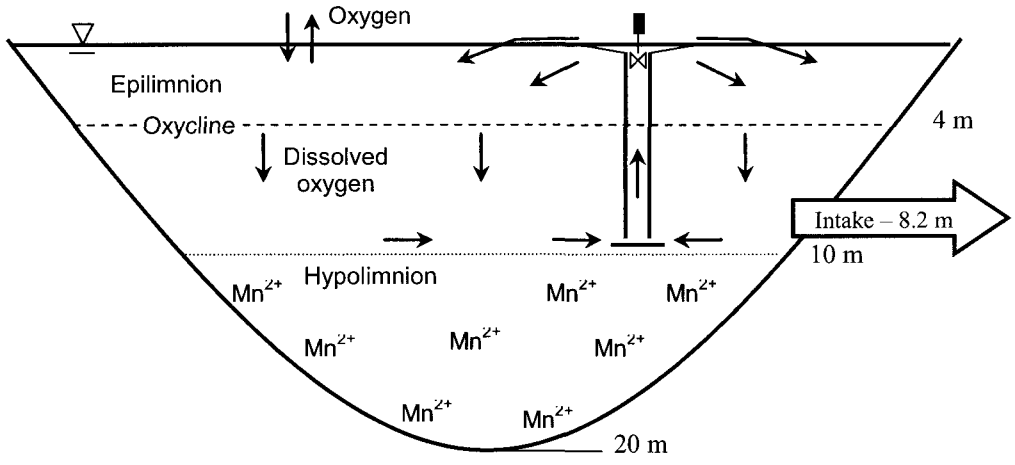

Figure 43. Schematic of surface circulator in Occoquan Reservoir.

Based on historical data the redoxcline in Occoquan Reservoir develops naturally at four meters depth during the summer with water above the redoxcline well oxygenated and near the saturation limit. For oxygenation to improve by circulator operation oxygenated water would need to be transported vertically to depths below the historical oxycline. The maximum depth of Occoquan Reservoir is 20 meters, so water below 10 meters would purposely not be oxygenated by the operation of the surface circulators. This condition would result in sediments below 10 meters depth becoming anoxic during stratified periods and releasing Fe, Mn, ammonia and sulfide to the water column. The amount of these reduced substances present in the hypolimnion would be significantly influenced by the sediment surface area subjected to anoxic conditions. If the oxycline can be lowered from 4 to 10 meters, the sediment area exposed to oxygenated water would decrease from 49 to 14% of the total sediment area in the reservoir. While accumulation of Fe, Mn, and other reduced substances would occur in the hypolimnion the continuous circulation and downward transport of oxygen has been conceptually

suggested to prevent lower quality waters below the circulator intake depth from negatively impacting the water above.

3.4 Methods and Analysis

Many of the methods used for this research were related to measuring dissolved oxygen. During the monitoring conducted from late April 2007 to late October 2007 dissolved oxygen concentrations were measured with a HydroLab DS5 multifunctional probe containing a Hach luminescent dissolved oxygen (LDO) sensor. The sensor was operated and calibrated by the Hydras 3 LT v.2.02 software from OTT and calibrated every two or three weeks. The calibration procedure was based on immersing the sensor in water with 100% oxygen saturation, which was created by vigorously bubbling air through deionized-distilled water in a 1000 mL beaker for over 10 minutes. The LDO sensor was never far off the calibration during these procedures.

During the first sample trip, dissolved oxygen recordings were triggered manually as the datasonde was held motionless at 0.5 meter increments through the water column. For all remaining monitoring efforts, the system was set to collect data automatically every second while the datasonde was lowered slowly through the water column. It took approximately 10 to 15 minutes to lower the datasonde through the water column slowly enough to ensure an accurate characterization of the profile. The benefit of this collection method is an increased resolution of the dissolved oxygen distribution over narrow depth intervals where dissolved oxygen concentrations change dramatically (e.g. redoxcline).

Measurements of manganese concentrations at the WB site were conducted during five sample trips from June 21, 2007 to July 26, 2007. Water samples were collected using a sample rig consisting of high density polyurethane tubing and a peristaltic pump. A sample was collected every other meter from the surface to the bottom, except at 4 meters, which was expected to be similar to the surface sample (collected at 10 cm depth) due to the homogeneous epilimnion. The sample containers were 500 mL polycarbonate bottles that were prepared by washing, acid soaking, and DI rinsing before sampling. The samples were stored in an ice chest during transport to the laboratory. A 100 mL sample aliquot was then poured into a separate container, acidified by addition of 5 mL concentrated trace metal grade nitric acid, and stored at 4 degrees Celsius until analyzed. A model 2100 Perkin Elmer atomic absorption spectrophotometer operated in flame mode was used to analyze manganese concentrations.

To study the circulator's impact on far-field dissolved oxygen conditions, measurements were taken between the NW and WB sites on three dates in June 2007. On each date a series of vertical profiles were recorded 200 meters apart using the same procedures used at the main sampling locations (and described earlier). The location for each profiling site was located by a GPS. Post-processing of field collected data was conducted in Excel, and isopleths were generated in OriginPro v.8.

Exploring the near-field conditions was an important step in understanding the circulator's potential impact on circulation/mixing in the reservoir. The dissolved oxygen concentrations and water velocities were recorded within a plane starting at the edge of the distribution pan and extending from the surface to five meters deep and extending

five meters perpendicular to circulator 3. Two instruments were used in recording oxygen concentrations and flow velocities: the HydroLab DS5 and an acoustic Doppler velocimeter (Nortek Vectrino AVD). Because each circulator had free movement within the slack of its chain to the mooring, circulator 3 was fixed in position by setting two additional anchors. A 5-meter-long wooden support was attached to the circulator's solar panel and supported by a flotation device (empty ice chest) at the opposite end; this assembly can be seen in Figure 16. The wooden support was used to attach the datasonde and cable while the boat was kept 8 to10 meters away to avoid influencing the circulator's flow pattern. Vertical profiles were collected at 0.0, 0.25, 0.5, 0.75, 1.0, 1.5, 2.0, 2.5, 3.0, 3.5, 4.0, and 5.0 meters lateral distance from the circulator's distribution pan.

Understanding the flow behavior of water directly discharged from a circulator and induced circulation from circulator operation is critical in understanding the affect on temperature and dissolved oxygen levels in the lake. The acoustic Doppler velocimeter (ADV) was used for recording flow velocities around circulator 3. The Vectrino is a high resolution acoustic velocimeter which measures the water velocity in an x, y, and z-direction. The Vectrino's local coordinate system is fixed in relation to a marked "finger" on the probe with the marked "finger" indicating the positive x-axis, the y-axis 90 degrees to the left, and the z-axis pointing outward. The Vectrino records x, y, and z-velocities according to its local coordinate system, so keeping the instrument oriented in a purposeful orientation is crucial. A PVC apparatus was made to keep the Vectrino in position and orientation during the measurements of the near-field. This apparatus had a T-section at the end where the Vectrino was attached by tie wraps. The pole was

sectioned so that it could be lengthened to record velocities up to a depth of 5 meters. The pole attachments were marked with a line which helped point the Vectrino when it was too deep to virtually observe. The pole also had depth markings so that the Vectrino could be positioned at 0.1, 0.5, 1.0, 2.0, 3.0, 4.0, and 5.0 meter depths. Velocity measurements at these depths were recorded at 0.5, 1.0, 2.0, 3.0, 4.0, and 5.0 meters from the circulator's distribution pan. The system has been shown previously (Figures 16 and 17).

The Vectrino was operated from a laptop using the Vectrino Plus software at a sampling rate of 50Hz. Each recording was initiated after the data (velocities) settled down after moving the instrument to the new position. Each recording was set to terminate after 2000 samples, so the total sampling time lasted 40 seconds from start to finish; 40 seconds was considered a sufficient duration to cancel out the instrument motion from small waves. Only the x and y-velocities (horizontal and vertical velocities in the vertical plane) were used to describe the two-dimensional flow field. The post-processing involved several steps before a vector-field plot could be made in OriginPro v.8. Each recording (a series of 2000 x and y-velocities) was saved with the appropriate depth and distance designation then exported in ASCII format to Excel where the x and y-velocities were averaged. In order to generate a vector plot in OriginPro v.8, the x and y-velocities were transferred to a velocity and angle format. To better assess the effects of circulator operation, the velocity vector field was finally plotted with near-field plots of the temperature and dissolved oxygen.

The mass of dissolved oxygen contained in the epilimnion and hypolimnion were calculated for Occoquan Reservoir's lower basin, defined as the region extending from

the dam to a point 1000 meters upstream and including Hooes Run (Figure 44). These calculations were conducted for 2007 and for previous years to evaluate total dissolved oxygen content and to calculate depletion rates. An AutoCAD file from OWML's bathymetric survey from 2004 to 2005 with contour lines every two feet was used to find the depth to volume relationship for this region of the reservoir. The lower basin was separated from the remaining reservoir, and the surface area of each depth contour was found by AutoCAD's area calculation tool. The volume of each contour segment was then found by multiplying each contour area by the distance between them (two feet). The depth to volume relationship was then represented as a polynomial equation by using Excel's curve fitting tool. The total oxygen mass for the lower Occoquan Reservoir was calculated by multiplying the volume of depth intervals by the dissolved oxygen concentrations measured at each depth interval. For calculations before 2007 the dissolved oxygen concentrations recorded by OWML at site RE02 were used; site REO2 is closest to site WB1. For the purposes of the analysis the hypolimnion was defined as the depth below five meters. The total hypolimnetic oxygen mass was therefore found by adding the oxygen mass of each depth interval below five meters. The total hypolimnetic oxygen demand (THOD) was determined by characterizing (least-square linear regression) the total hypolimnetic oxygen mass versus time after the spring thermal stratification and extending into May. The THOD was calculated for years between 2000 and 2007 except 2006, which was eliminated from examination as it was a year of partial aeration.

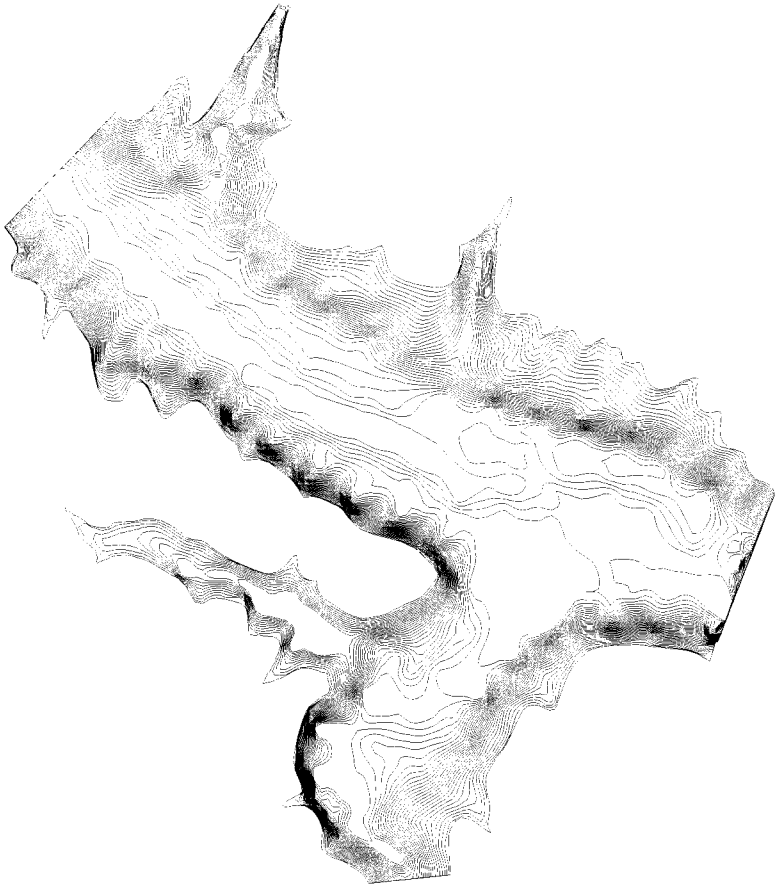

Figure 44. Lower Basin of Occoquan Reservoir with two feet increments between the contour lines.

3.5 RESULTS

3.5.1 Historical Patterns of Dissolved Oxygen

Similar to the examination of temperature profiles presented in Chapter 2, late July dissolved oxygen profiles from 2000 to 2007 were examined to assess the influence of surface circulation relative to years when the aeration system was operated. Late July dissolved oxygen profiles were used because this is the seasonal period when the total oxygen mass is at a minimum in the reservoir. As in Chapter 2, 2006 data are not

included due to failure of the aeration equipment during the middle of the aeration season.

The late July dissolved oxygen concentrations for 2000 to 2007 are plotted in Figure 45 for comparison. The dissolved oxygen profiles for the aeration years from 2000 to 2005 had a gradual oxygen gradient that is typical for a vertically mixed water column. For the 2000 to 2002 seasons the dissolved oxygen was measured at >1mg/L down to 10 meters depth, while for years 2003-2005 only the top 6 meters of the water column had a dissolved oxygen concentration >1mg/L. The dissolved oxygen concentrations at the surface were comparatively lower during 2000-2002, which is another indication of the elevated vertical mixing with the anoxic water from the hypolimnion that took place during these seasons. The other three aeration profiles from 2003 to 2005 showed higher dissolved oxygen concentrations at the surface consistent with lower mixing with oxygen depleted lower waters and the transport of oxygen demanding substances (e.g. Fe^{2+}, Mn^{2+}, H_2S) to the surface. Although the vertical mixing in 2003-2005 appears to have been reduced relative to 2000-2002, all six years exhibit trends that vertical mixing in each of these years was greater and substantially influenced dissolved oxygen concentrations more than in 2007.

It is clear that the 2007 dissolved oxygen profile is different from the other seasons when the aeration system was operating. The 2007 profile has a sharper oxycline, slightly higher near surface oxygen concentrations but a lower volume of oxygenated water (>1mg/L). This vertical dissolved oxygen distribution suggests that in 2007 vertical mixing in the water column was reduced from the previous years of aerator operation.

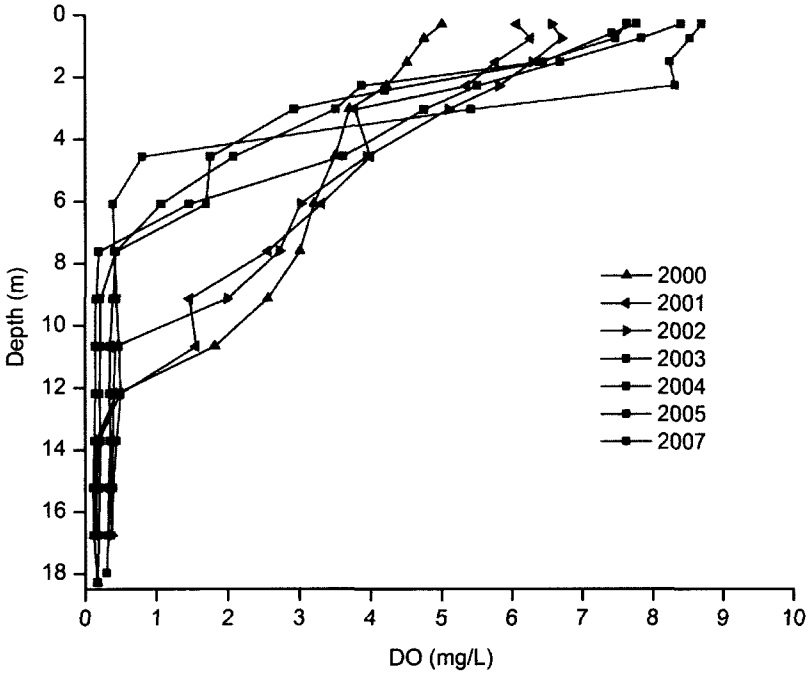

Figure 45. Late July dissolved oxygen profiles at RE02 for Occoquan Reservoir from 2000 to 2007

The trend of decreasing penetration of dissolved oxygen to deeper depths could potentially reflect changes in reservoir operations (e.g. water withdrawal, elevation) or hydrologic or meteorological conditions that influenced stratification and mixing. No changes of this nature occurred during this period; instead, the changes appear related to changes in the condition of the aeration system. Aging of the diffuser system and wear from repeated hydrogen chloride gas exposures to clean the diffusers were considered by Fairfax Water to be the major causes of decreased performance of the aeration grid as evidenced in lower dissolved oxygen concentrations (Greg Prelewicz, personal communication). The decreased penetration of dissolved oxygen could also reflect a change (i.e. increase) in the amount of oxygen demanding constituents in the water

column or the rate at which oxygen demand was exerted. Neither was considered to have occurred or was evident from historical monitoring.

Since the July dissolved oxygen profiles (Figure 45) represent just one period of time and condition and may not reflect other important differences between the circulation period and the previous periods where aeration was occurring, the dissolved oxygen concentrations at specific depths from near surface to near the bottom of the water column were examined (Figure 46).

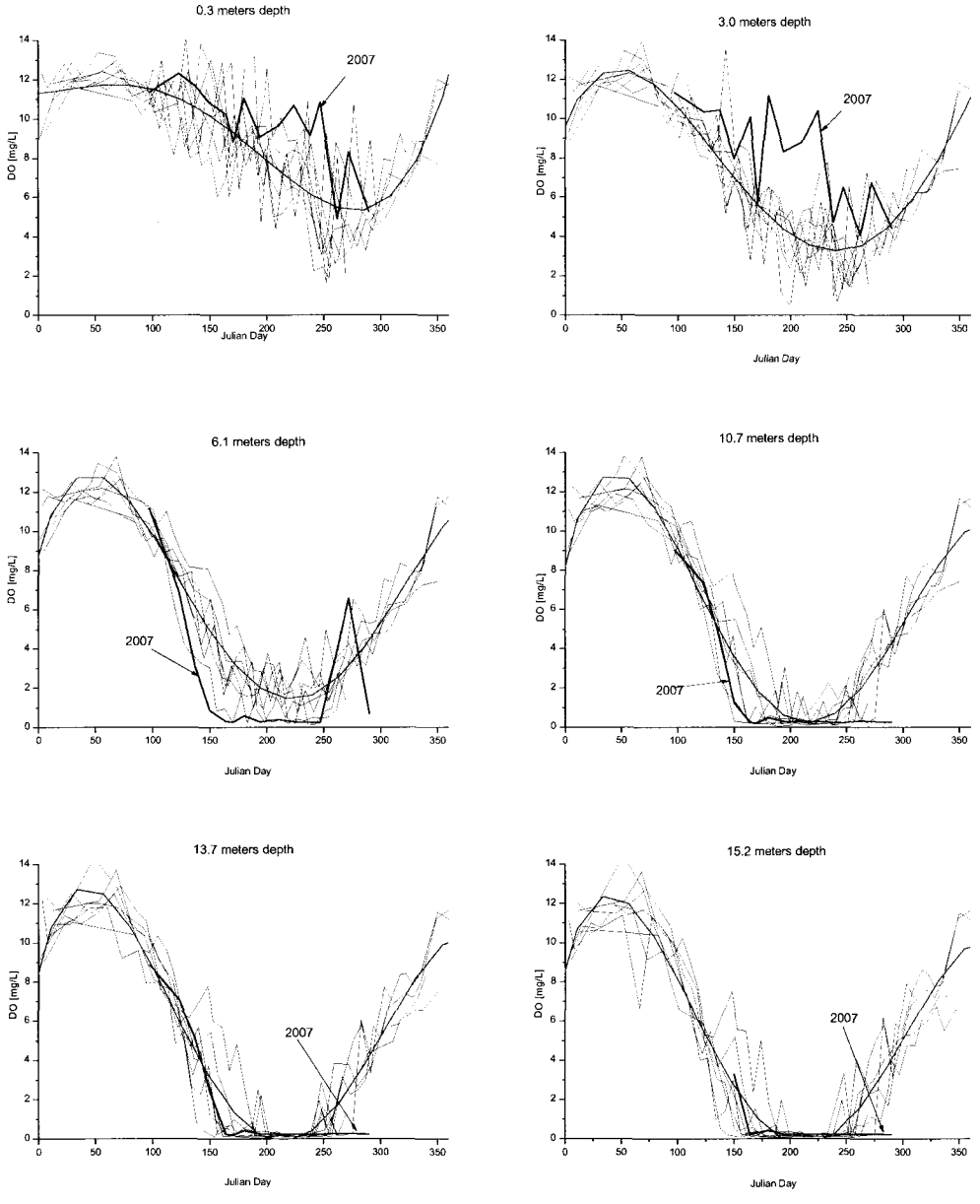

Figure 46. Temperature [C] at various depths of Occoquan Reservoir's lower basin from 2000 to 2007. Smooth blue line indicates the average of years 2000-2005.

The 0.3 meter and 3.0 meter depths were both within the epilimnion, and the dissolved oxygen concentration at these depths was higher than the average oxygen concentration based on the aeration years (2000-2005). Three factors likely contributed to the high

dissolved oxygen concentrations in the epilimnion during 2007. The first factor is a lower degree of mixing and dilution by oxygen poor hypolimnetic water in 2007 compared to aeration years due to aerators producing a much larger vertical flow rate than the circulators. A second factor is the aeration system's ability to introduce more oxygen demanding substances into the epilimnion by its large vertical flow rate compared to the circulators' vertical transport and the knowledge that the diffuser grid is known to re-suspend sediments (Greg Prelewicz, personal communication), thus increasing the oxygen demand in the epilimnion and throughout the water column.

The 6.1 meter and 10.7 meter plots show the opposite trend of the two shallower depths with dissolved oxygen concentrations generally lower during the circulation season of 2007 than the previous aeration seasons. This condition also likely results in the aeration system's addition of oxygen at the lower depths as well as vertical mixing and downward transport of oxygen to a larger degree compared to the circulators. Due to the aeration system enhancing mixing between the epilimnion and hypolimnion, the 6.1 meter and 10.7 meter depths contained more dissolved oxygen due to downward mixing of oxygen-rich epilimnetic water during the operation aeration system. The dissolved oxygen concentration in the 13.7 meter and 15.2 meter plots are not significantly different between the aeration seasons and the circulator season indicating that both systems failed to maintain dissolved oxygen at these depths through the summer period. Once dissolved oxygen is depleted, it is apparent that only destratification and water column mixing following the "natural" cooling of the upper waters in the fall causes reoxygenation of the lower waters. This occurred sooner during aeration years due to the enhanced vertical mixing.

3.5.2 Circulators Influence on the Anoxic Duration

The duration of the anoxic event during aeration versus during circulation was studied during 2002 and 2007 (Figure 47). 2002 was chosen as a representative year for the aeration period because OWML's dissolved oxygen monitoring data appeared to be consistent with the seasons from 2000 to 2005. The 2002 season was also chosen because of a relatively higher sampling frequency than the other seasons.

The length of the anoxic period is primarily controlled by vertical convective transport, which is strongly influenced by the thermal distribution of the water column. After the establishment of thermal stratification in early May, oxygen transport from the surface to the hypolimnion and the sediments essentially ceases and oxygen demand in the water column and the sediments consumes the available oxygen that was present in the hypolimnion at the time of the thermal stratification (Mohseni and Stefan, 2001). The development of anoxia started around May 15 for both the aeration season (2002) and the circulation season (2007) with the difference between the two seasons being the very low oxygen conditions progressed through the water column. The aeration system, with its substantial vertical mixing and addition of oxygen to the hypolimnion, showed a gradual transition of the anoxic boundary from the sediments up to 8 meters depth in the middle of June. Evidence of mixing taking place and influencing water column dissolved oxygen concentrations is evident in the lower oxygen concentration at the surface water during 2002 compared to the circulation season in 2007. The circulation season had rapid oxygen depletion throughout the hypolimnion up to about 6 meters with a sharp oxycline between the epilimnion and metalimnion. A broad oxycline during the aeration

year illustrates the influence of aeration on vertical mixing and suggests a much smaller influence of surface circulators.

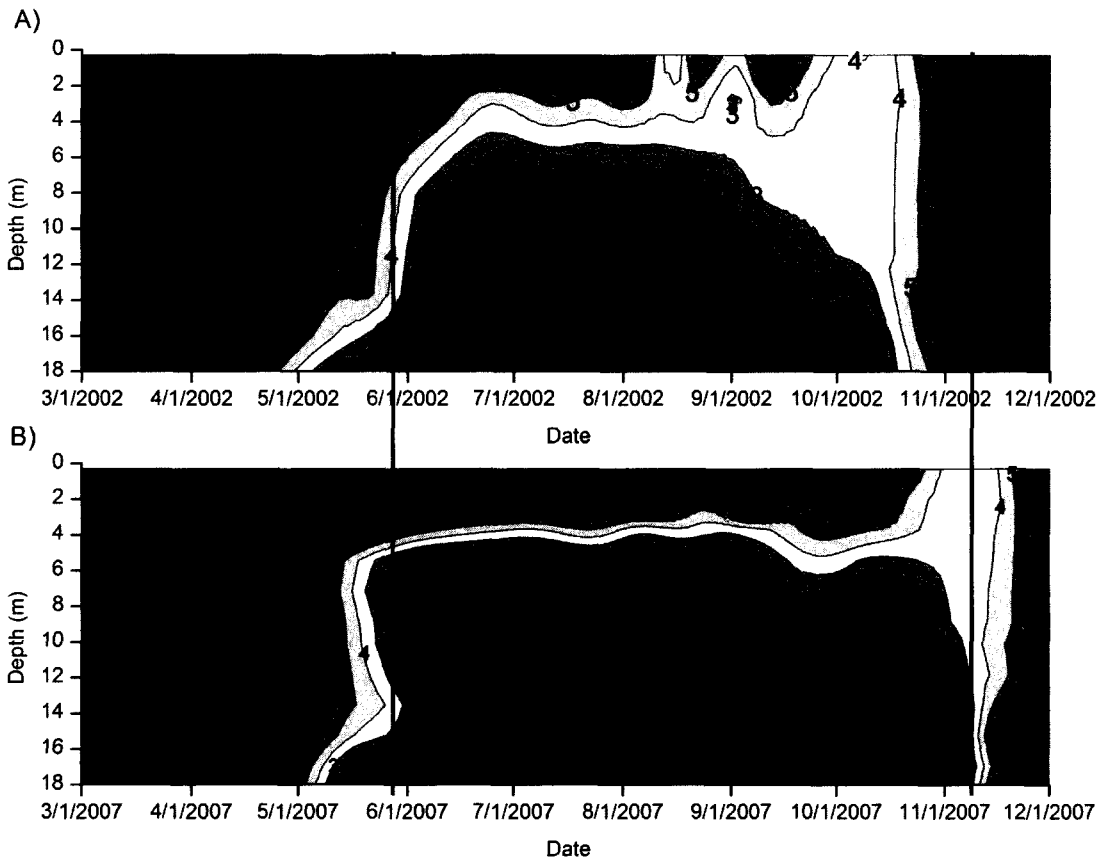

Figure 47. A) Dissolved oxygen concentration [mg/L] at WB location for the 2002 season during the aeration period. B) Dissolved oxygen concentration [mg/L] at WB location for the 2007 season during the surface circulation period.

The aeration system and the circulation system had dramatically different influences on the duration of the anoxic period. It is clear that the aeration system triggered an earlier turn-over and water column than the circulation system with

reoxygenation occurring almost a month earlier during the aeration period compared to the circulation period. Under aeration conditions the reoxygenation occurred over a long period and was a more gradual (but earlier) reoxygenation. This occurrence is consistent with the earlier and more gradual erosion of thermal stratification shown in chapter 2. In 2007, dissolved oxygen conditions were more stable but changed dramatically when destratification occurred. The destratification and reoxygenation appeared similar to unaerated/uncirculated lakes and reservoirs and suggests that the circulators did not substantially influence the event.

3.5.3 Circulators Impact on Gas Transfer

Oxygen diffusion from the atmosphere through the reservoir surface is commonly treated as a two-film process, a condition first postulated by Lewis and Whitman (1924). A thin film is thought to exist on both sides of the gas/liquid interface considered stagnant with gas transport occurring across the interface only by molecular diffusion through the film. Molecular diffusion is a slow transport process, driven by differences in oxygen concentration between the atmosphere and the concentration in the bulk liquid. The overall oxygen transportation rate is limited by the transportation rate through the liquid film (Metcalf and Eddy, 2003) and will therefore be the focus of this discussion.

Figure 48 illustrates the transportation of gas through a two-film model. The main assumptions with this model are that the concentration within the gas bulk phase and the liquid bulk phase are homogeneous (i.e. mixed completely) and that the rate of oxygen mass transfer through a quiescent medium (i.e. liquid film) is linearly correlated

with the mass transfer coefficient through the film and the difference in concentration between the interface and the bulk liquid (3-1).

$$r = k_L * A * (C_s - C_L) \quad (3\text{-}1)$$

where: r = *Rate of oxygen mass transferred per unit area per unit time*

k_L = *Liquid film mass transfer coefficient (e.g. kg/day)*

A = *Interfacial area of oxygen transfer (i.e.* m^2*)*

C_S =*Saturation oxygen concentration (i.e. mg/L)*

C_L = *Oxygen concentration in the bulk liquid (i.e. mg/L)*

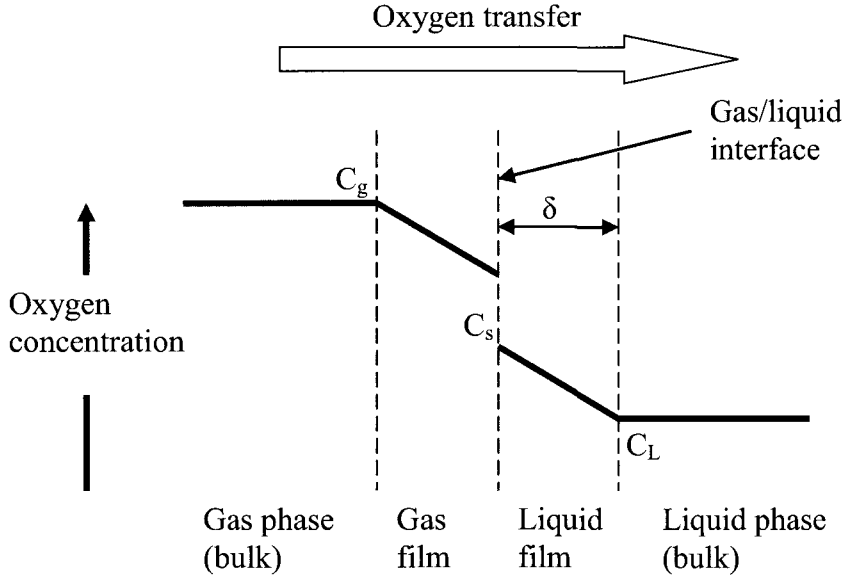

Figure 48. Illustration of oxygen concentration distribution in the two-film theory.

In addition to the effect that the hypolimnetic surface circulators have on the vertical oxygen distribution due to physical mixing, the circulators also affect the oxygen transfer that is taking place locally at each circulator from the atmosphere to the water. Several mechanisms are involved in this process. Because the eight hypolimnetic surface circulators installed in Occoquan Reservoir have intakes set at a depth of 10 meters, the dissolved oxygen concentration of the water rising through the circulators is close to zero from June through October, as can be seen in Figure 47. According to equation (1), the overall oxygen mass transfer rate increases locally at each circulator as the difference in oxygen concentration between the atmosphere and the water flowing over the distribution pan increases. This increased oxygen gradient caused by introducing anoxic hypolimnetic circulation water at the surface is a major contributor to the enhanced oxygen transfer taking place over the distribution plate. As water leaves the distribution plate, it mixes with the epilimnetic water in the reservoir, so the resulting dissolved oxygen concentration will increase to saturated levels. The dissolved oxygen mixing in the near-field will be addressed later in this chapter.

The second factor influencing the oxygen transfer rate through the surface of a lake is to introduce turbulence within the liquid. The result of turbulence near the surface is a reduction of the liquid film thickness so that the distance for molecular diffusion is shortened, and the K_L value and the overall oxygen mass transfer rate are increased. Alves et al. (1970) derived an equation for calculating the oxygen transfer coefficient for an eddy cell model:

$$k_L = 0.40\ (\upsilon/D_m)^{-1/2}\ (\varepsilon\upsilon)^{1/4} \qquad (3\text{-}2)$$

where: υ = *kinematic viscosity of water*

ε = *rate of energy dissipation*

D_m = *molecular diffusivity of oxygen*

When the rate of energy dissipation (ε) is increased in equation (3-2), the overall liquid oxygen mass transfer coefficient (K_L) also increases. Bimlesh and Rao (2009) describe how the energy dissipation rate correlates with the power input and the water volume. Although equation (3-3) is developed for a cylindrical tank with a paddle-type rotor, it is assumed that the conditions are similar for the surface circulators that are deployed in Occoquan Reservoir with a shallow depth (15 cm) over the impeller and significant turbulence visible at the surface over the distribution pan.

$$\varepsilon = (P/V)^{1.08}\ e^{0.005\ (P/V)\text{^}-6.02} \qquad (3\text{-}3)$$

According to the manufacturer, it takes 24 watts of power to rotate the impeller at 60 rpm. The volume of water inside the distribution pan of a circulator is estimated at 0.40 m^3. Using (3-3), an energy dissipation rate of 84.11 W/kg was calculated. Plugging this value into (3-2) with the kinematic viscosity of 0.903 x 10^{-6} (m^2/s) at 25 °C, and a molecular diffusivity of oxygen of 2.0 x 10^{-9} (m^2/s), one gets a k_L value of 6.34 m/h. Finding the rate of oxygen mass transferred per unit area per unit time by using (3-1) with C_S equal to the oxygen saturation concentration of water at 25 °C (8.5 mg/L) and a C_L of 0.0 mg/L dissolved oxygen for the hypolimnetic circulation water. The circulator surface area is 2.63 m^2. It was found that the oxygen mass transfer rate was 142 g/h oxygen per circulator.

A similar calculation was conducted for a lake surface area similar to a circulator but without any turbulence. This was so that a comparison of oxygen transfer rate could be completed. The most basic method of calculating the oxygen transfer rate (k_L) is described by the Whiteman film model shown in (3-4), and found by dividing the molecular diffusivity of oxygen of 6.7 x 10^{-6} m^2/h by the estimated liquid film-thickness 2.0 x 10^{-5} m (Metcalf and Eddy, 2003). Based on the coefficient of molecular diffusion for oxygen and the estimated film thickness (Becker, 1924), the oxygen transfer rate (k_L) was calculated to be 0.335 m/h.

$$k_L = D_m/H_l \tag{3-4}$$

where: D_m = molecular diffusivity of oxygen

H_1 = liquid film thickness

By plugging this value into equation 1, the overall oxygen mass transfer rate is calculated. The surface concentration is assumed to be equal to the oxygen saturation in water at 25 °C of 8.5 mg/L; however, the bulk liquid concentration was assumed to be 8.0 mg/L. The overall oxygen mass transfer rate was calculated to be 0.44 g/h for the lake surface without any agitation.

It has been shown that the surface area over the circulator transfers significantly more oxygen to the reservoir than a similar natural surface area on the reservoir with no circulation. The area over the distribution pan therefore has about 325 times the oxygen transfer to the reservoir than a similar lake surface with no agitation (i.e. absolute quiescent condition).

3.5.4 Vertical Oxygen Mass Distribution in the Lower Basin

Eight surface circulators were deployed in Occoquan Reservoir's lower basin in an effort to raise the dissolved oxygen level in the water column during the thermal stratification and prevent manganese from accumulating in the upper hypolimnion where it would be withdrawn to the water treatment plant. The lower basin of the reservoir was defined as the area between the dam and 1000 meters upstream. The volume to depth relationship for this part of the reservoir was calculated based on OWML's bathymetry survey from 2005. The method for deriving this hypsographic relationship is described in the method section earlier in this chapter. The oxygen mass generated by the surface circulators could not be determined by comparison with the natural oxygen distribution of Occoquan Reservoir because artificial mixing has been conducted every year since 1970. Therefore, the oxygen mass had to be compared between the aeration period and the circulation period. The oxygen mass was divided into epilimnetic oxygen mass (above 5 meters) and hypolimnetic oxygen mass (below 5 meters). Oxygen masses were calculated from 2000 to 2005 representing the aeration period and for 2007 representing the surface circulation season. OWML's vertical oxygen profiles at RE02 were the basis for these calculations, which are described in detail in the methods section in this chapter.

The total epilimnetic mass of oxygen (kg) for the lower basin was calculated for 2000-2005 and for 2007, as shown in Figure 49. There is a strong seasonal influence on total mass that directly derives from the temperature influence (inverse relationship) on the solubility of dissolved oxygen. It is important to note that 2007 was an unusual year with respect to winter temperatures. Ice formation developed in early January — a rare event for Occoquan Reservoir — due to the cold weather. This can be seen in the

weather buoy temperature and dissolved oxygen data displayed in Figure 50, where 2007 conditions are compared with 2006 conditions.

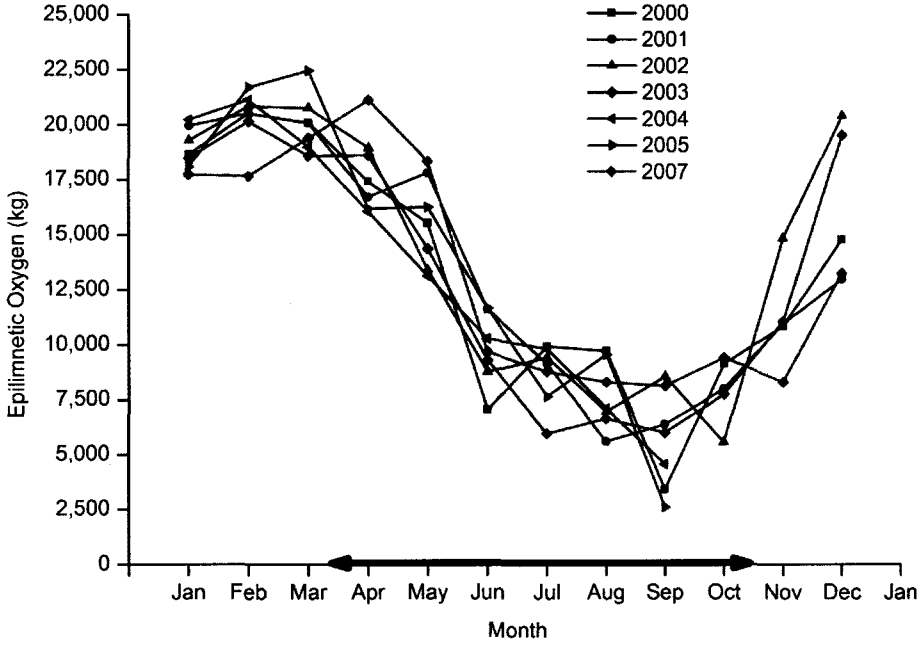

Figure 49. Total epilimnetic oxygen mass (above five meter) for Occoquan Reservoir's lower basin. Arrow along the horizontal axis indicates the period over which the aerators operated in 2000-2005.

Figure 49 shows that the total epilimnetic oxygen mass during January and February 2007 were lower than the previous years. This is likely a reflection of the ice cover that occurred during this period hindering oxygen exchange with the atmosphere. The total epilimnetic oxygen mass was a little higher in April and May 2007 compared to the other seasons (2000 to 2005). This likely reflects the seasonal start-up of the aeration system that typically took place during this period (personal communication with Fairfax Water).

It is observed that the oxygen masses during June to November were very stable compared to the previous six seasons. This reflects the high stability of the water column during 2007 with little influence from vertical lake transport.

The epilimnetic oxygen mass is affected by temperature and vertical mixing of the water column. The vertical mixing was much more significant during the aeration period (2000 to 2005) than during the circulation period (2007). The aeration system introduced a larger flow of low oxygen hypolimnetic water to the epilimnion, thus lowering the oxygen concentration and oxygen mass in the epilimnion. As discussed earlier, the aeration system triggered an earlier fall turn-over but also resulted in a higher oxygen transfer to the reservoir as seen in Figure 47. Therefore, the reservoir had a quicker oxygen recovery after the turn-over event during the aeration years (2000 to 2005), which can be seen as higher oxygen mass in the entire water column (Figure 49 and Figure 51) in November compared to the circulation year (2007). The circulators produced a lower epilimnetic oxygen mass in November due to a later turn-over date due to increased water column stability, increased buildup of oxygen demand in the hypolimnetic water due to a longer and more severe anoxic period, and less overall oxygen transfer to the reservoir from the atmosphere compared to during the aeration period. A general observation is that the circulation season (2007) had a slightly elevated epilimnetic oxygen mass during the late summer (August to October) than the average aeration seasons. This is related to the relatively small vertical mixing produced by the circulators and the relatively small volume of oxygen poor hypolimnetic water that the circulators introduced to the epilimnion.

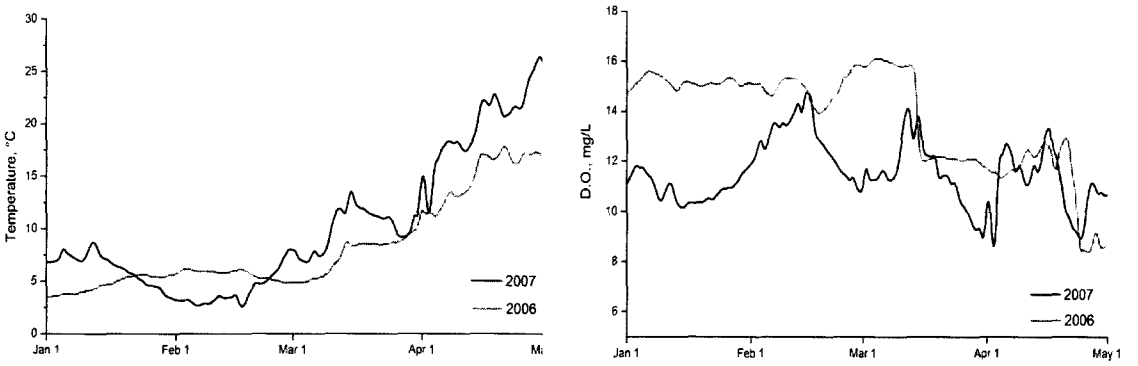

Figure 50. Weather buoy data from the lower reservoir during 2006 and 2007 at 2 feet below the surface.

The monthly hypolimnetic oxygen mass was calculated in a similar manner as the epilimnetic oxygen mass and is displayed in Figure 51. The monthly hypolimnetic oxygen masses were generally lower during the circulation period (2007) compared to the aeration years (2000 to 2005) and, as noted earlier, are likely due to the aeration system's inducement of greater vertical mixing. The oxygen mass in January and February, 2007 are thought to be due to the ice formation mentioned earlier. An interesting observation is that the 2007 season had the highest oxygen mass in May and the lowest oxygen mass in June. This observation is discussed in more detail in the next chapter.

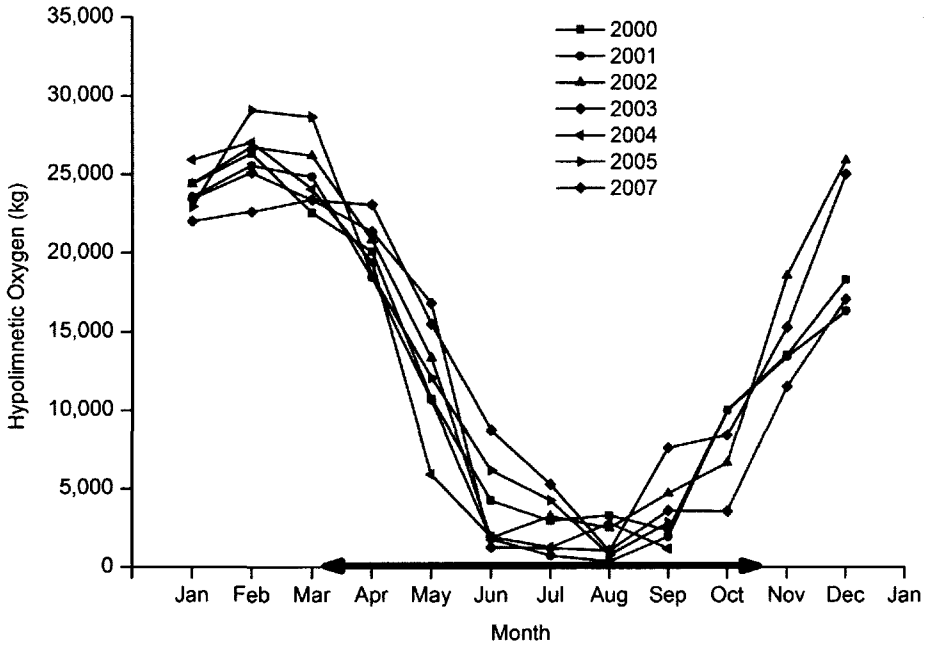

Figure 51. Total hypolimnetic oxygen mass (below five meter) for Occoquan Reservoir's lower basin. Arrow along the horizontal axis indicates the period over which the aerators operated in 2000-2005.

The low hypolimnetic oxygen mass during October and November 2007 is related to the circulator's later turn-over date due to increased water column stability, increased buildup of oxygen demand in the hypolimnetic water due to a longer and more severe anoxic period, and less oxygen transfer and vertical transport to the hypolimnion compared to during the aeration period. During the aeration years, the thermal stratification was weaker, and the stratification period ended earlier. Therefore, the oxygen levels recovered quicker during the period of aeration (2000 to 2005).

3.5.5 Oxygen Depletion

Understanding the sources and sinks of oxygen is important when designing or evaluating an oxygenation system in a reservoir. To maintain dissolved oxygen concentrations throughout a stratified period the oxygenation system must transfer oxygen at a sufficient rate such that anoxia does not occur before destratification, when natural mixing and oxygen transfer from the atmosphere is resupplying oxygen to the lower waters. It has been observed in many systems that the oxygen demand increases when lake aeration is initiated. Soltero et al. (1994) explain this phenomenon as a shift from anoxic to aerobic decomposition and an increase in the bacteria concentration. It has also been suggested that increased hypolimnetic aeration results in a higher flow velocity over the sediments that will increase the oxygen demand as demonstrated by Mackenthun and Stefan (1998). Re-suspension of sediments can also occur which will increase the oxygen demand. This increase in oxygen demand in response to long term oxygenation has caused many aeration systems to be under sized (McQueen et al., 1984). When evaluating an oxygenation system for a reservoir, studying the oxygen source and sink dynamics during the operation of the oxygenation system is crucial. It is therefore important to quantify the oxygen demand of the reservoir which has to be overcome by the system's oxygen supply, if anoxic conditions are to be avoided. The oxygen budget will therefore be studied during the operation of the surface circulators and compared with the oxygen budget from the aeration period.

The total net-hypolimnetic oxygen demand (net-THOD) was calculated for Occoquan Reservoir's lower basin each year from 2000 to 2007 to assess any differences between the years when the aeration system and the one full stratification season the

circulation system were operated. The net-THOD values represent the rate that hypolimnetic dissolved oxygen was consumed while the aeration system or the surface circulation system was adding oxygen. For each year, hypolimnetic oxygen mass from early May, after stratification was established, until the mass decreased to below 2,000 kg was used to calculate the net-THOD. As an example, Figure 52 shows three dissolved oxygen profiles recorded at W2 during different dates in May 2007 (circulation period) that clearly illustrate how hypolimnetic oxygen was consumed as a function of time.

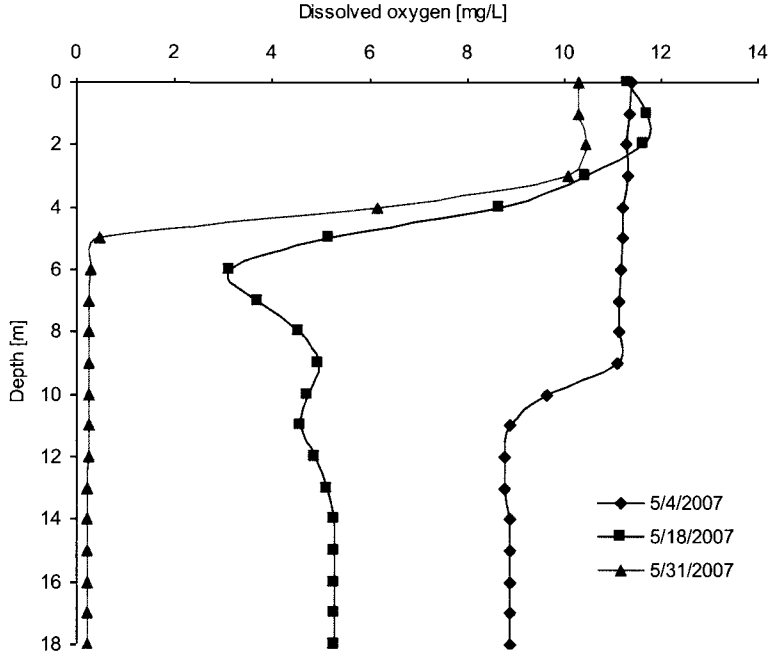

Figure 52. Three dissolved oxygen profiles from site WB during May 2007.

It is clear that the oxygen supply from the circulators did not satisfy the oxygen demand exerted by the water column and the sediments during May 2007. The change in the

hypolimnetic mass of oxygen for all the years evaluated in this study shows that the depletion occurs largely over a period of one month (Figure 53). The start date and the end date for the net-THOD and the net-AHOD are displayed in Table 6.

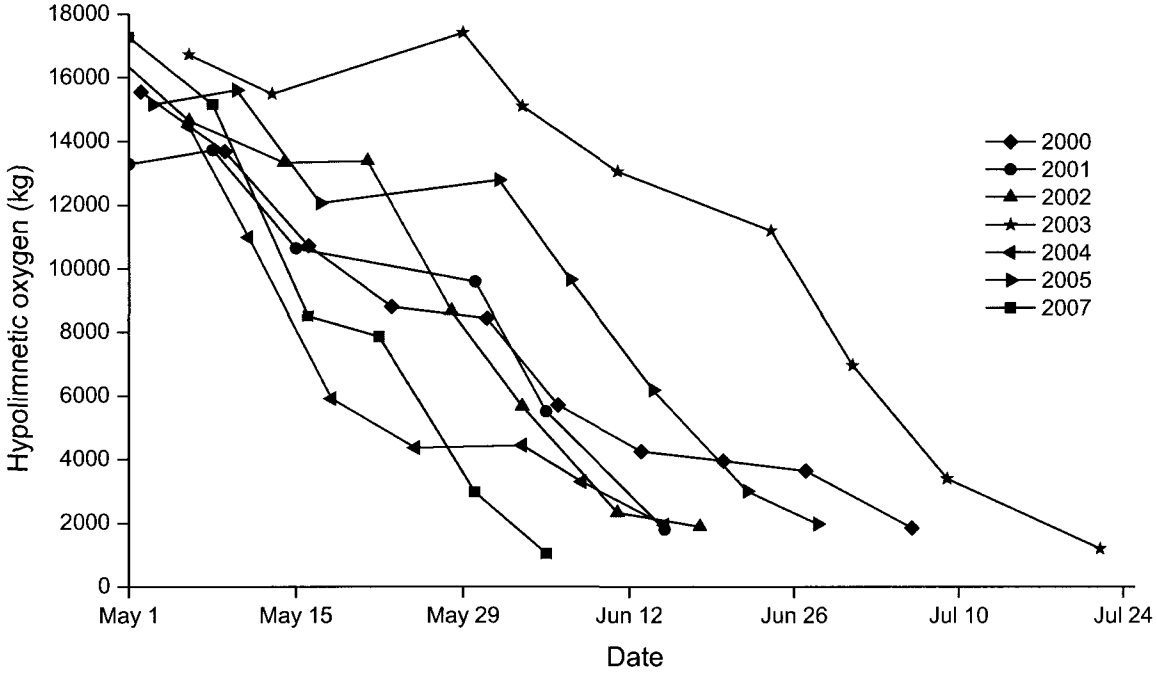

Figure 53. Plot of total hypolimnetic oxygen [kg] for Occoquan Reservoir's lower basin. The slope represents the hypolimnetic oxygen demand.

Table 6. Summary of data involved in calculating the HOD and the AHOD.

Year	Start Date	End Date	HOD [kg/d]	Std. Error +/-	AHOD [mg/m^2 d]	Std. Error +/-
2000	5/2	7/6	264	9.4	974	34.7
2001	5/1	6/15	292	19.7	1,080	72.5
2002	4/30	6/18	335	10.9	1,240	40.0
2003	5/6	7/22	268	18.2	989	67.0
2004	5/6	6/15	279	28.0	1,030	103.1
2005	5/3	6/28	236	5.7	871	21.0
2007	5/1	6/5	482	18.7	1,780	68.8

Dissolved oxygen mass was relatively similar in early May, and for the 2000-2005 seasons it appeared to decrease at similar rates. It is assumed that the natural oxygen demand was similar for all the seasons considered, leaving the difference in the rate that the dissolved oxygen disappeared to represent the differences in the amount of dissolved oxygen that each oxygenation system provided. A linear regression analysis was conducted for each season displayed as a curve in Figure 53 to find the slope which represents the rate of decline in oxygen mass. This oxygen decline can only be observed in spring at the onset of the thermal stratification. During this period the oxygen concentration is high, but the thermal stratification efficiently cut the supply of oxygen to the hypolimnion. The results of these regressions are displayed in Figure 54. The error bar represents the standard error from each season's linear regression.

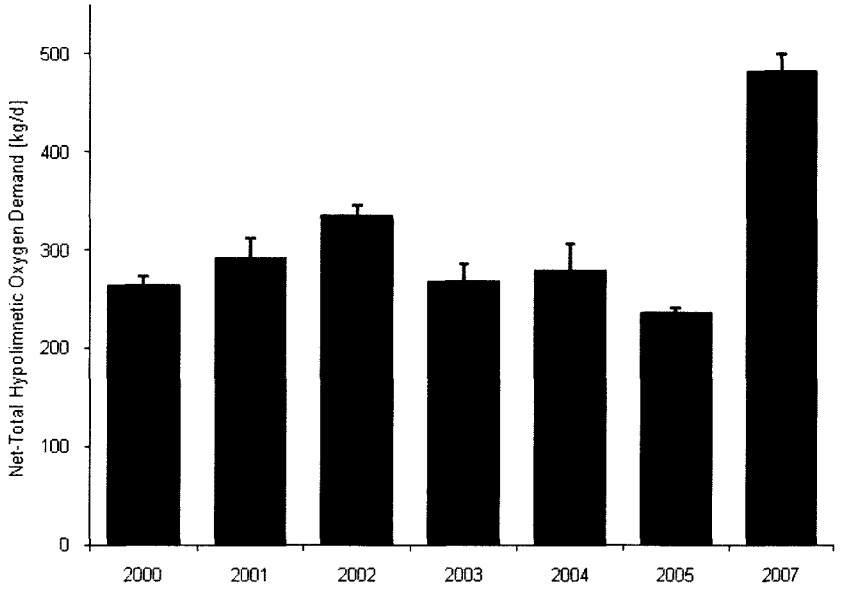

Figure 54. Net hypolimnetic oxygen demand [kg/d] from 2000 to 2007 representing the deficit in oxygen supply to the hypolimnion in Occoquan Reservoir lower basin.

As previously noted the net-THOD values reflect the net rate of depletion with the gross rate of depletion (THOD) unknown but higher than these values. The aeration seasons (2000 through 2005) had similar net-THOD values averaging 279 kg per day and ranging from 236 to 335 kg/d during this period. During the circulation season of 2007, the oxygen mass disappeared more than 200 kg/d faster than the average decline rate during the aeration seasons. The likely reason for the high THOD in 2007 was that the circulators provided less oxygen to the hypolimnion than the aeration system provided in previous years. It is entirely likely that the gross THOD during aeration years exceeded the gross THOD of 2007 due to the increased mixing and likely higher velocities at the sediment water interface.

A reservoir's oxygen demand is often reported on an areal basis, allowing lakes and reservoirs to be compared and is referred to as the areal hypolimnetic oxygen demand (AHOD). The net-AHOD for the Occoquan Reservoir was calculated by dividing the net-THOD by the surface area of the reservoir at the depth of the hypolimnion. The hypolimnetic boundary typically descends gradually from May through October but was set at 5 meters below the surface for these calculations. The average net-AHOD value of the aeration years (2000 through 2005) was about 1,000 mg/m^2 d, while the 2007 net-AHOD value was 1,780 mg/m^2 d. (Figure 55). Similar to the net-THOD values, it is assumed that the sediment oxygen demand is relatively consistent within these years, leaving the net difference to represent the differences in the efficiency to supply dissolved oxygen to the hypolimnion.

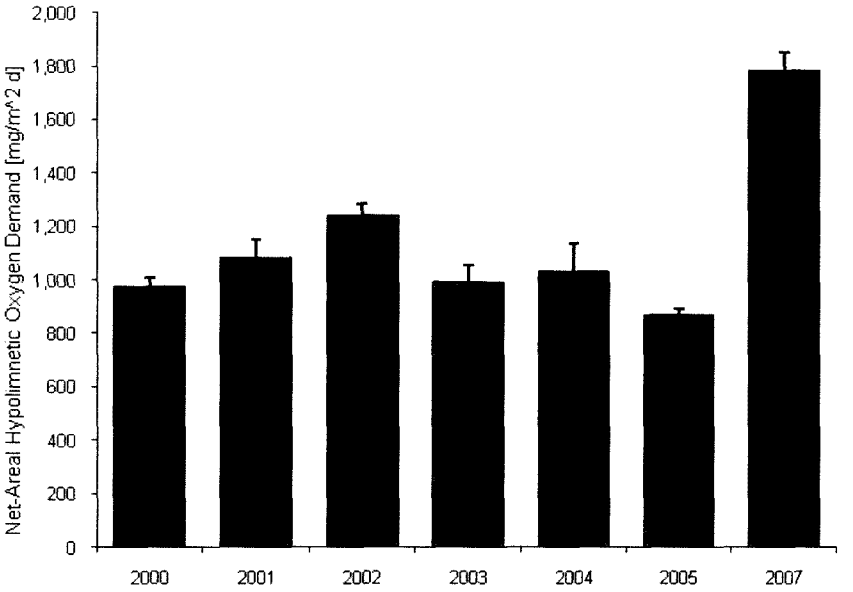

Figure 55. Hypolimnetic areal oxygen demand [mg/m^2 d] from 2000 to 2007.

If one assumes that the surface circulators supplied an insignificant amount of dissolved oxygen to the hypolimnion, then the net-AHOD value of 2007 (1,777 mg/m^2 d) would become the AHOD, which can be compared with other AHOD values from lakes in the literature (Table 7). It can be seen that the calculated AHOD value for Occoquan Reservoir falls within the natural range; however, it is likely that the actual AHOD value of the reservoir is a little higher than the calculated value due to the effect of operating the surface circulators.

Table 7. Comparison of yearly mean AHOD values for various lakes.

Site	AHOD [mg O_2/m^2 day]	Reference
New Meadows upper lake, MA	2,000	Bridges, 2009
Lake Ewana, OR	1,800	Doyle, 2005
Lake Lyndon B. Johnson, MI	1,700 – 5,800	Schnoor, 1979
Broken Bow	1,490	Veenstra, 1991
Texoma	1,690	Veenstra, 1991

Birch	3,200	Veenstra, 1991
Pine Creek	3,390	Veenstra, 1991
Lake Sammamish, WA	1,000	Bella, 1970
Occoquan Reservoir, VA	1,780	This study

Ultimately, the AHOD for a specific reservoir is dependent on the external and internal loading of organic matter to the hypolimnion and the oxygen demand that has accumulated in the sediments. It has been suggested that long term (10 years +) oxygenation of a reservoir will reduce the AHOD by allowing a more complete degradation of the organic matter in the sediments by increasing the hypolimnetic oxygen concentration (McQueen et al., 1984), but more frequently it has been reported that the AHOD increases with long term oxygenation. The main causes for this are decreased settling velocity of the detritus (Ashley, 1983) and a shift from an anaerobic microorganism community in the hypolimnetic water column and in the sediment to a more effective and oxygen consuming aerobic community (Soltero et al. 1994).

3.5.6 Impact of Circulator Operation on Dissolved Oxygen in the Near-Field

The near-field spatial distribution of dissolved oxygen was studied to better understand the mixing induced by circulator operation, the fate of the hypolimnetic circulation water, and the impact of releasing anoxic water at the reservoir surface. Most of the measurable water movement was taking place a few meters from the circulator, so the near-field was defined as the distance out to five meters from the circulator. During initial measurements, it became clear that there was no apparent influence on the

dissolved oxygen concentration below the thermocline, so the near-field was limited to a depth of five meters.

The near-field dissolved oxygen distribution is represented with near-field velocities (represented as a vector field) to better explore the relationship between water movement and the dissolved oxygen concentration (Figure 56); each arrow represents a water velocity at the arrowhead and a flow orientation. The range of velocities was within 0.001 and 0.057 m/s indicated by the length of the arrows. The orientation of the flow is indicated by the direction of the arrows.

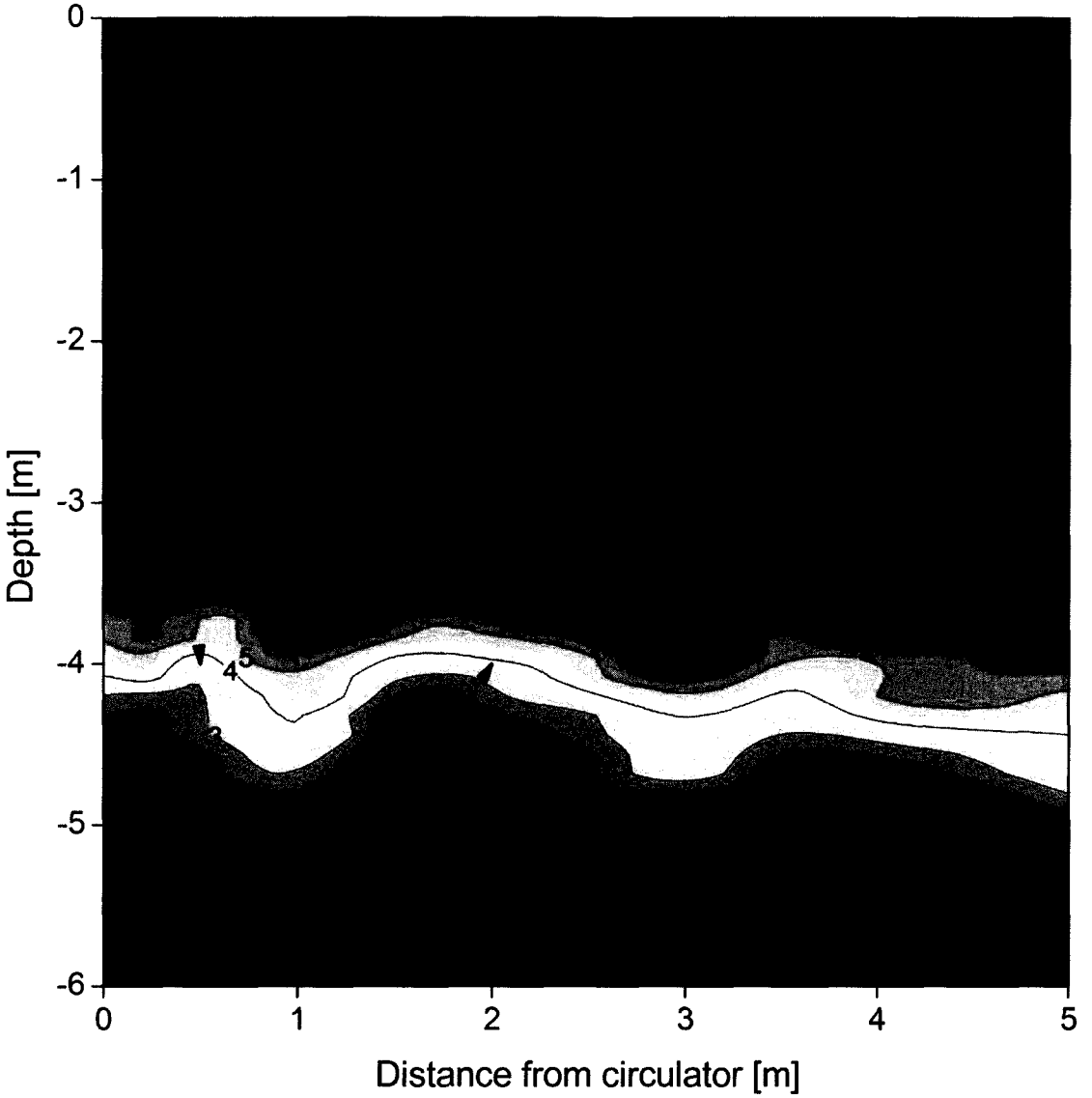

Figure 56. Near field dissolved oxygen isoplot including the flow field described by vectors around circulator 2 in July 2007.

In this graphic, flow from the distribution pan enters at the upper left corner, as can be seen by the velocity vector field and also by observing the slightly lower dissolved oxygen concentration in this area. The lower dissolved oxygen concentration dissipates quickly after leaving the circulator indicating that substantial mixing is taking place

between the water exiting the circulator and the surrounding water. It appears that a weak "plume" was descending from the distribution pan down to about four meters due to the colder, denser water from the hypolimnion being released into the warmer, less dense epilimnion. This density driven transport was apparent with the near-field temperature profiles and velocity vectors as shown in Chapter 2 (Figure 33). This density current was not well formed and was difficult to track outside three to four meters from the circulator. From the velocity vector profile it appears that water that is discharging from the circulator is entraining water from underneath the pan as it leaves the circulator. This flow pattern is likely the result of viscous shear forces between the water layers, although there is an opening/slot at the top of the riser tube below the distribution pan that might release water and contribute to the observed velocity field. However, no evidence of low levels of dissolved oxygen is seen, so it is unlikely that water discharge through this slot is significant if it occurs.

The composition of water inside the distribution pan of circulator 3 was measured multiple times during 2007 by submerging the field probe into the pool of circulation water inside the distribution pan. All the monitored parameters showed similar values as was recorded at 10 meters by the WB, except for the dissolved oxygen concentration which was on average 2 mg/L higher inside the distribution disk (Table 8). This could either be the result of rapid oxygen transfer from the atmosphere accelerated by the turbulent flow that exists inside the circulator distribution pan, or it could be the influence of water flowing into the slot beneath the distribution pan and being mixed into the hypolimnetic circulation water. A reverse flow through the slot into the distribution pan (Figure 57 B) is contrary to the manufacturer's flow description (Figure 57 A) and is

unlikely based on multiple temperature comparisons between the pan and the adjacent water column at intake depth (10 meters). Table 8 also shows the water quality parameters at 1 meter depth. These values suggest that the water was flowing into the hidden slow below the distribution pan as shown in Figure 57 b.

Table 8. Comparison of water quality parameters inside circulator 3 and at WB at 1 and 10 meter.

	6/14/2007			6/29/2007			7/14/2007			7/21/2007		
	Circ. - 3	10 m	1 m	Circ. - 3	10 m	1 m	Circ. - 3	10 m	1 m	Circ. - 3	10 m	1 m
Temp	13.3	13.4	25.9	15.8	16	29.1	16.4	16.5	28.6	16.2	16.3	28.8
DO	1.93	0.22	8.8	2.4	0.24	13.0	2	0.3	9.2	2.7	0.3	10.4
pH	7.8	7.6	8.5	9.7	9.6	11.1	10.1	10.1	11.3	10.5	10.4	11.9
Chl-a	5.5	4.4	10.0	2.4	3.2	1.8	4.7	3.6	10.0	6.6	3.7	16.7

The temperatures were consistently similar, which suggests that the 2 mg/L oxygen increase must occur at the distribution pan of the circulator. It is believed that a rapid increase in the dissolved oxygen concentration is possible at the top of the distribution pan based on observations of the turbulent mixing occurring directly above the impeller during circulator operation.

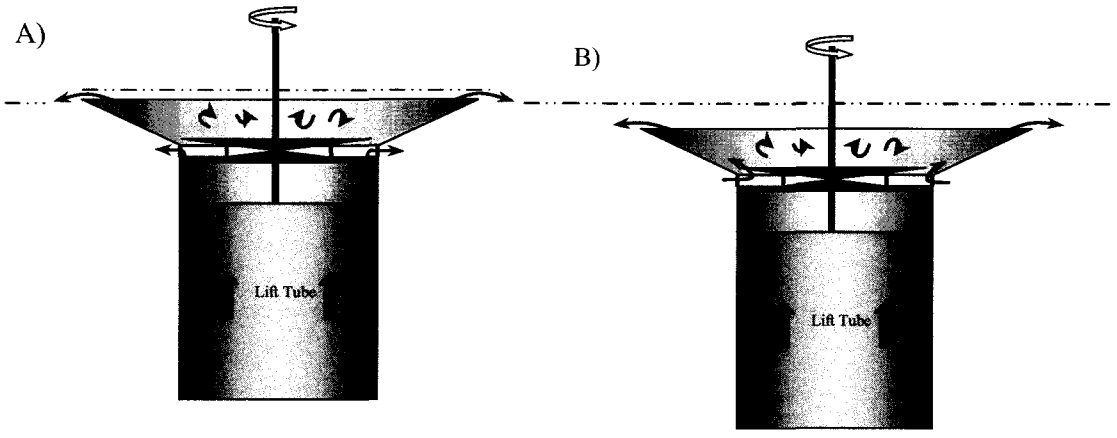

Figure 57. A) Flow pattern illustrating water leaving the slot below the distribution pan. B) Reversed flow through the slot under the distribution pan.

The existence of the circulator slot was discovered during the late summer of 2007 after ADV measurements of velocity were completed. Consequently, examination of the velocity field immediately adjacent to the slot was not conducted. The flow through the slot is assumed to be affected and possibly dictated by the head above the pan. If the pan is positioned deeper below the surface, the lack of head on top of the pan could possibly allow water to enter through the slot (reverse flow) as the head pressure is less prominent. In Occoquan Reservoir, the distribution pans were about 7 cm below the surface and consequently a small head condition would follow. This suggests a reversed flow through the slot as shown in Figure 57 B. The flow pattern described by the velocity vectors in Figure 56 does not show any evidence of water flowing through the slot as shown in Figure 57A. Judging by how fast oxygen was introduced to the hypolimnetic circulation water inside the distribution pan, it is likely that oxygen rich epilimnetic water (at one meter) was entering through the slot in the reverse flow direction.

The circulator's ability to lower the oxygen concentration in the epilimnion is dependent on the hypolimnetic circulation flow rate, the epilimnetic volume, and the reoxygenation rate. A reservoir with a small epilimnetic volume and a large hypolimnetic circulation flow rate will likely show signs of reduced oxygen concentration in the epilimnion under a normal reoxygenation rate. Occoquan Reservoir's epilimnetic volume is relatively large related to the circulation flow rate. This makes the reoxygenation rate less likely to be the limiting factor in the process of reaching epilimnetic oxygen saturation. It is clear that the flow rate is too small to reduce the epilimnetic dissolved oxygen concentration significantly by studying the near-field in Figure 56.

3.5.7 Circulator's Dissolved Oxygen Impact on the Far-Field

Occoquan Reservoir has a relatively long and narrow morphology that is typical for run-of-the-river reservoirs. The main body of the reservoir is 16 km long but only a few hundred meters wide. The circulators were located at the basin close to the dam and potentially influenced conditions in this region of the reservoir in a manner that differed from the upstream reservoir, referred to here as the "far-field." To determine to what extent the circulators may have influenced the spatial distribution of dissolved oxygen a series of profiles collected between NW and circulator 3 (referred to as WB) at the same time that temperature measurements were collected as described in Chapter 2 and illustrated in Figures 36 to 39. The vertical profiles on the three sampling dates were used to decipher whether circulator operation influenced the spatial distribution of dissolved oxygen between WB and NW. Based on the vertical profiles from each sample

date an isoplot was generated. The circulators' general location along the transect line is indicated with arrows (each circulator's lateral distance from the transect line is not indicated). The depth scale was set to 6 meters for the first transect recorded June 15, 2007 and 5 meters for the other two transects recorded June 21, 2007 and June 30, 2007. The illustration of just the upper 5 or 6 meters was created to accentuate the details of the dissolved oxygen in the upper water strata.

The first transect (Figure 58) showed a different dissolved oxygen distribution than the transects on the following two dates, but the trend that circulator operation was lowering the oxycline was obvious in all three transects. The depth of the oxycline from NW to a 600 meter distance from NW was approximately 4 to 4.5 meters.

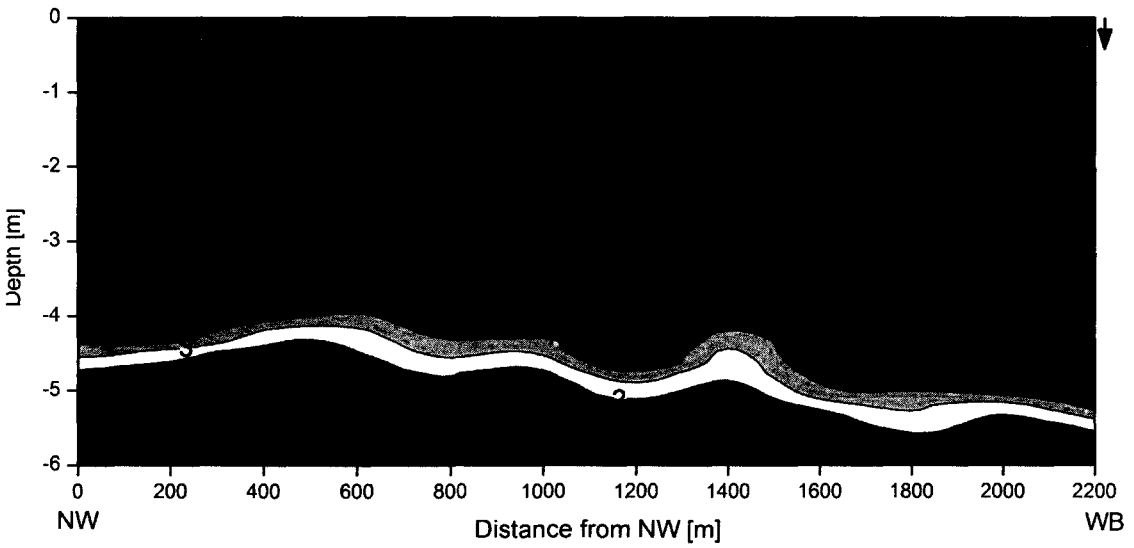

Figure 58. Dissolved oxygen [mg/L] isoplot of transect from NW to WB recorded the 06/15/2007.

The oxycline was at 5.5 meters near the WB site. This observation is consistent with introducing additional water to the epilimnion by the circulators. Although this hypolimnetic water is anoxic when removed from the hypolimnion, aeration at the circulator distribution pan and mixing with a large well-oxygenated epilimnetic volume resulted in an increased epilimnetic volume that displaced lower water strata of lower dissolved oxygen in the water column by displacement. The first transect shows reduced dissolved oxygen concentrations near the surface in approximation of the circulators. This was thought to be caused by the physical mixing of oxygen-poor water at the surface by the circulators, although this was not seen in the following two transects. It is possible that the first transect was conducted during the influence of a seiche, as high winds of 17 to 20 mph occurred five days prior to the transect (Figure 59). Another possible reason for the different dissolved oxygen distribution during the first transect was the possibility that Fairfax Water operated the aeration system prior to the data recording. Based on information from Fairfax Water, the aeration system was operated in early May for a few days. This was obvious, as the aeration system increased the turbidity (resuspended sediments) in the lower part of the reservoir. As the turbidity settled out of the upper water column a few days later, a monitoring trip was conducted (5/4/2007). A plume of turbid water was then observed around each circulator (Figure 60), as the turbidity at the intake depth (10 meters) was still high. Despite this event, Fairfax Water had no record of operating the aeration system after early May, so there is little chance that there is an influence from this event on the first transect (6/15/2007).

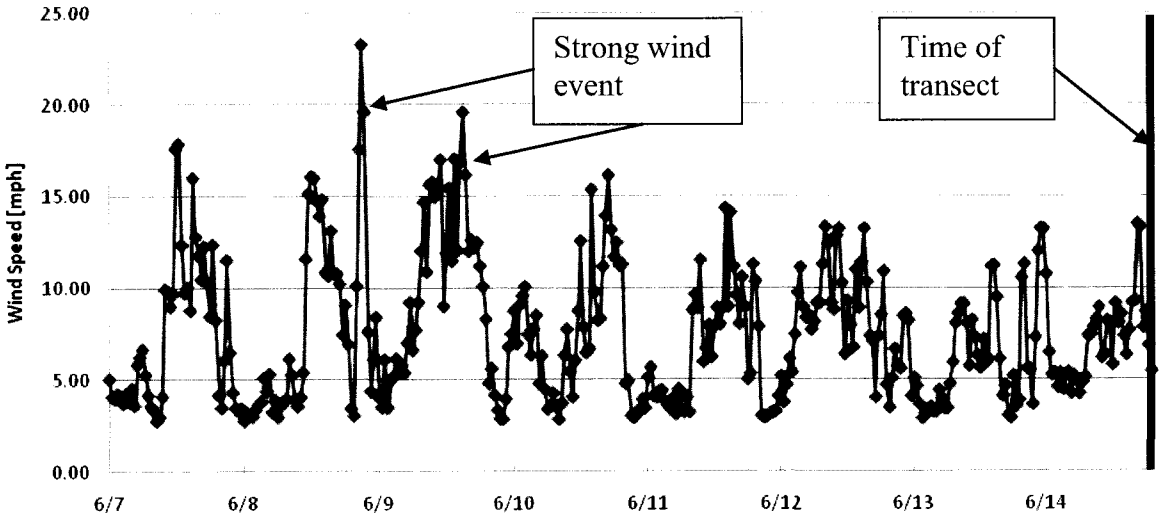

Figure 59. Wind conditions during seven days prior to the first transect (6/15/2007).

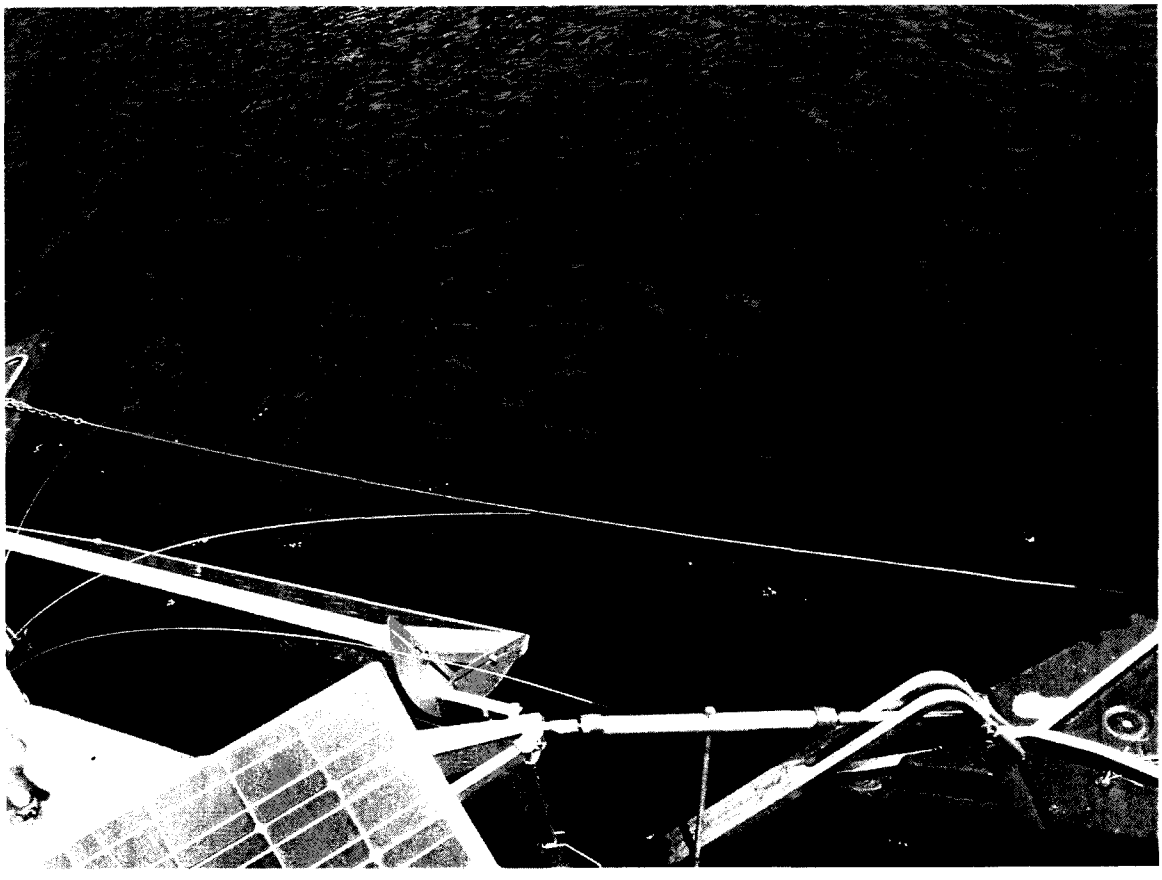

Figure 60. Picture taken of turbid discharge plume around circulator 3 at 5/4/2007.

On June 21, 2007 and June 30, 2007, the second and third transects were conducted (Figure 61 and Figure 62). The dissolved oxygen distribution during these transects were similar but different than the distribution of the initial transect. The last two transects showed little or no reduction of dissolved oxygen above 3 meters depth by the WB site. The June 21, 2007 transect showed a slight reduction in the dissolved oxygen at the WB site within this depth, but the June 30, 2007 transect had a slightly higher oxygen concentration in this region. This is evidence against strong vertical mixing from the circulators. The elevated dissolved oxygen levels at the last transect may have been due to phytoplankton activity or possibly the effect of the wind direction. The lack of discernable oxygen depletion in the region surrounding the circulators may reflect the rapid mixing (particularly horizontal) that occurs in the reservoir related to the circulator discharge.

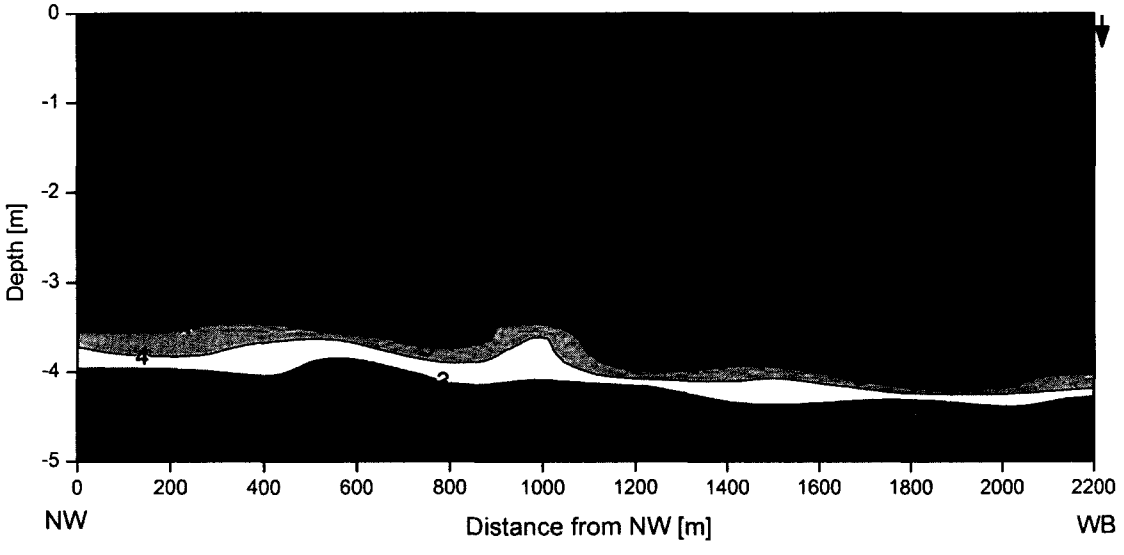

Figure 61. Dissolved oxygen [mg/L] isoplot of transect from NW to WB recorded the 06/21/2007.

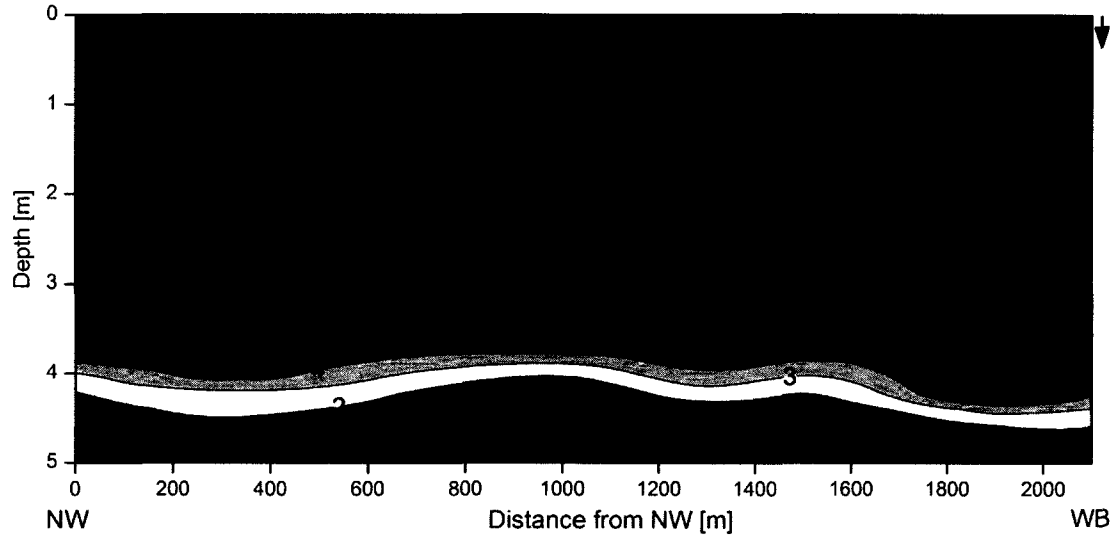

Figure 62. Dissolved oxygen [mg/L] isoplot of transect from NW to WB recorded the 06/30/2007.

The main observation from all three transects is that the oxycline is deeper near the circulators (WB) than at the NW site. The June 15, 2007 transect had a 1 meter difference in oxycline depth between the NW and WB site (4.5 and 5.5 meters), the June 21, 2007 transect had a 0.5 meter difference in oxycline depth between the NW and WB site (3.5 and 4.0 meters), and the June 30, 2007 transect had a 0.5 meter difference in oxycline depth between the NW and WB site (4.0 and 4.5 meters). The first transect had a greater difference in oxycline depth but also a deeper depth for the oxycline than the other two transects. This may be evidence of the strong wind event five days before the event. The next two transects had similar differences in oxycline depths between the two sites, but the last transect had a 0.5 meter deeper oxycline than the previous one. This is consistent with the deepening of the thermocline and oxycline in lakes/reservoirs with the thermal stratification season. This trend suggests a volumetric increase in the upper

water column due to the operation of the circulators. This influence was also noted with the temperature profile and described previously in Chapter 2.

In addition to the transects discussed above, dissolved oxygen profiles were recorded regularly at the monitoring stations (WB, NW, and WB2) from April to October 2007. These monitoring stations represented the lower, middle, and the upper part of the reservoir, respectively. As a part of studying the far-field influence of the circulators, these vertical profiles were compared to develop an understanding of how far the influence of the circulators would reach. There were small variations between the oxygen profiles from the monitoring stations suggesting that deeper penetration of oxygen through the water column was limited. Vertical temperature and oxygen profiles from WB, NW, and WB2 recorded within one hour on August 13, 2007 are provided as an example of the variation observed (Figure 63). The WB temperature and oxygen profiles in the circulator region are homogeneous down to four meters which was deeper by approximately one meter than the profiles recorded at NW and WB2. It appeared that the operation of the circulators lowered the depth of the thermocline and the oxycline but not enough to oxygenate the deeper depths. Based on this observation, one can conclude that the influence from the circulators was limited to somewhere between WB and NW.

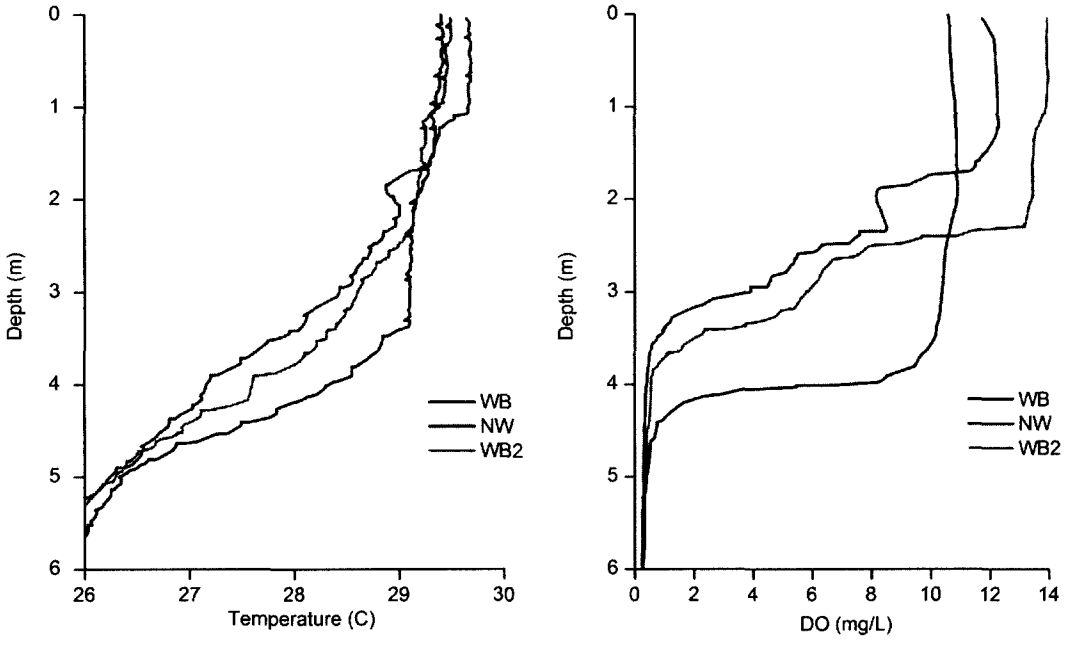

Figure 63. Temperature and dissolved oxygen profiles August 13, 2007.

3.5.8 Circulators Impact on Biogeochemical Processes

Biogeochemical processes in a reservoir are mainly controlled by the ambient dissolved oxygen concentration, which is primarily controlled in the water column by vertical transport. For reservoirs deep enough to develop thermal stratification, vertical transport is substantially limited (i.e. slow) across the thermocline and mesotrophic, and eutrophic lakes can become substantially or completely depleted of dissolved oxygen in the hypolimnion. Under these conditions, organic matter decomposition proceeds with microorganisms using alternative electron receptors in the absence of dissolved oxygen. This situation can result in the accumulation of iron, manganese, ammonia, sulfide, and other byproducts in the water column.

Cooke and Kennedy (2001) describe how artificial circulation can eliminate iron and manganese development and increase the dissolved oxygen concentration so that phosphorus can be retained in the sediments. End products from anoxic biogeochemical processes such as iron, manganese, hydrogen sulfide, and phosphorus will be avoided if dissolved oxygen is available at the sediment-water interface as an electron acceptor (Zaw and Chiswell, 1999). Occoquan Reservoir installed an aeration system in the lower basin in 1970 to alleviate the negative impact of these end products. The performance of the aeration system was initially deemed a success; however, historic water quality data show that the aeration system's impact on the reservoir has been varying. It can be seen in Figure 45 that the performance of the oxygen transfer declined from 2000 to 2005. According to Fairfax Water, this drop in performance was caused by aging diffuser hoses that had suffered irreversible fouling. The diffuser hoses were replaced but then ruptured in 2006, which led to the deployment of eight surface circulators in late July 2006 to provide oxygen to the lower waters.

The goal that was defined for circulator operation was to inhibit manganese from entering Fairfax Water's middle intake located at 8.2 meters. The eight solar-powered surface circulators were configured for hypolimnetic oxygenation by setting the circulator intakes at 10 meters. The manufacturer's conceptualization of circulator operation was that the circulators could create an oxidation barrier at the circulator intake depth strong enough to keep manganese from entering the middle intake of Fairfax Water. Data collected here illustrates that this penetration of dissolved oxygen to the desired depths did not occur (Figure 47 B). As a consequence, hypoxia developed at the sediment-water interface and throughout the hypolimnion over a large sediment area resulting in a sizable

release of manganese to the water column. All collected monitoring data illustrate that the circulators did not provide oxygen below five meters during the stratification period, which is well above the depth of Fairfax Water's middle water intake.

Manganese measurements were not conducted regularly as part of long-term monitoring in Occoquan Reservoir until after the aeration system failed and was shut down in June 2006. In July 2006, Fairfax Water started monitoring manganese concentrations at the surface and at their three intakes to the treatment plant. These intakes were located at 3.6 meters, 8.2 meters, and 12.8 meters below the spillway crest.

The manganese concentrations for each intake depth are shown for April 2007 to November 2008 (Figure 64). The 2007 period represents the reservoir under surface circulation while in 2008 the reservoir was again under aeration system operation conditions. The manganese concentrations at the bottom intake were highest during 2007 when the surface circulators were operating; however, only the middle intake and the top intake were used during that period (Greg Prelewicz, personal communication). An interesting observation is that the top intake had higher manganese concentrations during the aeration season in 2008 than during the circulation season in 2007. This situation is consistent with the aeration system's ability to vertically mix the water column, thus causing manganese released from the sediments to be transported by convection to shallower depths.

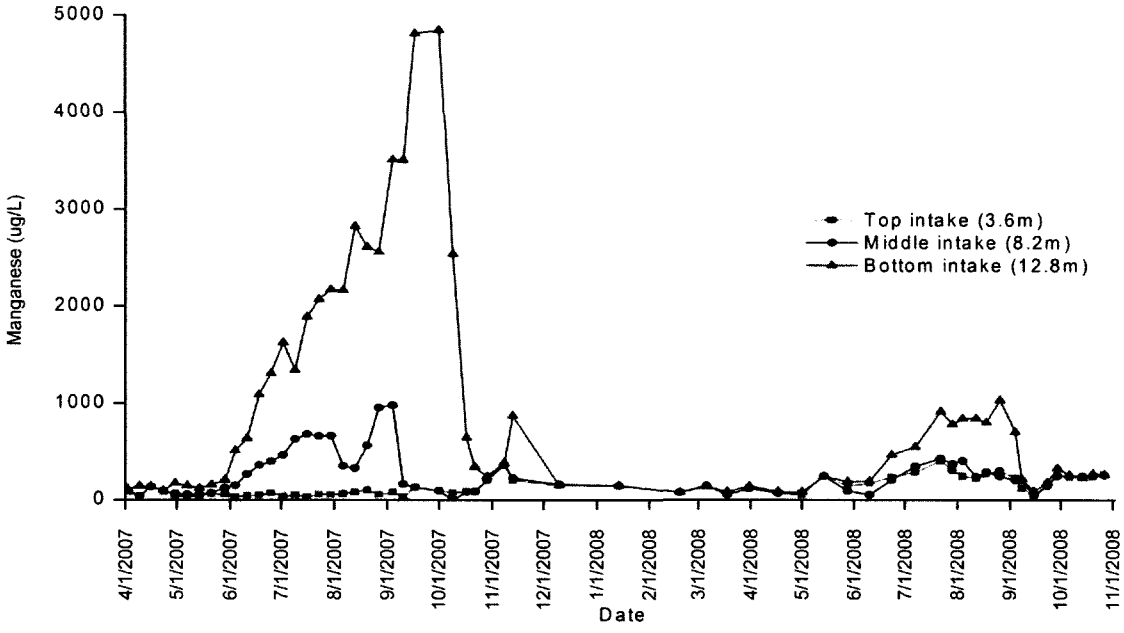

Figure 64. Manganese concentrations at the top, middle and bottom intakes from April, 2007 to November, 2008.

During the circulation year in 2007, there were distinct differences between the top, middle, and bottom intakes in terms of manganese concentrations with manganese concentrations as high as 5 mg/L at the bottom intake while the top intake measured concentrations that were two orders of magnitude lower, indicating a much lower degree of vertical mixing.

Samples for manganese analysis were collected at 0, 4, 6, 8, 10, 12, 14, 16, and 18 meters depth five times at the WB site between June and July 2007 and are used to further examine temporal and spatial variations under circulation conditions (Figure 65). The manganese concentrations at 12 meters agree with Fairfax Water's concentrations at the bottom intake during June and July 2007 increasing from the first vertical profile in

June 21, 2007 to July 26, 2007. Manganese concentrations continued to rise at 12 meters depth peaking at the beginning of October (Figure 64).

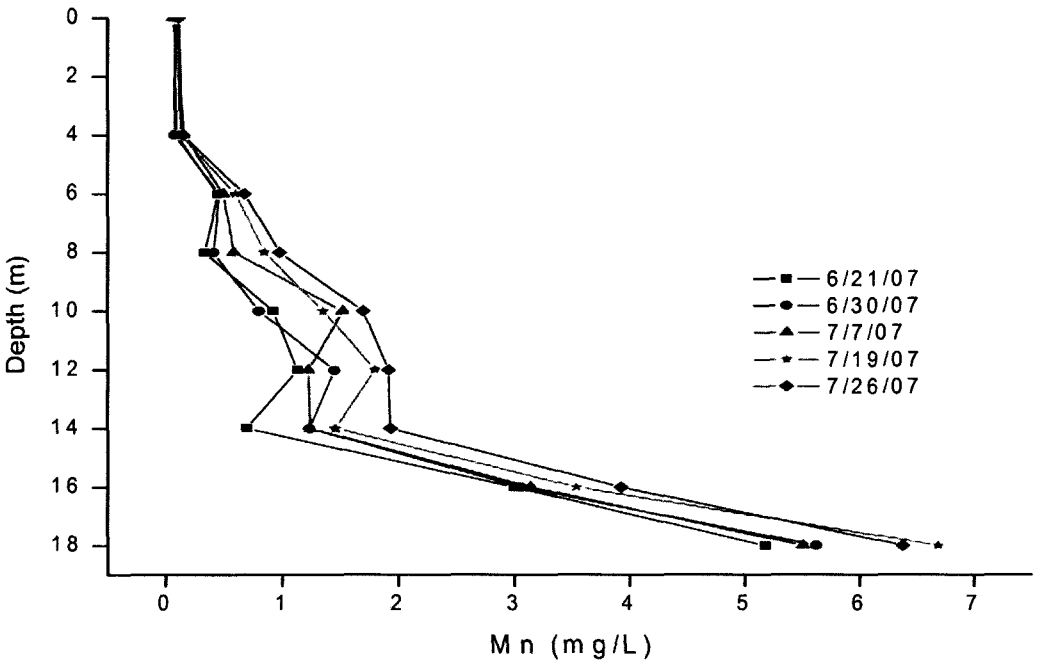

Figure 65. Manganese profiles at WB from June and July 2007.

The manganese concentrations below 14 meters were much higher than the concentrations above this depth, and the sharper gradient in concentration with depth suggests that this deeper layer of water had less mixing than the region between 6 and 14 meters. Figure 65 shows that a slightly higher manganese concentration occurs at 12 meters depth than at 10 and 14 meters depth, except for the June 26, 2007 profile. These elevated manganese concentrations at 12 meters are possibly related to the large sediment area in Hooves Run which ranges between 10 and 15 meters in depth.

Historically, Fairfax Water shifts withdrawing water from the middle intake at 8.2 meters to the top intake to 3.6 meters sometime in late July to avoid high manganese levels entering the treatment plant. The manganese concentrations at the top intake during the stratified season in 2007 (surface circulation) and 2008 (bubble aeration) were approximately 50 µg/L throughout the summer season while in 2008 they exceeded 200 µg/L for most of the summer. The higher manganese concentrations in 2008 were caused by greater mixing and transport of manganese to shallower depths by the aeration system. The circulators did not produce the same amount of vertical mixing as the aeration system; therefore, less manganese was transferred to the top intake in 2007. The main observation is that manganese concentrations were lower at the top intake during 2007. However, this condition reflects more on the aeration system's inability to control Mn release from the sediment than on improvements from the circulators. It is likely that manganese concentrations at 3.6 meters depth would be even lower in the absence of both aeration and circulation (from surface circulators).

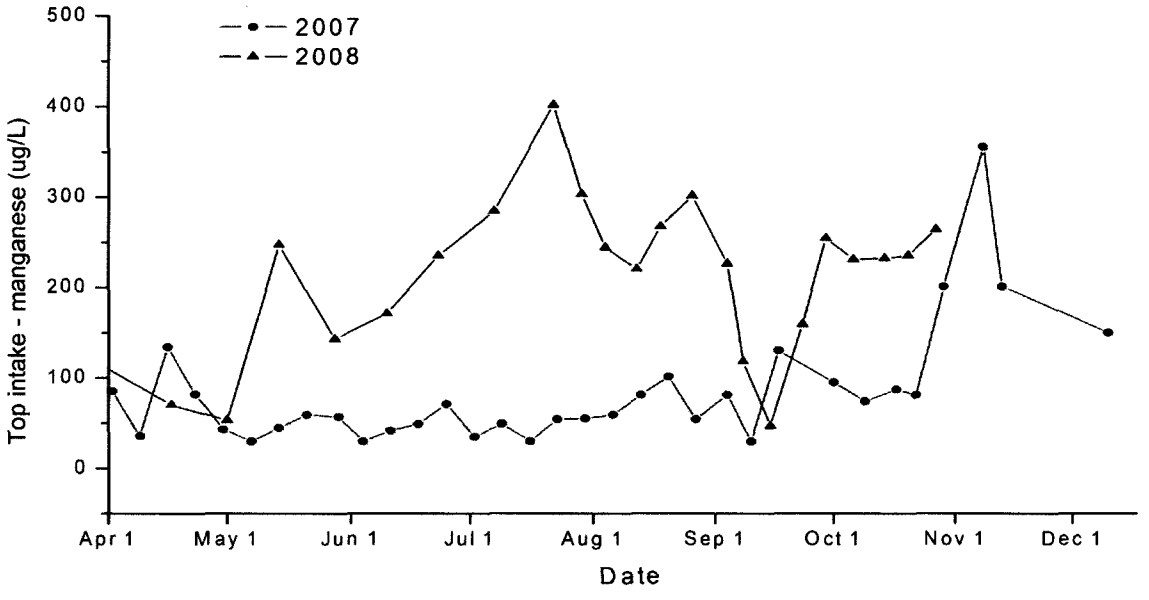

Figure 66. Manganese concentrations at the top intake (3.6 m) from April to December.

The peak in manganese concentration during November 2007 indicates that the elevated hypolimnetic manganese mass was released to the entire water column by water column mixing at fall turnover.

3.6 Conclusions

The aeration system was operated in Occoquan Reservoir for 36 years until the summer of 2006. Eight surface circulators were installed at the lower part of the reservoir next to the dam. Water quality monitoring showed that the dissolved oxygen distribution in the reservoir during the stratified period of 2007 (surface circulator influence) resembled a water body without mixing. The oxycline was sharply defined at about 4 meters with anoxic conditions below this depth during this period. Comparison between the dissolved oxygen distribution in the reservoir during the aeration period from

2000 to 2005 and the circulation year of 2007 was clear (Figure 45), although the years from 2003 to 2005 showed significantly less oxygen transfer below 8 meters than the previous three years (2000 to 2002). The surface circulators failed to induce oxygen below 5 meters during the summer months of 2007.

Based on long term dissolved oxygen data for the reservoir, but also long term temperature data, it was clear that the vertical mixing in the reservoir was significantly higher during the aeration years than during the circulation year. This was substantiated by the low flow through the circulators as discussed in Chapter 2. Consequently, the anoxic conditions started earlier and ended later in the circulation season of 2007 compared to 2002, which was chosen as a representative year for aeration.

The THOD and AHOD was calculated for the lower part of the reservoir from 2000 to 2005 (aeration period) and for 2007 (circulation period). It was found that the THOD and AHOD were much larger for 2007. This was mainly a consequence of the lack of oxygen transport provided by the circulators. It was calculated that the AHOD was 1,780 $mg/m^2\ d^{-1}$.

The oxygen transfer through the surface was calculated for the surface area of the circulator distribution pan and for a similar area without the agitation of the circulator impeller. It was found that the oxygen transfer was 325 times faster through the surface area over the circulators compared to a similar surface area on the reservoir without any external forces (wind and waves). The two main contributors for the larger theoretical oxygen transfer over the circulators were the higher difference in oxygen concentration at the surface and in the bulk liquid due to the introduction of anoxic hypolimnetic water and the increased rate of energy dissipation from the impeller.

The dissolved oxygen near-field study of a circulator (Figure 56) showed that the low oxygen hypolimnetic discharge water mixed quickly with high oxygen ambient surface water. The oxygen concentration was therefore quickly restored to near ambient surface water levels. The far-field impact showed little or no reduction in dissolved oxygen concentration in the epilimnetic water near the surface circulator. The main observation was that the epilimnetic volume was increased in the vicinity of the circulators as the discharge volume lowered the oxycline by displacement. A 0.5 meter difference in oxycline depth was found through the entire length of the 2,000 meter transect.

Manganese data was compared between 2007 (circulation period) and 2008 (aeration period). It was found that the manganese concentrations at the bottom intake to the WTP (12.8 meters) were significantly higher in 2007 than 2008. This contributed to the significantly worse oxygen conditions that occurred in 2007 versus 2008. This observation was also seen at the middle intake to the WTP (8.2 meter). The top intake (3.6 meters) did not show this trend. The manganese concentrations were actually lower in 2007 than in 2008. This contributed to the lack of vertical mixing induced by the circulators. A similar result would likely occur even if no mixing was conducted. Based on the manganese data available, it was clear that the circulators did not inhibit the manganese from entering the top intake by an oxygen barrier at the circulator intake depth at 10 meters.

CHAPTER IV

MODELING TEMPERATURE AND DISSOLVED OXYGEN CONDITIONS IN OCCOQUAN RESERVOIR

4.1 Introduction

Water quality modeling is a developing field within limnology and as water quality models become more complex, their ability to simulate more advanced physical, biological, and chemical processes increases. The water quality models available today are capable of modeling complex eutrophic water systems using the processing capabilities of personal computers, making them accessible to a potentially large user group. These models are becoming invaluable tools in studying the response of a given water system, however, the model user must know the actual water system in sufficient detail if accurate predictions are to be made.

A modeling effort was undertaken complementing the field studies to determine if the surface circulation technology that was deployed in Occoquan Reservoir's lower basin could be represented in an advanced water quality model. If this is possible, the temperature and dissolved oxygen conditions could be simulated for Occoquan Reservoir during 2007 and also simulated under other operational scenarios. In this chapter is a description of the procedure to configure and calibrate a water quality model for Occoquan Reservoir with respect to temperature. Dissolved oxygen is conducted and then the model is used to assess the influence of surface circulator operations and selected reservoir conditions.

There are currently several water quality models available that are capable of modeling reservoirs and lakes. The most widely used models based on a literature search and USGS's SMIC (The Surface Water and Water Quality Models Information Clearinghouse) are listed in Table 9. The criteria for selecting a modeling platform for Occoquan Reservoir was to model temperature and dissolved oxygen accurately in at least 2 dimensions. Because the dissolved oxygen concentration in a reservoir is closely linked to all the eutrophic processes such as biological, geochemical, and physical processes, it was decided that the model for this study had to be able to simulate all the major eutrophic processes. This excluded HEC-5Q, WASP, and RMA10. CAEDYM with DYRSEM was also excluded because it was only capable of simulation in one dimension. CAEDYM, ELCOM, MIKE 3, EFDC/HEM3D, and CE-QUAL-W2 were deemed all acceptable candidates for this effort.

Table 9. List of commonly used Eutrophication models.

Model	Dimensionality	Constituents modeled	Comments
CAEDYM	0-D	Eutrophication, nutrients, phytoplankton, oxygen	Eutrophication model only
HEC-5Q	1-D vertical	Temperature, 7 water quality const., 22 optional const.	
WASP	1-D vertical	Eutrophication, DO, temp. nutrients, OM, velocities	
DYRSEM	1-D vertical	Temperature, salinity, density	Hydrodynamic model. Use with CAEDYM
CE-QUAL-W2	2-D longitudinal and vertical	Eutrophication, DO, BOD, nutrients, toxic pollution	Suitable with long and narrow water bodies
MIKE 3	3-D	Eutrophication, nutrients, phytoplankton, oxygen	Hydrodynamic and eutrophic model
RMA10	3-D	Temperature, salinity, suspended sediments	Not eutrophic model
EFDC/HEM3D	1,2,3-D	Eutrophication, nutrients, phytoplankton, oxygen	Hydrodynamic model and eutrophication model
ELCOM	3-D	Velocities, temperature, salinity, density	Hydrodynamic model. Use with CAEDYM

It was decided that CE-QUAL-W2 was the best overall choice for this research due to its proven eutrophic algorithms, large number of registered applications (783 registered U.S. applications), and free download with an active online support forum. Another reason weighing heavily for deciding on CE-QUAL-W2 was that OWML had configured CE-QUAL-W2 to model Occoquan Reservoir and had published a paper discussing the model set up and simulation. This previous work provided some guidance on setting up the model for simulations in this study.

4.2 CE-QUAL-W2

CE-QUAL-W2 is a two-dimensional laterally-averaged water quality and hydrodynamic model for lakes, reservoirs, estuaries, and river basins. It simulates basic eutrophication processes such as temperature-nutrient-algae-dissolved oxygen-organic

matter and sediment interactions. The CE-QUAL-W2 model was developed by the Army Corps of Engineers and Portland State University (Cole and Wells, 2000). It has been under development since 1975 when it was known as LARM (Laterally Averaged Reservoir Model) developed by Edinger and Buchak. Further modifications allowed for multiple branches and estuarine boundary conditions. Later the model was known as GLVHT (Generalized Longitudinal-Vertical Hydrodynamics and Transport Model). Finally, the first version of CE-QUAL-W2 was released in 1986. The model has gone through many versions since then and has gained broad acceptance for modeling water quality in rivers, lakes, reservoirs, and estuaries worldwide. The latest version of the model in 2007 was 3.5 which is the version used for all the modeling work in this study effort. The Water Quality Research Group affiliated with Portland State University is responsible for maintaining the CE-QUAL-W2 code and administering the web site for downloading the CE-QUAL-W2 model. According to WQRG, the current registered numbers of CE-QUAL-W2 applications at the time of writing are described in Table 10.

Table 10. The number of applications for several types of water bodies (WQRG March 2009).

Water body	Number of applications
Reservoirs	319
Lakes	287
Rivers	436
Estuaries	82

Transport within CE-QUAL-W2 is calculated based on solving a set of two-dimensional (longitudinal and vertical), unsteady, hydrodynamic advective-diffusion equations (Cole and Wells, 2001), solved by a finite difference method. The model domain is illustrated (Figure 67) where a typical river-reservoir-dam layout is assumed. The main governing equations are also provided (Table 11).

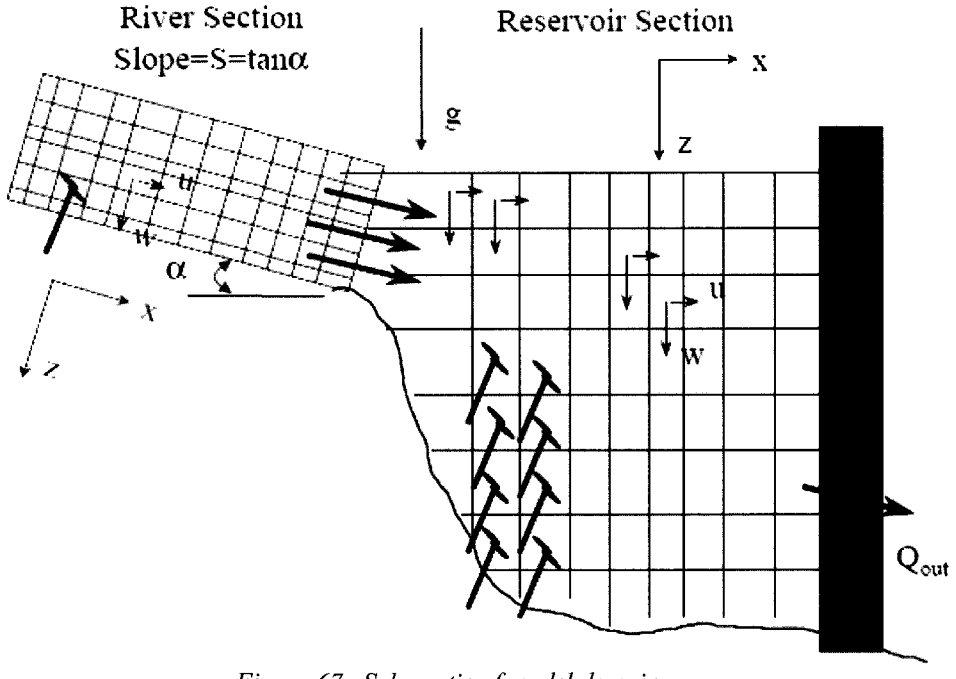

Figure 67. Schematic of model domain.

Table 11. Governing Equations for CE-QUAL-W2

Equation	Version 3 governing equations
x- momentum	$\frac{\partial UB}{\partial t} - \frac{\partial UUB}{\partial x} - \frac{\partial WUB}{\partial z} = gB\sin\alpha + g\cos\alpha B\frac{\partial \eta}{\partial x} - \frac{g\cos\alpha B}{\rho}\int_{\eta}^{z}\frac{\partial \rho}{\partial x}dz + \frac{1}{\rho}\frac{\partial B\tau_{xx}}{\partial x} - \frac{1}{\rho}\frac{\partial B\tau_{xz}}{\partial z} + qBU_x$
z-momentum	$0 = g\cos\alpha - \frac{1}{\rho}\frac{\partial P}{\partial z}$
free surface equation	$B_\eta\frac{\partial \eta}{\partial t} = \frac{\partial}{\partial x}\int_{\eta}^{h} UBdz - \int_{\eta}^{h} qBdz$
continuity	$\frac{\partial UB}{\partial x} + \frac{\partial WB}{\partial z} = qB$
equation of state	$\rho = f(T_w, \Phi_{TDS}, \Phi_{ss})$
Conservation of mass/heat	$\frac{\partial B\Phi}{\partial t} + \frac{\partial UB\Phi}{\partial x} - \frac{\partial WB\Phi}{\partial z} - \frac{\partial\left(BD_x\frac{\partial \Phi}{\partial x}\right)}{\partial x} - \frac{\partial\left(BD_z\frac{\partial \Phi}{\partial z}\right)}{\partial z} = q_\Phi B - S_\Phi B$
where B is the width, U is the longitudinal velocity, W is the vertical velocity, q is the inflow per unit width, α is the channel angle, Φ is the concentration or temperature, η is the water surface elevation, P is the pressure, h is the depth, T_w is the water temperature, Φ_{TDS} is the concentration of TDS, Φ_{ss} is the concentration of suspended solids, ρ is the density	

A basis for the numerical solution to replicate the behavior of a reservoir is the computational grid. The water body is divided into longitudinal segments and vertical layers. Variables can either be located at the center of a computational cell or at the boundary. Variables that are defined at the computational cell boundary include horizontal and vertical velocity, eddy viscosity and diffusivity, and shear stress. Variables that are defined at the center of a cell include density, temperature, constituent concentration, and hydraulic pressure. Boundary parameters will affect velocities and transport and center parameters involve other properties that a cell holds. There are three

numerical formulations for mass and heat transport within CE-QUAL-W2. The earliest to be developed were the UPWIND and QUICKSET algorithms. The latest heat and mass convective algorithm is ULTIMATE (Leonard, 1991) which was used for all the modeling work in this research. The ULTIMATE transport scheme performs better than the UPWIND or the QUICKSET schemes during challenging conditions such as when sharp gradients occur causing oscillations or wider gradients by the UPWIND or the QUICKSET scheme.

Surface shear stresses from wind forcing are accounted for by a formula that is based on water surface velocity, wind velocity at a given height over the surface, drag coefficient, and the air density. The default settings set the wind velocity height at 10 meters above the surface, but all the parameters can be altered to a desired behavior. The bottom shear stresses are based on a simpler equation involving only the Chezy friction coefficient, longitudinal velocity, and the density of water. CE-QUAL-W2 gives the user a choice of six solutions to the vertical shear stress equation (4-1). The recommended method to solve for wind shear is the latest TKE (Turbulent kinetic energy) formulation (Wells, 2003) shown in Table 12. This was used for all the modeling work in this study.

$$\frac{\tau_{xz}}{\rho} = \nu_t \frac{\partial U}{\partial z} = A_z \frac{\partial U}{\partial z} \qquad (4\text{-}1)$$

Table 12. Numerical Solution to the Surface Shear Stresses from Wind.

TKE (Turbulent kinetic energy)	$\nu_t = C_\mu \frac{k^2}{\varepsilon}$ where k and ε are defined from $\frac{\partial kB}{\partial t} + \frac{\partial kBU}{\partial x} + \frac{\partial kBW}{\partial z} - \frac{\partial}{\partial z}\left(B\frac{\nu_t}{\sigma_k}\frac{\partial k}{\partial z} \right)$ $-\frac{\partial}{\partial x}\left(B\frac{\nu_t}{\sigma_k}\frac{\partial k}{\partial x} \right) = B(P + G - \varepsilon - P_k)$ $\frac{\partial \varepsilon B}{\partial t} + \frac{\partial \varepsilon BU}{\partial x} + \frac{\partial \varepsilon BW}{\partial z} - \frac{\partial}{\partial z}\left(B\frac{\nu_t}{\sigma_\varepsilon}\frac{\partial \varepsilon}{\partial z} \right)$ $-\frac{\partial}{\partial x}\left(B\frac{\nu_t}{\sigma_\varepsilon}\frac{\partial \varepsilon}{\partial x} \right) = B\left(C_{\varepsilon 1}\frac{\varepsilon}{k}P + C_{\varepsilon 2}\frac{\varepsilon^2}{k} - P_\varepsilon \right)$	Wells (2003)

where:

ℓ_m =	mixing length	C =	constant (assumed 0.15)	k =	wave number
z =	vertical coordiante	u =	shear velocity	ρ =	liquid density
H =	depth	κ =	von Karman constant	Ψ(x) =	max(0,x)
u =	horizontal velocity	τ_{wy} =	cross-shear from wind	ν =	molecular viscosity
Ri =	Richardson number	Δz_{max} =	maximum vertical grid spacing	C_1 =	empirical constant, 100

All numerical solutions are approximations to the actual physical processes, and every water quality model must go through extensive testing before considered validated. CE-QUAL-W2 has found a good balance of representing the physical river/lake/reservoir/estuary system with relatively little model calibration required and without requiring high computer processing capabilities allowing the model to be run on personal computers.

CE-QUAL-W2 is based on an automatic timestep algorithm that calculates the maximum time step based on estimated hydrodynamic numerical stability. The actual time step used is a fraction of this calculated maximum timestep. The timestep

controlling parameters are located in the control file. The minimum time step was set to 1 second, and the maximum time step was set to 1 hour.

4.3 Assumptions within CE-QUAL-W2

A reservoir is a highly dynamic and complex system influenced by numerous chemical, physical, and biological processes. Every biological or biogeochemical process that is taking place in a reservoir can be represented by a mathematical expression with a kinetic reaction coefficient used to quantify rates of conversion. Most of these processes are influenced by factors such as temperature and pH but often also other factors such as light availability, oxygen concentration, or nutrient availability. Several assumptions must always be made during any modeling effort; however, it is important that the major controlling processes be well described. At a minimum the effort requires detailed bathymetry, water quality, hydraulic, and meteorological data. All models are essentially built on assumptions in the form of mathematical representation of the various processes and transport mechanisms that are taking place in a reservoir. These mathematical representations typically capture the main behavior of the actual process but often not every aspect of the physical system.

The main assumption associated with the CE-QUAL-W2 model is that it is laterally averaged. The benefit of this assumption is that fewer calculations are required compared to a three-dimensional model, so computational time is reduced. The assumption that the water quality is laterally similar is generally good for long and narrow water bodies (like typical run-of-river reservoirs) but may not be a good match for a wider water body (Martin et al., 2007). Despite the assumptions that are involved in the

CE-QUAL-W2 model, accurate representation of many different water systems has been demonstrated (Wells et al. 2004; Martin et al., 2007).

4.4 Methods

The following sections describe the configuration of CE-QUAL-W2 to represent Occoquan Reservoir. The model consists of a control file and several input files. Running the model generates an output file that can have various formats and information depending on how the user sets up the control file. The manual that was provided with the CE-QUAL-W2 (version 3.5) was the basis for setting up and calibrating the model (Wells, 2003). The overall order of setting up the model was to first develop a bathymetry file and a meteorological file. All the other input files necessary to run the model had to be initially set up with "first guess" values as space holders so that the model could be executed so that error messages could be debugged. The next task after generating a bathymetry file and a weather file was to set up and calibrate the model hydrologically. Input and output volume files were developed so that the hydrological aspects of the reservoir were represented, then the temperature related files adjusted so that the thermal outputs represented field data collected from Occoquan Reservoir. Finally, constituent related input files were adjusted so that the basic eutrophication processes led to a dissolved oxygen distribution that matched field data from the reservoir through 2007.

4.4.1 Bathymetry file

The focus of the modeling effort was the temperature and dissolved oxygen response in the lower basin of Occoquan Reservoir. It was decided that the reservoir should be modeled far enough upstream so that the natural behavior of the reservoir was represented and boundary influences avoided. Ryan's Dam was used as an upper boundary of the model because it was far upstream of the lower basin and a shallow threshold exists across the reservoir from the ruins of the old dam. The Occoquan Reservoir was modeled as a single water body from Ryan's Dam to the main dam at the lower basin. The small coves and side branches were excluded in the model because they were considered insignificant to the reservoir's behavior due to their lack of depth and insignificant inflow; the computational speed of the model was also improved by excluding the coves and side branches.

The bathymetry file for CE-QUAL-W2 was based on a detailed bathymetric survey conducted by OWML in 2005. The main water body was divided into 36 longitudinal segments with an inactive boundary segment at the beginning and at the end of a water body, which is why the first segment displayed is number 2 (Figure 68). Vertically, the reservoir was divided into 40 layers, each being 0.5 meters high (Figure 69). Each layer was given a width to best replicate Occoquan Reservoir's bathymetry at the location of each segment, and all segments were given a length and a compass orientation. The average length of the segments upstream of NW was 450 meters, and the average length of the segments downstream of NW was 115 meters each. The increased spatial resolution below NW was established since it was within the area that was under the most significant influence of the surface circulators. Google Earth, which

displays aerial photographs relative to a global coordinate system, was used to find the approximate length of each segment. These lengths and the main compass orientation of the segments were used to generate the bathymetry file.

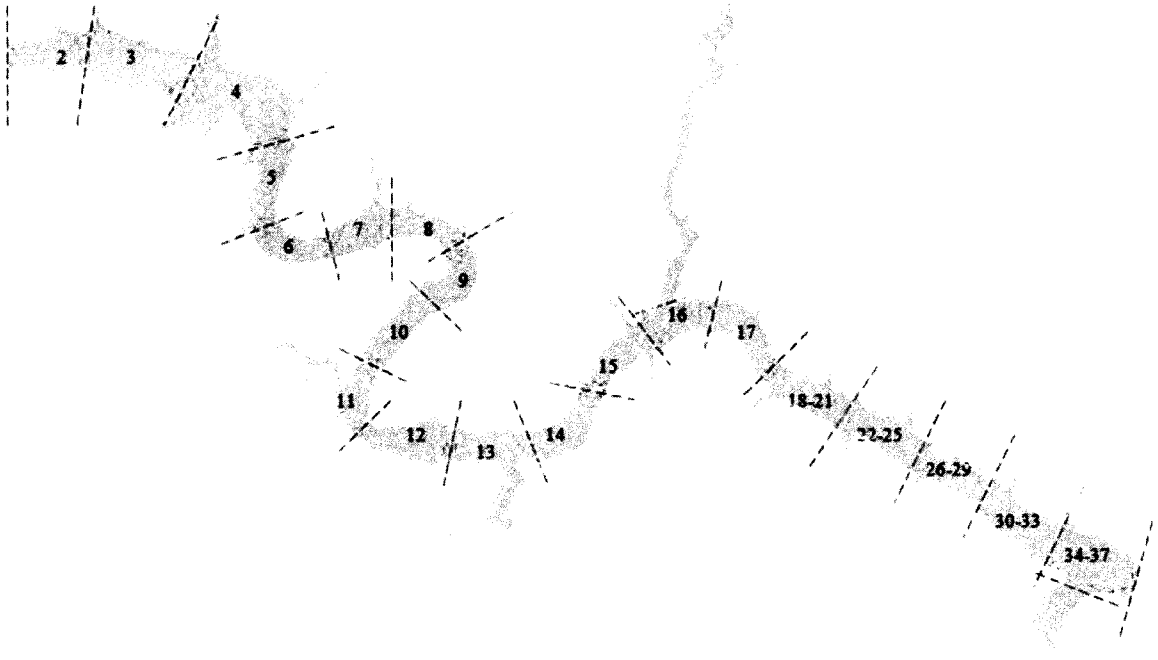

Figure 68. Occoquan Reservoir from Ryan's dam to the outlet. CE-QUAL-W2 segment numbers are shown.

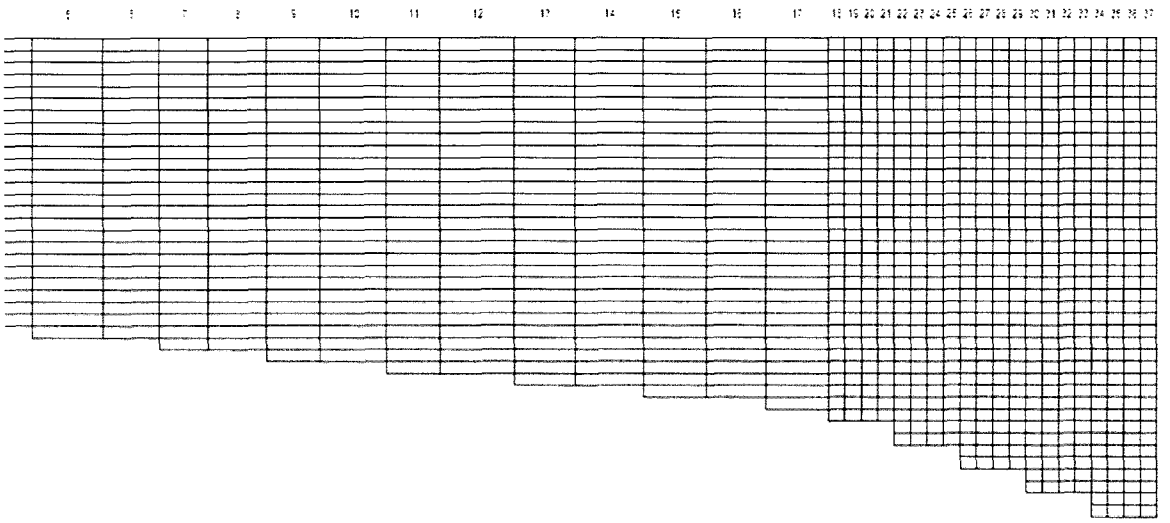

Figure 69. CE-QUAL-W2 segment numbers from 5 to 37 by the dam including the active layers at each segment.

4.4.2 Metrological file

Data from Fairfax Water's weather buoy (WB) was first used to create a metrological input file for the model, but the wind speed sensor produced many periods of unrealistically high values during several periods lasting for several days (i.e. wind velocities from 50 to 270 mph). A new meteorological input file was created based on wind velocity data from Dulles Airport; historical weather data including wind velocity for 2007 were downloaded from National Weather Service's archive. The air temperatures from Dulles Airport and the weather buoy were compared by plotting them together (Figure 70). The spurious data from the weather buoy wind instrument was removed for this comparison. This plot shows a strong agreement between the two data sources. The Spearman (non-parametric method for paired dataset) correlation coefficient was 0.98 for the two data sources, which indicates a high correlation. A test

of hypothesis was conducted comparing the average values of the two data sets. A Wilcoxon's signed rank test (distributions were not normal) revealed that the Weather Buoy had slightly higher temperatures than Dulles Airport. This can be seen by observing where the regression line intersects the y-axis (1.19 at Dulles air temperature of zero).

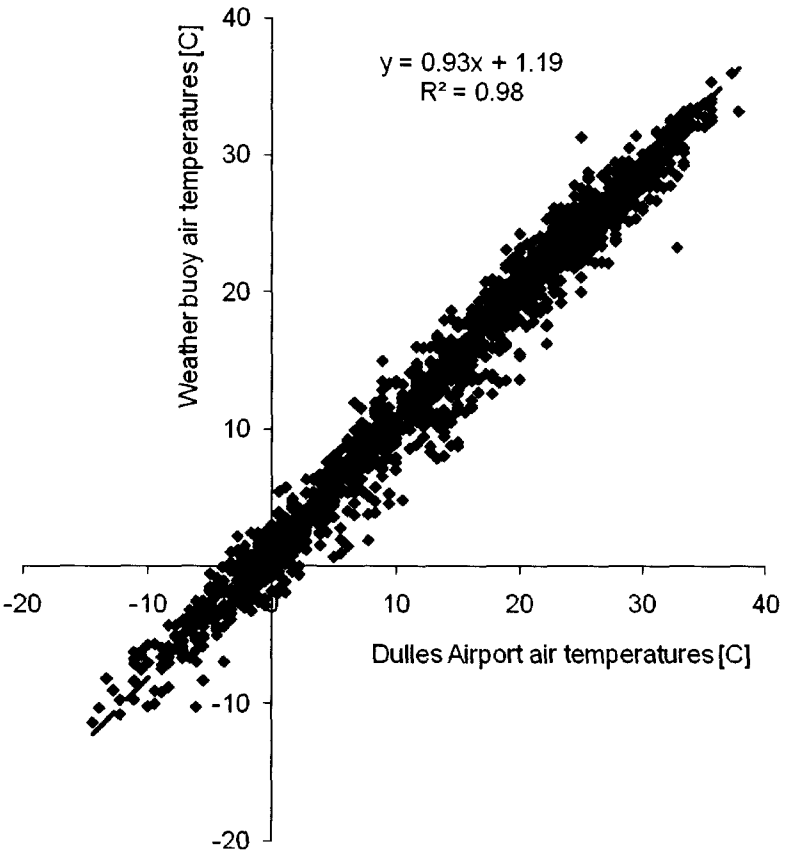

Figure 70. Comparison of air temperature data from the Weather Buoy and Dulles Airport for 2007

A similar comparison was conducted with the wind speed of the two weather data sources and illustrated a greater scatter than the previous temperature comparison plot (Figure 71). The wind speed at the Dulles Airport weather station is about two times the wind speed measured at the weather buoy in the reservoir ($wind_{WB} = 0.43\ wind_{dulles}$; $R^2 = 0.47$). This relationship is not surprising as Dulles Airport is located in a flat open region with few trees or other geological features that would likely result in higher wind speeds. By contrast Occoquan Reservoir lies within a river valley with wooded, tall, riverbanks that would be expected to block the wind. To compensate, the wind file for Occoquan Reservoir conditions, wind speeds at Dulles Airport was multiplied by 0.5. These values were considered representative of wind speed 3 meters above the reservoir surface.

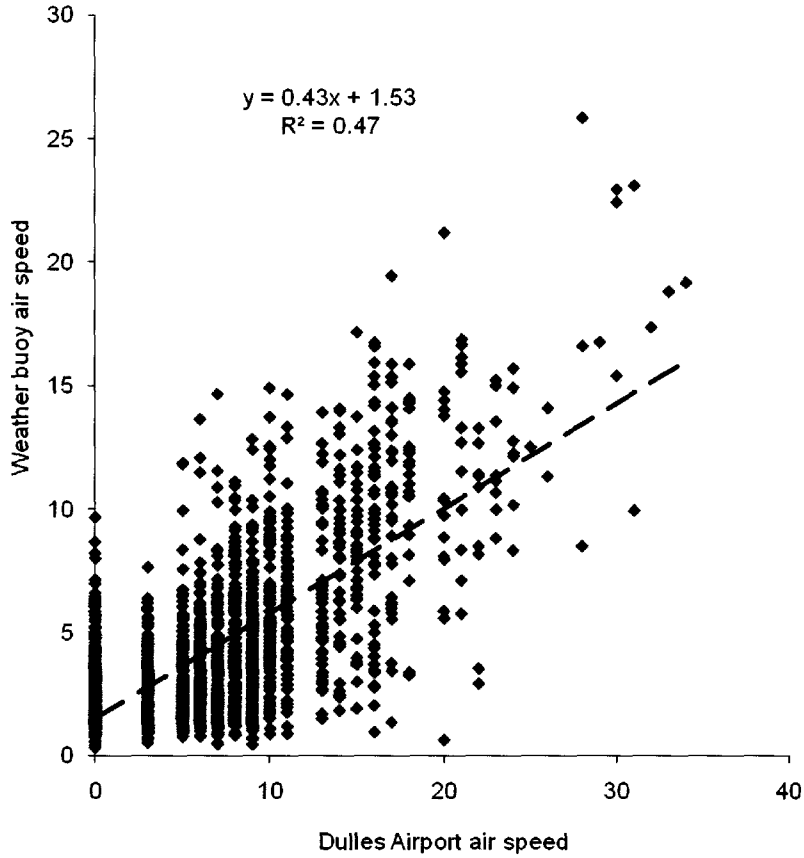

Figure 71. Comparison of wind velocity data from the Weather Buoy and Dulles Airport for 2007

The meteorological file for CE-QUAL-W2 that was based on modified data from Dulles airport included air temperature, dew-point temperature, wind direction, wind speed, and cloud cover data in three hour increments. The drawback of such high temporal resolution is longer computational runtime, but the weather input file is very influential on the reservoir behavior, so this was considered necessary.

The dew-point temperature was not provided by National Weather Service. Therefore, a well known simple approximation (Lawrence, 2005) was used to calculate the dew-point temperature from the relative humidity that was provided in the weather

data from Dulles Airport. The equation (4-2) for the relative humidity to dew-point conversion is:

$$T_d = T - \frac{(100 - RH)}{5} \tag{4-2}$$

Where:

T_d is the dew-point temperature in Celsius.

T is the temperature in Celsius.

RH is the relative humidity in %.

This simple approximation of dew-point temperature is considered accurate within ± 1° Celsius when the relative humidity is above 50%, which is likely always the case over Occoquan Reservoir. It was decided that the simple approximation for calculating the dew-point temperature was satisfactory for this modeling project.

4.4.3 Inflow volume file and withdrawal volume file

Water inflow to Occoquan Reservoir is monitored by OWML on Bull Run and Occoquan Creek on a weekly basis, but inflow is not monitored on the many smaller inflows (small creeks) to the reservoir. Groundwater inputs to, and/or seepage losses from, the reservoir are also not monitored and unknown and could not be directly accounted for. To simplify the model, all inflows were represented as a lumped input from the two main contributors (Bull Run and Occoquan Creek). The inflow volume file was used to calibrate the model hydrologically and hydrologic calibration was first conducted before modeling other conditions in the reservoir.

The Occoquan Reservoir model had three paths by which water could leave the reservoir: over the spillway (depending on the surface elevation), withdrawal to the treatment plant, or surface evaporation. The amount of water that flowed over the spillway was dependant on how the surface elevation in the model related to the spillway crest elevation (defined in the control file). The relationship between water elevation above the spillway and the discharge flow rate was developed based on a spillway discharge curve that was provided by Fairfax Water. If the surface elevation was above the crest, then water would flow over the spillway and exit the model. No outflow volume input file was necessary for this discharge flow, as it was calculated by the model. Surface evaporation was also calculated and removed by the model automatically and was dependent on air temperature, relative humidity, and wind speed. The main volumetric outflow of the model was the intake to Fairfax Water's WTP. An outflow volume input file was created based on Fairfax Water's operational data, which accurately described the withdrawal volume on a daily basis.

The inflow volume file was developed by first specifying Fairfax Water's average daily withdrawal rate (3.45 $m^3 s^{-1} d^{-1}$) as entering the reservoir at Ryan's Dam. Then the daily inflow volumes were adjusted manually up and down until rough agreement was obtained between the simulated surface elevation and the observed surface elevations. To accurately fine-tune inflow volumes, the water balance tool that is provided with the model was used to make the daily adjustments so that the modeled surface elevation corresponded with the observed surface elevation.

4.4.4 Inflow Temperature File and Initial Temperature Condition File

The tributary temperature input file entering the top of the model (Ryan's Dam) was set up for the entire 2007 season with a temporal resolution of 15 days, as the model interpolates the temperature values between these dates. The selected values were based on OWML's measured temperature profiles through the 2007 season near Ryan's Dam (RE15). The temperatures for the tributary inflow are listed in Table 13. The density inflow distribution was selected for the tributary inflow, so that a more realistic inflow scenario would be modeled as the inflow passes over the shallow submerged dam-structure at Ryan's Dam.

Table 13. Estimated Initial Temperatures for Tributary Input

JDAY	Temp. (°C)	JDAY	Temp. (°C)	JDAY	Temp. (°C)	JDAY	Temp. (°C)
1	5	105	11	210	27	315	22
15	5	120	15	225	29	330	19
30	5	135	17	240	29	345	16
45	6	150	20	255	29	360	14
60	6	165	21	270	28	366	10
75	7	180	23	285	26		
90	9	195	25	300	25		

The initial temperature profile for the Occoquan Reservoir model was simplified by defining the same temperature (5 °C) throughout the reservoir. This was justified by examining the temperature profiles recorded by OWML during early January 2007. The modeling period started January 1, 2007 and ended December 31, 2007. It appeared that CE-QUAL-W2 was insensitive to the exact initial temperature, as the cold weather

during January and February 2007 took precedence over the temperature distribution for the following season.

4.4.5 Inflow Constituent File and Initial Constituent File

Modeling of any constituent in CE-QUAL-W2 should only be attempted after the hydrological and temperature calibration is completed. This is because the transport mechanisms in the reservoir are strongly affected by these factors. Dissolved oxygen is considered a constituent in CE-QUAL-W2, and its concentration is dependent on several other processes controlled by other constituent concentrations and kinetic coefficients. It was decided that only the most influential processes on dissolved oxygen in a reservoir should be included in the modeling effort. The selected constituents were totally dissolved solids, phosphate, ammonia, nitrate, organic matter (divided into labile dissolved organic matter, refractory dissolved organic matter, labile particulate organic matter, and refractory particulate organic matter), biochemical oxygen demand, and algae concentration. A schematic of these dissolved oxygen related processes is shown in Figure 72.

The initial constituent concentrations (on January 1 2007) and the tributary constituent concentrations were unknown for Occoquan Reservoir. Therefore, typical constituent concentrations were selected (Table 14) based on a ten-year water quality database collected from Western Branch Reservoir in Suffolk, VA (unpublished data) and CE-QUAL-W2 simulation of Cedar Creek Reservoir, TX (Debele et al., 2006). Experimentation showed that output of the model was not sensitive to these nutrient and organic matter values. The initial concentrations of these constituents were defined for

the entire reservoir by programming them into the control file. The constituent concentrations in the tributary inflow were set up in a separate input file to the model. The values were specified with 30 day increments through the season. CE-QUAL-W2 has an interpolation option that was selected so that the periods between the values would automatically be generated.

Table 14. Estimated initial concentration of the active constituents in CE-QUAL-W2 on January 1, 2007.

JDAY	TDS	PO_4	NH_4	NO_3	LDOM	RDOM	LPOM	RPOM	BOD	ALG	DO
	(g m^{-3})	(g m^{-3})	(g m^{-3})	(g m^{-3})	(g m^{-3})	(g m^{-3})	(g m^{-3})	(g m^{-3})	(g m^{-3})	(g m^{-3})	(g m^{-3})
Initial concn.	100	0.03	0.3	0.3	0.1	0.3	0.05	0.2	1	0.01	10
1	100	0.03	0.3	0.3	0.1	0.3	0.05	0.2	1	0.01	10
30	100	0.03	0.3	0.3	0.1	0.3	0.05	0.2	1	0.01	13
60	150	0.03	0.3	0.3	0.1	0.3	0.05	0.3	1	0.02	13
90	150	0.04	0.4	0.3	0.1	0.3	0.08	0.4	2	0.02	13
120	200	0.05	0.5	0.4	0.2	0.5	0.1	0.6	2	0.03	11
150	200	0.05	0.5	0.4	0.3	0.5	0.1	0.6	2	0.03	10
180	200	0.05	0.5	0.4	0.3	0.5	0.1	0.6	2	0.03	10
210	200	0.05	0.5	0.4	0.3	0.5	0.1	0.6	2	0.03	9
240	200	0.05	0.5	0.4	0.3	0.5	0.1	0.6	2	0.03	9
270	200	0.05	0.5	0.4	0.3	0.5	0.1	0.6	2	0.02	8
300	200	0.05	0.5	0.4	0.3	0.5	0.1	0.6	2	0.01	8
330	150	0.04	0.5	0.3	0.2	0.3	0.1	0.4	2	0.01	8
360	150	0.03	0.3	0.3	0.1	0.3	0.05	0.3	2	0.01	9
366	100	0.03	0.3	0.3	0.1	0.3	0.05	0.2	1	0.01	9

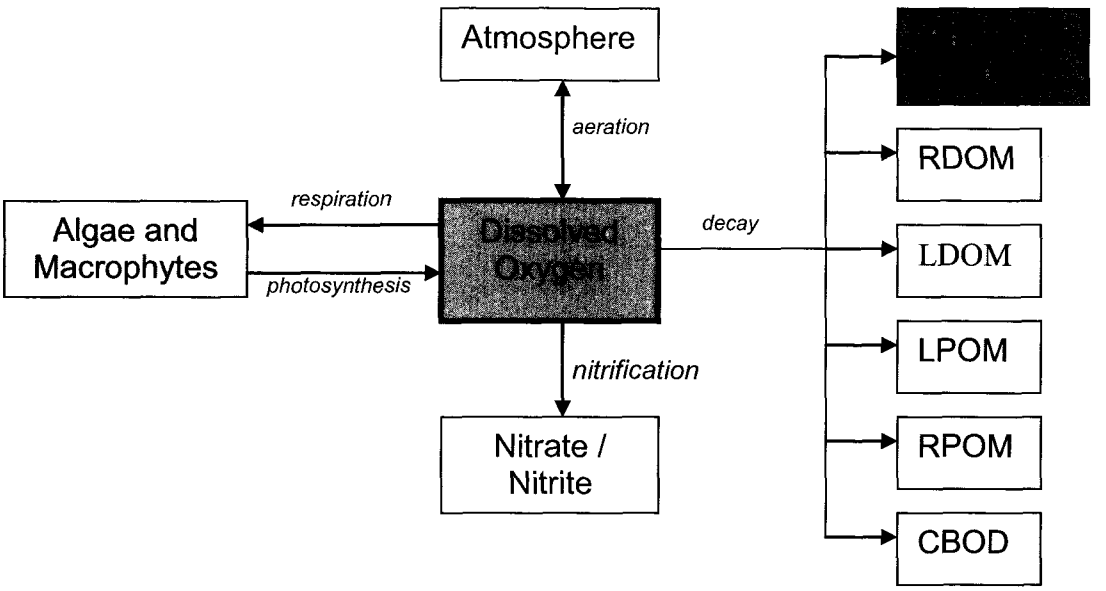

Figure 72. Schematic showing processes that is influencing Dissolved oxygen in CE-QUAL-W2 for the active constituents. (Modified from Cole and Wells, 2000).

4.4.6 Circulator Representation in the Model

The objective of this modeling effort was to simulate the circulators in the model and to replicate the temperature and dissolved oxygen concentration in Occoquan Reservoir during 2007. Representing the surface circulators in the model was one of the major challenges of this modeling effort. There was no literature available describing similar modeling efforts or solutions to the circulator representation within the model. Initially, an attempt was made to add a separate tributary inflow at the surface layer of segment 35 located in the lower basin of the reservoir, and then subtract the same amount of water from the same segment, but at 10 meters depth. This attempt was a poor representation of the surface circulators, since the actual water was not transferred from the intake to the surface with its temperature, dissolved oxygen, nutrients, and constituent

concentrations. These values are constantly varying throughout the season and would be difficult to replicate accurately in an inflow file and a withdrawal file. A second attempt was made to represent the surface circulators, using the model's pump device. A pump was configured to transfer water from 10 meters depth to the surface within the same segment. The model's selective withdrawal inflow algorithm was set up to draw water from 10 meters and the surface so that the effect of the intake plate was represented. The selective withdrawal calculations are mostly affected by water density. The inflow was discharged to a 10 cm surface layer. This circulator representation was representing the surface circulators much more favorably due to a direct transfer of water properties such as temperature and other constituents from the intake to the surface. This dynamic water transfer concept was a key factor in selecting it for surface circulator representation in the model.

The year of this study, 2007, was a year of extreme surface fluctuations on Occoquan Reservoir providing a bigger modeling challenge (Figure 8). The spillway crest was 37.2 meters above mean sea level (AMSL), which was considered the main surface elevation for the reservoir. The circulators float on the surface of the reservoir, and will therefore change their elevation in response to changes in surface elevation of the reservoir. To represent this behavior within the model, six circulation scenarios were defined, each at one meter depth interval. Each of these circulation scenarios would represent the total circulation flow, so only one scenario could be operated at any given time depending on the water level in the reservoir and corresponding starting and ending dates (Table 15). Four circulation scenarios represent the slow decline in water level from the end of May to the end of October, each with one meter difference in elevation.

Because the water level rose almost instantaneously through the interval corresponding to scenario 3, this scenario was not represented as the water ascended to the normal (spillway) elevation.

Table 15. Summary of circulation scenarios.

Circulator Scenario #	Discharge Elevation [m]	Intake Elevation [m]	Active range of surface elevation [m]	Start - Julian Day	End - Julian Day	Circulator Flow Rate [m^3/s]
Scenario 1	37.2	27.2	38.7 - 36.7	1	189	0.8
Scenario 2	36.2	26.2	36.6 - 35.7	190	251	0.5
Scenario 3	35.2	25.2	35.6 - 34.7	252	283	0.4
Scenario 4	34.2	24.2	34.6 - 33.7	284	301	0.3
Scenario 5	36.2	26.2	36.6 - 35.7	302	352	0.3
Scenario 6	37.2	27.2	38.7 - 36.7	353	366	0.3

One major assumption in the representation of the eight circulators in the model was that they all were represented as one single circulator unit. The justification for this simplification was that the horizontal advective transport is much larger than the vertical advective transport in a lake/reservoir (Martin et al., 2007), so that their exact location would not be essential to the overall outcome of the circulator operation. Six of the circulators were longitudinally within 300 meters from each other with the remaining two circulators about 100 and 300 meters upstream of this group. This is a relatively narrow spatial distribution.

The circulator representation in the model was set up to draw water from 10 meters below the surface and discharge it into a 10 cm layer below the surface. During

the thermal stratification period the discharged water would have a higher density mostly due to the lower temperature than the surrounding water. The circulator flow enters a receiving computational cell which is 115 meters long, 263 meters wide and 0.5 meters deep. As the water enters this volume, the simulated cell temperature will be averaged over volume affected by the flow rate. This surface cell will naturally also be subjected to solar heating and shear forces from wind and waves similar to all the surface cells in the model. During thermally stratified periods, a vertical density current occurs mostly due to thermal differences between the hypolimnetic water and the ambient surface water of the reservoir. The model calculates the total density (4-3) based on thermal influence, salinity influence, and suspended solids influence.

$$\rho = \rho_{Tw} + \Delta\rho_{sal} + \Delta\rho_{ss} \qquad (4\text{-}3)$$

Where: ρ_{Tw} = density of water as a function of temperature.

$\Delta\rho_{sal}$ = density of water as a function of salinity (TDS).

$\Delta\rho_{ss}$ = density of water as a function of suspended solids.

The vertical transport that is driven by the density difference will be transferred between the cells based on the governing transport equations listed in Table 10. In a fresh water reservoir the temperature becomes the main factor that is affecting the water density and the vertical advective transport. As cold water enters the surface cell (due to discharge of cold hypolimnetic water) a weak plume would be expected to descend towards the thermocline as it spreads out and becomes diluted with the surrounding surface water. Diffusive and advective heat exchange will occur during this process which will have a

local effect on the temperature distribution around the circulators. This will be discussed in more detail in a later section.

4.4.7 General Model Calibration Procedures

The previous sections describe how the CE-QUAL-W2 model was set up to represent Occoquan Reservoir during 2007. Modeling the impact of the surface circulators on the reservoir was particularly difficult because the natural undisturbed condition of the reservoir is unknown. The reservoir has continuously been vertically mixed by an aeration system from 1970 to 2006. This aeration system considerably affected all the constituent concentrations in the lower basin of the reservoir during this period. The challenge that had to be overcome in order to calibrate the model for 2007 conditions was to do so while the circulators were operating in the model.

CE-QUAL-W2 has three aspects which must be calibrated separately in a distinct order for a complete model calibration (Cole and Wells, 2001). The first aspect to be calibrated was the hydrologic input and output of the model. The approach is different for every modeling project and must be conducted appropriately so that each is correctly represented in the model. The hydrologic in-flows and out-flows of Occoquan Reservoir are described in section 4.4.3 (i.e. inflow volume file and withdrawal volume file) and the approach to establish the hydrologic budget for Occoquan Reservoir.

The second aspect of the model to be calibrated was the temperature. The manual for CE-QUAL-W2 suggests an approach for this procedure, but little detail was provided as CE-QUAL-W2 is written to simulate a wide variety of aquatic systems such as rivers, lakes/reservoirs, and estuaries (tidal). The simulated temperatures from CE-

QUAL-W2 during calibration efforts were compared to the temperatures recorded in the reservoir using panel plotting software (Origin Pro 8). A date at the end of each month where field monitoring occurred was selected and compared to the simulated temperature profile recorded at noon on the same dates as the field monitoring. A large amount of effort was invested in finding the effects of adjusting each parameter in the model. In the end, the model obtained a good agreement with the reservoir behavior without adjusting any parameters significantly away from the default values (Table 16). While it is not conclusive evidence of each process being accurately represented it is an indication that the meteorological file, bathymetry file, and the other input files were represented reasonably well in the model.

Table 16. CE-QUAL-W2 Control File Settings.

Card	Description	Code	Default value	Used value	Comment
	Wind Height (m)	WINDH	10.0	3.0	Instrument height in reservoir
	Wind shield factor	WSC	NA	0.50	To match res. conditions
EXCOEF	Extinction coefficient for pure water (m^{-1})	EXH2O	0.45	0.45	Default value
	Extinction coefficient due to inorg. SS (m^{-1})	EXSS	0.1	0.1	Default value
	Extinction coefficient due to org. SS (m^{-1})	EXOM	0.1	0.1	Default value
	Fract. of abs. solar energy at surface	BETA	0.45	0.45	Default value
ALG EX	Algal light extinction coefficient	EXA	0.2	0.2	Default value
ALGAL RATE	Max. algal growth rate (day^{-1})	AG	2	1.1	To match res. conditions
	Max. algal respiration rate (day^{-1})	AR	0.04	0.04	Default value
	Max. algal excretion rate (day^{-1})	AE	0.04	0.04	Default value
	Max. algal mortality rate (day^{-1})	AM	0.1	0.1	Default value
	Algal settling rate (m day^{-1})	AS	0.1	0.1	Default value
DOM	Labile DOM decay rate (day^{-1})	LDOMDK	0.1	0.12	Value from example
	Refractory DOM decay rate (day^{-1})	RDOMDK	0.001	0.001	Default value
	Lab. To refr. DOM decay rate (day^{-1})	LRDDK	0.01	0.001	Value from example
POM	Labile POM decay rate (day^{-1})	LPOMDK	0.08	0.08	Default value
	Refractory POM decay rate (day^{-1})	RPOMDK	0.001	0.001	Default value
	Lab. To refr. POM decay rate (day^{-1})	LRPDK	0.01	0.001	Value from example
	POM settling rate (m day^{-1})	POMS	0.1	0.5	Value from example
OM STOICH	Stoich. OM/phosphorus	ORGP	0.005	0.005	Default value
	Stoich. OM/nitrogen	ORGN	0.08	0.08	Default value
	Stoich. OM/carbon	ORGC	0.45	0.45	Default value
	Stoich. OM/silica	ORGSI	0.18	0.18	Default value
OM RATE	Lower temp. for OM decay (°C)	OMT1	4	4	Default value
	Upper temp. for OM decay (°C)	OMT2	25	25	Default value
	Fraction of decay at OMT1	OMK1	0.1	0.1	Default value
	Fraction of decay at OMT2	OMK2	0.99	0.99	Default value
CBOD	5-day decay rate (day^{-1})	KBOD	0.1	0.25	Value from example
	Temperature coefficient	TBOD	1.02	1.0147	Value from example
	Ratio of CBOD to ultimate BOD	RBOD	1.85	1.85	Default value
	CBOD settling rate (m day^{-1})	CBODS	0	0	Default value
COD STOICH	P. stoic. for COD decay	CBODP	0.004	0.004	Default value
	N. stoic. for COD decay	CBODN	0.06	0.06	Default value
	C. stoic. for COD decay	CBODC	0.32	0.32	Default value
PHOSPHOR	Sediment SOD release	PO4R	0.001	0.03	Highest value recommended
	P fraction of suspended solids	PARTP	0	0	Default value
AMMONIUM	Sediment release rate of NH4	NH4REL	0.001	0.4	Highest value recommended
	Ammonium decay rate (day^{-1})	NH4DK	0.12	0.12	Default value
NH4 RATE	Lower temp. for NH4 decay (°C)	NH4T1	5	5	Default value
	Upper temp. for NH4 decay (°C)	NH4T2	25	25	Default value
	Fraction of decay at NH4T1	NH4K1	0.1	0.1	Default value
	Fraction of decay at NH4T2	NH4K2	0.99	0.99	Default value
NITRATE	Nitrate decay rate (day^{-1})	NO3DK	0.03	0.05	Value from example
	Denitrification rate from sediments (day^{-1})	NO3S	1	1	Default value
NO3 RATE	Lower temp. for OM decay (°C)	NO3T1	5	5	Default value
	Upper temp. for OM decay (°C)	NO3T2	25	25	Default value
	Fraction of decay at NO3T1	NO3K1	0.1	0.1	Default value
	Fraction of decay at NO3T2	NO3K2	0.99	0.99	Default value
SED CO2	Sed. CO2 release rate	CO2REL	1.2	1	Value from example
O2 LIMIT	Half-saturation const. for O2 proc. (g m^{-3})	KDO	0.1	0.1	Default value
S DEMAND	Zero-order SOD value (g O_2 m^{-2} day^{-1})	SOD		3.5	To match res. conditions
SOD RATE	Lower temp. for SOD decay (°C)	SODT1	4	5	To match res. conditions
	Upper temp. for SOD decay (°C)	SODT2	25	25	Default value
	Fraction of decay at SODT1	SODK1	0.1	0.1	Default value
	Fraction of decay at SODT2	SODK2	0.99	0.99	Default value

The next task was to configure and calibrate CE-QUAL-W2 for the dissolved oxygen section of the model. This task was much more complicated than setting up and calibrating the temperature section of the model since dissolved oxygen is effected by many more processes in a reservoir and therefore a much larger set of algorithms and parameter values has to be examined. It was decided that only the most influential processes affecting dissolved oxygen should be incorporated into the simulation. These processes included the effect of and/or conversation of total dissolved solids, phosphate, ammonia, nitrate, organic matter (divided into labile dissolved organic matter, refractory dissolved organic matter, labile particulate organic matter, and refractory particulate organic matter), biochemical oxygen demand, and algae concentration and activity. The initial concentration of these constituents for January 1, 2007 was unknown as was the inflow concentration of these constituents at Ryan's Dam. In order to provide these values to the model, estimation was conducted based on data from a similar reservoir in Virginia. A ten-year water quality data set from Western Branch Reservoir in Suffolk, VA was used to create the initial concentrations and inflow concentrations, as described in section 4.4.5 (inflow constituent file and initial constituent file). The phosphorus, ammonia and nitrate concentrations and coefficients was set up in the model. Then these concentrations were verified through several simulation runs to make sure that a good agreement occurred with concentrations measured in Western Branch Reservoir, VA. Then the algae (chlorophyll-a) module was set up and calibrated using a similar method. Again, a series of model runs were conducted while the kinetic algae coefficients were adjusted so that the modeled algae concentrations were similar to the measured chlorophyll-a concentration in the reference reservoir. Finally, the BOD in the inflow

was set up following the same approach. The contributory constituents and the initial concentrations are listed in Table 14.

The AHOD (discussed in Chapter 3) was determined to be 1,780 mg m^{-2} d^{-1} for the lower basin of Occoquan Reservoir. Beutel (2003) suggests that for reservoirs of high productivity the sediment oxygen demand (SOD) is typically 75% of the AHOD in moderately deep lakes (10 to 15 meters). Based on Beutel's observations, it was estimated that the SOD was approximately 1,340 mg m^{-2} d^{-1} during May (1,780 mg m^{-2} d^{-1} * 0.75). CE-QUAL-W2 represents the SOD as a zero-order process. In doing so, CE-QUAL-W2 uses a single maximum SOD value with two rate multipliers (SODK1 and SODK2) with corresponding temperatures (SODT1 and SODT2) as shown in Figure 73. The first rate multiplier was 0.1 at 5 °C, and the second rate multiplier was 0.99 at 25 °C. These values are shown in Table 16 under SOD RATE. The multiplier rates and temperatures is to account for the influence that temperature has on SOD (Seiki et al., 1993). Since the SOD was observed at 1,340 mg m^{-2} d^{-1} in May, the maximum SOD value entered into the model was 3,500 mg m^{-2} d^{-1}.

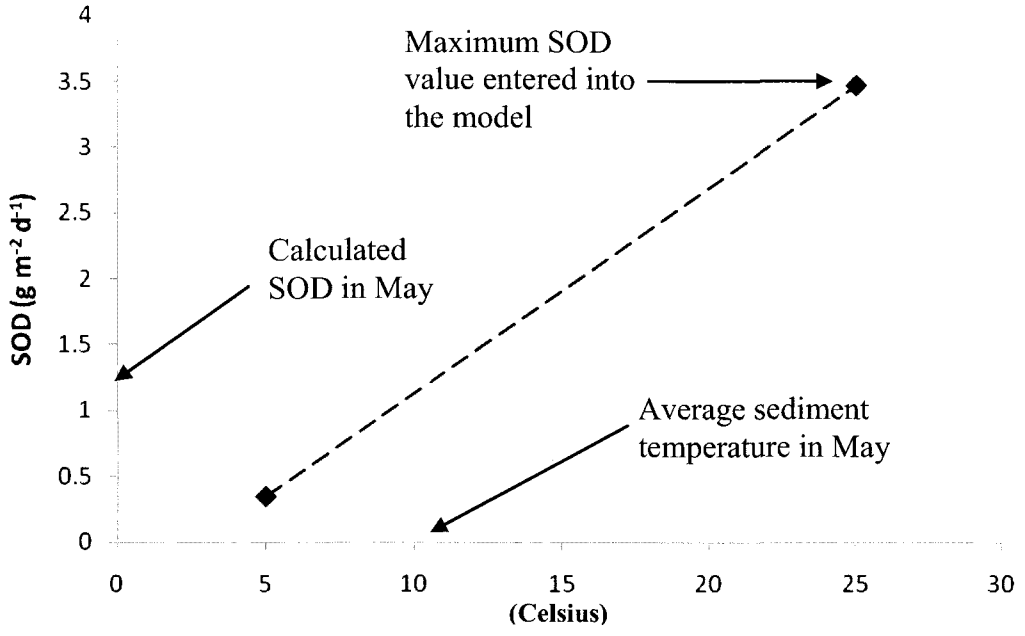

Figure 73. Illustration of the SOD-temperature relationship used for modeling Occoquan Reservoir.

4.4.8 Circulator Flow Rate

The Occoquan Reservoir model could not be calibrated to the measured temperature and dissolved oxygen profiles without simulating the circulation from the surface circulators at the same time. The manufacturer of the circulators listed a direct flow of 3,000 gpm passing through the lift tube and discharging at the surface/near-surface. Based on the manufacturer's statement, the highest possible combined flow rate was therefore assumed to be the sum of the direct flow rates for eight surface circulators, calculated as1.5 m^3/s. Field studies suggested a much smaller flow rate based on measurements of water velocities as the water was flowing over the distribution pan (Chapter 2). It was also found that the circulators were programmed to reduce flow between 9:00 pm and 5:00 am in order to preserve battery life. Based on this down-time

and the lower flow rate measured with the ADV, the smallest combined flow rate was estimated as 0.5 m^3/s. Another factor of uncertainty is the existence of a slot below the distribution pan that was unknown during the time when ADV velocity measurements were made (Chapter 3). If water flows through this slot during circulator operation, then the low estimate of the total circulator flow rate is underestimated.

During the temperature calibration of the model, it was found that the agreement between the modeled and the measured profiles in early 2007 were best when the flow rate was set at 0.8 m^3/s. This flow rate corresponded reasonably with the measured flow rate (ADV). Model results for the summer and later periods were not well characterized at this flow rate but were observed to be better simulated by a reduced flow rate. These model changes reflect changes observed in the field during this period when it was observed that the circulators' performance declined significantly during the late summer and through fall as a result of impeller fouling. A photograph of the condition in August 2007 illustrates conditions on a circulator distribution pan (Figure 74). Not shown in the photograph but also observed was fouling occurring on the impeller. No flow measurements were conducted within this period to quantify the apparent lower flows because the ADV instrument was unavailable. Based on field observations, it was clear that the flow rate became significantly reduced during late summer and fall. To reflect this decline in the circulator flow rate, the model was set up to circulate 0.8 m^3/s from January through June, then reduced to 0.5 m^3/s for July, 0.4 m^3/s for August and 0.3 m^3/s the following months as shown in Table 15. This circulation flow rate scheme produced satisfactory simulated temperature profiles and was therefore used for the remaining modeling.

Figure 74. Picture showing fouling on circulator distribution pan during August, 2007. The thin detached band of algae was loosened upon touching the distribution pan.

4.5 RESULTS

4.5.1 Hydrologic Model

The hydrological model in CE-QUAL-W2 was adjusted to represent Occoquan Reservoir using known daily withdrawal volumes and surface elevations provided by Fairfax Water. The evaporation losses were automatically subtracted by the model and other losses were assumed to be insignificant. The tributary inflow volume at Ryan's Dam was adjusted in the model on a daily basis so that the simulated surface elevation would correspond to the observed surface elevations of the reservoir.

Figure 75 displays the simulated and observed surface elevations as well as withdrawal volumes. There is good agreement between the modeled surface elevation and the measured elevation through the entire 2007 season except for small differences in surface elevation that can be observed between January and April (Julian Day 1-120). Differences during this period were related to debris (such as tree trunks) that accumulated on the spillway and changed the flow dynamics over the spillway were not accounted for in the model. It was decided that a perfect hydrological calibration was not essential during this period, as the reservoir was not stratified and the effect of the circulator operation was insignificant. The flow over the spillway ended in late April at the same time as the thermal stratification established. The tributary inflow was adjusted to achieve a reasonable agreement between the model and the observed surface elevation during the remaining season, as can be seen in Figure 75.

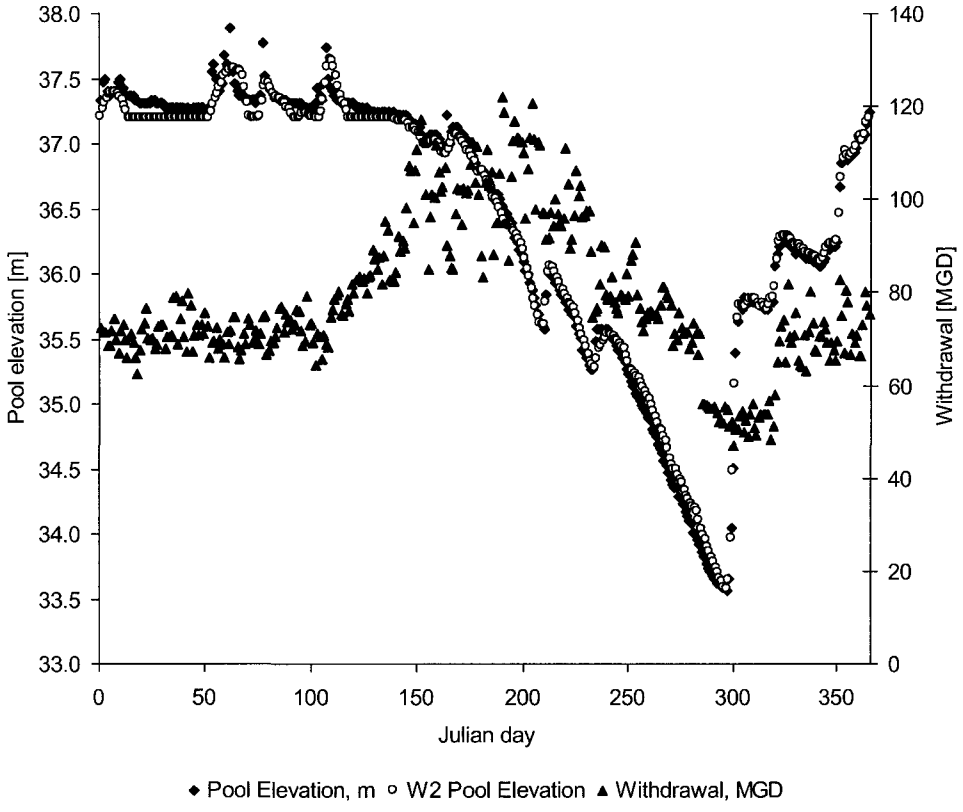

Figure 75. Comparison plot of Fairfax Water's daily measured surface elevations and CE-QUAL-W2's simulated surface elevations through 2007.

4.5.2 Temperature

The seasonal temperature distribution in a monomictic reservoir such as Occoquan Reservoir strongly influences the transport mechanisms that are taking place in the water column, as discussed in Chapter 2. It is therefore necessary to calibrate the temperature segment of the model before other constituents such as dissolved oxygen but after the hydraulic conditions have been accurately represented. The circulator flow rate was set to 0.8-0.5 m^3/s during the temperature calibration as discussed in Section 4.4.8 and calibration was conducted as described in section 4.4.7. Simulated temperature

profiles for each month from February through November are shown, and it can be seen that there is good agreement between the simulated and the observed temperature profiles through the entire 2007 season (Figure 76). Despite a satisfactory temperature calibration of the model, some deviations in the observed and modeled profiles exist at certain depths and times. CE-QUAL-W2 replicates the measured temperature profiles satisfactory through May. Then the simulated temperatures from 3 to 12 meters become slightly colder than the measured profiles. This starts in June and continues in July. This is potentially caused by the model failing to capture the dynamics in the light extinction coefficient during algae blooms. If the light extinction coefficient contributed by the algae was over-represented, the temperature penetration could become colder in this depth. Another possible cause for this discrepancy is an under-represented circulator flow rate within this period. A higher circulation flow rate would draw down the temperature curve above the intake depth (10 meters). The simulated and measured monthly temperature profiles generally corresponded for the remaining months of the year.

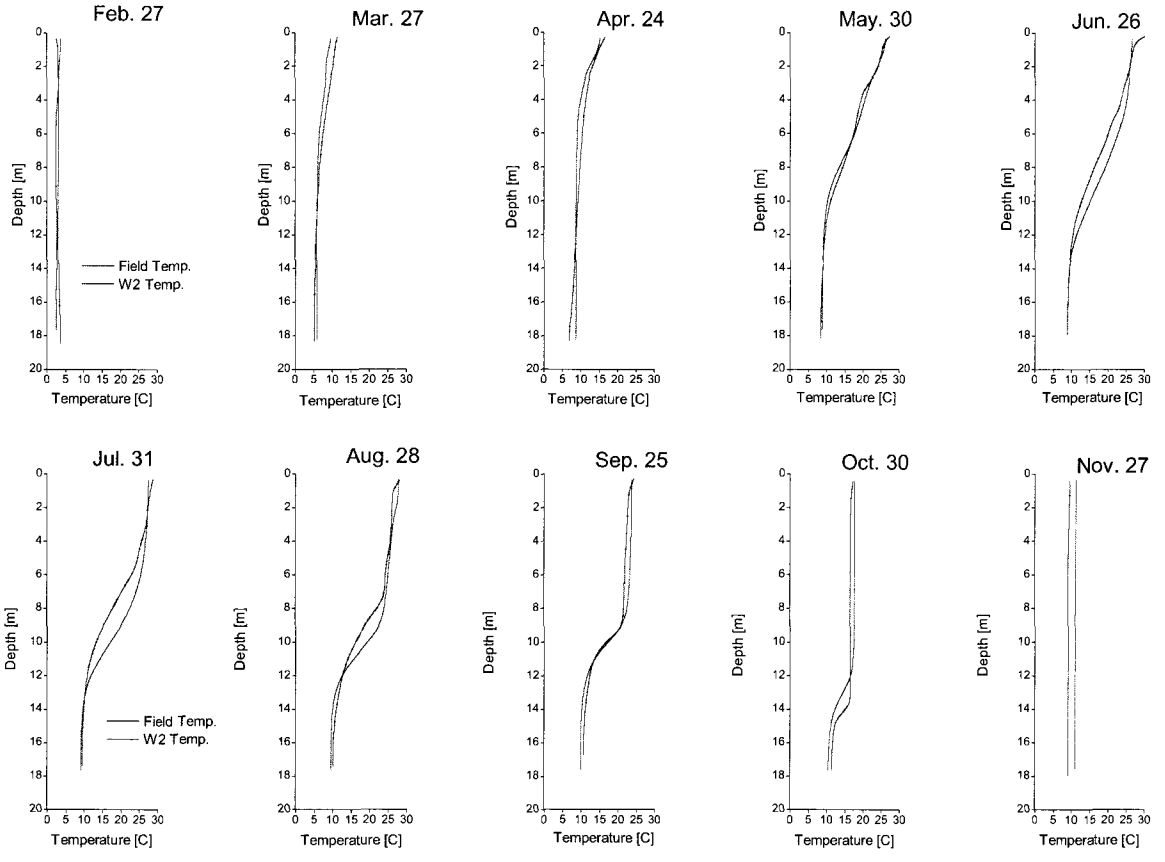

Figure 76. Comparison of OWML's field temperatures at RE02 with CE-QUAL-W2 simulated temperatures.

4.5.3 Dissolved Oxygen

The dissolved oxygen concentration was set up and configured after the temperature segment of the model was calibrated. The method for calibrating reservoir dissolved oxygen concentrations is described in section 4.4.7 and proved to be much more difficult than the temperature calibration. Simulated and measured dissolved oxygen profiles for every month during the 2007 season were similar (Figure 77). Simulated dissolved oxygen profiles deviated from the observed conditions more than the previous temperature profiles which is typical of modeling efforts in general due to the greater

number of factors that can affect dissolved oxygen concentrations and the difficulty of representing all of these processes (e.g. quantifying coefficients) in the model. Simulations using CEQUALW2 have been reported to under represent dissolved oxygen in the surface layer (Cole and Wells, 2000), which was observed from March through June. Another factor to consider when comparing the profiles is that the measured dissolved oxygen profiles (OWML data) were provided for every 1.5 meters, but the dissolved oxygen profiles that the model generated were based on predictions at 0.5 meter intervals. This difference in profile resolution can result in more significant differences between the simulated and the measured profiles where water column concentrations change noticeably over depth intervals of one meter or less (e.g. across the metalimnion).

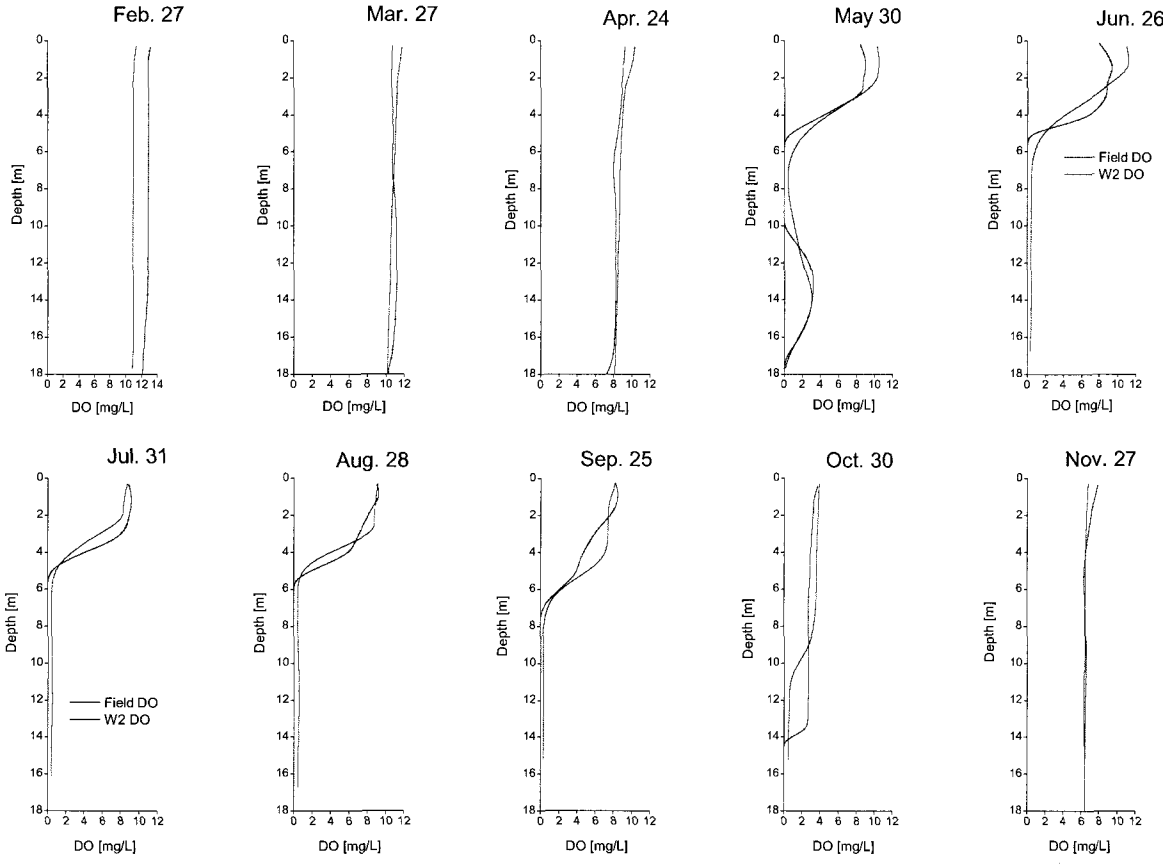

Figure 77. Comparison of Occoquan Reservoir's field dissolved oxygen concentrations with CE-QUAL-W2 simulated dissolved oxygen concentrations.

4.5.4 Spatial Impact from Circulation

The spatial impact from circulator operations on temperature and dissolved oxygen conditions is presented and discussed in Chapter 2 and Chapter 3 but will now be considered based on modeling. Field measurements established a modest depression of both the thermocline and oxycline in the vicinity of the surface circulators as a result of the circulator's discharging at the surface. Examination of model output was conducted to determine whether a similar influence was predicted through simulation.

A spatial (approximately sites NW to WB) temperature and dissolved oxygen distribution was obtained by setting the model to produce a temperature and dissolved oxygen profile for every segment from the dam (segment 37) up to 1,500 meters upstream (segment 25). This is equivalent to the transects that are discussed in Chapter 2. Figure 78 shows the temperature distribution within this lower section of the reservoir on Julian Day 225 (August 13, 2007) at noon; the modeling conditions were identical to the final calibrated simulation run shown in Figure 76. The location of the modeled circulation is shown by a blue line at segment 35. One can see that the spatial temperature distribution is uniform throughout the lower basin and no depression of the thermocline or mixing is predicted in the vicinity of the circulators.

A similar modeling effort was conducted without any circulation to explore the natural condition of the reservoir that would develop without any agitation (Figure 79). The results of the simulation show a dramatically different vertical temperature distribution compared to circulation conditions. The metalimnion (roughly the layer between 14 and 27 °C) under no circulation condition is much narrower in depth (4.2 to 7.0 meters) than circulation conditions (4.5 to 10.2 meters). From this observation it can be inferred that in the absence of circulation the distribution of heat is differently distributed and leads to a stronger density gradient across the metalimnion.

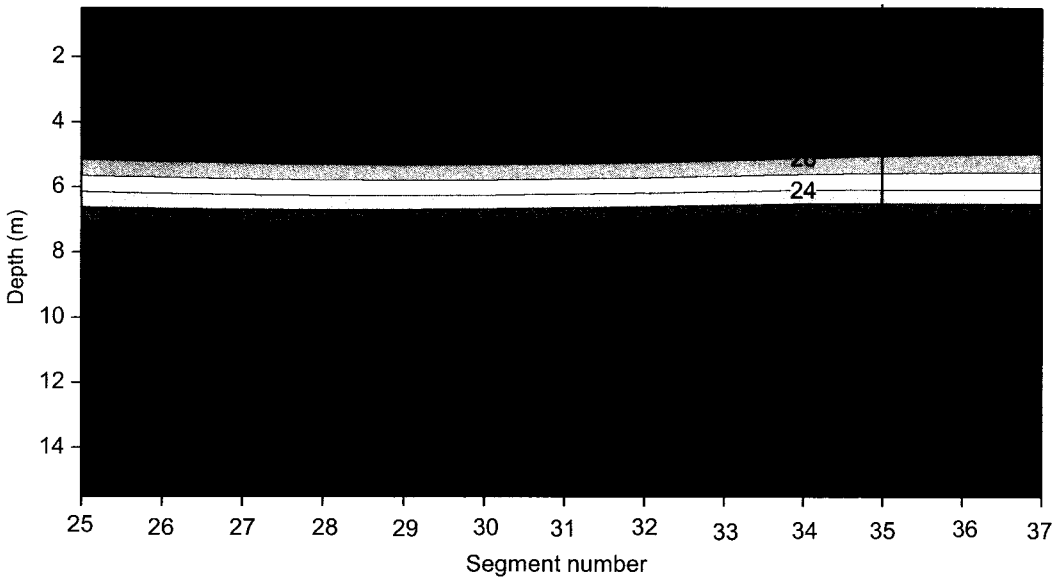

Figure 78. Temperature (°C) transect plot of lower basin of model at Julian Day 225 under regular flow conditions (0.8 to 0.5 m^3/s). The circulator is located at segment 35.

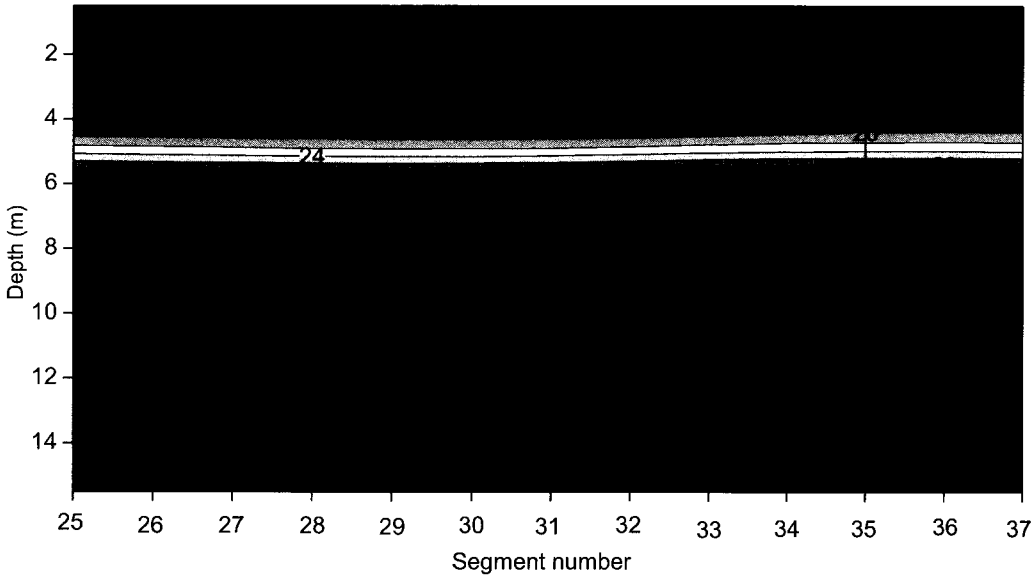

Figure 79. Temperature (°C) transect plot of lower basin of model at Julian Day 225 under no-flow conditions. The circulator is located at segment 35.

Similar to the modeled temperature transects, the spatial dissolved oxygen distribution was also modeled and examined from the dam to 1,500 meters upstream. Similar to temperature, the dissolved oxygen profiles from segments 25 to 37 on Julian Day 225 illustrate the potential impact that circulation had on dissolved oxygen relative to (modeled) no-circulation conditions (Figure 80). For comparison, the prediction of dissolved oxygen concentrations but with no circulation is also shown (Figure 81). By comparing the two simulated oxygen transects, it is clear that the modeled results show that circulation lowers the depth of the oxycline slightly.

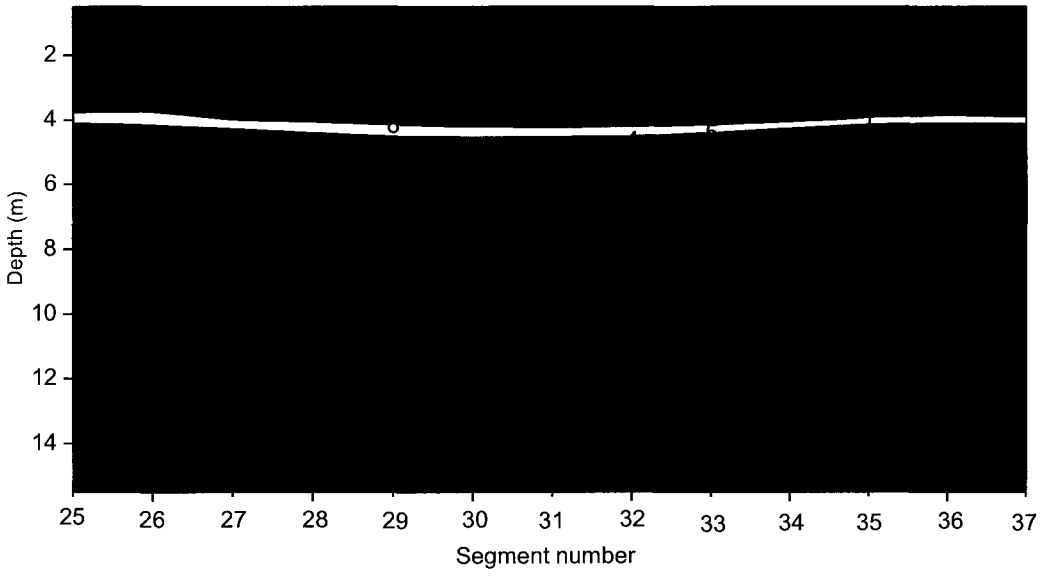

Figure 80. Dissolved oxygen (mg/L) transect plot of lower basin of model at Julian Day 225 under regular flow conditions (0.8 to 0.5 m^3/s). The circulator is located at segment 35.

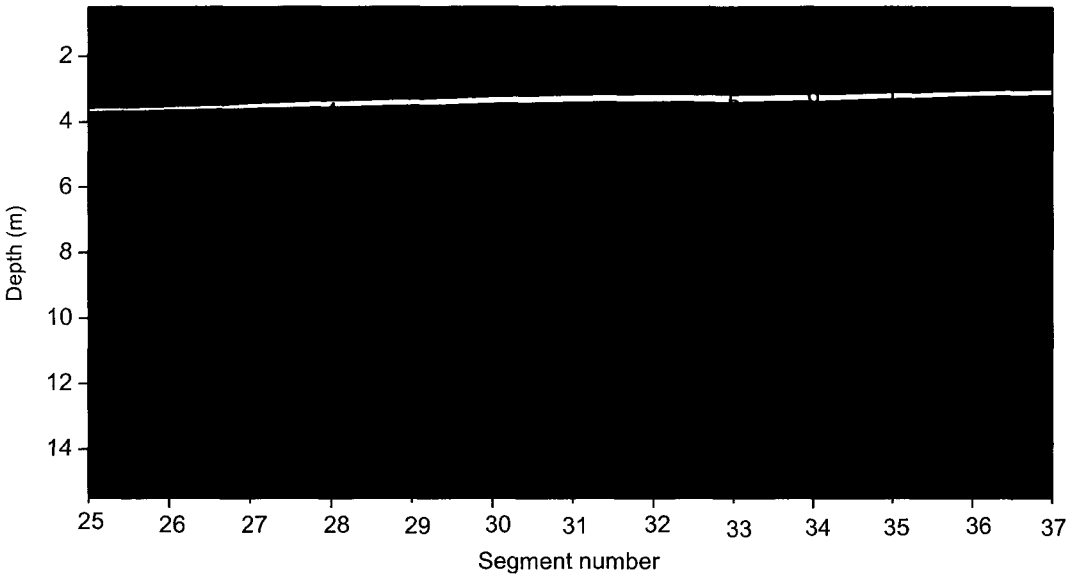

Figure 81. Dissolved oxygen (mg/L) transect plot of lower basin of model at Julian Day 225 under no-flow conditions. The circulator is located at segment 35.

4.5.5 Simulated No-flow Condition in Occoquan Reservoir

In Section 4.4.7 the challenges of calibrating a model that was under the influence of artificial vertical mixing (surface circulators) were discussed. Calibration for circulation condition and assumption that the model reasonably represents processes in the absence of circulation was necessary since "natural" temperature and dissolved oxygen distributions of Occoquan Reservoir were unknown due to oxygenation activities that have been operating continuously during the stratification season since 1970. In the previous section the temperature and dissolved oxygen profiles were examined under circulation flow and under no circulation flow on Julian Day 225 (August 13, 2007). In this section, the full impact of circulation versus no circulation will be studied on a monthly basis during the full season of 2007. This temporal study will give a better understanding of what the behavior of the reservoir would be without any circulation.

Figure 82 shows simulated temperature profiles for every month through 2007 for circulation flow conditions and for no-circulation conditions; the profiles for circulation flow conditions (blue) are identical to the profiles shown in Figure 76. The profiles for the no-circulation conditions (red) were simulated with the same model as the flow profiles, except circulation flow was defined as 0 m^3/s. Assuming that the model with the circulation flow was calibrated correctly, the no-flow temperature distribution should represent the natural behavior of the reservoir without the eight surface circulators. Figure 81 shows that there was no difference between the two scenarios from January, 2007 up to the thermal stratification season started in May 2007. This indicates that the natural vertical mixing prior to thermal stratification provides greater transport than the surface circulation system that was deployed in 2007. In May, just after the establishment of the thermal stratification, the thermocline for the circulation flow scenario gradually established deeper in the water column than the no circulation scenario. This difference grew more pronounced as the stratified season progressed. From August through October, the difference in thermocline depth was as much as 2 to 3 meters between the two flow scenarios.

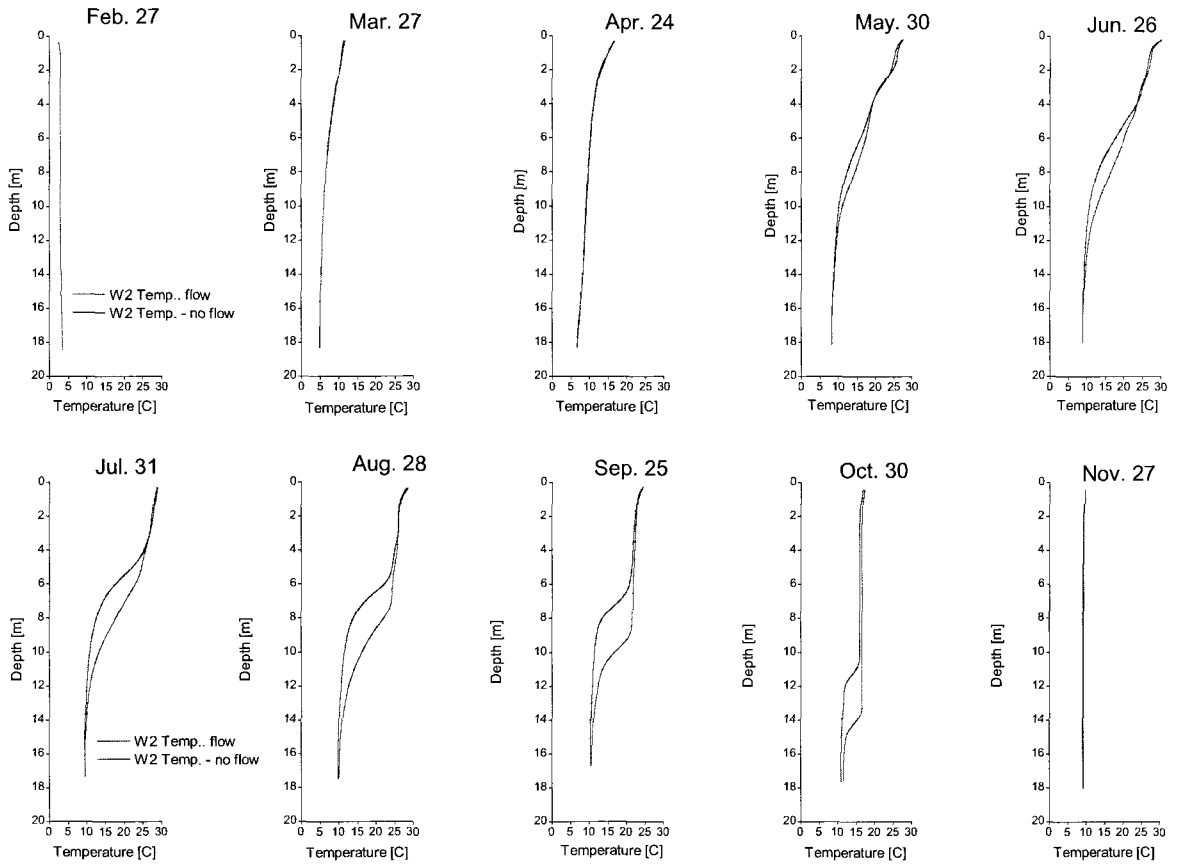

Figure 82. Temperature profiles under regular circulator flow rates and zero circulation flow rate.

Dissolved oxygen profiles were similarly studied through the full season of 2007 under both circulation conditions and under no-flow conditions (Figure 83). Prior to the thermal stratification, the circulation did not have any impact on the oxygen concentration of the water column. As the thermal stratification established in early May, the oxygen profiles started to deviate. It can be seen that the circulation flow scenario generally established the oxygen profile deeper in the water column than the no-flow scenario, consistent with hypolimnetic surface circulators removing volume from the hypolimnion and adding volume to the epilimnion. Based on the flow and no-flow

temperature profiles on September 25, 2007 (greatest difference in thermocline depth), it was found that the hypolimnetic volumes ($5.7 * 10^6$ m^3 and $3.0 * 10^6$ m^3 respectively) differed by $2.7 * 10^6$ m^3. This volume was much less than the pumped volume through the circulators from the start of the thermal stratification period (approximately $6.0 * 10^6$ m^3). The difference is assumed to be related to the withdrawal of water to the WTP from the middle intake (8.2 meter) until June and from the top intake (3.6 meter) for the remainder of the period. The withdrawal volume to the WTP was $49.9 * 10^6$ m^3 during this period.

An observation from Figure 83 is that the greatest difference between the circulation scenario and the no-circulation scenario occurred in October and November. The total oxygen mass in October, according to the model, was 52,000 kg in the reservoir during circulation and 87, 000 kg during no-flow conditions. A possible cause for a higher oxygen mass in the reservoir during no-flow conditions is that the circulators may have eroded the thermal stratification much earlier and deeper, introducing a higher oxygen demand in October. In November there was no thermal stratification in any of the scenarios. Figure 83 shows that the circulator scenario resulted in a dissolved oxygen concentration of about 6.5 mg/L (150,000 kg total oxygen mass), while the no-circulator scenario resulted in about 5 mg/L dissolved oxygen concentration (116,000 kg total oxygen mass). It was calculated that the circulators transfer about 30 kg oxygen to the reservoir every day based on 8 circulators with 142 g/h O_2 (Chapter 3).

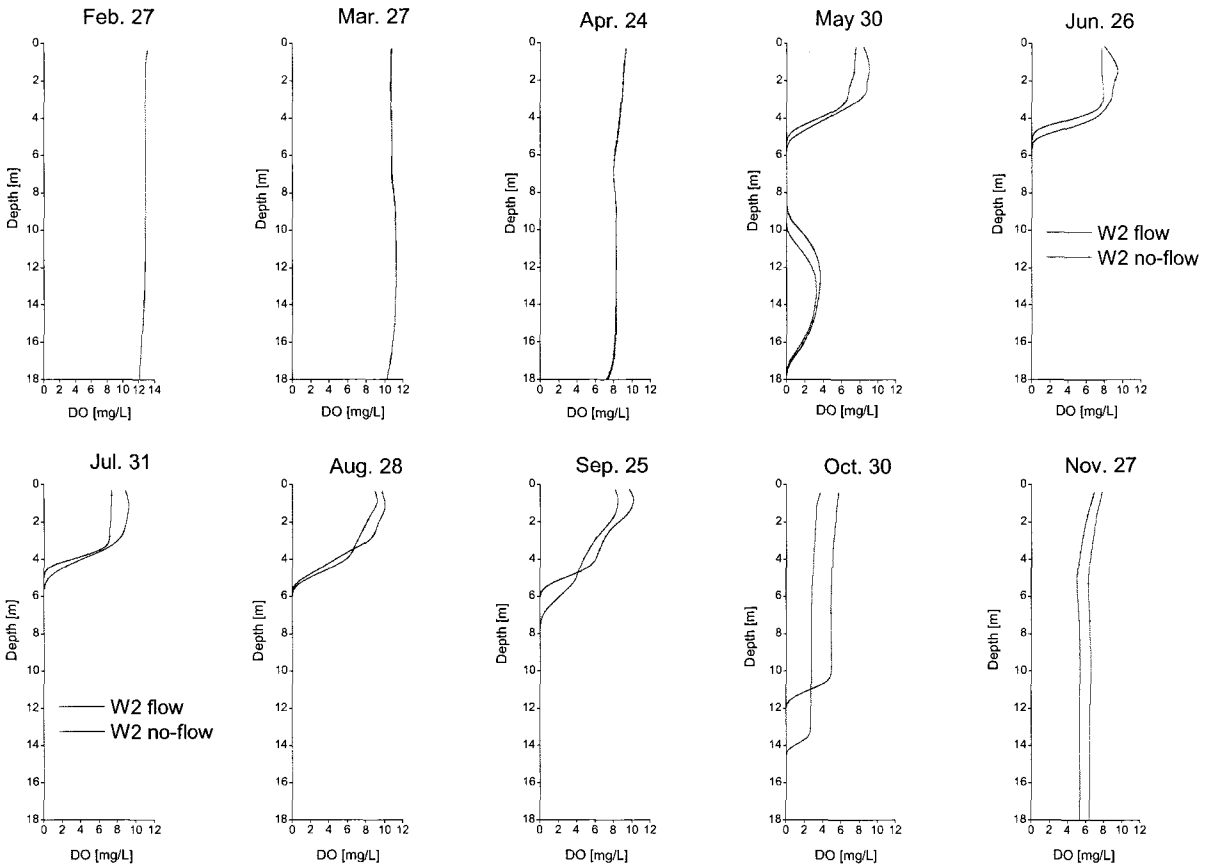

Figure 83. Dissolved oxygen profiles under regular circulator flow rates and zero circulation flow rate.

4.6 Conclusion

This chapter described the process of setting up and calibrating CE-QUAL-W2 to represent Occoquan Reservoir during the 2007 surface circulator year. The combined flow of the eight circulators was represented in the model using the pump algorithm. Water was withdrawn at 10 meters depth and released at the surface. After the hydrological conditions, such as in and out flows and surface elevations, were configured, the input files were developed (i.e. metrological file, tributary temperature file, and tributary constituent file). Finally, the model's process parameters were adjusted

until a good agreement between the simulated and the measured temperature profiles and dissolved oxygen profiles were achieved (at WB site near the dam). The temperature representation in the model was relatively easy to adjust, but the dissolved oxygen component of the model was significantly more difficult to calibrate. This is because dissolved oxygen is involved in many processes in a lake/reservoir system. Despite having to adjust many process parameters in the model, adequate agreement with measured oxygen profiles was achieved.

From volume calculations of the hypolimnion between circulation and no-circulation condition it was found that the withdrawal volume to the WTP (from the epilimnion) interfered with the lowering of the thermocline. Because of the large withdrawal volume ($49.9 * 10^6$ m^3) from the epilimnion, it is likely that this would reduce the temperature and dissolved oxygen impact that the circulators would have on the reservoir.

The spatial distribution of temperature and dissolved oxygen in the lower section of the reservoir was simulated during flow and no-flow conditions (flow rate = 0 m^3/s). It could be observed how the circulator operation lowered the thermocline about one meter. The circulator operation also made the thermocline less sharp. The simulated oxycline was less affected by the operation of the circulators. The depth of the oxycline was only slightly affected, and there was no significant difference in the sharpness (transitional depth) of the oxycline during circulation flow and no-flow conditions.

Finally, a temporal comparison of the model under normal circulator flow and no-flow condition was conducted. It was found that there was about a 2 to 3 meter difference in oxycline depth during July, August, September, and October. There was no

temperature difference between the two flow scenarios in November. It is assumed that the no-flow temperature represented the natural behavior of the reservoir (no mixing). The dissolved oxygen distribution showed only minor differences through February to September for the two flow scenarios. The October total oxygen mass in the reservoir was reduced during the circulation simulation compared to the no-circulation scenario. This was assumed to be related to the circulators' early erosion of the thermal stratification, introducing oxygen demand. The total oxygen mass and the oxygen concentration in November ended up significantly higher for the circulation scenario compared to the no-circulation scenario.

4.7 Future Research

Future efforts should be focused on including other water quality parameters in the modeling such as phytoplankton. A more in depth development of the algae segment of the model based on algae kinetics would be beneficial when studying the hypolimnetic surface circulator's affect on the algae concentration. Manufacturers claim that surface circulation can reduce the algae growth rate by pushing the algae deeper in the water column. This supposition is based on the assumption of light starvation that algae would experience at deeper depths from the surface. In particular, cyanobacteria behavior is of interest when predicting taste and odor events by modeling. This is of particular interest for lake/reservoir managers and the source water community.

This research has studied the impact of up-flow surface circulation on temperature and dissolved oxygen. Future efforts should also look at the impact of down-flow

circulation for comparison. Both modes of circulation are reported in the literature and a comparison of the two circulation modes by modeling would be beneficial.

Future efforts may also be aimed at representing other circulation equipment within CE-QUAL-W2, such as free bubble plume aeration systems. Aeration systems are the most common lake and reservoir oxygenation solution due to their relatively simple design and reputation for efficiently increasing the oxygen concentration of many reservoirs. If the bubble plume process could accurately be represented within CE-QUAL-W2, then the model would become a valuable tool for feasibility studies of aeration solutions in reservoirs. The model would possibly also become a tool for sizing aeration systems in lakes or reservoirs.

CHAPTER V

MODELING THE OF EFFECT OF LAKE SIZE, FLOW RATE, AND INTAKE DEPTH

5.1 Introduction

The objective for this chapter is to develop an understanding of the conditions or limits under which surface circulation can improve the dissolved oxygen distribution in reservoirs. In Chapter 4, modeling was used to replicate the temperature and dissolved oxygen profiles in Occoquan Reservoir and to approximate/simulate what the conditions would likely be under no circulation conditions. In this chapter, modeling will be used to study the impact of various circulation configurations in various virtual lakes of different configurations to assess whether consistent relationships are observed that can be developed into a guidance procedure for sizing circulators to various lakes and reservoirs. All natural water bodies will respond differently to surface circulation due to their differing biological, chemical, and physical properties; however, modeling surface circulation in hypothetical/conceptual lakes is valid when exploring the general influence that the technology has on temperature and dissolved oxygen conditions. To investigate the ability of the surface circulation technology to oxygenate lakes and reservoirs is an important contribution to lake/reservoir management since reservoir managers are always looking for solutions for reducing the anoxic conditions that typically accompany eutrophication.

In this effort, four hypothetical reservoirs of different volumes were chosen; each with different depths, so that the impact from a circulation system could be explored under various conditions. The four conceptual lakes had identical surface areas but different depths. The maximum depths were 7, 10, 15, and 20 meters, all deep enough to establish thermal stratification during summer, which is known to establish at about 5 meters depth in Virginia. The bathymetries of these lakes are illustrated in Figure 82.

CE-QUAL-W2 was used for simulating the temperature and dissolved oxygen conditions in the four hypothetical lakes. Each lake was modeled similarly to Occoquan Reservoir, described in Chapter 4 except for the bathymetry files which were configured to represent the lakes as shown in Figure 82. The bathymetry files for the 7, 10, 15, and 20 meter lakes each had 22 longitudinal segments of 250 meters, and 40 vertical layers, each with respectfully 0.175, 0.25, 0.375, and 0.5 meter height. Each layer was given a lateral width so that it would correspond with its bathymetry. These lateral layer widths were the same for all the hypothetical lakes, allowing the use of the same basic bathymetry file design. A summery of the segments, layers, and volumes is shown in Table 17.

During the simulations that were conducted on the four virtual lakes, all the initial water quality concentrations and the model configurations were the same as the Occoquan Reservoir simulation described in Chapter 4. It was assumed that the weather file used for the Occoquan Reservoir (Chapter 4) would be appropriate for all lakes within this region, thus ensuring a reasonable weather influence on the hypothetical lakes. The hydraulic residence time among natural lakes and reservoirs vary greatly. So does the influence from the constituents in the tributaries. This influence particularly affects

the vertical dissolved oxygen distribution high inflow rates. It was decided that no inflow or outflow would occur for the four hypothetical lakes to ensure constant surface elevations and otherwise equal conditions, under which a comparison of the circulator influence would be possible.

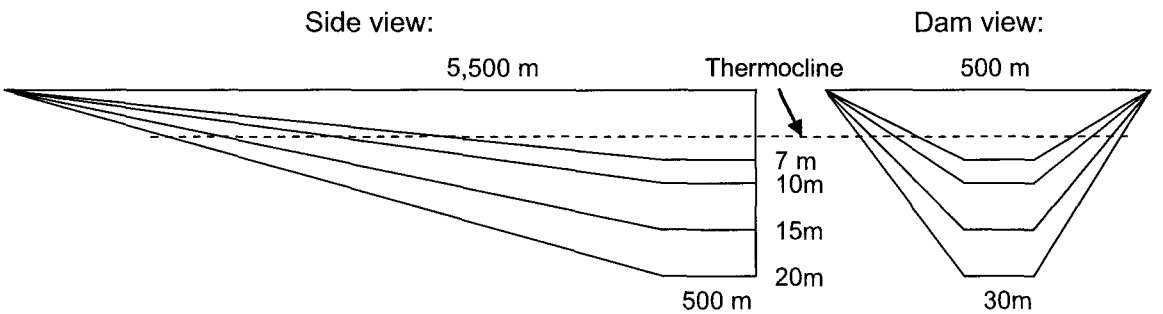

Figure 84. Physical features of all four hypothetical lakes. All the lakes have the same surface area, but the maximum depth is respectfully 7, 10, 15, and 20 meters. Horizontal and vertical distances are not to scale.

Table 17. Summary of hypothetical lakes bathymetry grid, surface area, and lake volume. Occoquan Reservoir (O.R.) information is also included.

Maximum lake depth [m]	Number of segments	Number of layers	Segment length [m]	Layer height [m]	Surface area [10^6 m^2]	Total volume [10^6 m^3]	Volume above 5 meter [10^6 m^3]	Volume below 5 meter [10^6 m^3]
7	22	40	250	0.175	2.75	6.99	6.72	0.27
10	22	40	250	0.250	2.75	9.98	8.45	1.53
15	22	40	250	0.375	2.75	14.98	9.53	5.44
20	22	40	250	0.500	2.75	19.97	10.93	9.04
O.R.	36	40	Varies	0.500	3.37	21.53	13.01	8.52

The surface circulator representation within CE-QUAL-W2 for the four hypothetical lakes was similar to the previous Occoquan Reservoir simulation, described in Chapter 4. The circulation was placed in the middle of segment 20, near the deepest part of each lake. This was done to potentially influence the largest water column, and the intake depth was set as deep as possible (0.5 meter above the maximum depth) for the same reason. Each model run-time was conducted over a 365 day period in order to capture an entire seasonal cycle.

CE-QUAL-W2 is an advanced hydrodynamic water quality model capable of simulating all typical eutrophic processes that take place in a lake. The model numerically determines the concentration of the active constituents at any point in the bathymetry throughout the run-time. In order for the model to provide output data, such as temperature and dissolved oxygen profiles, a segment must be defined in the control file along with a time for the profiles to be recorded. It was decided that the best location for recording temperature and dissolved oxygen profiles was at the middle of the last segment before the dam (Figure 85 segment 22). The benefits of this location were a full lake depth and an entire segment between the circulation and the data recording (500 meters). The sensitivity of the circulator location was tested by moving the circulator to segment 19, but it was found that the difference in vertical temperature and dissolved oxygen profiles was negligible, so it was decided to locate the circulation in segment 20 as shown (Figure 85).

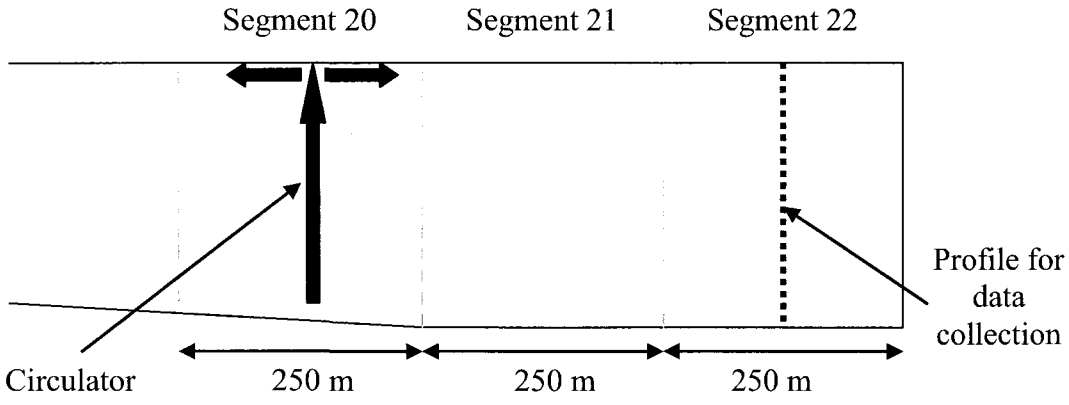

Figure 85. Conceptual representation of the location of the circulator and the data recording.

Before the simulated temperature and dissolved oxygen impact from the surface circulation could be examined, the natural behavior of each lake was modeled throughout a full year without circulation (i.e. flow rate = 0 m^3/s). The resulting temperature and dissolved oxygen distributions were compared to similar lakes in Virginia to ensure that the model generated reasonable values. The temperature distribution of these simulations is shown as isopleths in the first column of Figure 86.

Next, a new set of simulations was conducted with a modest circulation so that the temperature influence from the circulation could be compared to the previous zero-flow conditions. A modest circulation flow rate of 0.5 m^3/s was provided because this flow rate is relatively easily produced with commercially available equipment. Figure 84 displays the resulting temperature isopleths under a 0.5 m^3/s circulation rate of all four hypothetical lakes in the second column.

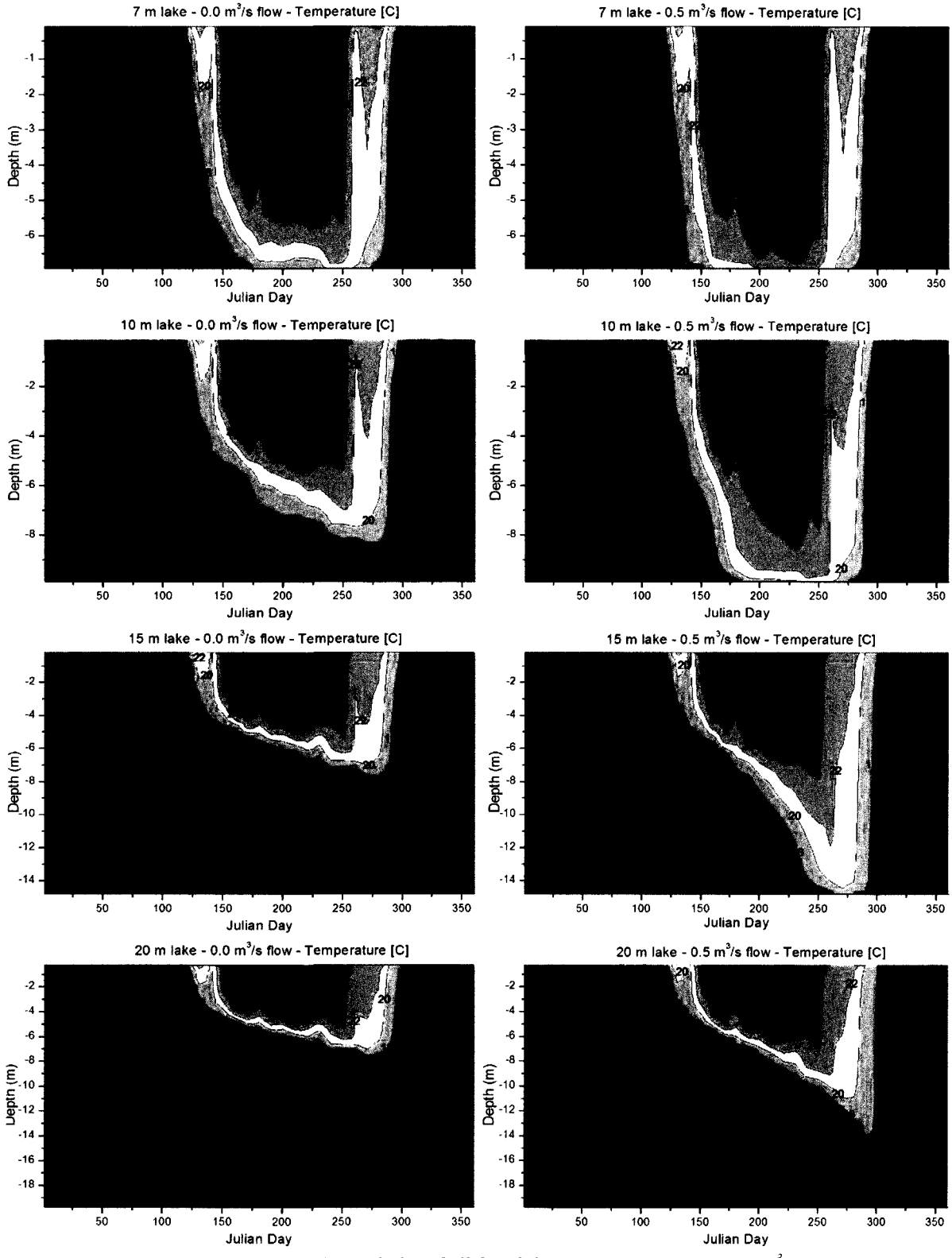

Figure 86. Temperature [C] panel plot of all four lake sizes under zero and 0.5m^3/s circulation flow. The plots are based on the 220th Julian day (August 8) conditions

The impact on the temperature distribution from circulator operation on the 7-meter lake was not as pronounced as for the other lake sizes. This is related to the fact that the thermocline naturally (no circulation) develops near the sediments. Figure 86 shows that the thermocline occurs at 6.5 meters on Julian Day 220 (August 8) without circulation, but when 0.5 m^3/s circulation rate is applied, the thermocline is eliminated resulting in only minor temperature changes in the water column. The greatest temperature impact from circulation occurs at the lower water column, where warmer water reaches the sediments.

The circulation influence on the 10-meter lake was more pronounced than the 7-meter lake. A well defined thermocline developed naturally (no circulation) at about 6.5 meters for Julian Day 220 (August 8), but when the 0.5 m^3/s circulation rate was applied, the 10 meter lake quickly became destratified. This can clearly be seen in the dT/dy plot in Figure 87. Based on Figure 86, it appears that the thermocline is pulled down to the sediments in approximately 35 days after thermal stratification was established. This period corresponds to the time it would take for the circulator to draw down the thermocline at 0.5 m^3/s circulation flow rate. This response suggests that the vertical temperature distribution in this lake was substantially altered by physical mixing. The largest temperature increase occurred at the sediment-water interface for the 10-meter lake, which would be expected to have a large impact on biogeochemical reactions and rates at which they occur (Wetzel, 2001).

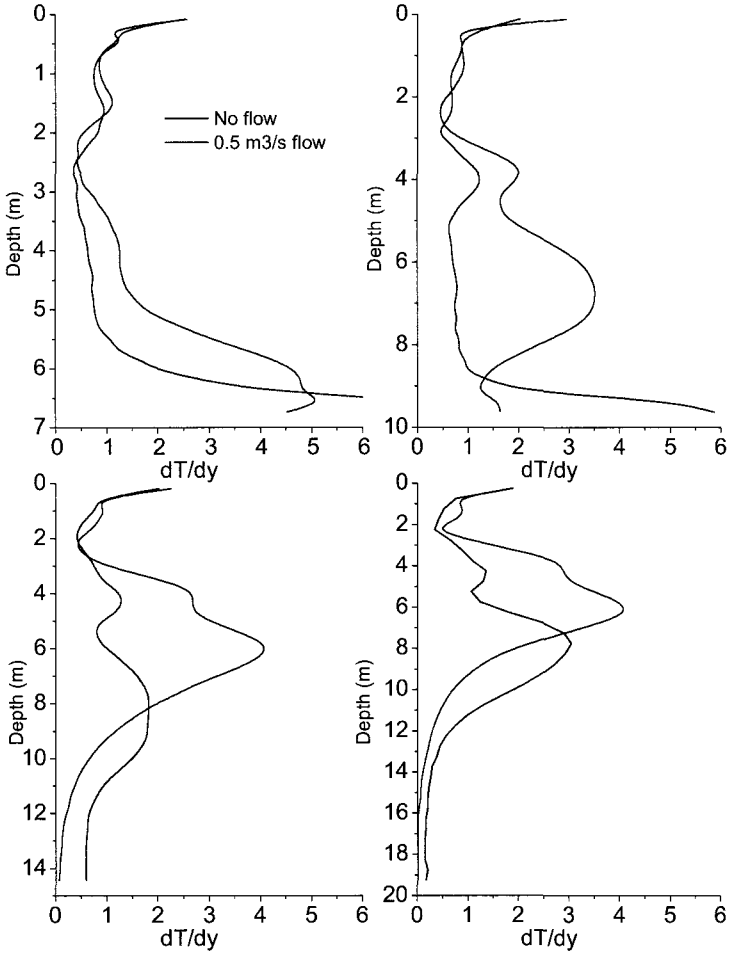

Figure 87. dT/dy plots for all four hypothetical lakes at Julian Day 220 (August 8).

The 15-meter lake was also significantly influenced by the circulation. The thermocline naturally occurred at 6 meters on Julian Day 220 (August 8) with no circulation. When the 0.5 m^3/s circulation was applied, the temperature increased in the hypolimnion (Figure 86) and the thermocline was pulled down gradually until it reached the sediments around the 240th Julian Day (August 28), approximately 120 days after the establishment of the thermocline. This period corresponds with the time required for the circulator to pump a volume similar to the hypolimnetic volume. There is a good

correspondence between the hypolimnetic volume listed in Table 17 ($5.4 * 10^6$ m^3) and the pumped volume at the time that the thermocline reaches the sediments ($5.2 * 10^6$ m^3). This response is similar to the 10-meter lake and illustrates the capability of circulation to alter the vertical temperature distribution.

The 20-meter lake was also significantly influenced by circulation. The lake naturally developed a thermocline at 6 meters (Figure 86), but when the 0.5 m^3/s circulation rate was applied, the thermocline migrated downward in response to hypolimnetic withdrawal. The hypolimnetic volume was too large for the circulation rate to draw the thermocline down to the sediments before the stratification season ended. This corresponds with the calculated 200 days it would take to draw down the hypolimnetic volume at 0.5 m^3/s, when the stratified season only lasted about 160 days. Despite failing to pull the thermocline down to the sediments, the temperature was approximately increased 5 °C at the sediment water interface towards the end of the stratified period.

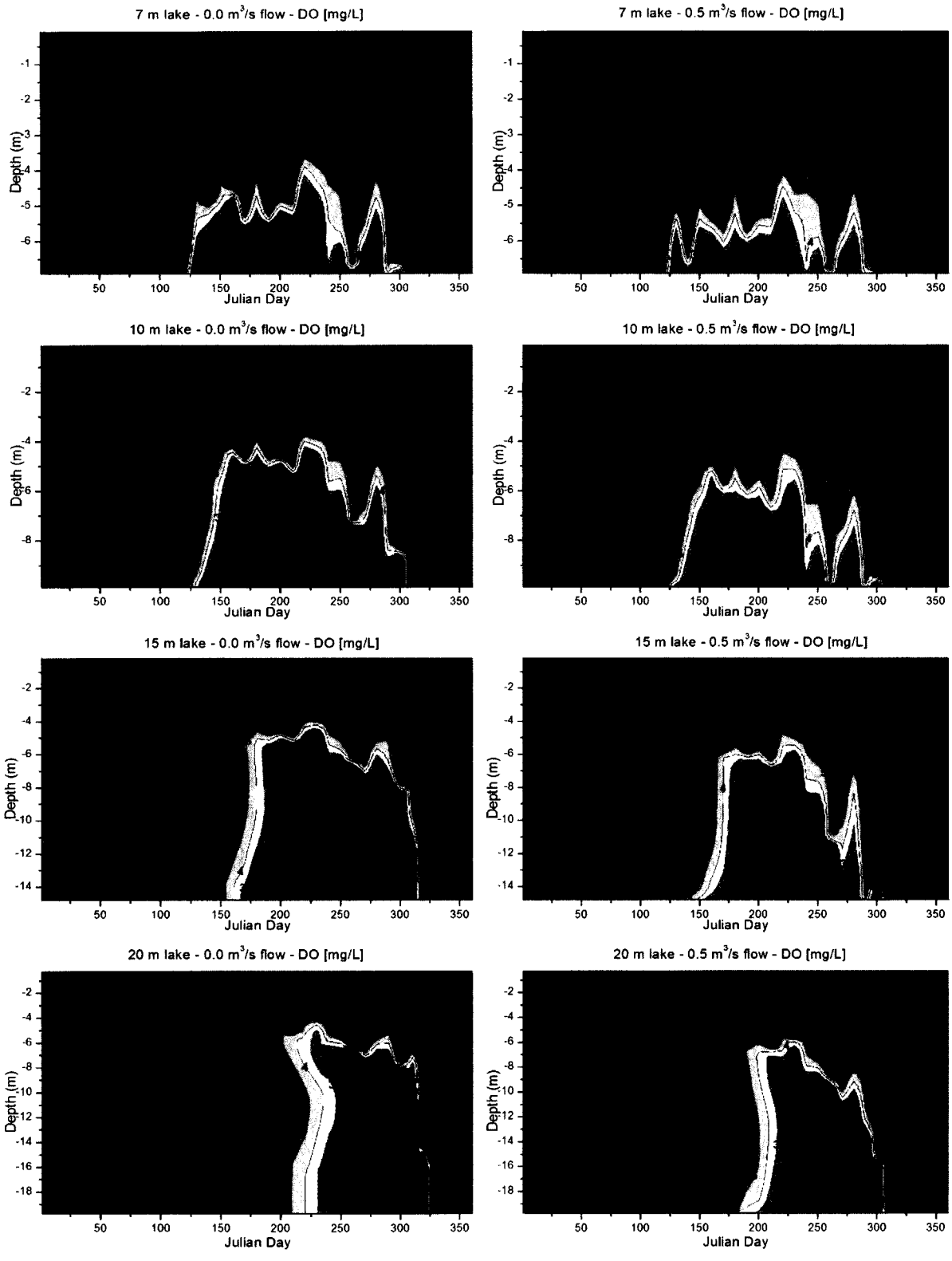

Figure 88. Dissolved oxygen [mg/L] panel plot for the four lake sizes under zero and 0.5m3/s flow. The plots are based on the 220th Julian day(August 8) conditions

Similar to the previous temperature simulations, dissolved oxygen conditions were examined in all four hypothetical lakes simulated by CE-QUAL-W2 under circulation and no circulation conditions. The results of these dissolved oxygen simulations are shown in Figure 88.

The 7-meter lake developed an oxycline around Julian Day 125 (May 5). It developed first at the sediment water interface and ascended to a depth of approximately 5 meters below the surface around Julian Day 140 (May 20). It stayed at this depth until Julian Day 220 (August 8), then fluctuated between 4 meters and 7 meters until the oxycline was eliminated at Julian day 290 (October 20). It appears that the oxycline was pushed down to the maximum depth of 7 meters around Julian Day 260 (September 17), temporarily eliminating the anoxic event. When 0.5 m^3/s circulation rate was simulated, the oxycline generally established at 6 meters. This is about one meter deeper than during the no circulation condition. It can be seen that the oxygen condition was improved by the circulation, but the anoxic condition was not eliminated in the 7-meter lake.

The 10-meter lake showed similar behavior as the 7-meter lake. The establishment of an oxycline occurred around Julian Day 130 (May 10) during no circulation, which was a few days later than the 7-meter lake. The oxycline developed at 5 meters depth, then fluctuated as it descended and finally disappeared around Julian Day 300 (October 27). During the 0.5 m^3/s circulation rate the oxycline was lowered one meter, similar to the 7-meter lake. The 10-meter lake lost the oxycline during fall turnover at Julian Day 260 (September 17). Similar to the 7-meter lake, the anoxic conditions were not eliminated by the circulation.

The 15 meter lake developed an oxycline 30 days later than the 7 and 10 meter lakes (Figure 88). This is likely related to a deeper lake having a higher oxygen mass than a shallow lake, thus taking longer for the water column oxygen demand and the sediment oxygen demand to consume the available oxygen. The oxycline disappeared about 15 days later than for the 7 and 10-meter lakes. This is likely related to the delayed turnover for the deeper lakes, which can be observed in Figure 86. The 0.5 m^3/s circulation rate caused the oxycline to develop at 6 meters depth, one meter deeper than for the shallower lakes. The weather event on Julian day 260 (September 17) was not able to destratify the 15 meter lake, as it did with the shallower lakes.

The 20-meter lake showed a similar trend to the 15-meter lake with a delayed onset of oxygen depletion. Similar to the 15-meter lake, the high oxygen mass in the 20-meter lake caused the anoxic event to develop later in the season compared to the shallower lakes. It can also be seen that the oxygen depletion rate in the hypolimnion was slower in the 20-meter lake than the shallower lakes. Because the oxycline developed late in the season, the oxycline only occurred at 5 meters depth for a short period before descending to 6 to 7 meters depth.

Surface circulation improved the vertical oxygen condition in all four hypothetical lakes, but anoxic conditions were not eliminated by circulation (Figure 88). The sediment oxygen demand was particularly dominant in the shallow lakes (7 and 10-meter), and the water column oxygen demand was more prevailing in the deeper lakes (15 and 20-meter). The sediment oxygen demand was similar in all four lake models, which may be an oversimplification of the variation that would occur in similar lakes. Beutel (2003) suggests that the sediment oxygen demand is higher in shallow lakes and

lower in deeper lakes. This relationship is related to little of the total oxygen demand of the organic matter being consumed in the water column due to the shorter residence in the water column. Deeper lakes provide a longer period of time for organic matter to oxidize so the detritus will have less oxygen demand remaining when it reaches the sediments and therefore less sediment oxygen demand to be exerted than a shallow lake.

The oxycline was lowered by approximately one meter at all four lake sizes as a result of the 0.5 m^3/s circulation flow rate. This appears to be a small improvement with respect to the oxygen condition of the lakes, but the consequence of lowering the oxycline by one meter is that less sediment surface is subjected to overlying anoxic water. It is assumed that undesirable anoxic biogeochemical processes such as iron and manganese reduction are proportional to the sediment area that is exposed to anoxic conditions. Therefore, the total production of iron and manganese will be reduced when the oxycline is lowered in the water column, and consequently the sediment area exposed to anoxic condition is reduced. Based on this concept, the circulator performance could therefore be evaluated with respect to the reduction in the sediment water area under anoxic overlaying water.

All four hypothetical lakes were evaluated based on the fraction of the sediments that were exposed to low-oxygen conditions during no circulation and during circulation. A low-oxygen condition for the purpose of this analysis is defined as less than 4 mg/L oxygen, which was considered a critical value below which manganese mobilization from sediments has been observed (Giblin, 2009). In order to explore the improvement of the circulation in the four hypothetical lakes in terms of sediment surface that is no longer

exposed to low-oxygen conditions, a new set of plots was generated illustrating the effect of circulation (Figure 89).

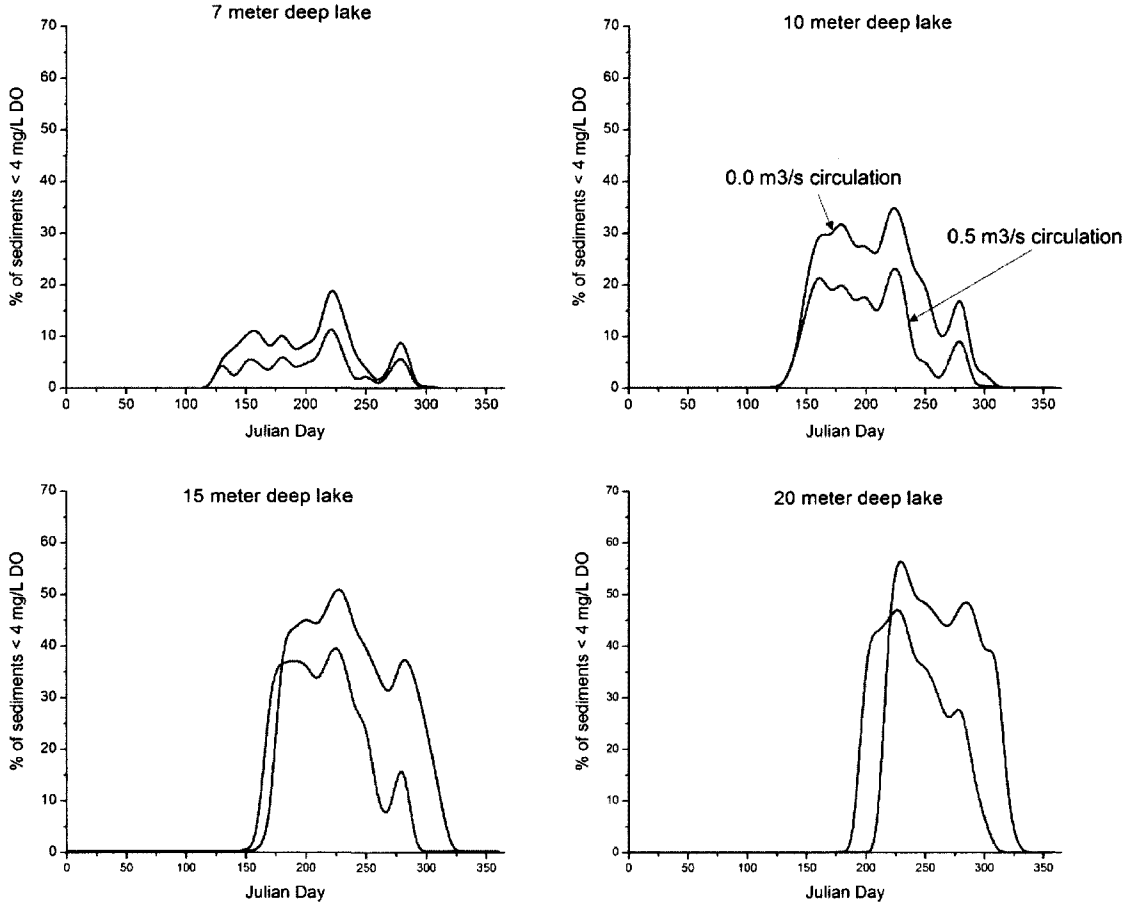

Figure 89. Percent of sediments exposed to less than 4 mg/L dissolved oxygen under no circulation and under 0.5 m3/s circulation. The plots are based on the 220th Julian day (August 8) conditions.

It is clear that the impact of circulation, as described with CE-QUAL-W2, is a decrease in the sediment area exposed to low oxygen conditions. The difference between no circulation and a moderate circulation rate of 0.5 m^3/s was less significant in the 7-meter

lake than in the deeper lakes. This is related to the large sediment surface (oxygen demand) to water volume ratio that occurs at the deepest part of a lake. It is therefore difficult to overcome the oxygen demand that exists in this region. The deeper lakes showed a more pronounced reduction in the sediment surface area exposed to low-oxygen condition, as the anoxic depth developed naturally further from maximum depth. The 7-meter lake had approximately 10% of the sediment surface area exposed to low-oxygen conditions without any circulation. This percentage was reduced to about 5% during 0.5 m^3/s circulation rate. The 10-meter lake had approximately 30% of sediment surface exposed to low-oxygen condition, but this was reduced to 20% with circulation. The 15 meter lake naturally exposed 45% of the sediment surface to low-oxygen condition without any circulation, but when circulation was applied, the initial percentage was 35%. The difference was growing significantly towards the end of the stratified season. The 20-meter lake had about 55% of the sediment surface area exposed to low-oxygen conditions, but this percentage was reduced to 45% under a circulation rate of 0.5 m^3/s. As in the 15-meter lake, the difference increased between the no circulation curve and the 0.5 m^3/s circulation curve at the latter part of the stratified season. These percentages represent the highest anoxic condition that occurred in the lakes (around Julian Day 220) as shown in Figure 89 and will depend on the time considered.

5.2 Effect of Intake Depth on Water Column Stability and Dissolved Oxygen

When considering the implementation of circulation in lakes/reservoirs there are two main parameters to establish before acquisition of a circulation system: (1) the intake depth(s) and (2) total circulation flow rate. In this section the focus is on the intake depth

The 10 and 15-meter lakes were chosen for this modeling effort because circulation was observed to have a larger impact on these lakes (Figure 86 and 88). Simulation runs were conducted for both lakes with the intake set at a single depth during each run. Intake depths were varied during model runs at one-meter intervals between the surface and the sediment. Similar to the initial impact simulations (Figure 86 and Figure 88), the circulation flow rate was set to 0.5 m^3/s for all the model runs in this intake depth study. The temperature and dissolved oxygen profiles reported here are based on the 220th Julian day (August 8th) because this date represents the middle of the thermal stratification period for both the 10 and 15-meter lakes.

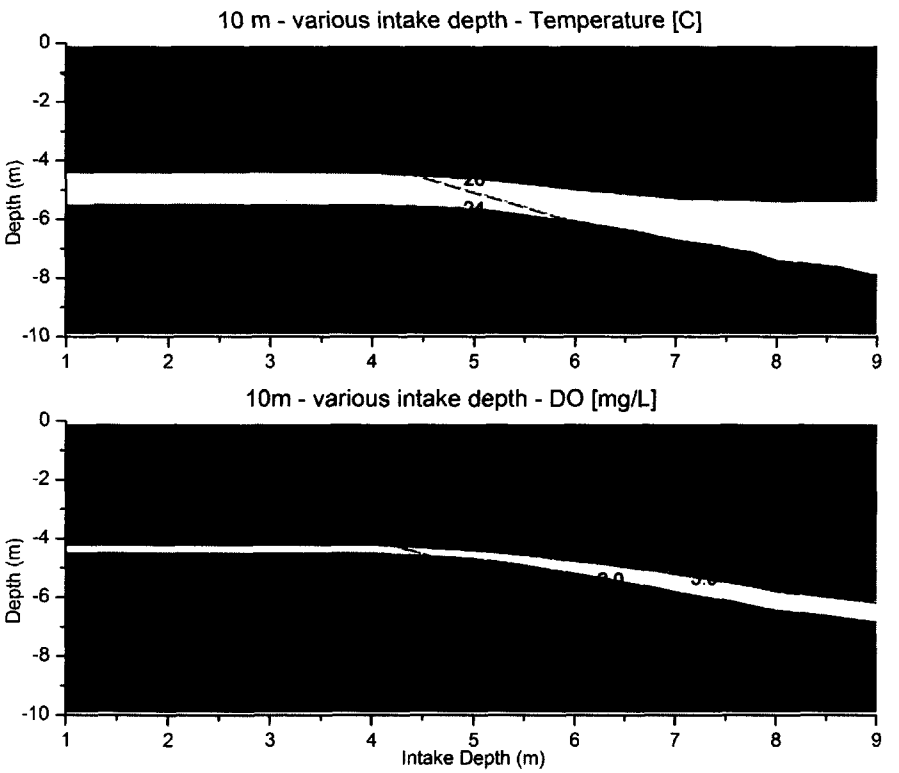

Figure 90. CE-QUAL-W2 prediction of temperature and dissolved oxygen for the 10 meter lake as a function of circulator intake depth. Flow rate = 0.5 m^3/s; Julian Day 220 (August 8). Dashed line represents depth of intake.

Figure 88 shows the vertical temperature and dissolved oxygen distribution in the 10 meter deep lake under the influence of various intake depths. One can see that there was no significant influence on the temperature profile as long as the intake depth was set within the epilimnion (about 3 meters). This finding was expected, since the variation in temperature is small within the epilimnion and, consequently, the specific gravity of the water. The density of the withdrawn water will therefore be similar to the density of the surface water, so the impact of the physical mixing is minimal.

Once the intake was set within the thermocline, a small change occurred in the vertical temperature profile followed by a larger impact as the intake was lowered towards the sediments. The epilimnion deepened but did not become much colder. This may result largely from the short residence time of colder and denser water at the surface. Another influence was the draw-down effect caused by water being removed through the circulator intake. The flow rate (0.5 m^3/s) was sufficient to completely draw the thermocline down to the sediments (22 °C isoline) for the 10-meter lake simulation. This is reasonable when considering the circulated water volume from the beginning of the stratified period (about 3,000,000 m^3) and the hypolimnetic volume (about 1,000,000 m^3). Because the amount of hypolimnetic water that is removed by the intake is so large? Small?, it is clear that the thermocline would reach the intake depth sooner than the 75 days from the onset of the thermal stratification to Julian Day 220 (August 8). This can clearly be seen for the 10-meter lake in Figure 84 during 0.5 m^3/s circulation rate. Based on the observations above, it appears that circulation can substantially impact vertical temperature distribution.

The 10-meter lake's dissolved oxygen response to the various circulator intake depths showed a similar behavior as the temperature response discussed above. There was no significant impact while the intake was defined within the epilimnion (above 4 meters), but when the intake depth was set below the depth where oxycline developed without circulation, the dissolved oxygen distribution was altered. One can see that the oxycline became less sharp as the intake was introducing oxygen poor hypolimnetic water to the circulation mixing zone from the surface to the intake depth. In contrast to the temperature simulation, the dissolved oxygen distribution was not affected by the circulation to the same degree. Figure 88 shows that the oxycline was not drawn down to the intake when the intake depth was close to the sediments. This indicates that substantial mixing and draw down of surficial waters is not sufficient alone for oxygenation of the lower waters of a lake.

The 15-meter lake (Figure 91) showed a similar response to the various circulation depths as the 10-meter lake; however, the hypolimnetic volume was larger than the pumped volume by the circulator on Julian Day 220 (August 8). As a result, the thermocline (22 °C isoline) was not pulled down to the intake when located close to the sediments. Similar to the 10-meter lake, the temperature distribution showed a behavior that was controlled by the physical mixing. The dissolved oxygen plot (Figure 91) showed that there was no additional impact of lowering the intake beyond 10 meters.

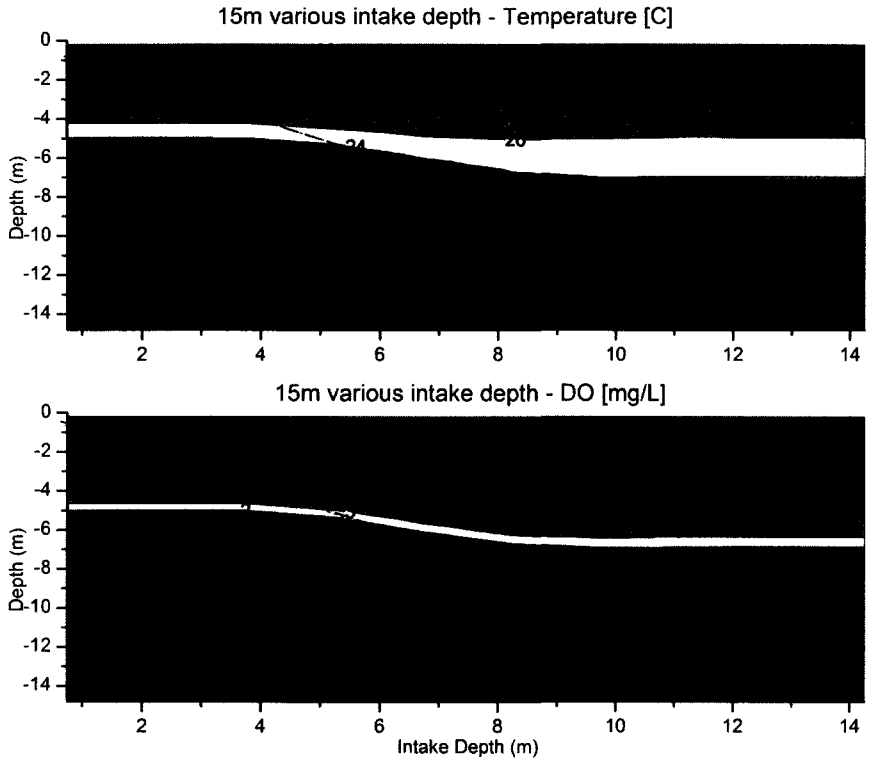

Figure 91. CE-QUAL-W2-prediction of temperature and dissolved oxygen for the 15 meter lake under various as a function of circulator intake depth Flow rate of 0.5 m^3/s Julian day 220 (August 8).

It has been shown how the temperature distribution is highly affected by surface circulation with the thermocline becoming less sharp as a consequence of the increased mixing provided by deeper intake depths (Figures 90 and 91). This shift in temperature distribution will naturally affect the density of water at various depths, and therefore affect the thermal stability of the water column. Thermal stability of a lake/reservoir arises from buoyancy forces within the water column and is commonly quantified by a Schmidt's stability number (eq. 8). Schmidt's stability represents the energy required to overcome the thermal buoyancy forces within the water column and obtain a completely mixed thermal distribution (Idso, 1979).

$$S = A_o^{-1} \sum_{z_0}^{z_m} (z - z_{\bar{p}})(p_z - \bar{p})\, A_z\, \Delta z \qquad (8)$$

A_0 = Lake surface area (cm^2)

p_z = Density at depth z (g/cm^3)

$\bar{p}$ = Mean density (g/cm^3)

z = Depth at measurement point in centimeters

z_p = Depth in centimeters where mean density is found

A_z = Area at depth z (cm^2)

Δz = Incremental change in depth (cm)

Schmidt's stability increases as the temperature gradient in the water column sharpens. Figure 92 illustrates how the Schmidt's stability of the 15-meter lake is affected when the intake depth was located at various depths. It can be seen that there was no change in stability as long as the intake was confined within the epilimnion (from the surface down to 5 meters). This agrees with the temperature distribution of various intake depths (Figure 91). When the intake depth was located within the metalimnion, the Schmidt's stability increased (Figure 92), along with the temperature gradient ($\Delta T/\Delta h$) (Figure 93) that was calculated for the water column under the various circulator intake depth conditions on Julian Day 220 (August 8).

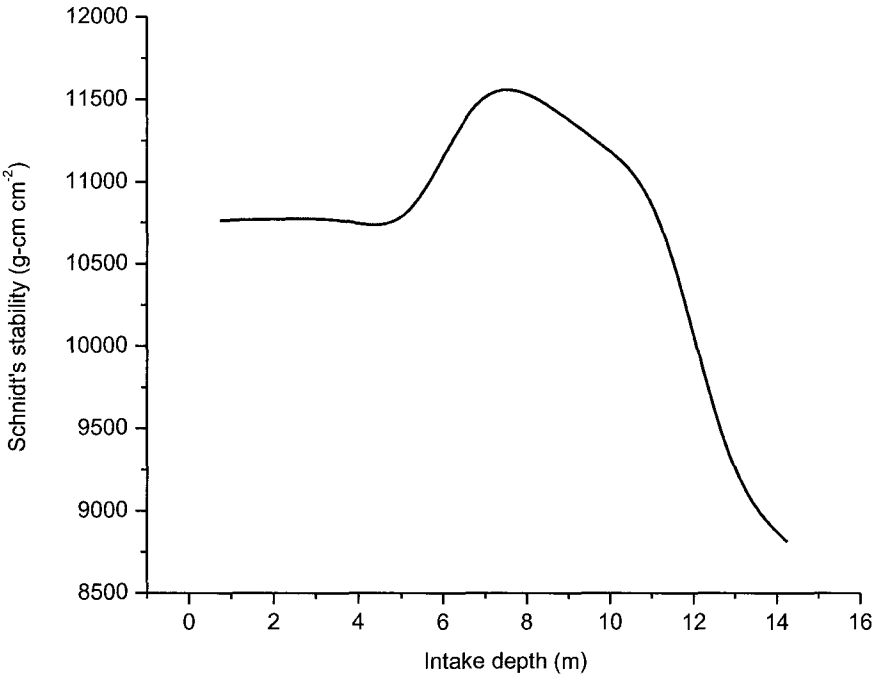

Figure 92. Schmidt's stability curve for the 15 meter lake under various intake depths at Julian Day 220 (August 8).

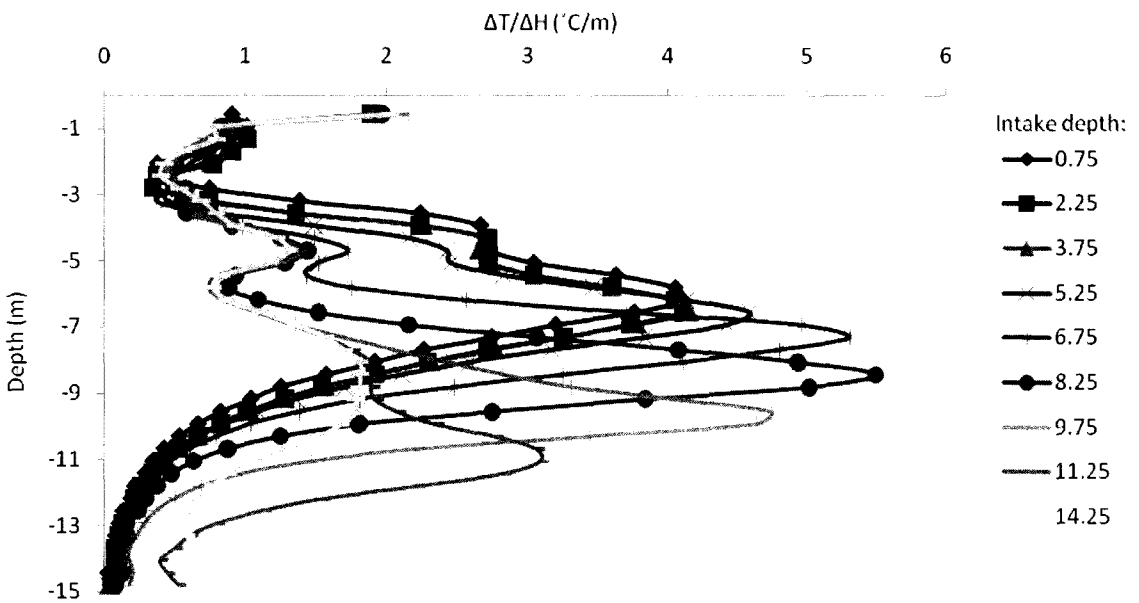

Figure 93. ΔT/Δh at Julian Day 220 (August 8) with the intake depth at various depths in the 15 meter lake.

The maximum stability of the water column occurred when the intake depth was set at about 7 meters (Figure 92), which corresponded to the highest temperature gradient also occurring when the intake was set at 7 meters (Figure 93). As the intake was lowered beyond this depth, the stability decreased due to a warming of the hypolimnion and cooling of the epilimnion making the temperature gradient less sharp.

In general, it is desirable to decrease the thermal stability of a lake/reservoir. A lower thermal stability will most often result in a shorter period of thermal stratification, therefore reducing the time of anoxic conditions with associated iron and manganese problems. If a shallow lake with a low thermal stability is subjected to circulation, thermal stratification may be prevented from forming. Water quality issues associated with anoxia will likely be prevented.

5.3 Effect of Circulation Flow Rates on Water Column Stability and Dissolved Oxygen

The second main consideration for sizing a surface circulator system in a lake is the total circulator flow rate. A new series of simulations was conducted in order to study the impact of various flow rates on several different lake sizes. A medium-small lake (10 m) and a larger lake (15m) were subjected to a wide range of flows in the CE-QUAL-W2 model and the effect on the water column temperature and dissolved oxygen concentration. Physical mixing of the water column during the formation of the thermal stratification has been shown to delay this process, and when applied during summer and fall, will weaken and dissolve the stratification, resulting in an earlier fall turn-over (Schladow, 1995).

This research will focus on the hypolimnetic surface circulator's effect on breaking down the thermal stratification during the middle of the stratification season. The temperature and dissolved oxygen profiles were simulated on the 220th Julian day (August 8) under various flow rates. This date represents the middle of the stratification period and is therefore considered representative of the circulation system's ability to influence the mid-season thermal stratification. The intake depth was located 0.5 meters above the sediments for the 10-meter lake model and 0.75 meters above the sediments for the 15-meter lake model. The reason for increasing the distance between the sediments and the intake of the 15-meter lake was to avoid flow restriction at the intake (segment 20) due to the steeper bottom slope of the 15-meter lake, as seen in Figure 85.

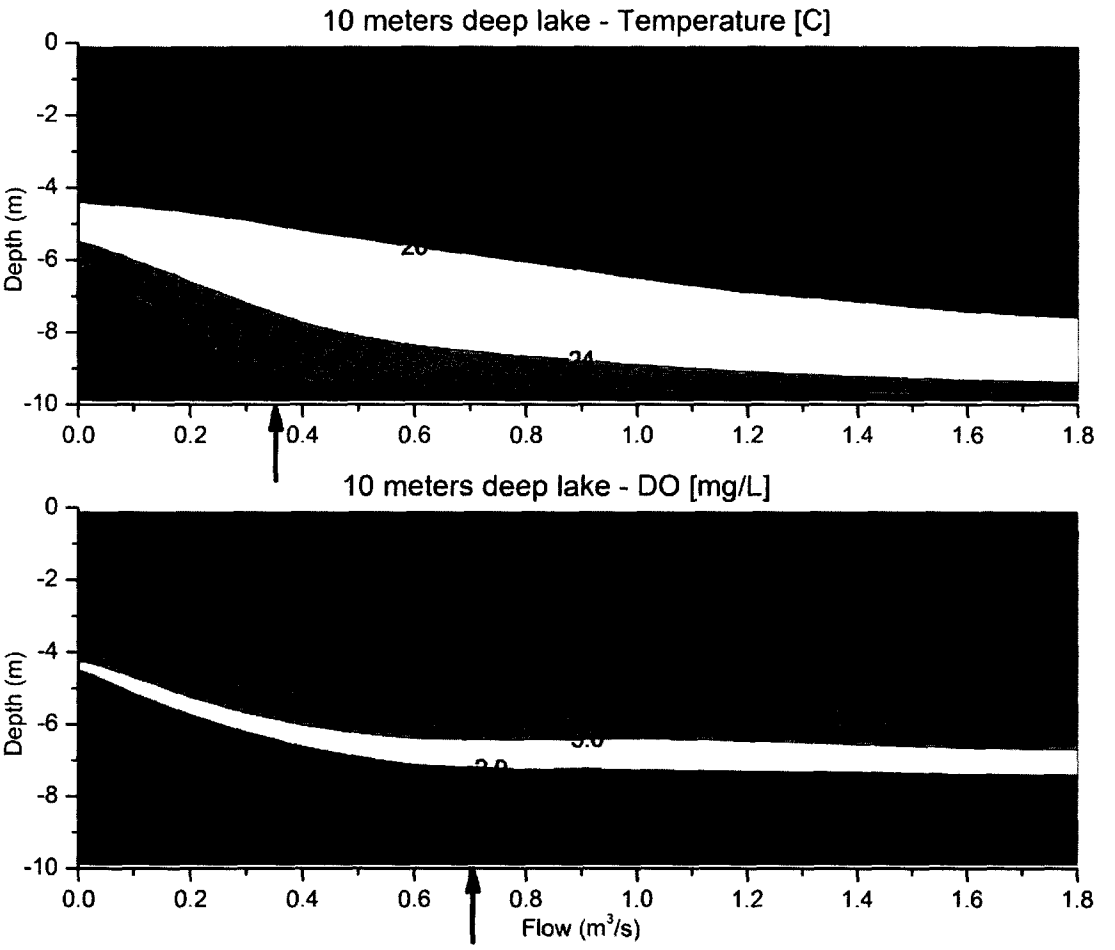

Figure 94. Temperature and dissolved oxygen distribution at Julian day 220 (August 8) of the 10 meter deep lake under various circulator flow rates. Arrows indicate the draw down flow rate for the thermocline and the oxycline.

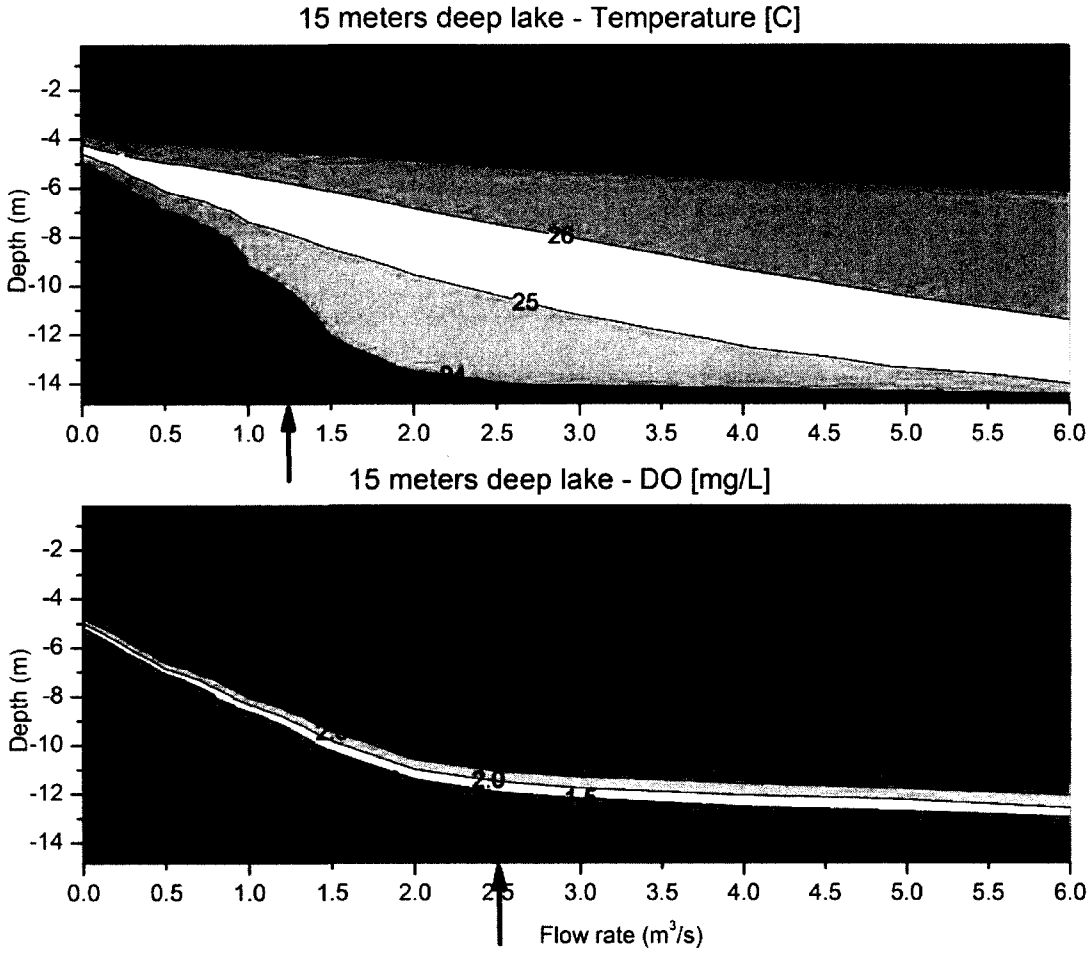

Figure 95. Temperature and dissolved oxygen distribution at Julian day 220 (August 8) of the 15 meter deep lake under various circulator flow rates. Arrows indicate the draw down flow rate for the thermocline and the oxycline.

The influence of circulation flow rate on thermal distribution was similar for both the 10 and 15 meter deep lakes (Figure 94 and 95) though the flow rates required for similar impacts, such as drawing the thermocline down, were higher in the 15 meter deep lake, consistent with the greater volume in the deeper lake. The thermal gradient decreased as the flow rate increased in response to the vertical mixing of colder bottom waters with warmer near-surface water. It is important to note that the 10 meter deep

lake had a warmer hypolimnion during similar external conditions than the 15 meter deep lake. Deep lakes will have a constant temperature in the hypolimnion throughout all the seasons if no vertical mixing is introduced. A direct comparison of the isolines between the two lake volumes is therefore not feasible, but a more general thermal comparison can be done. Both the isopleths of the 10 and 15-meter lakes showed that the temperature distribution was relatively unaffected above 4 meters by the circulation flow rate. This is related to how the density flow of the mixture between the hypolimnetic circulation water and the ambient surface water was sinking to its equilibrium depth below the four meter strata. These plots also show that the impact on the water column temperature distribution was substantial for the lower flow rates, but as the flow rate caused the thermocline to be drawn down to the intake depth, additional circulation flow rates made little additional impact on the temperature profile. Once the thermocline is drawn down to the intake, warmer water will be circulated to the surface; therefore, there is less thermal impact from the circulation. This flow rate causing the thermocline (about 22 °C) to be drawn down to the intake is indicated on the x-axis by a black arrow (Figures 94 and 95).

The dissolved oxygen distribution showed a similar trend as the temperature distribution. The oxycline was drawn down and the gradient diminished as the flow rate increased. It was observed that the dissolved oxygen distribution reached a circulation flow rate (0.7 $m^3 s^{-1}$ and 2.5 $m^3 s^{-1}$ for the 10 and 15 meter deep lakes, respectively) beyond which little additional impact was predicted by the model. A general observation of the 10 and 15-meter lakes was that they required approximately two times the flow rate for the dissolved oxygen to reach the point of a diminishing impact compared to the

temperature. The 10-meter lake needed a 0.35 m^3/s flow rate to draw down the thermocline and a 0.7 m^3/s flow rate to bring the dissolved oxygen profile to the point where little additional influence was predicted. For the 15-meter lake, the flows were 1.25 and 2.5 m^3/s respectively, indicated by the black arrows on the x-axis (Figure 95).

To explain the dissolved oxygen behavior, one must focus on the sources and sinks in a reservoir and how the operation of surface circulation impacts these sources and sinks – particularly the rate at which oxygen is transported to/from and consumed or produced at each location. The atmosphere serves as the oxygen source, which then diffuses into the water column through the surface boundary layer at a relatively slow molecular diffusion rate, as discussed in Chapter 1. Despite a slow oxygen transfer rate (during no wind and wave condition), the large surface area of a lake will result in an overall significant oxygen transfer to the lake. Once the oxygen has entered the water column it will be consumed by various oxygen demanding processes within the water column but also from the sediment oxygen demand (biogeochemical reactions resulting from the respiration of organic matter) at the bottom of the lake. The sediment oxygen demand is typically much larger than the oxygen demand within the water column. Beutel (2003) reports that the sediment oxygen demand is generally 75% of the total oxygen demand for moderately deep lakes. At the same time the horizontal transport within the lake is much more prominent than the vertical transport during the stratified period (Imboden, 2007). It can be seen in Figure 84 that the sediment area to water volume ratio of the hypothetical reservoirs increases with depth, which is why the oxygen concentration in the lower water column will be dominated by the sediment oxygen demand. During circulation, a draw-down effect of the oxycline will occur. Given a high

circulation flow rate scenario, the water column oxygen demand will be exceeded by atmospheric resupply from vertical mixing, resulting in an increased oxygen concentration in the middle to lower water column, but the oxygen demand in the sediment will exceed the oxygen supply at the deepest part of the lake/reservoir so that anoxia will still occur at the lowest depths of the water column. The draw-down effect of oxygenated epilimnetic water will play a significant role in transporting dissolved oxygen to the lower water column. It is estimated that a 0.5 m^3/s circulation flow rate will induce an oxygen flux of about 340 kg oxygen per day to the upper hypolimnion. The added oxygen will gradually be consumed by the hypolimnetic water column oxygen demand and increasingly by sediment oxygen demand with depth. This sediment oxygen demand influence becomes particularly influential at the maximum lake depth since the bottom surface is horizontal and will represent a high oxygen demand on a small volume of overlying water. The modeling reflected this tendency of sediment oxygen demand dominance at the deepest segment of the lakes (Figure 88). The sediment oxygen demand was too prominent to be eliminated by the 0.5 m^3/s circulation flow rate for all four hypothetical lake sizes. This was also the case when simulations of higher circulator flow rates were tried.

The goal for the hypothetical lake modeling was to develop a general understanding of how surface circulation affects the temperature and dissolved oxygen distribution within a lake. An attempt was therefore made to compare the vertical temperature and dissolved oxygen concentration distributions with respect to hypolimnetic turnover time, where hypolimnetic turnover time is considered the time it takes for the circulators to pump the equivalent volume of the hypolimnion (equivalent to

the hypolimnetic volume divided by circulator pumping rate). It was thought that the various lakes sizes would behave similarly when compared on a hypolimnetic turnover basis, and if so, then the temperature and dissolved oxygen distributions from circulation might be related to a common condition. New isopleths of oxygen and temperature were made based on hypolimnetic turnover time for the 10 and 15-meter lakes. The isopleths were generated based on Julian Day 220 (August 8) and are displayed below (Figures 96 and 97).

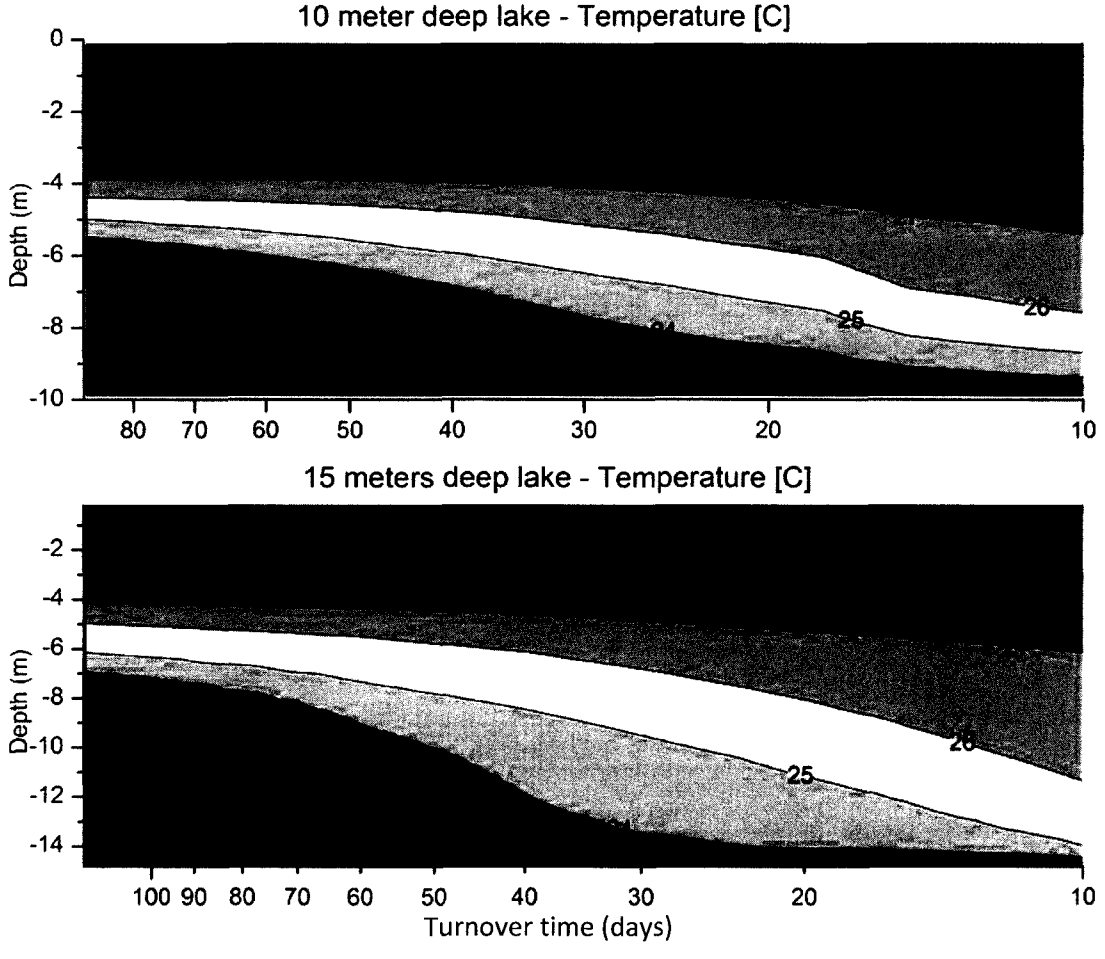

Figure 96. Temperature distribution of the 10 and 15 meter lake at Julian Day 220 (August 8) as a fraction of turnover time.

Both the 10 and 15-meter lakes were modeled up to circulation flow rates high enough to create a turn-over time of 10 days, which for the 10 and 15-meter lakes was 1.8 and 6 m^3/s, respectively; and 12 m^3/s for the 20-meter lake.

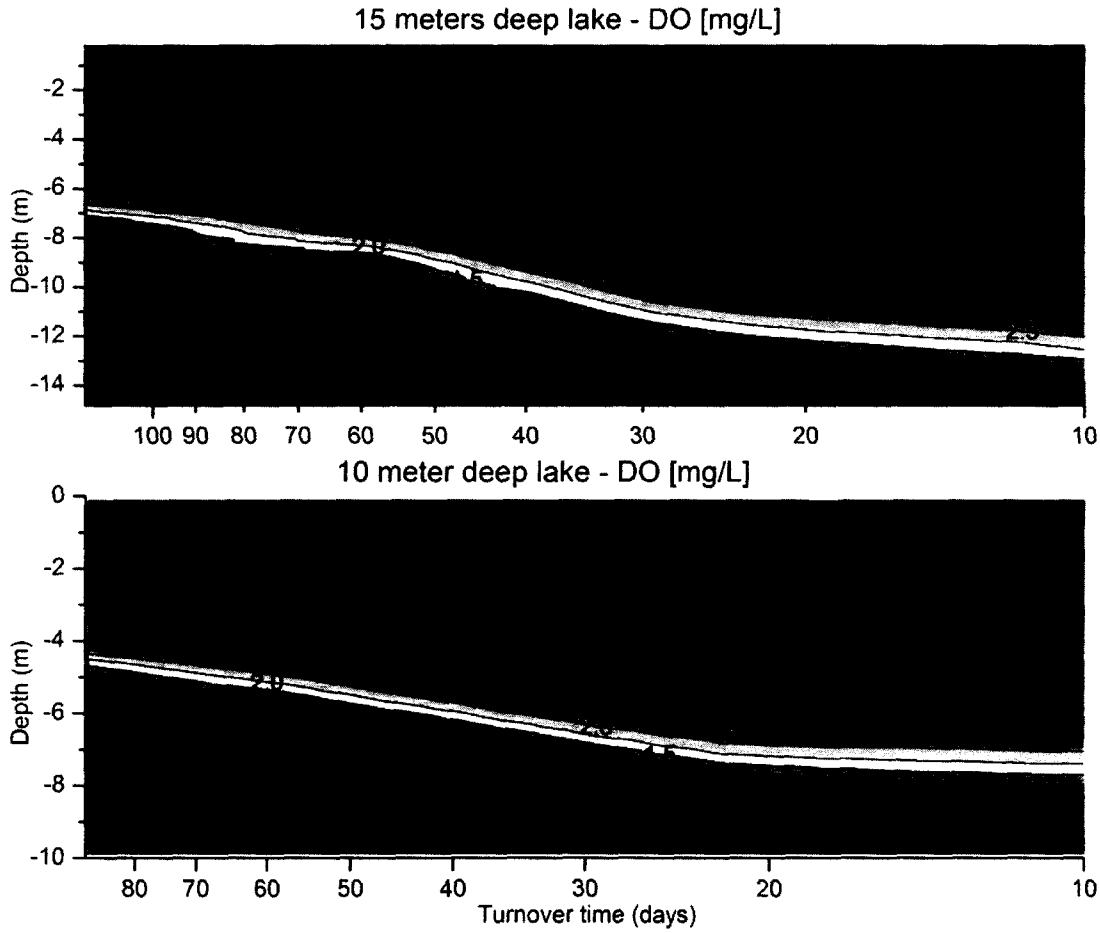

Figure 97. Dissolved oxygen distribution of the 10 and 15 meter lake at Julian Day 220 (August 8) as a fraction of turnover time.

The volumetric ratio between the epilimnion and the hypolimnion are different for the four lake sizes considered. The oxycline typically develops naturally at 5 meters depth without any circulation in all lake sizes independent of the maximum depth or the

surface area of the lake. If the four hypothetical lakes were to be completely homogenized, the volumetric ratio differences of the epilimnion and hypolimnion would cause the temperature and dissolved oxygen concentrations to be different. The ratio between the sediment area and lake volume is also different for the various virtual lake sizes resulting in sediment oxygen demand (SOD) having a varying influence on the oxygen distribution within lakes. Because the ratio between the sediment surface area to water volume is not the same for different lake sizes, it becomes difficult to generalize the temperature and dissolved oxygen distribution under surface circulation based on turnover time alone without taking the lake volume and bathymetry into account.

As previously illustrated (Figure 88), surface circulation improved the dissolved oxygen conditions in all the lake sizes by reducing the sediment area exposed to suboxic water through an entire season. The next step was to examine how various circulation flow rates would influence the anoxic fraction of the sediment surface area. The anoxic fraction was calculated based on temperature and dissolved oxygen profiles in the 10, 15, and 20-meter lakes on the 220^{th} Julian day (August 8, representing the middle of the stratification period) using the same definition of anoxia as < 4 mg/L at the sediment-water interface. The results are displayed in Figure 98 a. The initial fraction of anoxic sediments is different between the three lake sizes. The 10-meter lake has 38% of its sediment surface area exposed to water with less than 4 mg/L dissolved oxygen concentration, while the 15 and 20-meter lakes have 52% and 55% of the sediment area exposed to anoxic conditions, respectively. As the circulation flow rate increases (Figure 98 a) the 10, 15, and 20-meter lakes behave similarly but have a different anoxic sediment fraction relationship with flow rate. The 10-meter lake has the smallest

hypolimnetic volume and is therefore influenced by a relatively small range of flow rates. Figure 98 a shows that the 10-meter deep lake has a distinct change in slope at 1.8 m^3/s. A similar change in slope occurred in the 15 and 20-meter deep lakes at 6.0 m^3/s and 11.0 m^3/s, respectively. These flow rates all correlated to a 20 day turnover time based on each lake's hypolimnetic volume. Figure 98 b illustrates how each lake's anoxic surface area is reduced and thus improved as the circulation flow rate increases compared to the anoxic surface area that develops under the no-circulation condition. Similar to Figure 98 a, a slope-change occurs in the curve for each lake as the flow rate yields a 20 day turnover time. As the flow rate is increased beyond the point of 20 days turnover time, the impact on the reduction in anoxic sediment area is diminished.

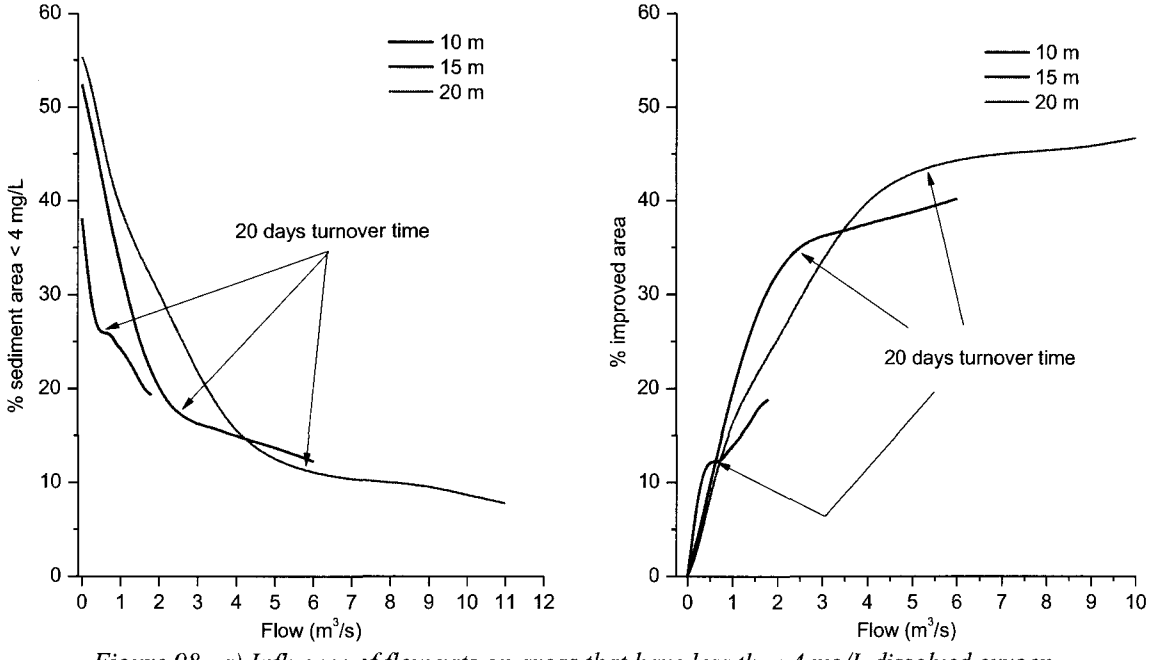

Figure 98. a) Influence of flow rats on areas that have less than 4 mg/L dissolved oxygen. b) Percent improved area that experiences more than 4 mg/L dissolved oxygen as a consequence of various circulation rates.

These slope changes are linked to the effect of drawing the oxycline down to the intake (about 0.5 meter above the sediments). Once the oxycline is drawn-down to the intake, the efficiency of the circulator to increase the oxygen condition diminishes. This is related to circulator operation not affecting the condition of the water column that is below the intake depth. Because Figures 98 a and 98 b are based on conditions on Julian Day 220 (August 8), and because the geometric shapes of the hypothetical lakes are similar for all the hypothetical lakes, the draw-down of the oxycline occurs on the same turn-over period (20 days). If similar curves were to be made based on conditions on Julian Day 200 (July 19), then a higher flow rate would be needed to draw-down the oxycline to the circulator intake due to a shorter time period available. Consequently, the point of slope change would also occur at a correspondingly higher flow rate. If the conditions were to be considered at a later date in the thermal stratification season, say Julian Day 250 (September 7), then a lower flow rate would be sufficient to draw-down the oxycline to the intake depth.

The reason that the 10, 15, and 20-meter lakes drew down the oxycline to the intake at the same turnover period (20 days) is driven by the geometric shape which was the same for the three hypothetical lakes. A natural lake/reservoir will have a different hydrographic relationship; therefore, the oxycline draw-down period for a given circulation flow rate will differ from the ones seen in Figure 98. For a given lake/reservoir, CE-QUAL-W2 can be set up, calibrated, and used for finding the required circulation flow rate necessary to meet a given set of design criterion related to anoxic

sediment fraction reduction. Alternatively, this procedure can be used for evaluating the dissolved oxygen depth penetration of particular circulation equipment and the sediment fraction implications that this equipment has on the lake/reservoir.

When looking at the modeling of Occoquan Reservoir, little impact was observed in terms of dissolved oxygen penetration (Figure 81). This is likely due to the large hypolimnetic volume of Occoquan Reservoir and the modest circulation flow rate. The hypolimnetic volume of Occoquan Reservoir is comparable with the 20-meter lake (9,000,000 m^3 below 5 meters), but the circulation flow rate was only about 0.5 m^3/s, as discussed in Chapter 4. Previous Occoquan Reservoir modeling (Figure 81) shows that the oxycline was drawn-down slightly; however, Figure 95 predicts that the reduction in anoxic sediment surface area should be close to about 5%. Although the reduced anoxic sediment area was not accurately calculated for Occoquan Reservoir, it appears that the small draw-down of the oxycline will result in a similar anoxic sediment surface reduction of 5%. The initial Occoquan Reservoir modeling is therefore consistent with the behavior of the 20-meter hypothetical lake and the predicted reduction of the anoxic sediment surface.

Being able to predict the reduction in sediment anoxic condition based on the circulation condition may be used to further predict the iron or manganese concentration in the reservoir. It can be assumed that the iron or manganese release rate from the anoxic sediment surface is constant; however, predicting these constituent concentrations accurately is challenging due to physical mixing and also oxidation aspects that will play a role. This is outside the scope of this research.

5.4 Summary

The surface circulator's impact on vertical temperature and dissolved oxygen was studied in detail with less emphasis on lateral effects as the lateral impact was without variation as seen in the Occoquan Reservoir modeling (Figures 76 to 79). The impact of circulation was examined through a series of simulation runs using CE-QUAL-W2. Despite reasonable modeling results, the simulations had several limitations. The model does not describe the near-field flow pattern that is present around an actual surface circulator, nor does it account for additional oxygen transfer from the atmosphere to the water due to turbulence at the surface over and around the circulator. As stated previously in Chapter 4, the oxygen that is generated by algae due to photosynthesis is only represented in a rudimentary manner. A more detailed algae study would allow the model to be set up to represent the actual conditions more closely. The model also uses a simple first order sediment oxygen demand, which is likely not to represent actual sediment behavior during all conditions. The last limitation listed here is related to the fact that not all constituents affecting dissolved oxygen are included in the model, such as reduced metals, silica, and macrophytes. The model was only set up to include the most influential constituents related to the dissolved oxygen concentration.

Four different lake sizes were studied under various flow rates and intake configurations. It was found that the modeled surface circulation was not able to eliminate the anoxic development of the lower water column during the thermal stratification period; however, it was found that the circulation did improve the oxygen conditions in all four hypothetical lakes. The oxygenation effect from surface circulation was found to be most significant when the intake was set as deep as possible. The

circulator influence on the temperature in the lakes was also most significant when the circulator intake was placed in this position. When the circulator intake was located below the thermocline, cold hypolimnetic water was transferred to the epilimnion where its temperature was increased by solar heating and mixing with the warm ambient surface water. The result of withdrawing hypolimnetic water and releasing it to the surface was a thickening of the epilimnion and deepening of the thermocline dependent on the hypolimnetic volume and the circulation flow rate. Although not confirmed by water quality data, CE-QUAL-W2 was set up to predict the thermal distribution of four hypothetical lakes during circulation conditions. As the simulated flow rate increases, the mixing also increases. This weakens the temperature gradient to a point where the strongest gradient occurs below or at the circulator intake. However, a complete destratification of a medium size lake requires a substantial circulation flow rate. It may not be practical to achieve this if solar-powered surface circulator units are deployed. Field studies in Occoquan Reservoir suggested that the circulated water remained in epilimnion after being released by the circulator. It appeared that the cold hypolimnetic circulation water was quickly mixed with the ambient epilimnetic water, and then descended to the lower part of the epilimnion at about 3 to 4 meters. The thermocline remains intact during the operation of the surface circulation, but it is gradually becoming less sharp as the circulation flow rate is increased substantially.

The vertical dissolved oxygen distribution has a response to surface circulation similar to that of temperature. Mixing of the water column and consumption within the water column and sediments cause dissolved oxygen behavior to be more dynamic than the temperature distribution, and changes are not just limited to the surface. From

studying the impact of various circulation flow rates, it was found that the oxycline reached a threshold where higher circulation flow rates were unable to improve the oxygen conditions of the lower water column. At this threshold the oxygen distribution was controlled by various oxygen demand rates in the water column and at the sediments. In a moderately deep productive lake, water column oxygen demand will be dominant in the upper water column (Cornett and Rigler, 1987), and the SOD will dominate the hypolimnion and lower water column (Burns and Ross, 1972). The modeling suggested that the sediment oxygen demand was controlling the dissolved oxygen concentration of the overlaying water at maximum depth. Consequently, anoxia developed at the deepest part of the lake despite increased circulation flow rate. The model suggested that surface circulation is not a suitable approach if anoxia is to be fully eliminated.

However, to improve the oxygen conditions in a small lake, only a small circulation flow rate is required. For these lakes the solar powered circulators may be an appropriate solution, but when the lake size increases, the necessary flow rate increases dramatically if a significant dissolved oxygen improvement is desired. For oxygen improvement, it is recommended to provide the largest possible circulation flow rate so that the turnover rate approaches 20 to 25 days. Naturally, there is a cost associated with any mixing or circulation activity, and a cost benefit analysis should be conducted for any circulation project. The temperature and dissolved oxygen plots that are presented in this chapter can serve as a guidance for specifying the circulation flow rate and the intake depth.

5.5 Future Research

This study focused on examining the impact of surface circulators (upflow mode) on temperature and dissolved oxygen in a water supply reservoir and through hydrodynamic/water quality modeling. Although the results in this chapter have been consistent with expected lake/reservoir behavior, a general lack of verification of the model is recommended. It is suggested that CE-QUAL-W2 is set up for a well studied lake/reservoir. The calibration of the model should ideally be done over multiple years to ensure a good representation of the physical system. Then a surface circulation system should be deployed in the lake. This circulation system should also be represented in the model. A thorough comparison of the lake/reservoir and the model could then be made over several years of operation. If a good agreement is found, then this would adequately verify the use of the model for this type of simulation.

It would be very desirable if CE-QUAL-W2 was set up to represent bubble plume type circulation systems in lakes/reservoirs, since these systems are widely chosen for their ability to circulate and oxygenate the water column. Being able to simulate the temperature and dissolved oxygen impact from a bubble plume would allow the model to be used to design the aeration system. It is therefore recommended that future research is aimed at representing the oxygen transfer, mixing, and transport mechanisms involved with bubble plumes produced within CE-QUAL-W2.

As in any research, there are many areas within surface circulation that can be explored further. This technology has recently been introduced on the commercial market to control the cyanobacteria concentration. Cyanobacteria has been of particular interest to the water treatment industry because even small amounts of geosmin or 2-

methylisoborneol (MIB) released by the cyanobacteria can cause taste and odor problems. Many of these species have a gas vacuole that makes them buoyant and therefore typically found at the surface. Surface circulators are believed to reduce the cyanobacteria growth by light starvation, as the cyanobacteria are forced deeper into the water column by mixing from the surface circulators. This has not yet been reported to occur in the literature; however, a manufacturer is currently advertizing that its circulators will cause a shift in the phytoplankton community from cyanobacteria dominance to a healthier green algae and diatom dominance. Further research is needed to identify the cause and effect relationship between surface circulator operation and changes in phytoplankton species and, if documented to occur, the mechanism that causes this shift.

The final research area suggested is based on the destratification system that is operating in Myponga, Australia (Lewis et al., 2001). Two large surface circulators are operating in a down-flow configuration assisting a bubble curtain aeration system in destratifying the reservoir. No literature is currently found describing the oxygenation efficiency of the up-flow circulation versus the down-flow efficiency. The thermal impact of both flow directions is also of importance, as it dictates the horizontal transport within the reservoir. This is a fundamental question related to the surface circulation technology and needs more research. A combination of field verification and modeling is suggested to explore the temperature impact and the oxygen transfer efficiencies to the reservoir. The down-flow circulator's influence on algae and cyanobacteria is also suggested and should be compared to the up-flow configuration.

References

Ashley, K.I. 1988. Hypolimnetic Aeration of a Naturally Eutrophic Lake: Physical and Chemical Effects. Can. J. Fish. Aquat. Sci. 40: 1343-1359.

Ashley, K.I. 1983. Hypolimnetic Aeration of a Naturally Eutrophic Lake: Physical and Chemical Effects. Can. J. Fish. Aquat. Sci. n40: 1343-1359.

Ashley, K.I. 1988. Hypolimnetic Aeration Research in British Columbia. Verhandlungen der Internationalen Vereinigung fur Theoretische und Angewandte Limnologie. Vol. 23 pp. 215-219.

Ashley, K.I. 1995. Hypolimnetic Aeration: Practical Design and Application. Water Research, Vol. 19. No. 6. pp. 735-740.

Berger, C.J., S.A. Wells, and R. Annear. 2005. Laurance Lake temperature model. Department of Civil and Environmental Engineering, Portland State University. Technical Report EWR-01-04. Portland, Oregon.

Beutel M.W., Leonard T.M., Dent S.R., Moore B.C. 2008. Effects of aerobic and anaerobic conditions on P, N, Fe, Mn, and Hg accumulation in waters overlaying profundal sediments of an oligo-mesotrophic lake. Water Research, 42 (8-9), pp. 1953-1962.

Beutel, M.W. 2003. Hypolimnetic Anoxia and Sediment Oxygen Demand in California Drinking Water Reservoirs. Lake and Reservoir Management 19 (3) p. 208-221

Bohm, H. L., McNeal, B. L., O'Connor G. A. 2001. Soil Chemistry, third edition. Wiley, New York.

Burris, V.L., D.F. McGinnis, J.C. Little. 2002. Predicting Oxygen Transfer and Water Flow Rate in Airlift Aerators. Water Research 36. pp. 4605-4615.

C.J. Watras, R.C. Back, S. Halvorsen, R.J.M. Hudson, K.A. Morrison, S.P. Wente. 1998. Bioaccumulation of mercury in pelagic freshwater food webs. Science of The Total Environment, Volume 219, Issues 2-3, Pages 183-208

Cole, T.M. and S. Wells. 2000. CE-QUAL-W2: A Two-Dimensional, Laterally Averaged, Hydrodynamic and Water Quality Model, Version 3. User's manual.

Cooke, G.D., E.B. Welch, S.A. Peterson and P.R. Newroth. 1993. Restoration and Management of Lakes and Reservoirs. 2nd Edition. Lewis Pub. Boca Raton, Fl.

Cooke, G.D., R.H. Kennedy. 2001. Managing Drinking Water Supplies. Lake and Reservoir Management 17 (3) p. 157-174.

Cornett, R. J., and F. H. Rigler. 1987. Decomposition of seston in the hypolimnion. Can. J. Fish. Aquat. Sci. 44: 146–151.

Csanady G. T. 1973. Turbulent Diffusion in the Environment. Dordrecht, Boston, D. Reidel Pub. Co.

Debele, B., R. Srinivasan, J.-Y. Parlange. 2005. Coupling upland watershed and downstream waterbody hydrodynamic and water quality models (SWAT and CE-QUAL-W2) for better water resources management in complex river basins. Springer Science + Business Media B.V. 2006

Dinehart, R.L., J.R. Burau. 2005. Repeated Surveys by Acoustic Doppler Current Profiler for Flow and Sediment Dynamics in Tidal River. Journal of Hydrology 314 1-21.

Engstrom, D.R., D.I. Wright. 2002. Sedimentological Effects of Aeration-Induced Lake Circulation. Lake and Reservoir Management 18 (3) p. 201-214.

Eunpu, F.F. 1973. Control of Reservoir Eutrophication. AWWA, Volume 65 Issue 4, April 1973, pp. 268-274.

Fenchel, T., T.H. Blackburn. 1979. Bacteria and Mineral Cycling. Academic Press. New York.

Fitzgerald G.P. 1970. Aerobic Lake Muds for the Removal of Phosphorus from Lake Waters. Limnol. Oceanogr., 15 (4), p. 550-555.

Floyd E. F. 1973. Control of Reservoir Eutrophication. Water Technology/Quality, Journal AWWA pp. 268 – 274.

G.S. Bilotta, R.E. Brazier. 2008. Understanding the influence of suspended solids on water quality and aquatic biota. Water Research, Volume 42, Issue 12, Pages 2849-2861.

Gachter, R., B. Wehrli. 1998. Ten Years of Artificial Mixing and Oxygenation: No Effect on the Internal Phosphorus Loading of Two Eutrophic Lakes. Environ. Sci. Technol. 32, pp. 3659 – 3665.

Gachter, R., B. Wehrli. 1998. Ten Years of Artificial Mixing and Oxygenation: No Effect on the Internal Phosphorus Loading of Two Eutrophic Lakes. Environ. Sci. Technol. Vol. 32. pp. 3659-3665.

VITAE

Paal Engebrigtsen was born in Bodo, Norway and raised in Oslo, Norway. At the age of 27 he married an American which eventually led him to live in Virginia. His passion for water and interest for the environment made the field of limnology a natural choice for his doctoral research.

Education:

Doctor of Philosophy - Environmental Engineering – May 2010

Department of Civil and Environmental Engineering

Kaufman Hall 135

College of Engineering and Technology

Old Dominion University

Master of Science - Environmental Engineering - May 2004

Old Dominion University, Norfolk, VA

Master of Science - Mechanical Engineering - July 1997

Norwegian University of Science and Technology, Trondheim, Norway

Bachelor of Science - Mechanical Engineering - December 1996

University of Colorado at Boulder, Boulder, CO

Mechanical Engineer - May 1993

College of Engineering, Oslo, Norway

Contact information:

Paal Engebrigtsen

5215 Bluestone Ave, Norfolk, VA 23508

engebrigtsen@gmail.com